NOTICE

CERTAIN DATA CONTAINED IN THIS DOCUMENT MAY BE DIFFICULT TO READ IN MICROFICHE PRODUCTS.

DISCLAIMER

Printed in the United States of America. Office of Scientific and Technical Information, Oak Ridge, Tennessee.

DOE/PC/79919-T2
(DE91002479)
Distribution Categories UC-102 and UC-113

Technical Progress Report for the Project

DOE/PC/79919--T2

DE91 002479

FLOTATION AND FLOCCULATION CHEMISTRY OF COAL AND OXIDIZED COALS

Principal Investigator : Prof. P. Somasundaran

Graduate Student : Rajagopalan Ramesh

FINAL REPORT

Reporting Period : September 15, 1987 to September 15, 1990

DOE Project Grant No. : DE-FG-2287-PC-79919

Contents

ABSTRACT xii

EXECUTIVE SUMMARY xiii

1 STATEMENT OF OBJECTIVES 1

2 INTRODUCTION 1

2.1 PREAMBLE 1

2.2 RESEARCH STRATEGY 4

3 REVIEW/BACKGROUND 5

3.1 CONTACT ANGLE 5

3.2 WETTING 9

3.2.1 Presentation of wetting behavior 11

3.2.2 Critical wetting surface tension 11

3.2.3 Film flotation 19

3.3 HEAT OF WETTING 25

3.4 ADSORPTION OF VARIOUS REAGENTS 27

3.4.1 Surfactants 27

3.4.2 Polymers 28

3.4.3 Fuel Oil 30

3.4.4 Frothers 31

3.5 OXIDATION 31

4 CRITICAL ISSUES 34

4.1 HETEROGENEITY 34

4.2 ROLE OF HETEROGENEITY IN INTERFACIAL PHENOMENA 35

4.3 ACCURATE CHARACTERIZATION OF COAL SURFACES . . . 36

5 MATERIALS AND METHODS 36

5.1 MATERIALS 36

5.1.1 Coal 36

5.1.2 Polymer 37

5.1.3 Other 38

5.2 METHODS 38

5.2.1 Morphological Studies 38

5.2.2 Adsorption Studies 38

5.2.3 Film Flotation 39

5.2.4 Centrifugal Immersion 39

5.2.5 Wax Vapor Deposition on Coal 40

5.2.6 Adsorption Gravimetry 40

5.2.7 Immersional Calorimetry 42

5.2.8 Spectroscopy 46

6 RESULTS AND DISCUSSIONS 48

6.1 MORPHOLOGY 48

6.2 WETTABILITY DISTRIBUTIONS 49

6.3 SURFACE SITE DISTRIBUTIONS 61

6.3.1 Effect of Oxidation on surface site distributions 68

6.3.2 Surface Modification:Polymer Adsorption 74

6.3.3 Effect of surface modification on surface site distributions . . 88

6.4 CONTACT ANGLE DISTRIBUTIONS 112

6.5 THERMODYNAMIC APPROACH TO SURFACE SITE DISTRIBUTION 117

6.5.1 Gas adsorption 117

6.5.2 Enthalpy of immersion 124

6.6 Spectroscopic investigations 128

6.6.1 DRIFT 128

6.6.2 LAMMA 134

6.6.3 D - ESCA 137

6.7 Other distributions 140

7 CONCLUDING REMARKS 141

7.1 Impact of study on advaced physical coal beneficiation processes . . 147

A SEM-EDX PHOTOMICROGRAPHS 163

B LASER MICROPROBE MASS ANALYZER 183

List of Figures

1 Contact angle of a sessile drop 6

2 The wettability "spectrum" for selected low energy surfaces (from Shaffrin, E.G. and Zisman, W.A., in J. Phy. Chem., vol 64, (1960), pp 519-524) 13

3 Schematic illustration of Lucassen-Reynders plot and Gamma flotation. 14

4 Schematic representation of film flotation process 21

5 Typical cumulative partition curve of a coal sample. 23

6 Typical frequency distribution diagram of critical wetting surface tension of coal particles: from reference [44]. 24

7 Adsorption density of dodecyl ammonium chloride concentration at pH 5.5 to 6.1 and at an ionic strength of 2×10^{-3} M KCl on coal. . 29

8 Schematic illustration of the apparatus used to coat coal particles with paraffin wax vapor. 41

9 Schematic illustration of the gravimetric gas adsorption apparatus. . 43

10 Cross sectional view of the Tian-Calvet calorimeter cell. 44

11 Cumulative partition curves constructed from film flotation data obtained using base coal and wax coated coal samples. 50

12 Cumulative wettability distribution curves of base coal, wax coated coal and oxidized coal constructed from centrifugal immersion experiments. 52

13 Differential wettability distribution curves of base coal, wax coated coal and oxidized coal constructed from centrifugal immersion experiments. 55

14 Cumulative wettability distribution curves of base coal in 1988 and in 1989 and oxidized coal constructed from centrifugal immersion experiments 56

15 Wettability distribution curves of base coal as a function of the surface tension of the wetting liquid 58

16 Schematic film flotation partition curves for a heterogeneous mixture of homogeneous particles. 63

17 Schematic film flotation partition curves for a population of heterogeneous particles. 64

18 Film flotation partition curves for base coal and various float fractions. 66

19 Film flotation partition curves of base coal and float fractions after treatment with 1000 ppm of cationic polyacrylamide for 24 hours . . 67

20 Site distribution curves of base coal and base coal heated at 70°C for different durations (in hours) and cooled under ambient conditions. . 69

21 Site distribution curves of base coal and base coal heated at 70°C for different durations (in days) and cooled under ambient conditions. . 70

22 Site distribution curves of base coal and coal heated at 70°C for 2 days and coal heated at 140°C for 24 hours. 72

23 Site distribution curves of coal heated at 70°C for 2 days and cooled under ambient conditions, and the same sample reheated at 70°C for 2 days and cooled under ambient condition. 73

24 Site distribution curves of coal sample placed in a dessicator under vacuum for 24 hours. 75

25 Site distribution curves of coal heated at 70°C for 2 days without cooling, cooled in a dessicator under vacuum and cooled under ambient condition. 76

26 Kinetics of adsorption of cationic polyacrylamide on coal. 78

27 Adsorption isotherm of 10% cationic polyacrylamide and nonionic polyacrylamide on coal based on residual concentrations measued by Ubbelhode viscometer. 80

28 Adsorption isotherms of polyacrylamide of various charge densities on coal based on residual concentration measurement using a Total Organic Carbon analyzer. 81

29 Fluorescence emission spectrum of pyrene labeled polyacrylamide in solution. 83

30 Fluorescence emission spectrum of pyrene labeled polyacrylamide in supernatant after adsorption. 84

31 Fluorescence emission spectrum of pyrene labeled polyacrylamide adsorbed on coal. 85

32 DRIFT spectrum of bituminous coal used in this study. 87

33 DRIFT spectrum of commercial grade nonionic polyacrylamide (10% cationicity). 89

34 DRIFT spectrum of commercial cationic polyacrylamide (10% cationicity) coal used in this study. 90

35 DRIFT spectrum of commercial cationic polyacrylamide (34% cationicity) bituminous coal used in this study. 91

36 Difference spectrum of base coal and nonionic polyacrylamide. . . . 92

37 Difference spectrum of base coal and cationic polyacrylamide (10% cationicty). 93

38 Difference spectrum of base coal and cationic polyacrylamide (34% cationicity). 94

39 Site distribution curves constructed from film flotation tests for base coal and coal treated with 1000 ppm of various polyacrylamides . . . 96

40 Evolution of site distribution curves constructed from film flotation tests for base coal as a function of the initial concentration of cationic polyacrylamide. 98

41 Site distribution curves constructed from film flotation tests for base coal as a function of the time of adsorption. 99

42 Site distribution curves constructed from film flotation tests of oxidized coal treated with polyacrylamide. 100

43 Cumulative partition curves for the base coal and oil agglomerated coal. 104

44 Cumulative partition curves for coal samples treated with n-dodecane in a denver cell (the amounts in the figure represent microlitres of n-decane per 5 gms of coal). 105

45 Cumulative partition curves for coal samples treated with dodecane in a waring blender. 106

46 Frequency distribution of γ_c for base coal, oil agglomerated coal and coal samples treatred with dodecane in a Waring blender. 108

47 Site distribution curves for base coal, oil agglomerated coal and coal samples treated with dodecane in a denver cell. 109

48 Site distribution curves for base coal, oil agglomerated coal and coal samples treated with dodecane in a Waring blender. 111

49 Distribution of contact angle on coal surface as calculated from γ_c distributions and Neumann's equation of state. 113

50 Contact angles *vs* surface composition: After Dettre and Johnson, (1964). 115

51 Adsorption isotherm of methanol vapor on coal at 30°C plotted as a function of partial pressure of methanol. 119

52 Adsorption isotherm of methanol vapor on coal at 30°C and at 11°C plotted as a function of partial pressure of methanol. 121

53 Isosteric heat of adsorption of methanol vapor on coal. 122

54 Low pressure region of the adsorption isotherm of methanol on coal at 11 degrees C and 30 degrees C plotted as a function of the relative pressure. 123

55 Heat of immersion of coal in methanol as a function of preadsorbed methanol. 125

56 Integral heat of adsorption of methanol on coal as a function of preadsorbed methanol. 127

57 DRIFT absorbance spectrum of base coal. 130

58 DRIFT absorbance spectra of base coal and float fraction obtained from film flotation and the corresponding difference spectrum. . . . 131

59 DRIFT absorbance spectra of float and sink fraction obtained from film flotation and the corresponding difference spectrum. 132

60 DRIFT absorbance spectra of base coal and sink fraction obtained from film flotation and the corresponding difference spectrum. . . . 133

61 Positive ion LAMMA spectral line scan profiles at intervals of 4 microns. 135

62 Water desorption spectra from silicate glass samples recorded by a mass spectrometer (top) and the energy distribution calculated from the spectra for sample II. 142

ABSTRACT

The objective of this research project is to understand the fundamentals involved in the flotation and flocculation of coal and oxidized coals and elucidate mechanisms by which surface interactions between coal and various reagents enhance coal beneficiation. It is well recogonized that coal surface is heterogeneous. Often only a small fraction of the surface needs to posses a given property to bring about a desired interfacial effect in flotation or flocculation. An understanding of the nature of the heterogeneity of coal surfaces arising from the intrinsic *distribution* of chemical moieties is fundamental to the elucidation of mechanism of coal surface modification and its role in interfacial processes such as flotation, flocculation and agglomeration.

A new approach for determining the *distribution* in surface properties of coal particles was developed in this study and various techniques capable of providing such information were identified. Distributions in surface energy, contact angle and wettability were obtained using novel techniques such as centrifugal immersion and film flotation. Changes in these distributions upon oxidation and surface modifications were monitored and discussed. An approach to the modelling of coal surface site distributions based on thermodynamic information obtained from gas adsorption and immersion calorimetry is proposed. New information on the surface structure of coal using Laser Microprobe Mass Analyzer and Derivatized Electron Spectroscopy for Chemical Analysis is presented.

The results of this research project should prove powerful for proper characterization of coal surfaces and for developing an accurate understanding of the fundamental nature of the complex interfacial reactions in flotation and flocculation of coal.

EXECUTIVE SUMMARY

This project is designed to develop an understanding of the fundamentals involved in flotation and flocculation of coal and of coals in various states of oxidation. The main objective of this study is to accu. ıtely characterize the coal surfaces and elucidate mechanisms by which surface interactions between coal and reagents enhance beneficiation of coals. Effects of oxidation on the modification of surface characteristics of coal by various reagents will also be studied

Understanding the nature of the heterogeneity of the coal surfaces arising from *distribution* of chemical moieties is fundamental to the elucidation of mechanisms by which reagents adsorb on different coals. Heterogeneities arise from a variety of chemical, minerlogical and morphological reasons. Such heterogeneities can play different roles in different interfacial phenomena. The scale of heterogeneity can also determine the behavior of the system in such processes as flotation and flocculation. In this study a variety of techniques each capable of yielding a set of useful information is employed to generate a comprehensive and accurate picture of both the chemical and morphological characteristics of coal particles. These include morphological investigations, centrifugal immersion, film flotation and different spectroscopies.

Proximate and ultimate analysis of Bruceton mines coal (supplied by PETC) revealed it to be of high volatile bituminous quality. SEM/EDX studies of coal morphology indicated that the coal samples contained iron disulfides, clayey matter, silicates and carbonates. Traces of titanium, manganese, fluorine, potassium and chlorine were also recorded. At moderately coarser sizes (i.e. +100 mesh and +200 mesh), the mineral matter was found to be locked with each other and the coal matrix. Only at 635 mesh individual liberated particles of mineral matter were noticed. In many instances the mineral matter is covered with a fine layer of coal

dust probably due to smearing during grinding and sieving.

Centrifugal immersion is a technique developed during this project to study the role of heterogeneity in wetting of coal particles. Centrifugal immersion of as received coal (base coal), oxidized coal and coal particles coated with paraffin wax vapor revealed that the partition curves constructed from centrifugal immersion experiments are a manifestation of the surface chemistry, surface heterogeneity, shape and edge effects, and the dynamics of the wetting process. These studies also showed that in the wetting of relatively hydrophilic particles, surface chemistry plays a critical role, whereas, in the case of relatively hydrophobic particles, the shape of the particle, and the dynamics of the process predominate. Centrifugal immersion experiments yield a more accurate characterization of the wetting behavior of hydrophobic particles as encountered in practice since the results obtained using this technique are functions of the heterogeneity of the solid, dynamics of spreading wetting and the shape of the particles.

Centrifugal immersion experiments conducted by varying the surface tension of the wetting liquid showed that the detachment of coal particles from the water-air interface is indicative of a fall-out phenomenon under stress. As the surface tension of the liquid phase is reduced this phenomenon appears to be less significant. The family of wettability distribution curves obtained as a function of the surface tension of the liquid phase is likely to be characteristic of the coal particles used. Development of a family of such distribution curves for various coal samples offers a sensitive means for characterizing the wettability of coal particles from different sources or with different history.

An approach consisting of study of surface site distributions on coal using film flotation, including the changes in these distributions upon surface modification, was developed during the course of this project. It was found that the site distribution or the heterogeneity of a group of coal particles essentially represented the site

distribution on a single coal particle (in the -35 +80 mesh range). In other words *the intrinsic heterogeneity of the surface of a single coal particle was demonstrated.* Surface site distribution curves yield the percentage of surface area on individual coal particles exhibiting a specific range of critical wetting surface tension values (γ_c).

Low temperature heating of coal at 70°C in air results in marked changes in the surface site distribution. The average γ_c shifts towards lower values indicative of a more hydrophobic surface. Adsorbed layers of nonionic and anionic polyacrylamide on heat treated coal were found to exhibit a markedly different site distribution from that of the base coal. More of the hydrocarbon part of the polymer is suggested to be exposed as compared to amide groups. An analysis of site distribution curves obtained by film flotation of coal heated at 70°C and cooled under different conditions as well as of the coal stored in a dessicator indicates that moisture on the coal is present in ordered but heterogeneous (various degrees of order) structures and not as random structures encountered in bulk water. Such ordered surface moisture could possibly lead to autophobic behavior of coals.

Polyacrylamide (PAM) polymer was used to alter the surface of coal. A relatively fast and accurate method of determining polymer adsorption by measuring its concentrations at the ppm level using a Total Organic Carbon (TOC) analyzer was developed. Adsorption data obtained from TOC is more representative of the actual adsorption than that obtained by nephelometry or titration. Based on adsorption results for polyacrylamide on coal, obtained by TOC and Ubbelohde viscometer, it was concluded that there is preferential adsorption of higher molecular weight component. Flourescence spectroscopic studies using pyrene labelled polyacrylamide polymers gave further support to this observation.

Site distribution curves constructed from film flotation of PAM treated coal suggest the cationic PAM of 34% cationicity and nonionic PAM to form a more

compact adsorbed layer than the cationic PAM of 10% cationicity or anionic PAM. As the charge density of the polymer increases, the ability of the adsorbed layer to retain water decreases with a corresponding increase in the fraction of surface area with exposed amide groups. Coal with the adsorbed nonionic PAM layer exhibits more heterogeneity than those with cationic or anionic PAM layers. There is no preferential adsorption of nonionic PAM or PAM of 10% cationicity on particular energy sites indicating an entropically driven adsorption process.

The effect of modification of the coal surface by dodecane was studied by analyzing site distribution curves obtained from film flotation data for dodecane treated coals. 75 percent of the surface of coal, agglomerated with dodecane, exhibited a γ_c of around 38 dynes/cm as compared to 30 percent of the surface with a γ_c of 30 dynes/cm for coal sample (5 grams) treated with 80 microlitre of dodecane. Relative hydrophobicity of dodecane treated coal samples was dependent on both the amount of various sites and the magnitude of the surface energy of such sites. An increase in the speed of the impeller employed to disperse the dodecane in water increased the degree of coating of the dodecane on coal surface. However, continued increase in the speed produced no detectable difference in the degree of coating indicating the role of other hydrodynamic factors such as the degree of turbulence.

A thermodynamic approach was used to study the heterogeneity of the coal surface wherein the heat of adsorption of methanol on coal was obtained by two different techniques viz. calorimetry and gas adsorption. Analysis of the isosteric heat of adsorption obtained by this method for this system provided a *qualitative picture of the surface sites distribution* on coal. It appears that the more hydrophobic sites on the coal surface are located in a dense manner such that the adsorbed molecules on these sites are in a highly condensed state. The (relatively) hydrophilic sites are probably more spatially spread out such that adsorbed molecules on these sites are less condensed than in the liquid state implying some degree of mobility of the

adsorbed layer. Integral heat of adsorption curves for the methanol-coal system obtained from the heat of immersion data of coal and coal with various degrees of precoverage of methanol in methanol are presented. A double differentiation of this curve provides a *quantitative measure of the heterogeneity* of the coal surface in terms of the site distribution function.

Laser Microprobe Mass Analyzer (LAMMA), a state of the art surface analytical technique, was used to study the spatial variation in the moieties on the coal surface. A line scan was conducted at 4 micron intervals over a 40 micron span. Inorganic species like sodium, aluminum, potasium etc. were noticed and are consistent with the SEM/EDX results. Most importantly, inorganic inhomogeneity could be observed at micron levels. Micron level spatial fragmentation pattern obtained from LAMMA indicates that the distribution of organic moieties is probably random. The study also reveals that the average structural unit or "molecule" in coal, if present, is urger than 4 microns and that this average unit is probably randomly oriented on the surface leading to exposure of different functional groups.

DRIFT spectroscopic studies of float and sink fractions with a critical wetting surface tension (γ_c) from 72 to 44 and from 44 to 32 respectively, revealed that this technique is insensitive to the distribution of functional groups responsible for the observed critical wetting surface tension values. Apriori the DRIFT technique was also unable to predict the relative flotability of Upper Freeport or Pittsburgh No.8 coal samples. It appears that the distribution of sites is more important in governing the wetting behavior than the absolute amount of the sites with various surface energies. DRIFT studies also support the view that γ_c distribution of a sample of group of coal particles obtained from film flotation is essentially the distribution on every single coal particle in the sample.

Derivatized ESCA is a new technique in which specific polar functional groups are molecularly tagged and subsequently analyzed quantitatively by ESCA. This

technique was adopted for determining the absolute amount of phenolic, carboxylic and carbonyl groups on the coal surface for the first time. The three functional groups are present in approximately equal quantities ranging from 1 to 2 functional groups per 100 atoms. Nitrogen in aromatic and aliphatic moieties was detected in quantities equal to the amount of polar groups. Derivatized ESCA is found to be a powerful tool for studying quantitatively the role of polar and nonpolar groups in determining the wettability and flotability of coal.

Contact angle distributions based on γ_c distributions and Nuemann's equation of state were calculated and are presented. Implications of contact angle distributions on the surface behavior of heterogeneous substances are discussed. Models which relate equilibrium contact angles to spatial distributions of moieties were analyzed based on these contact angle distributions. The analysis reveals that the difference between equilibrium contact angles of surfaces with macroscopic heterogeneity and those with molecular heterogeneity is of the order of 0.5 degrees.

The results of this study has direct practical implications to the performance of advanced physical coal beneficiation processes such as flotation, flocculation and agglomeration. Our approach for determining *distributions* of surface parameters such as contact angle, wettability and surface energy and surface site types shows potential for arriving at a method for proper characterization of heterogeneous surfaces like coal and thereby for understanding surface interactions more accurately. The multipronged approach used here has yielded new information on the chemical and physical heterogeneities of coal particles and the role of these heterogeneities including the scale of these heterogeneity in wetting.

1 STATEMENT OF OBJECTIVES

This project is designed to develop an understanding of the fundamentals involved in flotation and flocculation of coals, and of coals in various states of oxidation. The main objective of this study is to accurately characterize the coal surface and elucidate mechanisms by which surface interactions between coal and various reagents can enhance beneficiation of coals. It was also an objective to study the effects of oxidation on the modification of surface characteristics of coal by various reagents.

2 INTRODUCTION

2.1 PREAMBLE

Coal is by far the world's largest and most uniformly distributed fossil fuel resource. Coal in the United States accounts for about eighty two percent of the nation's recoverable energy reserves [1]. The energy information administration reports that the U.S. has 478.2 billion tons of demonstrated reserves, and that these reserves are sufficient to meet the demand for coal for 300 years at current consumption levels [2].

About 50% of all coal mined in 1983 was cleaned in order to produce a product acceptable to the market [3]. The number of preparation plants treating bituminous and lignitic coal has increased from 382 in 1973 to 501 in 1983 [4]. The amount of refuse being produced at the preparation plant has also increased by around 27 million short tons during the period 1973-1983 reflecting the trend that it is often cheaper to remove waste during preparation than during mining [5]. It is evident that preparation of coal is an important operation for its efficient use. The specifications required for different end uses of coal are becoming complex, in view of increasing economic, political, and environmental pressures. Characteristics

such as ash content, volatile matter, particle size, and sulfur content are important factors that govern the ultimate use of coals and are determined essentially by the methods used for gangue liberation and its removal by appropriate processing techniques. Studies are presently being conducted by utility companies on the effect of coal preparation on the power plant fuel cycle cost [6]. This reflects on the desire by the utilities to purchase quality coal at affordable prices rather than the cheapest coal available in the market. The trend towards purchasing coal on spot markets as opposed to the traditional long term contracts is also an indication of the quality consciousness of power plants. Careful process design and optimization of beneficiation techniques hold the key to meet the various market requirements.

With the drive towards reducing the overall mining cost, the modern mechanization and non-selective mining techniques used have led to increased production of fines. The fines content in ROM coal can vary between 10 and 35 percent by weight [7]. These fines form a significant portion of the beneficiation plant feed and their recovery is imperative for the preparation plant to break even. The recovery of coal fines was valued at $2.3 billion per year in 1983 [8]. The increasingly stringent specifications with regard to ash and sulfur content have necessitated the coal being crushed to very fine sizes to better liberate gangue minerals. Due to the large surface area of these fines, beneficiation processes for these particles are based on surface forces rather than bulk forces. Efficient coal cleaning requires separation of undesirable ash forming constituents and inorganic sulfur forms from the very fine coal particles, and hence techniques for the preparation of a clean coal product of required quality are those processes that exploit the differences in surface properties of carbonaceous material and mineral matter. Froth flotation, selective flocculation and agglomeration have been receiving much attention in recent years. Probably in excess of 200 preparation plants are currently using the froth flotation

process, though the aggregate tonnage treated is reported to be relatively small[1] [9]. However, in order to reduce sulfur dioxide emissions responsible for acid rain and in view of other new coal technologies like fluidized bed combustion, coal-oil and coal-water mixtures as fuels and microbially enhanced coal cleaning, all of which use fine coal, it is expected that tonnage of coal beneficiated by flotation and other surface based process will increase in the future. These beneficiation techniques, when applied to coal, are inefficient and the least understood. This results partly from the complex physical and chemical nature of the coal surface and partly from the variation in its properties from mine to mine, seam to seam and even within the same seam. Added to this, coal being a highly reactive substance oxidizes on exposure to ambient atmosphere over time resulting in its degradation. Oxidation of coal results in the coal surface undergoing drastic changes influencing subsequent processes.

Coal is a very complex and heterogeneous substance. The absence of any well defined coal "molecule" precludes the use of stoichiometric chemical equations. The highly reactive nature of the coal surface makes it difficult to adopt traditional analytical techniques used in organic chemistry. The porous nature of coal including the presence of a wide distribution in pore size implies that the area involved in a surface reaction would depend on the adsorbate molecule. In the case of spectroscopic techniques the black color of coal is responsible for the absence of any sharp well defined peaks in various spectra. Most importantly, the heterogeneous nature of coal is responsible for the absence of any generalized theory or approach to coal surface science. In fact, lack of complete understanding of the role of heterogeneity itself, has largely been responsible for the poor characterization studies often conducted in the past. This important issue is the subject of this project. An accurate characterization of coal surfaces will aid in the development of advanced

[1] Froth flotation accounts for 4.8% of the 425 million ST of raw coal to preparation plants during 1983 ([9].

beneficiation technologies.

2.2 RESEARCH STRATEGY

In order to meet the proposed objectives, it is essential that an accurate understanding of the coal surface structure be developed. Often in the past, the heterogeneity of the coal surface, the most important, intrinsic and fundamental aspect in coal surface studies, has been neglected. In fact, a good knowledge of the nature of the heterogeneity present on the surface of coal particles is lacking and published literature in this area is scarce. It is clear that research on coal surface interactions and surface modifications requires a proper understanding of the fundamental nature of the heterogeneity of the coal surface. This in turn requires a knowledge of the distribution (chemical and energetic) of various surface sites and their role in surface interactions. Understanding the nature of the heterogeneity of coal surfaces arising from the *distributions* of chemical moieties is fundamental to the elucidation of mechanisms by which reagents adsorb on different coals. It should be pointed out that only *minor* changes in surface properties are adequate to affect surface based phenomena. In the case of heterogeneous materials like coal, knowledge of average properties would not provide sufficient information to control interfacial properties.

Characterization studies, which take into account the heterogeneity of the coal surface is considered central to this project. The role of heterogeneity in adsorption and wetting is considered be of fundamental importance in surface based beneficiation processes like flotation and oil agglomeration. The research approach adopted in this project is to develop and use techniques capable of providing information on the role of the heterogeneity in wetting and adsorption of reagents on the coal surface. As a prelude to the results and discussion, relevent literature and fundamental principles pertaining to this study are discussed in the next section.

3 REVIEW/BACKGROUND

3.1 CONTACT ANGLE

Contact angle directly governs a number of important processes, such as wetting, penetration of porous solids by liquids, adhesion, flotation etc. The study of contact angle measurements are of two kinds:

a) Contact angle measurements can be used to study the interfacial properties of a solid-liquid-gas system from a macroscopic point of view.

b) Contact angles may be used to characterize the solid surface itself.

The equation of Thomas Young treated contact angle (θ) of a liquid as being the result of the equilibrium of a static drop resting on a plane solid surface and acted upon by three surface tensions in equilibrium, as shown by three coplanar vectors in Figure 1. γ_{lv} is the surface tension along the liquid/vapor interface, γ_{sl} is the surface tension along the solid/liquid interface, and γ_{sv} is the surface tension along the solid/vapor interface.

Young derived for the equilibrium of these surface tensions acting at any *point* of such a surface the following relation:

$$\gamma_{sv} - \gamma_{sl} = \gamma_{lv} \cos\theta$$

Young's equation is simple in form only, because both conceptual and experimental difficulties exist concerning it which have been the source of many discussions [10]. Implicit in the derivation of the Young's equation is the assumption that the measurable contact angle θ is independent of the volume of the drop. However, for best reproducibility of results, the same size of drops should be employed. Not only is the accurate measurement of the actual contact angle at the three phase line of contact difficult but also the theoretical treatment of the contact angles in the near

Figure 1: Contact angle of a sessile drop

vicinity of the three phase line of contact of an actual system in three dimensions is highly mathematical and complicated [11] and this is more so in the case of a heterogeneous system. Analyses of contact angles on rough surfaces, and idealized rough surfaces have been made by others also [11,12].

Young's equation describes the interplay of forces at the three phase boundary line. Since, force is the derivative of energy with respect to displacement, and a derivative can be evaluated only at a point, it is not the energies of the three phase interface that determine the contact angle but the derivatives of the energies with respect to the displacement of the line boundary. The major conceptual difficulty associated with the Young's equation is the fact that it is valid only at a point on the solid whereas the measured θ is assumed to be related to the entire system. This difficulty becomes evident in the case of heterogeneous solids. If the surface is grossly heterogeneous, there will be a driving force for local contact angles to be the local equlibrium ones, different on various portions of the surface. As a result, varying local curvatures would be introduced in the liquid surface and there would be a tendency for the liquid to extend over low contact angle regions and retreat from high contact angle regions. This indicates that contact angles measured at various places along a 360 degree arc centered about the drop would yield different values. Indeed for liquids of ordinary viscosity, in the case of homogeneous surfaces, the requirement of uniform hydrostatic pressure will be overriding and the various local contact angles may represent some compromise demanded by this condition. A second possibility is that the locally varying angles may be on such a small a scale as to average out to a single observable one. In a formal way ;

$$\theta_{av} = \sum_{\theta_{min}}^{\theta_{max}} f(\theta)\theta$$

where f(θ) is an appropriately defined distribution function.

Brady and Gauger [13] measured contact angle on polished coal specimens and

concluded that high rank bituminous coals give greater contact angle values than anthracites, which in turn give greater contact angles than lignites. This finding has since been verified by other researchers [14,15]. Brown [15] plotted contact angle as a function of carbon content of coal on a dry mineral matter free basis and showed a pronounced maximum at about 89% carbon. The reasons for this maximum are not known. Based on a hypothesis by Sun [16], however, a semi quantitative explanation has been proposed by Rosenbaum [17]. Horsely and Smith [14] showed that using the captive bubble technique, the contact angle on coal could be correlated with carbon content on a dry ash free basis. Their data indicate that coals of high carbon content would be hydrophobic, but below 80% carbon (DAF), corresponding roughly to coals of high volatile B (HVB) bituminous rank and below, are not very hydrophobic (that is $\theta \approx 0$). Aplan [18] cautioned that although this procedure may be reasonably accurate, it is an approximation, since, only one of the four ASTM criteria (%C, %VM, BTU, agglomeration characteristics) is used. Other data by Parekh and Aplan [19] indicate that if the sessile drop is used instead of the captive bubble method, a smooth transition in the value of contact angle of water on coal, ranging from 50° for lignite to 75° for LV bituminous occurs. These data indicate that coal is a much more hydrophobic solid than would be assumed from the captive bubble data.

Gayle and Smelly [20] investigated the effect of temperature on the contact angle of coals and found that contact angles vary in a marked and complex manner between 1 and 60 degrees. Other researchers [19,21] have also discussed the direct correlation between contact angle and oxidation at varying temperatures. Neumann and Good [22] gave a detailed summary of the techniques used for contact angle measurements and noted that the choice of the method depends on the gross geometry of the system. For example, the most convenient method for a flat plate is not suitable for the inner surface of a capillary tube, and fine textile fibers and

powders raise specific problems of measurement that are not present in other systems. Several values have been reported for the contact angle on coal such as 0° for lignite, 48° for anthracite, and 60° for high volatile bituminous coal [15]. No two measurements even for the same coal appear to be the same, especially if these measurements were taken on two different spots on the coal surface. Several reasons like surface roughness, chemical heterogeneity, have been given to explain this behavior [14].

Laskowski [23] has discussed the vital aspect of sample preparation for contact angle measurements. Both the reproducibility and the reliability of the results are dependent on how well the samples are prepared prior to the measurement. Moreover, because of the heterogeneous and easily oxidizable nature of the coal, sample preparation for coal contact angle measurements becomes even more important. Lastly, it should be noted that contact angle measurements do require special sample preparation and polishing, and therefore do not reflect the nature of particle surfaces encountered under operating conditions.

3.2 WETTING

Wetting is the most important phenomenon that controls a variety of surface based processes such as flotation, flocculation and agglomeration. Wetting, in the most general sense is the displacement of one fluid from a surface by another. This definition implies that wetting must always involve three phases of which at least two must be fluid. Wetting phenomena are generally classified as adhesional wetting, spreading wetting and immersional wetting. In adhesional wetting, a second fluid not originally in contact with the substance makes contact and sticks to it; in spreading wetting the liquid already in contact with a substance spreads and displaces the second fluid; and in immersional wetting the material is transferred from a gas phase into a liquid phase.

All wetting processes can be described in terms of the respective surface free energy changes involved. Equations describing the free energy changes for adhesional wetting (ΔG_a), spreading (ΔG_s) and immersional wetting (ΔG_i) in systems involving a solid, a liquid and a gas phase are the following:

$$\begin{aligned} \Delta G_a &= \gamma_{sl} - \gamma_{sg} - \gamma_{lg} \\ \Delta G_s &= \gamma_{sl} + \gamma_{lg} - \gamma_{sg} \\ \Delta G_i &= \gamma_{sl} - \gamma_{sg} \end{aligned}$$

where γ_{lg}, γ_{sl} and γ_{sg} are the surface tensions at the liquid-gas, solid-liquid and solid-gas interfaces respectively. Incorporating the Young's equation in above expressions, we can write:

$$\begin{aligned} \Delta G_a &= -\gamma_{lg}(\cos\theta + 1) \\ \Delta G_s &= \gamma_{lg}(1 - \cos\theta) \\ \Delta G_i &= -\gamma_{lg}\cos\theta \end{aligned}$$

Thus the wetting process can be described in terms of two measurable quantities: the surface tension of the liquid and the equilibrium contact angle.

There are two types of spreading of liquids on insoluble solids which resemble, respectively duplex and nonduplex spreading in liquid-liquid systems. Spreading and wetting usually occur when solids have a large surface free energy with respect to the liquid. Spreading of a liquid into a stable multimolecular film on the solid is often observed, and is analogous to the spreading of a liquid into a multimolecular film on another liquid. Such a film on another liquid is not stable, however, and thus reverts to a monolayer. The latter is called duplex spreading. Nonduplex spreading

of a liquid on another liquid has its counterpart in liquid-solid systems, in which an adsorbed, oriented, or close-packed monolayer is formed upon which the liquid cannot spread. These liquids, which cannot spread over their own monolayers, are referred to as autophobic. The distinction between nonspreading systems and solid/liquid autophobic systems can be subtle, since drops with finite contact angles are found in both cases.

3.2.1 Presentation of wetting behavior

Wetting behavior is frequently assessed by measuring the contact angle as discussed above. Because of the difficulty in evaluating contact angles on particulate materials, various techniques involving wetting of particles by solutions of different surface tensions have been used to measure wettability. One such technique involves the rate at which a powder transfers from a gaseous phase into a liquid phase. In an investigation of the action of surface active agents in coal dust abatement, Walker et al. [24] studied wettability by determining the surface tension of the solution into which individual particles would be imbibed immediately when dropped from a height of one centimeter. Another variation of their experiment involved dropping 100 μm particles onto the surface of solutions of wetting agents, and taking the time for the particles to disappear from the liquid surface as the time of wetting.

3.2.2 Critical wetting surface tension

Zisman with his co-workers devoted his whole career [25,26,27,28] measuring the spreading and wetting of liquids, such as homologous series of alkenes and surfactants, mostly on polymeric substances. This effort has provided the concept of critical wetting surface tension γ_c. From Young's equation, $\cos\theta = (\gamma_{sv} - \gamma_{sl})/\gamma_{lv}$; if the solid has a finite angle in a liquid phase, then $\gamma_{lv} > \gamma_{sv} - \gamma_{sl}$. By reducing

γ_{lv}, it is possible to bring the contact angle to zero. Accordingly, if one determines contact angles on solids and plots $\cos\theta$ versus γ_{lv}, a straight line is usually obtained which can be extrapolated to $\cos\theta = 1$ i.e. $\theta = 0$, on the Y-axis. Zisman defined the γ_c of a material as the surface tension of the liquid, γ_{lv}, at which θ just becomes zero. By deductive analysis and considerations regarding the orientation of solid surface groups, the classical diagram given in Figure 2 [29] has been generated with other relevant information. The standard polymer handbook [30] carries γ_c values for entire range of polymers.

Lucassen-Reynders [31] and Bergeman et al. [32] have derived correlations on the effects of surfactants on contact angles, and presented their data in the form of $\gamma_{lv}\cos\theta$ versus γ_{lv} plots, where the former expression corresponds to the well known adhesion tension. Kelebek and co-workers [33,34] have used these diagrams for discussing the wetting behavior of hydrophobic solids. The Lucassen-Reynders plots produce lines like (a) and (b) as shown in top of Figure 3. If θ is kept constant and γ_{lv} is varied, lines (c) and (d) result. Hornsby and Leja [35] have observed from such plots that, if two particles have different γ_c, they should be separable (by means of float-sink test) under the following conditions; $\gamma_{c1} < \gamma_{lv} < \gamma_{c2}$ where γ_{c1} and γ_{c2} are critical wetting surface tension of particle 1 and particle 2. Under such conditions particle 1 would be wetted by solution of γ_{lv} and should sink while particle 2 should float. These authors used teflon-coal mixtures to demonstrate their point in test tubes. Similar results were previously reported by Finch and Smith [36] using magnetite and silica, made hydrophobic by treatment with surfactants prior to mixing of powders. These observations have resulted in an approach to flotation called "Gamma Flotation" using liquid surface tension control. A schematic plot of Gamma flotation where flotation recovery versus γ_{lv} is plotted is shown in the lower part of Figure 3. The validity of these observations has been demonstrated with sulfide minerals, silica, and oil shale by others [37,38].

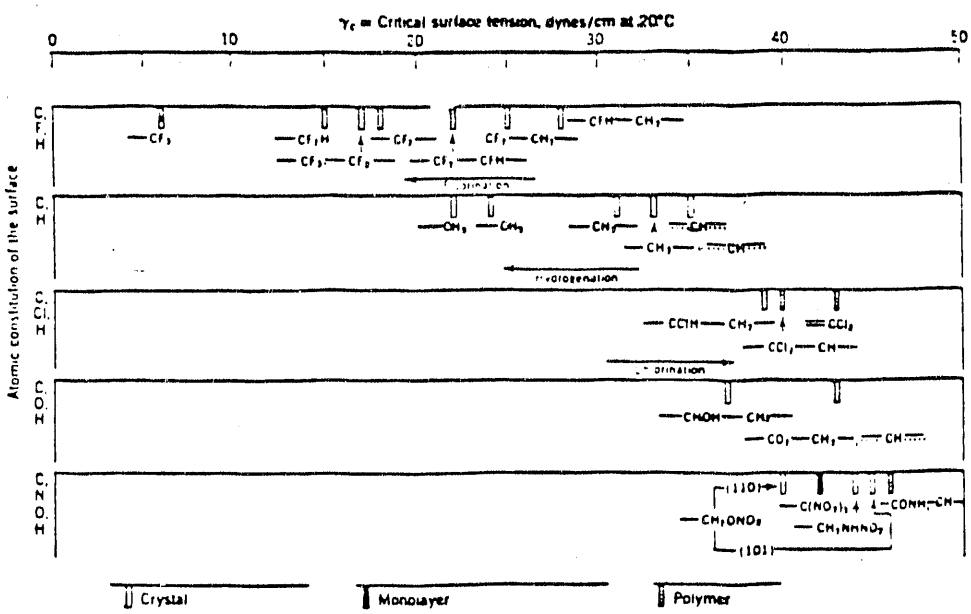

Figure 2: The wettability "spectrum" for selected low energy surfaces (from Shaffrin, E.G. and Zisman, W.A., in J. Phy. Chem., vol 64, (1960), pp 519-524)

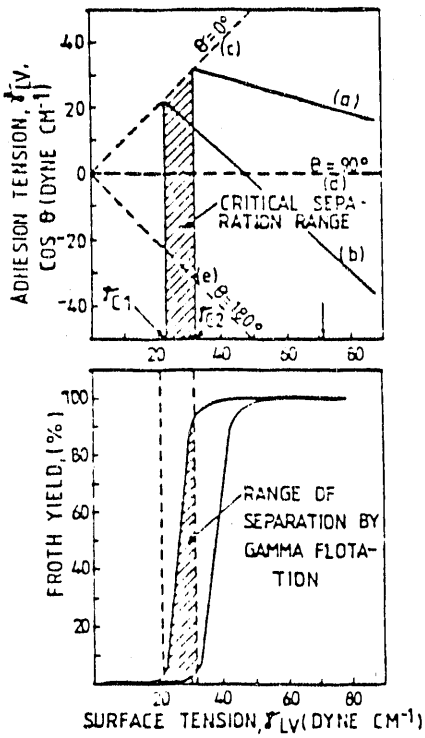

Figure 3: Schematic illustration of Lucassen-Reynders plot and Gamma flotation.

Yarar et al. [39] evaluated γ_c of minerals by extrapolating the "percent recovery versus surface tension" curve to zero recovery. Considering the linear part of the curve they derived the following relation

$$R_\gamma = \frac{dR}{d\gamma}(\gamma_{lv} - \gamma_c)$$

where R_γ is percent recovery at any given value of solution surface tension γ_{lv}.

The Zisman relationship is described by

$$\cos\theta = 1 - b(\gamma_{lv} - \gamma_c)$$

where b is the slope of the line in a $\cos\theta$ vs. γ_{lv} plot. Both γ_c and b (i.e the slope) values have been used to characterize the relative hydrophobicities of solids. For example, Shafrin and Zisman [29] used γ_c as a criterion to classify highly nonpolar polymers with respect to their atomic constitution, and others [19] have related b (i.e the slope) to the coal rank. Parekh and Aplan using pure liquids and the Zisman's approach found γ_c of coals ranging from anthracite to lignite to be nearly constant at about 45 mN/m. Yang [40] also observed that γ_c of a number of coals in alcohol-water mixtures to be constant but at about 23 mN/m. These results essentially indicated that γ_c was independent of the coal rank but the slope of the line (b) is strongly dependent on the rank. This is difficult to understand because it has been shown that different coals exhibit different degrees of hydrophobicities, more specifically different contact angles [14,15]. It is possible as pointed out by Good [41], that the lower values in the case of alcohol-water mixtures are due to preferential adsorption of one of the component of the binary solution used. This adsorption is also possibly the reason for the constancy of the γ_c obtained using aqueous solutions. Parekh and Aplan [19] postulated that the reason for the constancy of γ_c when measured using pure liquids may be related to the inherent surface moisture of coal.

It should be remembered that γ_c discussed above is an empirical parameter obtained from contact angle measurements. In general we would expect the γ_c to depend on the solid and the liquid series. However, when dealing with simple molecular liquids (where van der Waals forces are dominant), Zisman observed that γ_c is essentially independent of the nature of the liquid, and is a characteristic of the solid alone. In view of this, various authors have attempted to relate γ_c to physical parameters of the solid surface [11,41].

Young's equation gives $\cos\theta$ as a function of interfacial energies. The special case where $\gamma_{lv} = \gamma_{sv} - \gamma_{sl}$ and $\cos\theta = 1$ or $\theta = 0$ (complete wetting) leads to the concept of γ_c. In thermodynamic equilibrium $\gamma_{sl}+\gamma_{lv}$ can never be larger than γ_{sv}. If it were larger, this would imply that the free energy of a solid/vapor interface (γ_{sv}) could be lowered by intercalating a liquid film of energy ($\gamma_{sl}+\gamma_{lv}$). The equilibrium solid/vapor interface then automatically comprises such a film. Bangham et al [42] put forward the concept of equilibrium film pressure π_e

$$\pi_e = \gamma_s - \gamma_{sv} \tag{1}$$

where γ_s is the surface free energy of the solid in vacuum and is equal to one half the free energy of cohesion with respect to the specified surface dividing the bulk; γ_{sv} is the surface free energy when the solid is in equilibrium with the saturated vapor of the wetting liquid. The spreading coefficient S defined as $S = \gamma_s - \gamma_{sl} - \gamma_{lv}$ is related to π_e. It should be noted that π_e in some systems (water on metallic oxides) may be as large as 300 ergs/cm^2 [43] and this will affect the spreading coefficient if γ_{sv} is taken instead of γ_s.

Most molecular liquids achieve complete wetting with high energy surfaces. On the assumption that covalent bonding controls γ_s and van der Waals interactions control γ_{sl} we can write

$$\gamma_{sl} = \gamma_s + \gamma_{lv} - V_{sl} \tag{2}$$

$-V_{sl}$ describes the attractive van der Waals interactions between solid and liquid near the surface. The above equation shows that when liquid and solid regions are well separated the energy is $\gamma_s + \gamma_{lv}$; when contact is established the energy V_{sl} is recovered. Similarly, when two liquid portions are contacted, the original interfacial energy of $2\gamma_{lv}$ is reduced to zero. Therefore:

$$0 = 2\gamma_{lv} - V_{ll}, \tag{3}$$

where $-V_{ll}$ represents the liquid-liquid attractions. Using equations (2) and (3) the spreading coefficient S can be written as

$$S = -2\gamma_{lv} + V_{sl} = V_{sl} - V_{ll} \tag{4}$$

and the condition for complete wetting corresponds to

$$V_{sl} > V_{ll} \tag{5}$$

To a first approximation the van der Waals couplings between two species (i) and (j) are simply proportional to the product of the corresponding polarizabilities (α), therefore

$$V_{ij} = k\alpha_i\alpha_j \tag{6}$$

where k is roughly independent of (i) and (j). The condition for complete wetting corresponds to

$$\alpha_s > \alpha_l \tag{7}$$

Based on equations (2) to (7) and assuming polarizability of vapor to be negligible, Young's equation can be written as

$$\begin{aligned} \cos\theta &= \frac{\gamma_{sv} - \gamma_{sl}}{\gamma_{lv}} \\ &\approx \frac{\gamma_s - \gamma_{sl}}{\gamma_{lv}} \\ &\approx \frac{V_{sl} - \gamma_{lv}}{\gamma_{lv}} \\ &= \frac{2\alpha_s}{\alpha_l} - 1 \end{aligned} \tag{8}$$

When one constructs a Zisman's plot it is α_l that is varied. α_{lc}, the value of α_l at which $\cos\theta$ extrapolates to 1 is

$$\alpha_{lc} = \alpha_s \tag{9}$$

In terms of surface tensions $\gamma_{lv} = \frac{1}{2}V_{ll} = \frac{1}{2}k\alpha_l^2$. When θ just equals zero γ_{lv} equals γ_c; and equation (8) can be written as

$$\cos\theta = 2\left\{\frac{\gamma_c}{\gamma_{lv}}\right\}^{1/2} - 1 \tag{10}$$

$$\gamma_c = \frac{1}{2}k\alpha_s^2 \tag{11}$$

Numerically the above equation is a simplification. Good [41] has conducted a more rigorous discussion on the relation between γ_c andγ_s.

Even though the theoretical treatment of γ_c and its physical significance is still under development, and a direct relation between γ_c measured by the Zisman's

plot using mixed liquids and the surface energy has not yet been established [2], the concept of γ_c has been useful from a practical point of view as evidenced by works of Zisman and the Gamma flotation process. From a surface chemistry point of view, Zisman has demonstrated that surface functional groups can be characterized on the basis of γ_c. Parekh and Aplan have correlated surfactant adsorption mechanisms with γ_c. Fuerstenau et al [44] have used γ_c as a means to characterize coal surfaces by film flotation which is discussed below. It should be pointed out that γ_c obtained by contact angle measurements has the disadvantages associated with sample preparation which is ever more serious in the case of coal surface studies. Use of alcohol water mixtures gives low values due to adsorption of alcohol since contact angle measurements require that the liquid be in contact with the solid for a sufficient length of time to make multiple measurements. Also in certain instances it is the slope of the straight line drawn in a Zisman's plot that might be more meaningful. Finally it should be noted that γ_c obtained by contact angle measurements is only an average[3] value of the surface.

3.2.3 Film flotation

Film flotation is a technique based on the Walker's test for studying wettability of powders and which was further developed at the University of California, Berkely under a DOE project. The details of the technique and its efficacy is provided in the final report submitted to DOE (Grant No. DE-FG22-84PC70776). The researchers at California established the efficacy of this technique and used this technique mainly to characterize the surface of coal obtained from *various sources*. This technique was used here to study the surface of coal and modified coal surfaces from a *single source* (Bruceton mines, seam pgh) and extend the understanding of

[2] An indirect relationship does exist [41]

[3] The deviation from the actual statistical average is dependent on the spatial distribution of the measurements and the total number of measurements made

significance of film flotation bahavior from a more fundamental point of view.

Relevant sections from the above report are presented below.The concept of film flotation is based on wetting phenomena that occur when a particle is transferred from the vapor phase into a liquid phase as illustrated in Figure 4. This process can be divided into three steps. The first step when the particle is dropped onto the surface is adhesional wetting. As the particle begins to submerge, the process is immersional wetting. The final step as the particle is imbibed into the liquid as the film spreads over the solid surface is spreading wetting. For adhesional wetting the free energy change is given by

$$\Delta G_a = -\gamma_{lg}(\cos\theta + 1) \tag{12}$$

Equation (12) shows that adhesional wetting is spontaneous ($\Delta G_a < 0$) when the contact angle is less than 180 degrees. For the immersional wetting step, the change in free energy is

$$\Delta G_i = -\gamma_{lg}\cos\theta \tag{13}$$

which shows that immersion is spontaneous when the contact angle is less than 90 degrees. In the final step, namely spreading wetting, the change in free energy

$$\Delta G_s = \gamma_{lg}(1 - \cos\theta) \tag{14}$$

in which case spreading wetting is spontaneous when θ is equal to zero[4]. In the limit the film flotation process is ideally controlled by particles whose contact angle is just zero.

[4]In actual cases, due to gravitational effects the contact angle must be slightly greater than zero when the particles just sank.

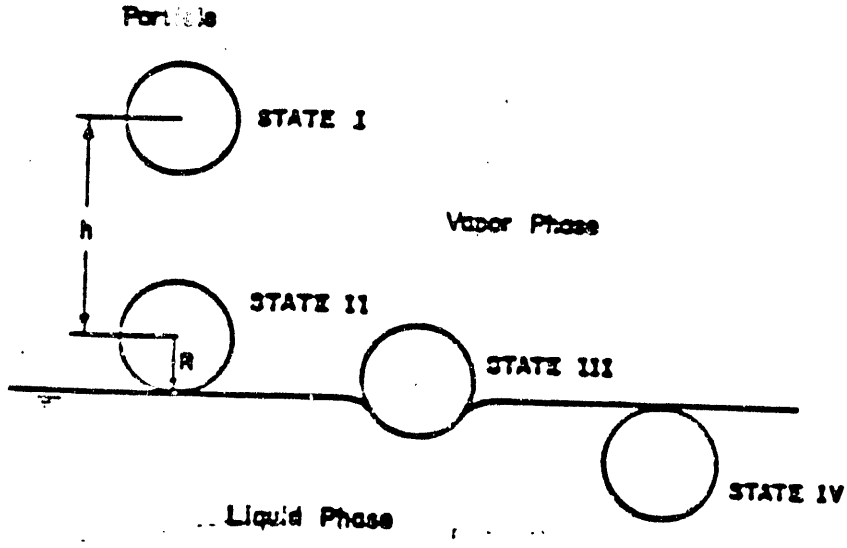

Figure 4: Schematic representation of film flotation process

In a typical film flotation experiment closely sized particles are sprinkled onto the surface of a liquid or aqueous solutions having different surface tensions. Normally sufficient material is sprinkled onto the liquid so that a layer of particles remains on the liquid surface. Depending on the surface characteristics of the material and the surface tension of the liquid the particles either remain at the liquid/vapor interface or are immediately imbibed into the liquid. After performing the film flotation the float and sink fractions are recovered by decantation, dried and weighed. The weight percent of the particles reporting as float for each solution is then determined and the results together with the surface tension of the solution are then used to construct the cumulative partition curve for the sample. A typical partition curve obtained during the present study is shown in Figure 5.

There exists a surface tension of the solution below which none of the particles will remain at the liquid surface, that is the surface tension below which all particles are wetted by the solution - γ_c of the most lyophobic[5] particles. Similarly the γ_c of the most lyophillic particles in the powder is the surface tension of the liquid at which all the particles are lyophobic, that is the surface tension above which none of the particles are wetted by the solution. Whereas conventional methods of γ_c estimation provide only one value irrespective of the heterogeneity of the sample, film flotation results can be used to obtain a distribution of γ_c values. A frequency distribution diagram can be generated from the partition curves as shown in Figure 6, implying the existance of a surface parameter distribution for coal particles.

Since the act of imbibation is instantaneous in the film flotation process the possibility of molecules adsorbing from the solution to change the surface characteristics is negligible. This indicates that γ_c obtained by film flotation does not have the experimental disadvantages associated with measurement of contact angles

[5]At a particular surface tension of the wetting liquid those particles that are wetted completely (sink) are lyophillic, and those that are not wetted (float) are lyophobic.

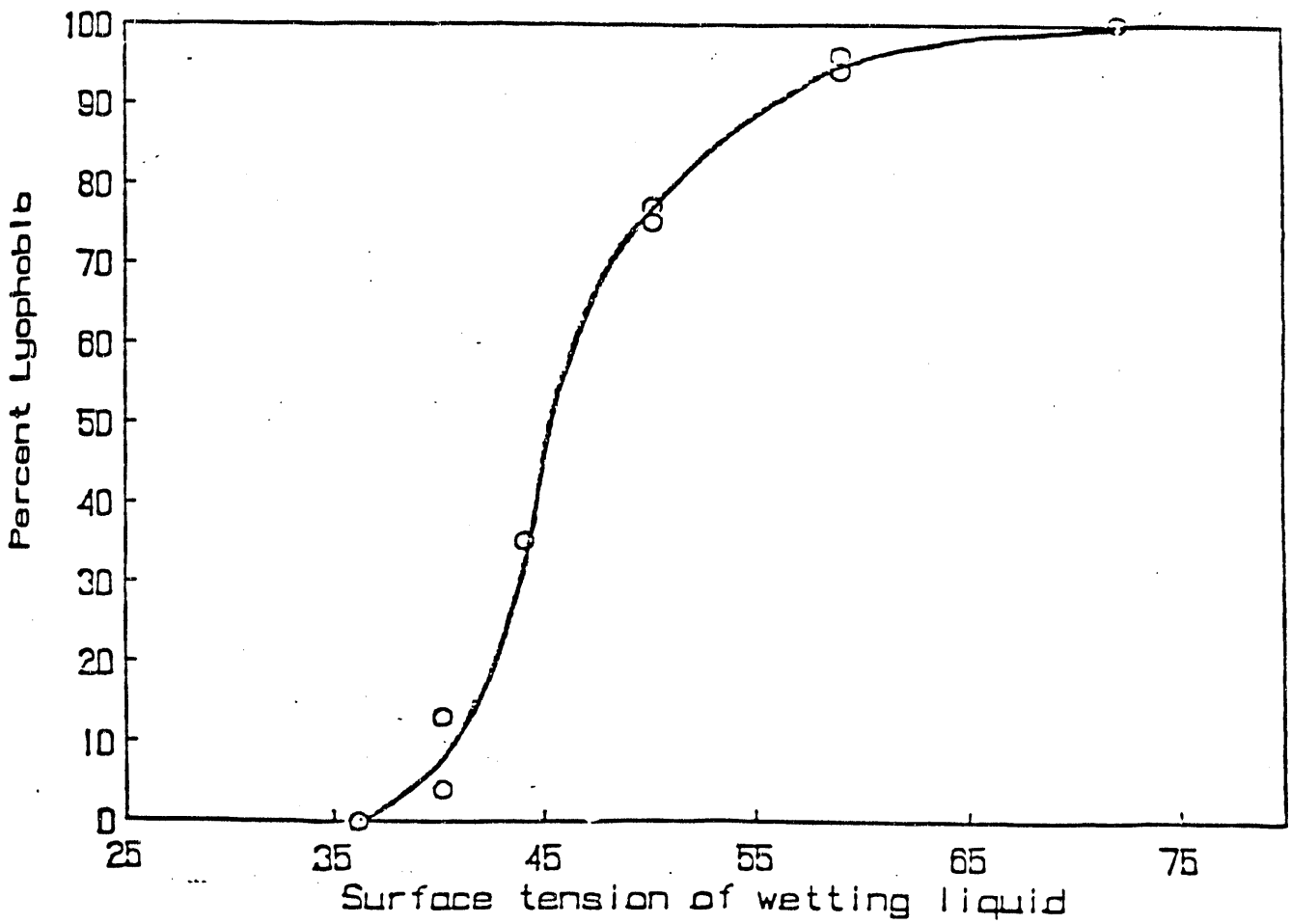

Figure 5: Typical cumulative partition curve of a coal sample.

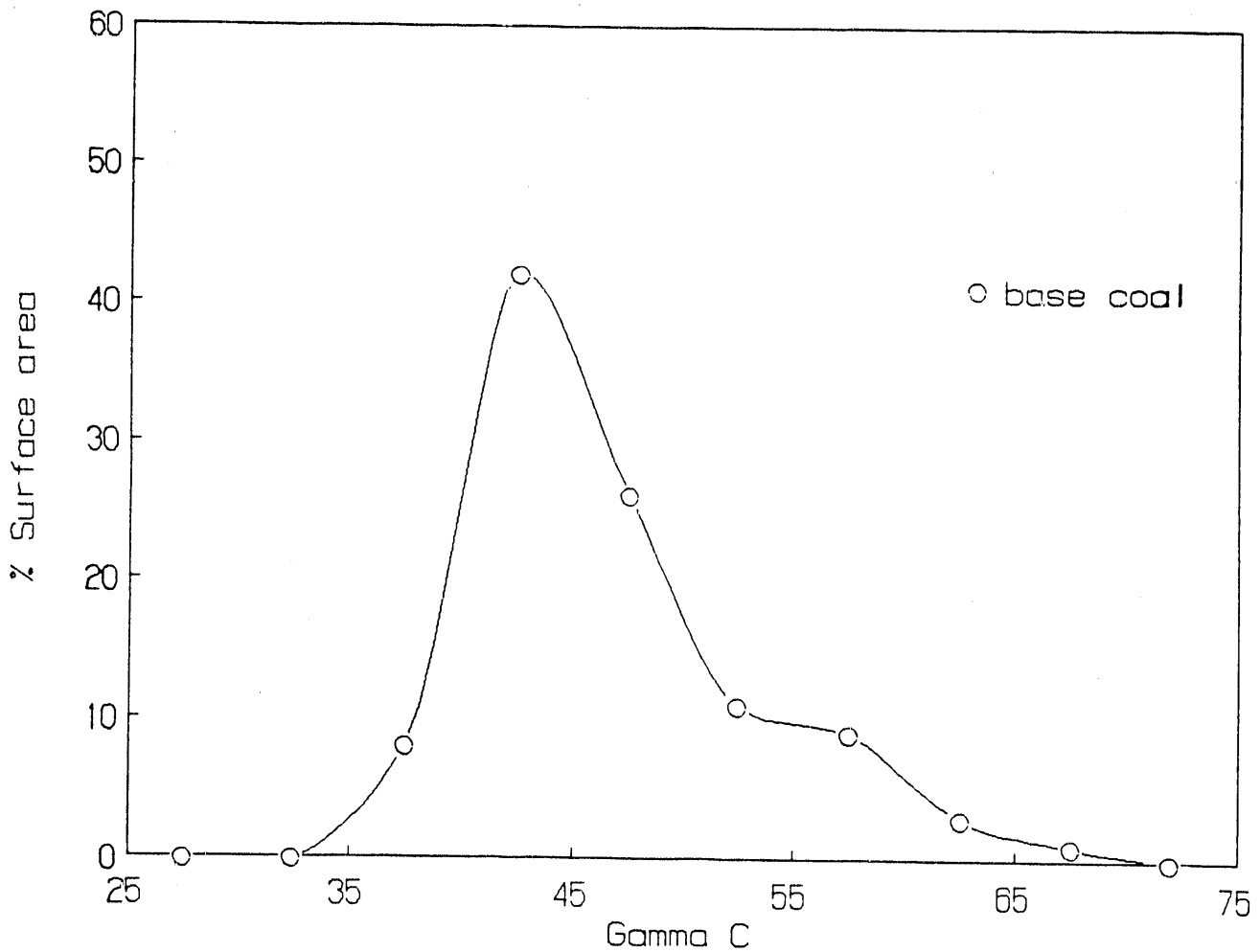

Figure 6: Typical frequency distribution diagram of critical wetting surface tension of coal particles: from reference [44].

using alcohol water mixtures.

It is also evident that since this process is based on the change in interfacial energy of the particle the weight percent lyophobic plotted on the Y-axis is actually proportional to the total surface area of the particles.

3.3 HEAT OF WETTING

Heat of wetting or heat of immersion (ΔH_{imm}) is a small exothermic quantity that is released when a clean solid is immersed in a pure liquid, and it can be used to characterize a solid in terms of hydrophobicity and hydrophilicity and to estimate the relative wetting tendency. Calorimetry, a fundamental analytical method is the widely used technique to study heat of immersion.

Chessick and Zettlemoyer [45] presented a detailed explanation of the thermodynamics involved in the heat of immersion. They measured the heat of immersion of various solids like teflon, Graphon, rutile, and clay, in various liquids (water, organics, surfactants etc.) to determine a number of properties like wettability, surface polarity and site energy distribution. They measured the heat of immersion of butylamine on attapulgite clay to determine the acid strength of exchange sites. The heat of immersion was measured as a function of surface concentration.

Marsh [46] presented a review on the surface area of coal determined by heat of immersion, neon adsorption and carbon dioxide adsorption methods. He concluded that the surface area of coals was around 200 to 300 m^2/gm.

Various researchers [47,48,49] working with Pittsburg and Illinois coals found that the heat of immersion for Pittsburgh coal increased linearly with increasing outgassing temperature; however, in the case of Illinois coal, there was a decrease in the heat of immersion with increasing outgassing temperature. Fuller [50] showed that the heat of immersion increases as the rank of coal decreases. The heat of

immersion was also reported to be higher for mineral rich fractions due to the greater polarity of the minerals and/or to the more open structure. Yang [40] reported that heat of displacement of methanol by water is a function of oxidation and rank. Oxidized coal evolves less heat due to the increase in the polar sites and preferential adsorption of water over methanol on coal. Nordon and Bainbridge [51] measured the heat of wetting of an Australian low rank bituminous coal with different initial moisture content and found that as moisture content increased the heat of wetting decreased. This study was related to the spontaneous combustion of low rank bituminous coal and it was concluded that under natural conditions heat of wetting could cause a temperature rise of only 2°C and is unlikely to contribute to spontaneous ignition.

Glanville and Wightman [52] have shown that the heats of immersion of powdered coal in water methanol mixtures vary with changing concentration. A maximum value of 16 J/gm at 30 mole % methanol was attained. The heat was also observed to be released upon immersion over a period of up to nine hours. Allen and Burevski [53] based on gas adsorption studies using a flow microcalorimetry concluded that, γ alumina is energetically heterogeneous and Degussa silica is energetically homogeneous. This study clearly demonstrated the utility of microcalorimetry to study the nature of surface heterogeneity.

Heat of wetting is essentialy equivalent to heat of adsorption. Heats of adsorption provide a means of characterizing surface properties. The classical text "Physical adsorption of gases" by Young and Crowell [56] provides an excellent exposition of the kinds of information obtainable from heats of adsorption and discusses the characterization of surfaces based on heats of adsorption.

It is clear from the published literature that heat of wetting studies can be used to characterize surfaces and provide a potential approach to the study of coal surface heterogeneity.

3.4 ADSORPTION OF VARIOUS REAGENTS

3.4.1 Surfactants

Adsorption of surfactants at solid/liquid interfaces is of practical importance in areas involving the control of wettability of solids. Coal, being naturally hydrophobic, can be usually floated without the addition of collectors or surfactants. However collectors are used in the flotation of poor quality or oxidized coals.

Adsorption of ionic surfactants results from their inherent amphiphatic nature, namely the presence of polar and nonpolar groups. The nature of the polar head group determines whether adsorption occurs by electrostatic or chemical interaction with sites at the solid surface, while the structure of the hydrocarbon chain controls the extent of adsorption and interaction with the aqueous medium. If the solid surface is hydrophobic, adsorption generally is controlled by interaction between the surface, water molecules and the hydrocarbon chain. Overall the adsorption of surfactants at the solid liquid interface may involve a complex combination of electrostatic, chemical and hydrophobic interactions.

In systems consisting of aqueous surfactant and carbonaceous material the adsorption of the surfactant clearly involves strong chain/solid, chain/chain, and electrostatic interactions. A number of adsorption studies on carbon black and activated carbon has been reported. Most of the systems are extremely complex, but were interpreted in terms of simple vapor phase adsorption concepts [54]. The main difficulty involved with surfactant adsorption on carbon blacks is the characterization of the surface. Graphon has been used as a model hydrophobic surface in many studies. Day et al [55] determined adsorption isotherms of sodium dodecyl sulfate on Spheron 6 and Graphon. It was noted that a marked point of inflection occured at an equilibrium bulk concentration below CMC in the case of Graphon but not in the case of Spheron 6 (i.e., two plateau regions were observed in the isotherms for

Graphon). Adsorption on Graphon remains constant above CMC, but on Spheron 6 the adsorption decreased at higher concentrations. After heat treatment Spheron behaved similar to Graphon; probably due to removal of surface oxygen groups. Similar results have also been reported by Tamamushi [57].

Adsorption of anionic surfactant (Aerosol OT) and cationic surfactant (CTAB) on carbon black shows typical Langmuir isotherms with long plateau [58,59]. This signifies that a high energy barrier to further adsorption exists after initial saturation. Effect of chain length of surfactants on their adsorption on carbon and coal has been studied and have been found to obey Traub's rule [60,61].

Adsorption of dodecyl ammoniumchloride has been studied by Yoo [62] and the isotherm is shown in Figure 7. The extent of experimental scatter points in this isotherm is indicative of the heterogeneity and is typical of such systems.

3.4.2 Polymers

Use of polymers in the selective flocculation of fine coal has been reported widely. Blaschke [63] reported studies in which coal slimes containing about 39% ash were selectively flocculated keeping the coal dispersed using sodium salt of carboxymethycellulose as the dispersent and an anionic, modified polyacrylamide ("Gigtar") as the flocculant. By this method ash content of the slimes could be reduced in one stage to about 20%, with coal recovery of about 40%. Hucko [64] conducted a detailed study on the selective flocculation of coal as a function of several important process parameters such as pH, dosage, and ionic strength of the medium. He concluded that selective flocculation is favored by alkaline conditions, and that naturally occuring organic colloids such as starches and guars were only moderately selective but low molecular weight nonionic polyacrylamides were more selective. A nonionic polymer with a molecular weight of about 4 million exhibited better se-

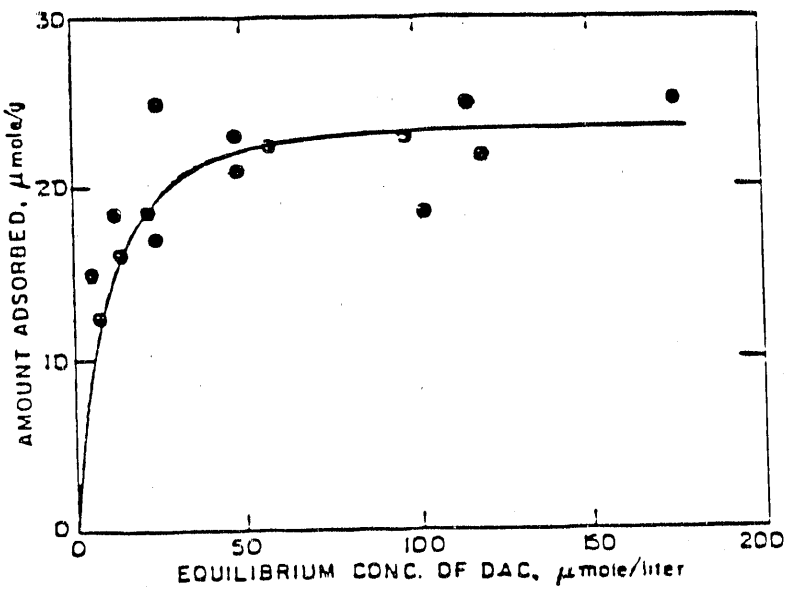

Figure 7: Adsorption density of dodecyl ammonium chloride concentration at pH 5.5 to 6.1 and at an ionic strength of 2×10^{-3} M KCl on coal.

lectivity than others in the 0.6 to 8 million range. Of the dispersants used, sodium hexametaphosphate was the most effective.

Commercial and modified polyacrylamide polymers tested with individual suspensions of coal, shale and mixtures of equal amounts of coal and shale revealed that anionic flocculants produced higher settling rates (about 25%) for shale than cationic flocculants. In the test with mixtures, both type of polymers produced low ash coal product [65]. The authors concluded that preferential adsorption of the flocculants onto the coal surface was responsible for the observed effect, the requirement for adsorption on coal being met prior to significant adsorption on shale. Krishnan et al [66] used water-dispersable flocculant containing hydrophobic functional groups and based on kinetic studies also concluded that there is significant adsorption on coal as compared to shale. Moudgil [67] has reported on the depressent action of polyacrylamide and polyethelyene oxide polymers on coal flotation. The author also reports that, based on visual observation polyacrylamide did not affect frothing characteristics but polyethelyne oxide tended to increase bubble size in the coal polymer systems studied.

3.4.3 Fuel Oil

Use of small amounts of collector, usually fuel oil or its derivatives in conjunction with frothers, is known to enhance flotation significantly [14,67]. The role of fuel oil as collector in coal flotation has not yet been fully understood. Explanations based on the electrokinetic properties of the oil droplets and coal surface have been proposed [69]. Other authors have examined the interfacial reactions of coal/ fuel oil on the basis of particle particle interactions [70]. It is possible that hydrophobic interactions would play a major role. Also, it apperas that the beneficial effect of fuel oil on coal flotation is governed by the probability of contact between coal and oil droplets than the energetics of adsorption.

3.4.4 Frothers

The mechanism of frother interaction with coal has been studied by Osaka [71]. His studies suggest the following : Typical frothers have both collecting and frothing properties. The amount of frother adsorbed on coal after periods of time such that equilibrium is not established are not in direct proportion to the total surface area of coal and is probably due to the ease with which these molecules can penetrate the pores of coal. The rate of adsorption of frothers decreases with time. The author suggests that there is a need to design larger molecular weight frothers, possibly with collecting properties incorporated.

Summarising, it is seen that reagents like surfactants, hydrocarbons, frothers and polymers have been studied for coal beneficiation. It is also noted that in many instances the optimum reagent scheme often consists of using a hydrocarbon. The hydrocarbon surfactant relationship is synergestic; Surfactants are used to emulsify the hydrocarbon before introduction into the flotation cell, and hydrocarbons are used to displace water from the coal surface and aid in the surfactant adsorption. Polymers have been used in selective flocculation; however, a high degree of selectivity has not been achieved and the mechanisms of polymer interactions with coal surface are not yet clear. It appears that there exists a multitude of reagents, each reagent scheme specific to a particular coal. Lack of efficient surface characterization coupled with our inadequate knowledge of reagent interaction mechanisms has been responsible for our inability to predict and control coal surface properties.

3.5 OXIDATION

In their natural state, most coals are susceptible to oxidation. Oxidation affects many of the surface-based processes employed in coal preparation and coal utilization [21,72]. Coal oxidation is particularly important in coal flotation since this

affects the wettability and hence floatability of the coal. In the future, oxidation will become even more important since advanced flotation processes will require fine grinding. Particles produced by fine grinding have an enormous surface area which will lead to extensive surface oxidation.

Coal oxidation progresses through a number of stages when coal is exposed to an oxidizing atmosphere [73]: i) surface oxidation, ii) production of alkali solubles, and iii) production of acid solubles. As oxidation continues and the oxygen content of the coal increases alkali-soluble compounds called humic acids are produced. On further oxidation, the humic acids degrade to low molecular weight acids that are soluble in acidic and neutral media as well as alkaline media. In the initial stages of oxidation, chemisorption of oxygen takes place leading to the formation of various functional groups, such as phenolic (-OH), carboxylic (-COOH) and carbonyl (C=O) [74]. As oxidation proceeds, gaseous products such as carbon dioxide and carbon monoxide together with water-soluble acids are produced. The exact nature of chemical changes that occur during coal oxidation is still not clearly understood.

Laboratory investigations concerned with the effects of oxidation on coal have usually been carried out either by air-oxidation or by the use of chemical oxidants. Air oxidation below 300°C normally stops at the formation of surface functional groups, whereas chemical oxidation in either an acidic or alkaline medium can form water-soluble products on coal surface.

Another important technique used for assessing the degree of oxidation is infrared absorption spectroscopy [75]. More recently, high speed and improved resolution FTIR (Fourier Transform Infrared Spectroscopy), a powerful tool, has been extensively used in the study of oxidized coal [76]. Modifications to this technique involving Diffuse reflectance (DRIFT) and Attenuated total reflection (ATR) are also employed to study coal [77,78]. These studies clearly show the formation of COOH and OH groups on coal surfaces upon oxidation.

An ion-exchange technique developed by Brooks, Sternhell and Schafer [79,80,81] is widely used for quantifying functional groups. However, this method determines only the leachable oxygen functional groups and cannot distinguish between surface and internal oxidized sites [40].

Oxidation of coal occuring in the bulk of the sample or the surface layer, can affect surface properties significantly. Studies by Sun [16] showed the flotation yield to decrease with increasing degree of oxidation, indicating increased hydrophilicity of the coal. He attributed this behavior to the accumulation of water-insoluble oxidation products at the coal surface. Chemical oxidation of coal, according to Celik and Somasundaran [82] can completely depress coal flotation. These researchers also found that ultrasonication restores the flotability of treated coals. Gutierrez-Rodrigues [21] inferred that at ambient temperatures aqueous oxidation decreases the hydrophobicity and hence the flotability of bituminous and lignitic coal.

Coals contain a variety of functional groups involving oxygen, nitrogen and sulfur. Among these oxygen groups, carboxylic and phenolic oxygen groups (-COOH, -OH) alter the wetting behavior of coals. The extent of change, however, depends on the susceptibility of a given coal to oxidation. Fuerstenau et al. [83] correlated the concentrations of phenolic and carboxylic groups with flotation response. Their results, indicate that the functional groups control wettability through the balance of hydrophobic/hydrophilic sites, and control flotation by their influence on surface charge. Oxidized coal floats less favorably because of the interaction between oxygenated sites and the polar water molecules. According to Rosenbaum [17] who measured contact angles on coal, the increasing hydrophilicity of coal with decreasing rank is due to the high concentration of oxygen groups on the surface.

Laskowski et al. [84] found that humic acids, which are products of coal oxidation, have a deleterious effect on coal flotability. They also observed the electronegativity of coal surface to increase with oxidation. The detrimental effect of

oxidation on coal wettability is evident, however there is no definite method by which their effect can yet be quantified.

Oxidation of coal has been shown to lead to the formation of polar groups on the surface. In view of the heterogeneous nature of coal, different moieties on the coal surface will probably oxidize to different extents. How oxidation affects the surface heterogeneity still remains an open question.

4 CRITICAL ISSUES

4.1 HETEROGENEITY

The above review of literature on coal beneficiation and coal surface science clearly shows that our knowledge is largely emperical and results on a particular coal sample is not necessarily valid for other samples. Often reagent consumption is found to differ even for coal samples from the same source as a function of time due to oxidation. This is due to the inherent heterogeneous nature of coal. Heterogeneity of coal consists of a) heterogeneity due to random dissemination of mineral matter in the coal matrix and b) The inherent heterogeneity of the coal surface itself. The former is related to the liberation of mineral particles during grinding. It is technically feasible, to a large extent, to control this type of heterogeneity by grinding coal to very fine sizes. This should liberate most mineral matter which can be subsequently separated by flotation or selective flocculation. The latter is due to the presence of various chemical moieties which form the organic matrix of coal and their distribution.

4.2 ROLE OF HETEROGENEITY IN INTERFACIAL PHENOMENA

Interfacial phenomena in heterogeneous systems will often be goverened by more than one mechanism. For example adsorption on a particle could be due to hydrophobic interaction on hydrophobic patches and by electrostatic interaction on oxidized patches. Also a small area on the surface with sites of a particular surface energy or charge could control the overall observed effect; for exarnple, lubricating property of graphite is greatly enhanced by adsorbed water on a few isolated hydrophilic sites [85]. Zettlemoyer and co-workers [86] have suggested that hydrophobic- hydrophilic ratio (3 or 4:1) may be an important parameter in determining the efficiency of ice nucleation. Recent surface studies have shown that important characteristics of adhesion, wettability, and printing are associated with a relatively few number of specific carbon-oxygen bonds within the outermost monolayer [87,88]. In the case of microbial adhesion and desulfurization it is quite possible that few isolated sites are points of attack in the gradual removal of sulfur. It is seen from the published literature that coal is often treated as any other homogeneous hydrophobic solid, neglecting the nature of heterogeneity. It should be pointed out that only minor changes in surface properties are adequate to affect surface based phenomena. In the case of heterogeneous material like coal, knowledge of average properties would not provide sufficient information for controlling the interfacial properties. The distribution of chemical moieties on coal surface is of direct significance in interfacial processes and a fundamental knowledge of their distribution is essential to design effecient flotation and flocculation systems.

4.3 ACCURATE CHARACTERIZATION OF COAL SURFACES

There exists no published material adressing the important issue of heterogeneity in coal surface characterization studies. Accurate characterization should include the heterogeneity of coal. Studies on the chemical structure of coal are numerous and are summarised in [89] with various types of models being proposed for various ranks of coal. However, there is no consensus regarding the nature of the average structural unit. It is evident that the average structural unit consists of various organic moieties; both aliphatic and aromatic in nature. Oxidation will induce polar groups like hydroxyl and carboxyl groups. The surface of coal is thus likely to be composed of varying quatities of polar and nonpolar sites of different degrees. From the works of Zisman, Good and others it is clear that characterization of coal surfaces based on the concept of critical wetting surface tension would be useful in understanding the chemical structure of the coal surface.

How chemical groups are distributed on a surface is a generic question in surface science having implications in the field of color sciences, drug delivery systems, molecular electronics, mineral processing and most importantly in coal cleaning.

5 MATERIALS AND METHODS

5.1 MATERIALS

5.1.1 Coal

Fifty two (52) pounds of coal from seam pgh, Bruceton mines in Alleghany county, PA was received from PETC. The tag on the package indicated that the coal was packed under argon atmosphere. Examination on delivery indicated that the plastic bags were ruptured probably during transport. The as received coal was in the form

Ultimate analysis: as received	
Description	Percent
Moisture	1.79
Carbon	80.65
Hydrogen	5.30
Nitrogen	1.74
Chlorine	0.10
Sulfur	1.12
Ash	3.29
Oxygen (by diff.)	7.80
Proximate analysis: as received	
Volatile matter	36.29
Fixed carbon	58.60
Calorific value	14000 BTU/lb
Sulfur Forms: as received	
Pyritic	0.28
Sulfate	0.0083
Organic	0.83

Table 1: Proximate, ultimate and forms of sulfur analyses.

of large pieces of rocks. The large pieces were broken down and crushed in a Quaker mill and subsequently dry ground in a ball mill using ceramic balls. The crushed product was sieved and various size fractions stored in plastic bottles in a glove bag under nitrogen atmosphere to minimize ambient oxidation. Proximate and ultimate analysis of the coal sample is shown in Table 1. The coal sample is high volatile B bituminous quality.

5.1.2 Polymer

Commercial polyacrylamide polymers were obtained from American Cynamid Company. Cationic polyacrylamides of 10% and 34% cationicity, anionic polyacrylamide of 30% anionicity and a nonionic polyacrylamide were used. The molecular weight of all the polymers used was approximately four million as specified by the manufacturer.

5.1.3 Other

All other chemicals used were reagent grade. Distilled water was used throughout the experiments.

5.2 METHODS

5.2.1 Morphological Studies

Systematic analysis of samples from +8, +100, +200, +635 mesh fractions were conducted using a SEM Cambridge 250 mark 2 coupled with a Kevax 8000 EDX analyzer. Samples for SEM were prepared from grain mounts fixed to aluminium stud sample holders and carbon coated prior to analysis. Representative photomicrographs of inclusions in coal and their elemental analyses were obtained.

5.2.2 Adsorption Studies

Adsorption isotherms were generated by the depletion technique. Typically 0.25 gram of coal was mixed with 5 ml of triply distilled water for one hour, after which 15 cc of polymer solution of the desired concentration was added. The suspension was conditioned for a known period of time, followed by separation of solids by centrifugation. All experiments were done under natural pH conditions. Adsorption experiments were conducted using the rest method (vials were allowed to stand in a stationary position and gently inverted by hand three times every 24 hours).

Polymer adsorption studies invariably require measurement of polymer residual concentrations. A survey of the literature on polymer adsorption reveals that polymer concentations at the ppm levels are usually measured by titration or nephelometry which are often very tedious and unreliable methods. During the course of this project we identified the Total Organic Carbon (TOC) analyzer as a simple

and reliable system for measuring polymer concentration at the ppm levels. The residual concentration of polymer was measured using a Dohrman DC-90 model TOC analyzer.

5.2.3 Film Flotation

The experimental technique involved sprinkling of coal (typically 0.25 gms.) on water-methanol mixtures of varying concentrations. The resulting float and sink fractions were separated by decantation and dried under ambient conditions and weighed. The weights recorded were used to construct cummulative site distribution curves. Experiments were conducted with coal samples subjected to heating in an air heated oven at 70°C and performing film flotation. The effect of cooling the sample under different conditions were also monitored. Film flotation experiments were also conducted after subjecting the sample to reoxidation at 70°C. Film flotation of coal oxidized at a temperature of 140°C in a muffle furnace for 24 hours was also performed. Samples of coal were placed in a dessicator under vacuum for twenty four hours after which film flotation was performed in order to study the effect of moisture removal on film flotation response.

5.2.4 Centrifugal Immersion

Typically about 0.1 to 0.2 gram of coal particles in the desired size range was gently placed on the surface of water in a centrifuge bottle and subjected to different degrees of centrifugal force for a constant time and temperature. The float and sink fractions were seperated, weighed and data used to construct partition curves. A Dupont Sorvall RC-5B refrigerated superspeed centrifuge was used.

5.2.5 Wax Vapor Deposition on Coal

In order to create a relatively homogeneous surface, the coal particles were coated with wax vapor. Chemical grade Paraffin wax from Aldrich Chemical Company was used. Granules of paraffin wax were placed in a conical flask and heated by an electric heating mantle. The wax was melted and subsequently vaporized. The vapors were passed through a bed of coal particles held in a fritted glass funnel by applying vacuum. After 10 minutes of vapor deposition the vacuum was broken and the bed gently tumbled in order to expose fresh surfaces to the vapor. This procedure was repeated 20 times. A schematic illustration of the experimental assembly is shown in Figure 8. The wax coated coal samples were stored in a desiccator and used for centrifugal immersion tests.

5.2.6 Adsorption Gravimetry

The experimental apparatus used in the present study has been reported in the literature [94,95,96] previously; however a brief description follows. The general arrangement of the system is shown in Figure 9. A symmetrical microbalance (Setaram MTB 10-8) is connected to vacuum pumps (oil diffusion pump and two-stage rotary pump) including liquid nitrogen trap, the vapor source , a gas manifold, and two pressure gauges: a Pirani gauge for the 10^{-6} to 10^{-1} torr range, a Texas fused silica Bourdon tube automatic gauge for the 10^{-2} to 500 torr range. The gas manifold and the associated valve set allow vacuum control and pressure measurements in different parts of the apparatus. A symmetrical thermostat around the balance allows a wide range of temperature conditions under which to conduct the experiment while simultaneously providing constant temperature control. The vapor supply is connected to the balance and the sample through a Granville-Philips leak valve, and is immersed in an air thermostat in which the balance and the

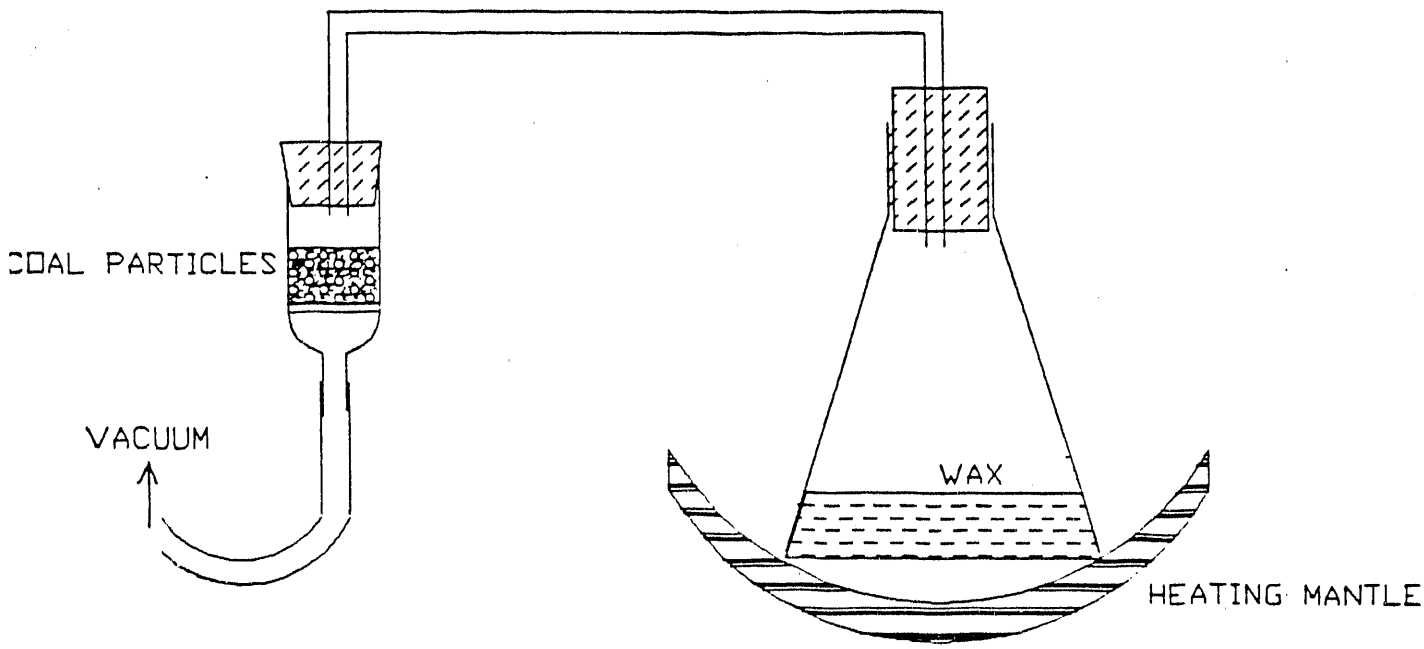

Figure 8: Schematic illustration of the apparatus used to coat coal particles with paraffin wax vapor.

manifold are encased. An XY recorder and analog to digital converter provide the necessary data acquisition hardware. A known amount of coal sample (typically a gram) is placed in the sample cell and the system subjected to degassing at room temperature for 14 hours.

Subsequently the entire apparatus is set to the desired temperature at which the adsorption isotherms are acquired and the system allowed to equilibrate for a further period of 4 to 5 hours. The pressure gauges and the leak valves are then set at their respective starting points and the experiment commenced. The change in weight of the sample is obtained as the output as a function of relative pressure. Thermodynamic equilibrium was checked over the entire relative pressure range. At a given p/p_0 value the adsorbate introduction was stopped and the system checked for any mass or pressure evolution. Error analysis reported earlier for this system [96] shows that the amount adsorbed can vary in the range $\pm 3.7 \times 10^{-6}$ mol/g and the relative pressure can vary by ± 0.03 units p/p_0. Coal samples used in the study were -200 mesh samples prepared by dry grinding of coal in a ball mill.

5.2.7 Immersional Calorimetry

A conventional Tian-Calvet differential microcalorimeter was used in the immersional calorimetry experiments. A brief description of the microcalorimeter however follows [97]., however a brief description follows. The microcalorimeter has two cells. The output of the microcalorimeter is connected to a digital millivolt meter and a chart recorder. A cross sectional view of the immersion cell is shown in Figure 10.

Sample (numbers refer to the preceeding figure) 1 is prepared in a glass bulb 2 with a brittle end 3 and sealed to a glass rod 4. When the experiment is started the glass rod is depressed and a small frictional heat takes place against the O-ring 5 which ensures an air-tight seal; nevertheless, since this O-ring is located about

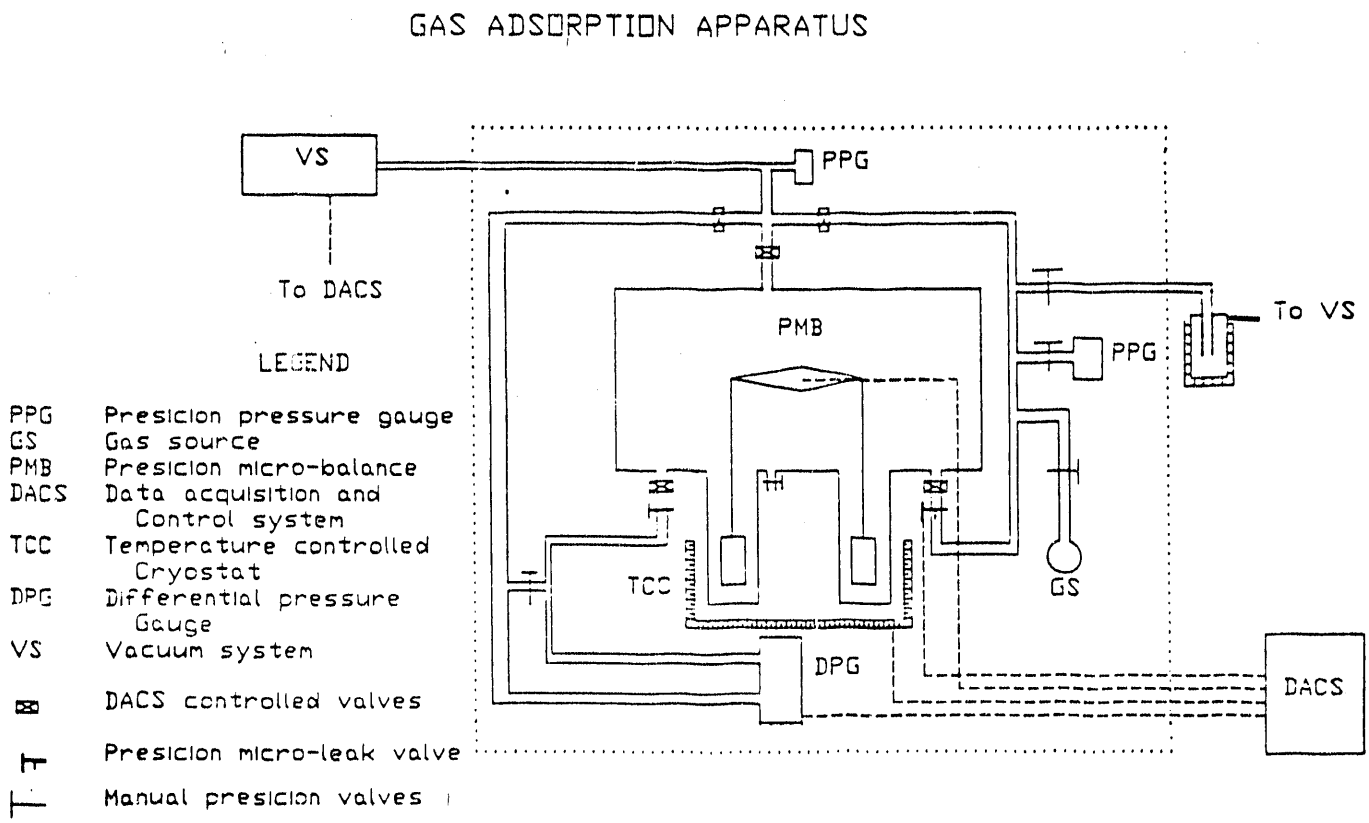

Figure 9: Schematic illustration of the gravimetric gas adsorption apparatus.

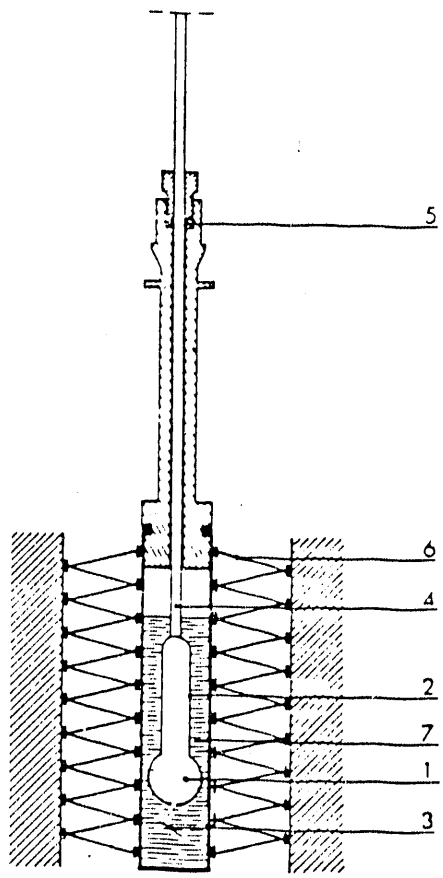

Figure 10: Cross sectional view of the Tian-Calvet calorimeter cell.

9 cm above the detecting thermopile 6, the microcalorimeter recording remains undisturbed by that friction as can be seen from a steady baseline in the output recorder. In the meantime when an extra volume v of the glass rod enters the liquid 7 there follows a rise in its level, a compression of the gas phase (air + saturated vapor of the liquid), and an exothermal effect approximately equal to $\int_0^v p_A dV$ (compression of the air phase with initial partial pressure p_A) + $(\Delta h_{liq})/RT \times p_0 \times v$ (liquefaction of the saturated vapor previously contained in v). Finally the brittle end breaks, with a small energy output W_B (typically around 10 ± 5 mJ), allowing the liquid to enter the bulb (in which the sample is kept either under vacuum or under a pressure p of the vapor) and to fill it completely. The heat effects detected then are: (i) the enthalpy of immersion ΔH_{imm}, (ii) the enthalpy of liquefaction $(\Delta h_{liq})/RT \times p \times V$ of the vapor previously filling the bulb (void volume V) at the pressure p, and (iii) the enthalpy of vaporization - $(\Delta h_{liq})/RT \times p_0 \times V$ of the saturated vapor which has to fill the volume liberated by the lowering of the liquid level. These heat effects finally result in a heat flow through the 400 junction thermopile 6 which delivers the calorimetric signal. A detailed thermodynamical analysis of this type of experiment is given elsewhere [98]. The magnitude of various terms are calculated by performing blank experiments. In a typical experiment the enthalpy of immersion contributes about 90 percent of the total heat, the enthalpy of liquefaction and vaporization *i.e.* items (ii) and (iii) above contribute about 7 percent while the other effects contribute around 3 percent.

The immersion experiments were performed with methanol as the immersional liquid. Calibration experiments were also performed to relate the area under a thermogram to the heat output. In experiments involving the enthalpy of immersion of coal samples with preadsorbed layers of methanol the following procedure was adopted. Samples held in the glass bulb were outgassed at ambient temperature for 14 hours and then kept for another 14 hours connected to the methanol vapor source

in a twin thermostat arrangement. The sample is always held at the temperature at which the adsorption study is conducted (30°C in this case) whereas the temperature of the methanol vapor source is varied in order to attain various degrees of partial pressures and hence various coverages. At the end of the equilibration period the sample bulb is sealed, attached to the glass rod and introduced into the calorimeter where thermal equilibrium at 30°C was awaited for about 4 hours before start of the immersion experiments. After thermal equilibrium has been attained the glass rod is depressed to break the brittle joint and the heat evolved measured. The output of the experiment in the form of a thermogram curve is available from the chart recorder connected to the calorimeter. The area under the thermogram was obtained using a planimeter and converted to heat units using calibration data.

5.2.8 Spectroscopy

Diffuse Reflectance Infrared Fourier Transform Spectroscopy (DRIFT)
Infrared spectroscopic investigations were conducted using a Perkin Elmer FTIR 1800 instrument. A Perkin Elmer DRIFT accessory was used to acquire the spectra of coal, oxidized coal and polymer treated coal. The spectra of float and sink fractions obtained (at 30% methanol concentration) from film flotation experiments were recorded. The typical spectral acquisition procedure involved the initial recording of a background spectrum of KBr powder in the single beam mode. Subsequently about 0.05 gram of the sample was mixed throughly with 0.25 to 0.5 gram of KBr powder, transferred to the sample holder and the spectrum was acquired in the single ratio mode. Typically 100 scans were collected. The difference spectrum was obtained using the interactive mode provided in the software.

Fluorescence Spectroscopy :

Pyrene labelled polyacrylamide polymer synthesized at National Chemical Laboratory, India, was used. Coal was treated with 250 ppm of polymer solution for 48 hours after which the slurry was separated by centrifugation. The supernatant and slurry were analyzed. A blank containing 250 ppm of polymer was also analyzed. The fluorescence spectra was accquired using a SPEX Fluorolog spectrophotometer.

Laser Microprobe Mass Analyzer (LAMMA) :

A brief description of LAMMA is given in Appendix C. A +8 mesh coal sample was analyzed using LAMMA along a line scan in thermal desorption mode to identify the desorbable components present (both elements and molecular fragments). The LAMMA spectra were obtained from Surface Sciences Laboratories Inc., California and are enclosed in Appendix D. Positive and negative ion spectra were acquired at locations identified on the spectral plot. Appendix C also contains the photomicrograph of the +8 mesh coal sample showing the analysis location and the LAMMA line profile end points.

Derivatized - Electron Spectroscopy for Chemical Analysis (D-ESCA)

An ESCA instrument comprising a Surface Science Instruments Inc., spectrophotometer, model SSX-100 equipped with a AlK alpha X-ray source was used. Typically during the experiments the pass energy was maintained at 25 eV at a pressure of 10^{-8} torr. The spectra were obtained from Surface Sciences Laboratories, California. A +8 mesh sample of coal was analyzed using ESCA to obtain surface elemental composition and chemical binding states. Subsequently the samples were submitted to site specific reactions resulting in the incorporation of fluorine and the spectra of derivatized samples obtained. The number of functional groups per 100 atoms is calculated by dividing the atom percentage of fluorine by the number of fluorine atoms in the tag molecule. The derivatization reactions which enabled the

quantitative determination of phenolic OH, carbonyl and carboxyl groups which were pursued in this study are as follows:

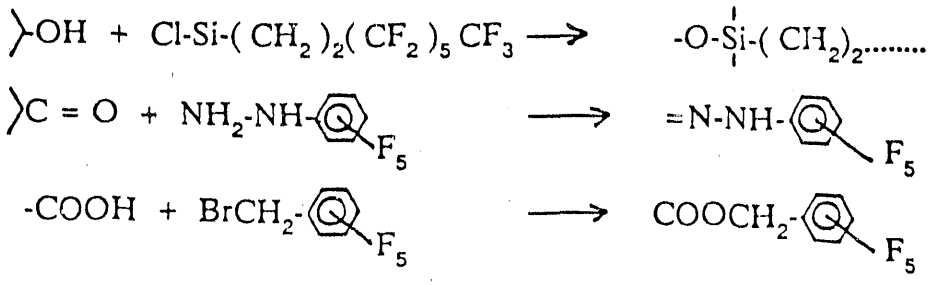

6 RESULTS AND DISCUSSIONS

6.1 MORPHOLOGY

The results of morphological studies are summarized below. Detailed discussion of the micrographs and elemental analysis is given in Appendix A. The coal sample contains iron disulphides refered to generally as pyrites, clayey matter, silicates and carbonates. Traces of titanium, manganese, fluorine, potassium and chlorine were also recorded. The mineral matter in coal is closely associated with the coal matrix and also with each other. Only at 635 mesh fraction individual particles of mineral matter are noticed. Single inorganic crystals of complex compositions were noticed in this size range. Even at moderately coarser sizes (such as +100 mesh and +200 mesh), the mineral matter was found to be locked with each other and the coal matrix.

In many instances the mineral matter is covered with a fine layer of coal dust probably due to smearing during grinding (dry) and sieving. This could have important implications for subsequent surface modification studies and advanced

cleaning processes based on surface properties.

6.2 WETTABILITY DISTRIBUTIONS

Wetting is an important phenomenon in physical beneficiation processes such as flotation and agglomeration. Since coal surface is heterogeneous it is to be expected that various domains on the coal surface would posses different degrees of wettability. Wettability distributions presented in this study were obtained from the centrifugal immersion technique which was developed during the course of this project. Centrifugal immersion involves forces required to detach particles from the liquid-air interface and to immerse them. The theoretical treatment of floating bodies has been undertaken in the past by means of force analysis [99,100] and free energy analysis [101,102]. These studies are for particles with simple geometries like those of spheres or cylinders. For a smooth chemically homogeneous particle with a single geometry there exists a single critical force for its detachment from the liquid-air interface. Recently the centrifugal immersion technique has been used to examine the role of collective adhesive effects (or ensemble effects) of particles on the force required to detach particles from the liquid-air interface [103]. This study showed that though significant ensemble effects were observed with particles smaller than 90 microns, larger particles did not produce any measurable effects. In other words the larger particles in a group behaved like single particles. The average size of the coal particles used in centrifugal immersion experiments is around 165 microns.

In order to obtain a chemically homogeneous surface while maintaing the shape, some samples of the coal particles were coated with wax vapor. Flotability of particles residing at the liquid-air interface in solutions of varying surface tension [104,105] was used to characterize the wax coated coal surface. Figure 11 shows the cumulative partition curve obtained from such flotation tests using wax coated coal

particles.

The wax coated particles yield an almost vertical partition curve. The minimum and maximum critical wetting surface tension (γ_c) values of wax coated coal particles are 25 and 30 mN/m respectively, as compared to 32 and 72 mN/m respectively for untreated coal. This shows that the wax coated particles have a more chemically homogeneous surface. The mean γ_c value for the wax coated coal particles is 26.5 mN/m and this is in general agreement with reported values for paraffin [104].

The wax coated particles were subjected also to centrifugal immersion experiments and the results are shown in Figure 12.

The curves corresponding to the untreated coal and coal oxidized at 140°C for 15 hours are also included in Figure 12. All coal samples are of minus 80 plus 100 mesh fraction (149 to 177 microns). It can be seen that at lower speeds the oxidized coal sinks more than the untreated coal or wax treated coal indicating that its relatively more hydrophilic. Similarly the detachment speeds for the wax treated coal is more than those for others. As expected wax treated coal is more hydrophobic than the untreated or oxidized coal samples.

The wide range of forces (corresponding to 2000 rpm to 16000 rpm) required to detach wax coated coal particles (which have a chemically homogeneous surface) from the liquid-air interface is illustrated in Figure 12. Such a wide range is not predicted for particles with chemically homogeneous surfaces by any of the models referred to herein. This is because these models take into account only bodies of well defined geometry. The works of Rapacchietta et al [101,102] and detailed calculations based on the approach adopted by Nutt [106] have demonstrated that shape does have a substantial effect on the force required to detach particles from the interface as is to be expected.

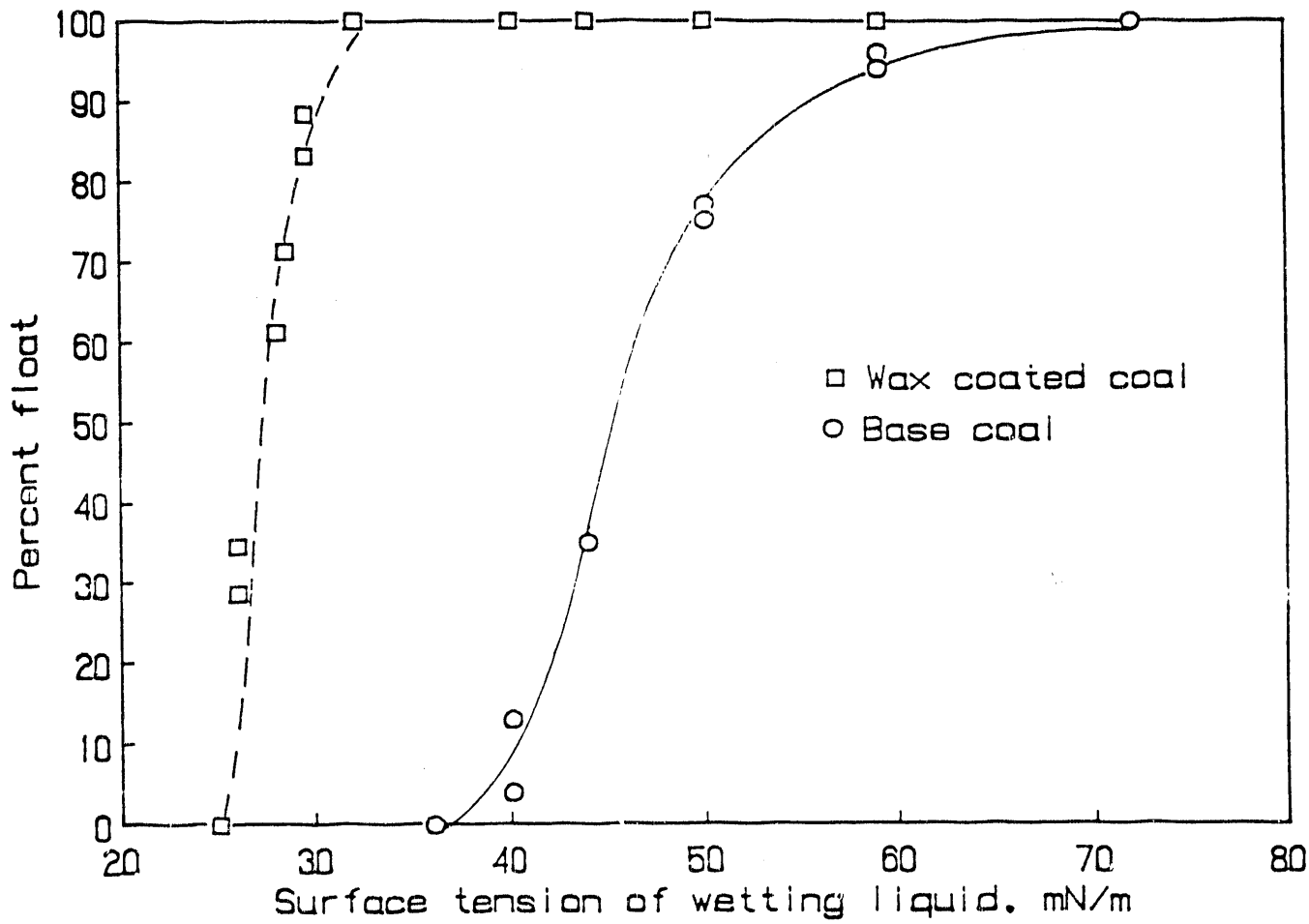

Figure 11: Cumulative partition curves constructed from film flotation data obtained using base coal and wax coated coal samples.

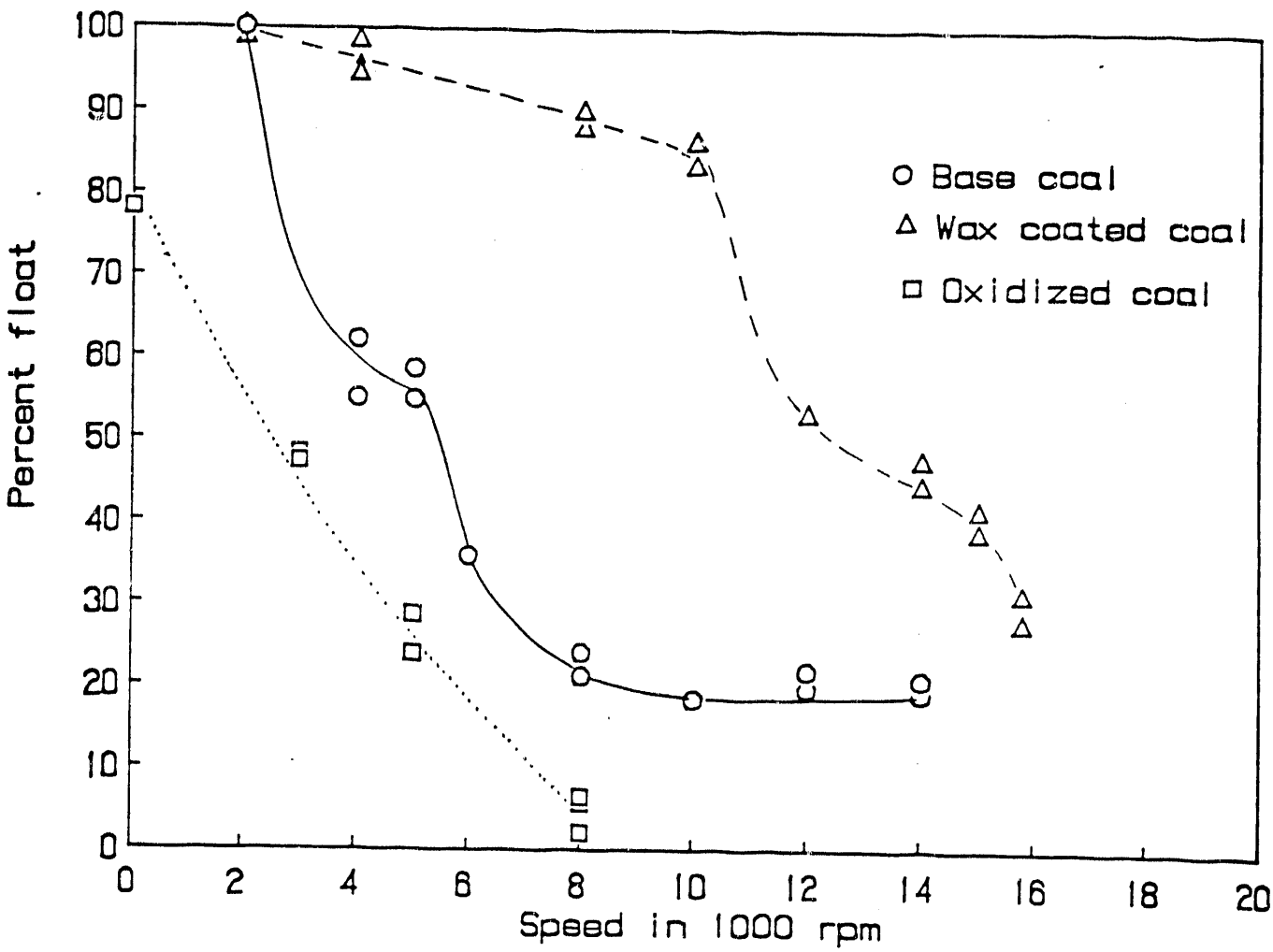

Figure 12: Cumulative wettability distribution curves of base coal, wax coated coal and oxidized coal constructed from centrifugal immersion experiments.

Homogeneous particles with a single specific geometry would yield a single value for the detachment force. A mixture of particles (contact angle being the same for all the particles) having a variety of shapes would yield a distribution of detachment force. Apart from the shape effects, edge effects [107] which can cause line pinning [11] and the dynamic effects of the moving interface [108,109] as the particle sinks could also contribute to the distribution of detachment force. We shall call these collectively as shape effects. The movement of the three phase contact line on hydrophobic surfaces is more akin to rolling than spreading. The rolling motion of the foot of the three phase contact line has been discussed by de Gennes [11]. The manifestation of these shape effects is more likely in the case of a rolling three phase line than in the case of spreading three phase line. To paraphrase, if a liquid is capable of wetting a solid then the geometry of the solid is not of primary importance, on the other hand if the liquid is incapable of wetting the solid then the geometry of the solid plays a significant role in the wetting process. This aspect is demonstrated in the design of many natural systems such as in the case of duck's feathers. Therefore, the collective shape effect can be expected to be more predominant in the case of hydrophobic surfaces.

The trends of curves for the untreated and wax treated coal in Figure 12 are similar, even though film flotation tests did indicate that the surface of the wax coated particles was more homogeneous. The only invariant property of the two samples is the collective shape effect. The shape of the curves in these cases is therefore a manifestation of the particle shape effects. The shape of the curve for the oxidized coal is different from that of the untreated coal curve. Oxidation is not expected to alter the shape of the particle; the difference in the curve of the oxidized coal sample cannot be due to shape effects. Oxidized coal is more easily wetted and the wetting fluid can easily spread around particles of various shapes. The shape of the curve in this case therefore can be considered to be determined

mainly by the moietic distribution on the surface.

Figure 13 shows the frequency distribution curves corresponding to the cumulative curves in Figure 12. The lateral shifts in the curves are indicative of the degree of hydrophobicity, and as expected, the curve for the most hydrophobic sample shifted towards higher detachment speed and that for the least hydrophobic shifted towards lower detachment speed. Since the particle size range of all coal samples is the same, the differences in the shape of the curve cannot be attributed to size effects.

The wettability site distribution diagram in Figure 13 shows the wax coated coal to exhibit bimodality. Since the surface of this sample is essentially homogeneous this can be attributed to the shape effects encountered during the immersion process. Since the shape effect is also a function of the hydrophobicity of the particle the modality will be influenced by the degree of hydrophobicity of the particle.

Clearly in the case of coal particles which posess hydrophobic and hydrophilic sites of varying degrees, the surface chemistry and shape effect are likely to play a role in determining the dynamics of the spreading wetting and the force required to detach particles from the liquid-air interface. The shape effects are likely to predominate in the case of relatively hydrophobic particles, and the surface chemistry to predominate in the case of relatively hydrophilic particles. Figure 14 shows the wettability site distribution diagram for the untreated coal sample constructed from data obtained from centrifugal immersion experiments conducted in April 1988.

Three major peaks at around 3000 rpm, 6000 rpm and 8000 rpm are noticed. The wettability site distribution diagram of the same sample obtained in April 1989 shows marked differences in the height of peaks corresponding to the above speeds. The peak at 8000 rpm is suppressed, and a significant increase in the height of the other two peaks is noticed. When the coal sample was oxidized at 140°C for 15 hours

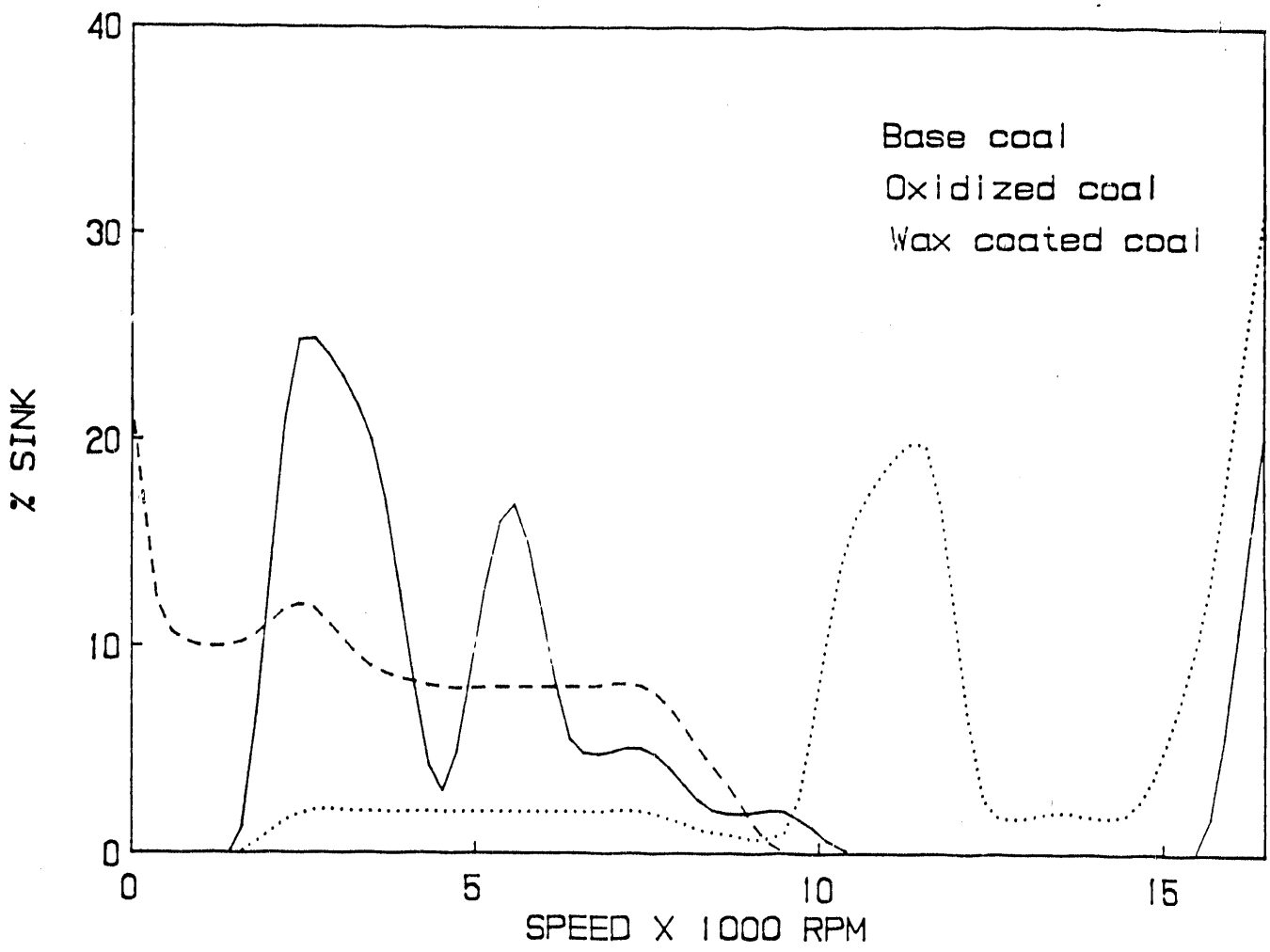

Figure 13: Differential wettability distribution curves of base coal, wax coated coal and oxidized coal constructed from centrifugal immersion experiments.

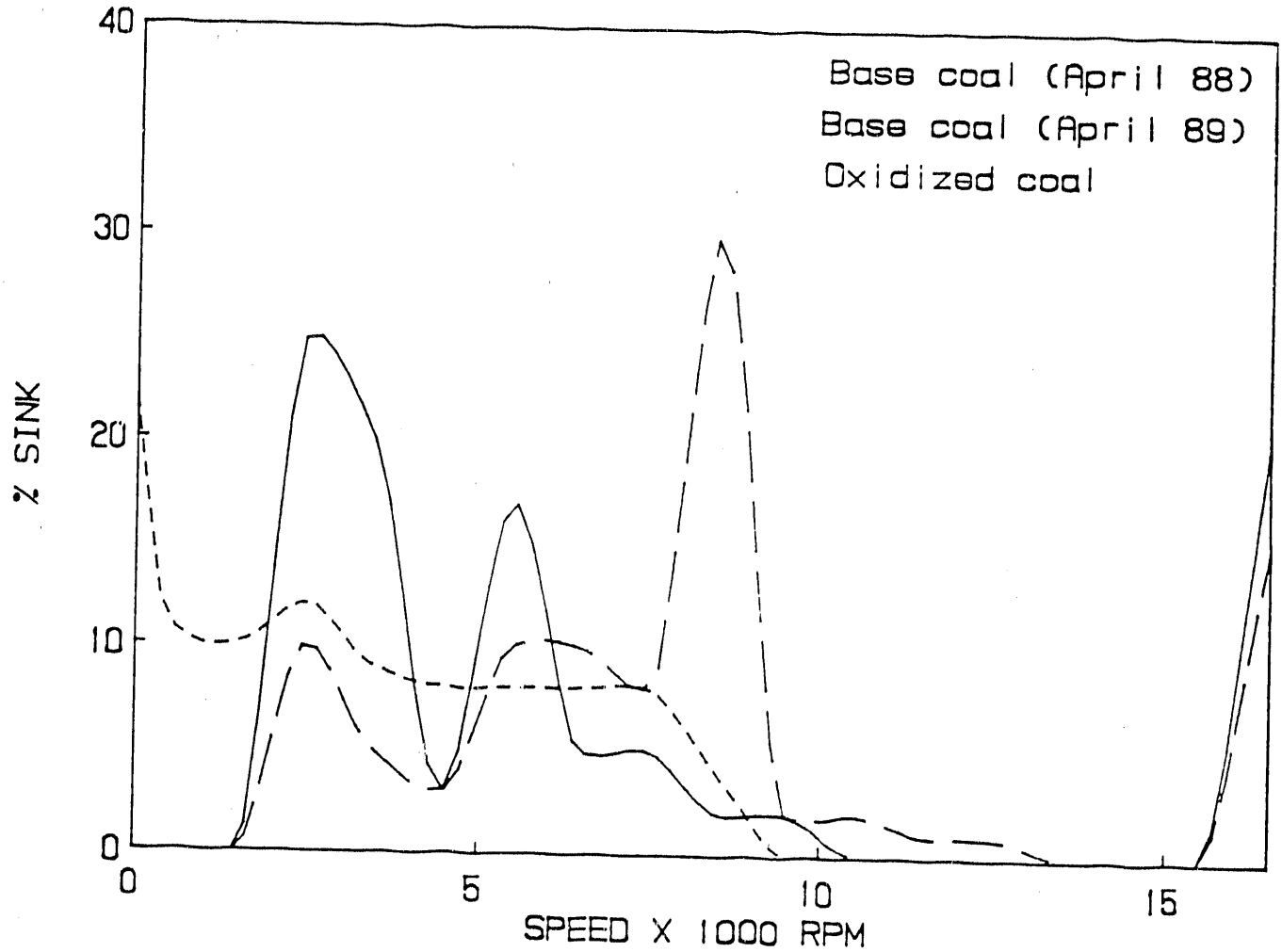

Figure 14: Cumulative wettability distribution curves of base coal in 1988 and in 1989 and oxidized coal constructed from centrifugal immersion experiments .

all the above mentioned peaks were suppressed. However, 20 percent of the coal sinks at zero speed. A general trend in the wettability site distribution diagram is noticed upon oxidation of the coal sample . As oxidation proceeds it is accompanied by a reduction in the height of peaks at high speeds with a corresponding increase in the height of those at low speeds. These changes can be attributed to a loss of nonpolar groups and the appearance of polar groups which accompanies oxidation [21,83].

Cumulative wettability distribution curves generated from centrifugal immersion experiments relate the forces required to detach heterogeneous coal particles from the liquid-vapor interface and the corresponding weights of the particles detached. Cumulative wettability distribution curves obtained from centrifugal immersion experiments conducted in methanol-water mixtures are shown in Figure 15.

Examination of the wettability distribution curves obtained for different surface tension of the liquid phase shows that as the surface tension of the liquid is lowered, the force required to immerse coal particles decreases as expected, since surface tension forces counteract the centrifugal force required to detach the particles from the liquid-vapor interface. Certain interesting features of these curves are to be noted. Firstly, in the case of liquids with surface tension of 72 mN/m and 59 mN/m, 80 percent of the particles are detached from the liquid-vapor interface between 5000 and 7000 rpm, indicative of a "fall-out" phenomenon under stress. However as the surface tension of the liquid phase is decreased this phenomenon appears to be of less significance. Secondly, the slope of the wettability distribution curve becomes less steep as the surface tension of the liquid is lowered.

The sudden increase in the amount of particles detached from the liquid-vapor interface warrants the description of this phenomenon in terms of probability distributions which relate fall-out under stress conditions. In the present case the amount

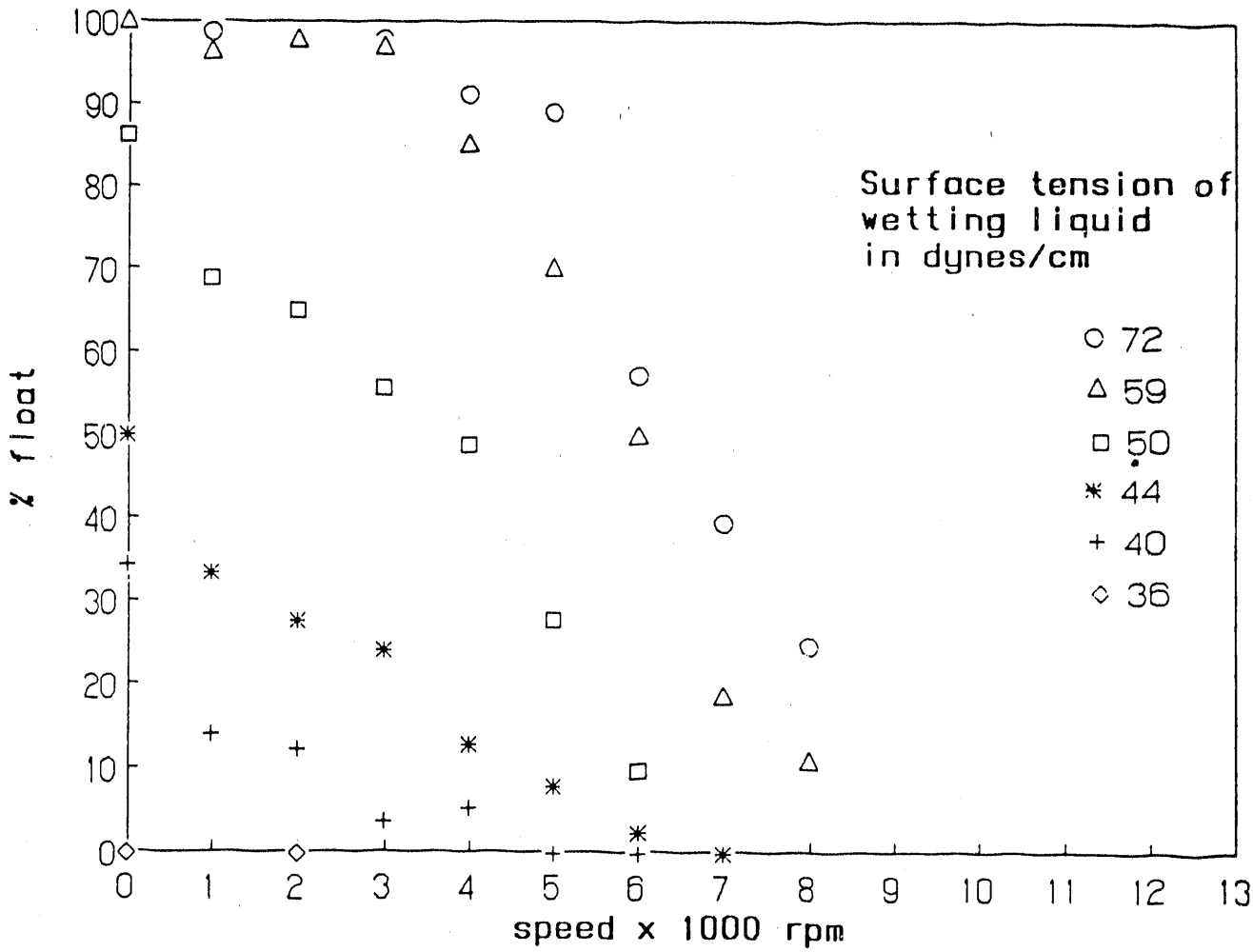

Figure 15: Wettability distribution curves of base coal as a function of the surface tension of the wetting liquid

of particles residing at the liquid-vapor interface is a measure of the probability of detachment or attachment. In fact, recently such a treatment has been suggested for the determination of adhesive strength of particles within the liquid-gas interface in flotation by means of a centrifugation method [110].

A Weibull distribution of the form $W_a = [1 - e^{-a_z/a_{z50}m}]$ was used to fit experimental data. W_a is the relative attachment probability which takes the value of 1 and 0 corresponding to 100 and 0 percent float respectively in the wettability distribution diagram. a_z is the centrifugal acceleration which can be calulated from the rpm values using tables given in the centrifuge (model Sorvall RC-5B, Du Pont Instruments) manufacturer's operating and maintenance manual. The parametrs a_{z50} and m are obtained by fitting the equation to experimental data. This distribution is a special case of gamma distribution which describes fall-out phenomena. Essentially the equations for such distributions have two parameters characteristic of the distribution curves *viz.* a_{z50} parameter which provides a measure of the average of the wettability distribution and another exponential parameter 'm' characterizing the width of the distribution. The latter depends on factors, such as irregularity of particle shape (varying extent of wetting), heterogeneity of particle surface (distribution function of contact angles) and polydispersity of the chosen particle size. Various modifications to the above equations are possible, one such modification for example is $W_a = e^{-ln2a_z/a_{z50}m}$. These equations can be linearized and parameters a_{z50} and m can then be obtained from the slope and intercept of the straight lines. It was found that these distributions did not provide a reasonable fit. However, reports of reasonable fit in the case of data obtained with mono-disperse glass spheres are available [110]. It apperas that the role of shape of particles in the present case is probably very significant.

A better method for characterizing the detachment of particles from the liquid-vapor interface could be obtained by adopting classical statistical methods for cal-

culating the moments of the frequency distribution curves which can be obtained from the experimental cumulative wettability distribution curves. For example, the moments of the detachment probability density distribution function can provide measures of the symmetry, skewness and flatness or steepness of the distribution.

It is possible that a family of wettability distribution curves obtained as a function of the surface tension of the liquid phase is characteristic of the coal particle used. In other words, development of a family of such distribution curves for various coal samples might offer a sensitive means for characterizing the wettability of coal particles from differing sources or with different history.

Wettability distribution curves constructed from centrifugal immersion data as a function of the surface tension of the liquid phase shows a complex and as yet undetermined relationship between the shape, surface tension and the force required to detach heterogeneous coal particles from the liquid-vapor interface. It appears that the series of wettability distribution curves as a function of surface tension of the liquid phase will be sensitive to the surface properties of coal particles in cases where a single wettability distribution curve is not sensitive.

Wetting of particles is a phenomenon with important effects on interfacial processes such as flotation and flocculation. Usually wetting is studied by measuring contact angles on polished surfaces. However such studies lack the ability to predict the macroscopic wettability of particles with irregular geometry and heterogeneous surfaces. This is because the dynamics (the movement of the three phase line), and the shape (edge) effects play an important role in the spreading wetting of particles. Further more the measurement of equilibrium contact angles provides little information on the ability of the liquid to spread over heterogeneous surfaces. The force required to detach particles from the liquid -air interface which is the measured parameter in centrifugal immersion experiments, is a function of the dynamics of spreading, surface heterogeneity, and shape effects. This technique

is clearly a powerful tool for studying the relative wetting behavior of irregularly shaped hydrophobic particles.

6.3 SURFACE SITE DISTRIBUTIONS

Partition curves constructed by film flotation yield a graph of the cumulative weight of the particles as a function of critical wetting surface tension (γ_c). It has been previously established by Zisman [26,27] that γ_c is a surface parameter which depends not only on the nature of the surface molecules but also on their orientation/ conformation. γ_c is also a measure of the surface energy and their relationship is given by $\gamma_s = \phi^2 \times \gamma_c$ where ϕ is the interaction parameter and γ_s is the surface tension of the solid in vaccum [43]. Assuming that the interactions at the interface are of the London type and spreading pressure (π_e) equal to zero, ϕ could be taken to be unity. As weight is proportional to the surface area and film flotation is a surface based process these partition curves essentially give distribution of the surface energy sites on the particles.

Surface heterogeneity in a particulate population can be of two kinds. In the first kind, individual members of the population can possess homogeneous surfaces but the population as a whole could be heterogeneous. A schematic illustration of such a population is shown below, typified by a mixture of particles having different surface features. However, each particle has only one type of feature on its surface (in this sense each particle is homogeneous). Such particulate populations are heterogeneous mixture of homogeneous particles.

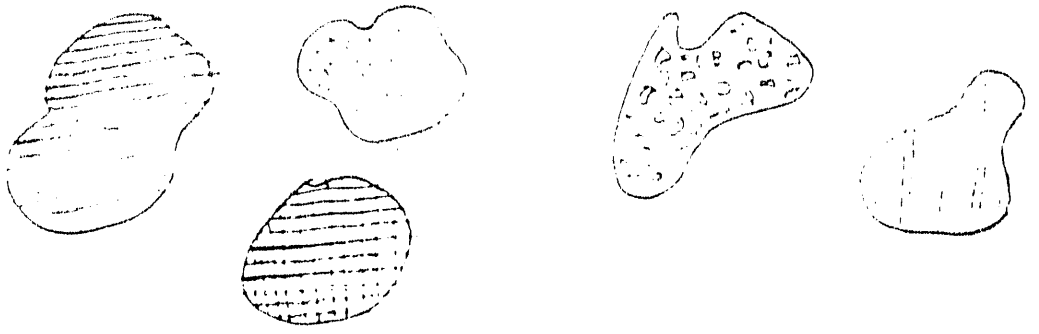

In the second case, the individual members of the population can be heterogeneous and therefore the population as a whole will be heterogeneous. An illustration of this is shown below, typified by a mixture of particles where each particle posses all of the features on its surface (in this sense each particle is heterogeneous). This category falls under a homogeneous mixture of heterogeneous particles.

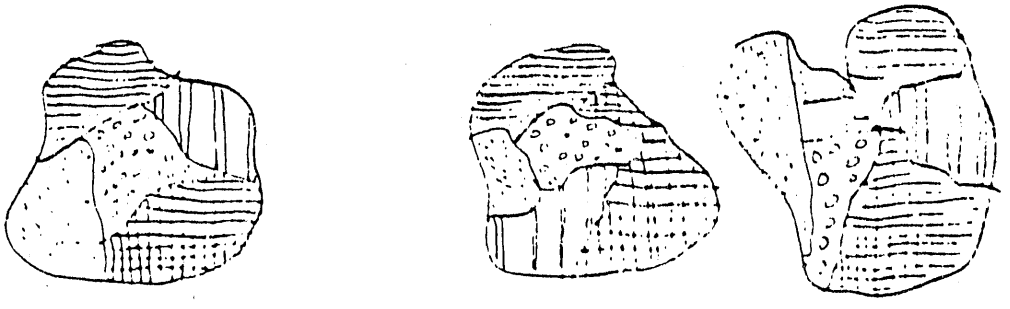

A partition curve obtained from film flotation is indicative of the gross heterogeneity. It cannot be distinguished from the partition curve if the heterogeneity is of the first kind (discussed above) or if it is of the second kind. Curves shown in Figure 16 and Figure 17 below are for illustrating a working hypothesis and are not constructed from experimental data. The working hypothesis is as follows: Construct a partition curve. Remove the material floating on solutions of various concentrations and repeat the experiment.

Figure 16 shows that if the heterogeneity in the population is of the first kind then one can expect a series of partition curves as shown; in other words it would be possible to separate the particles based on their surface features. Figure 16 is the basis of the "gamma flotation" process described earlier in the literature by Hornsby and Leja [37] and Yarar and co-workers [39]. Figure 17 shows the expected response of the second case where it would not be possible to separate the particles based on its critical wetting surface tension values (or its surface features). The mathematical model of the film flotation in terms of the differential free energy analysis has been provided in reference [46]

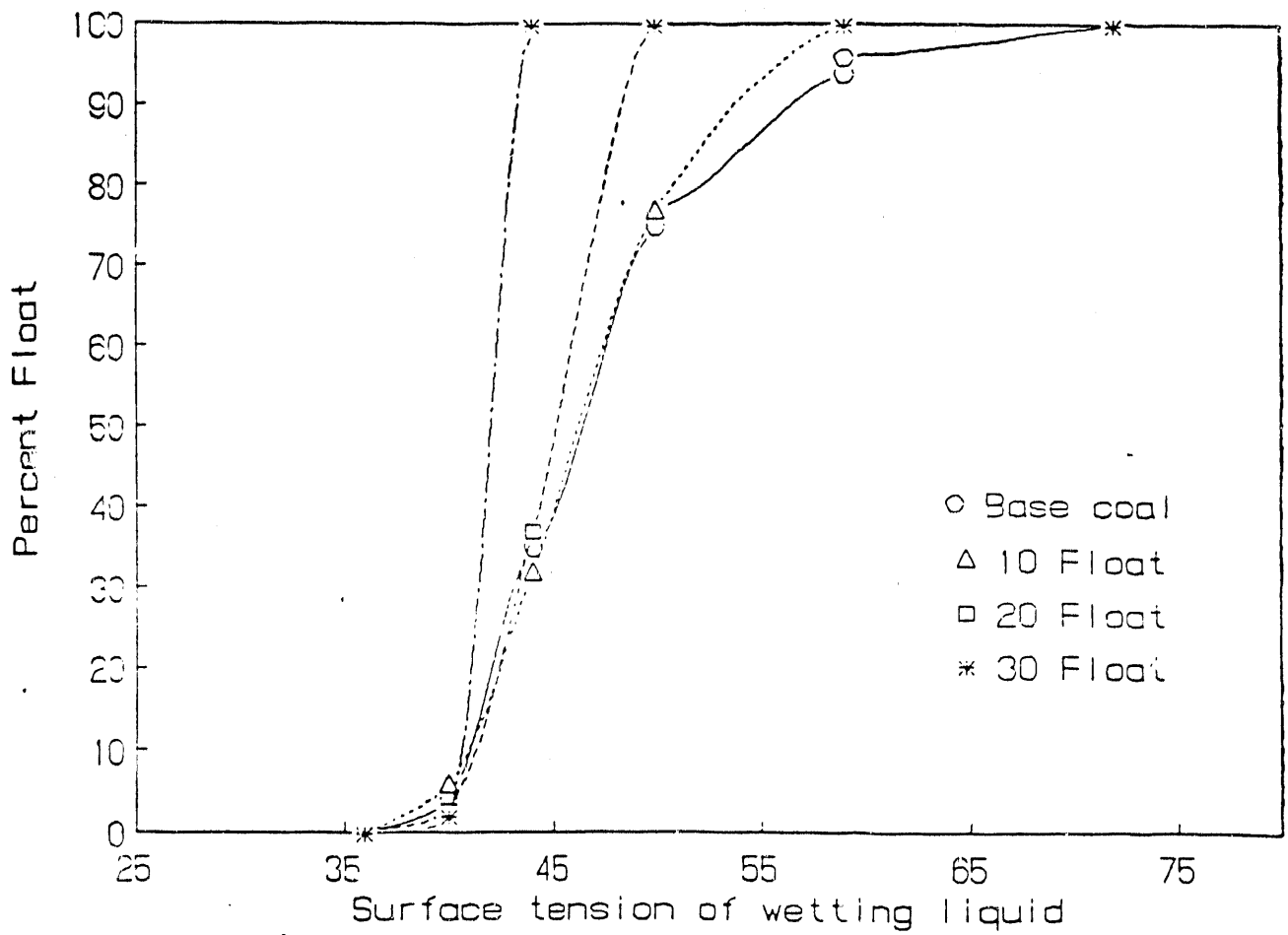

Figure 16: Schematic film flotation partition curves for a heterogeneous mixture of homogeneous particles.

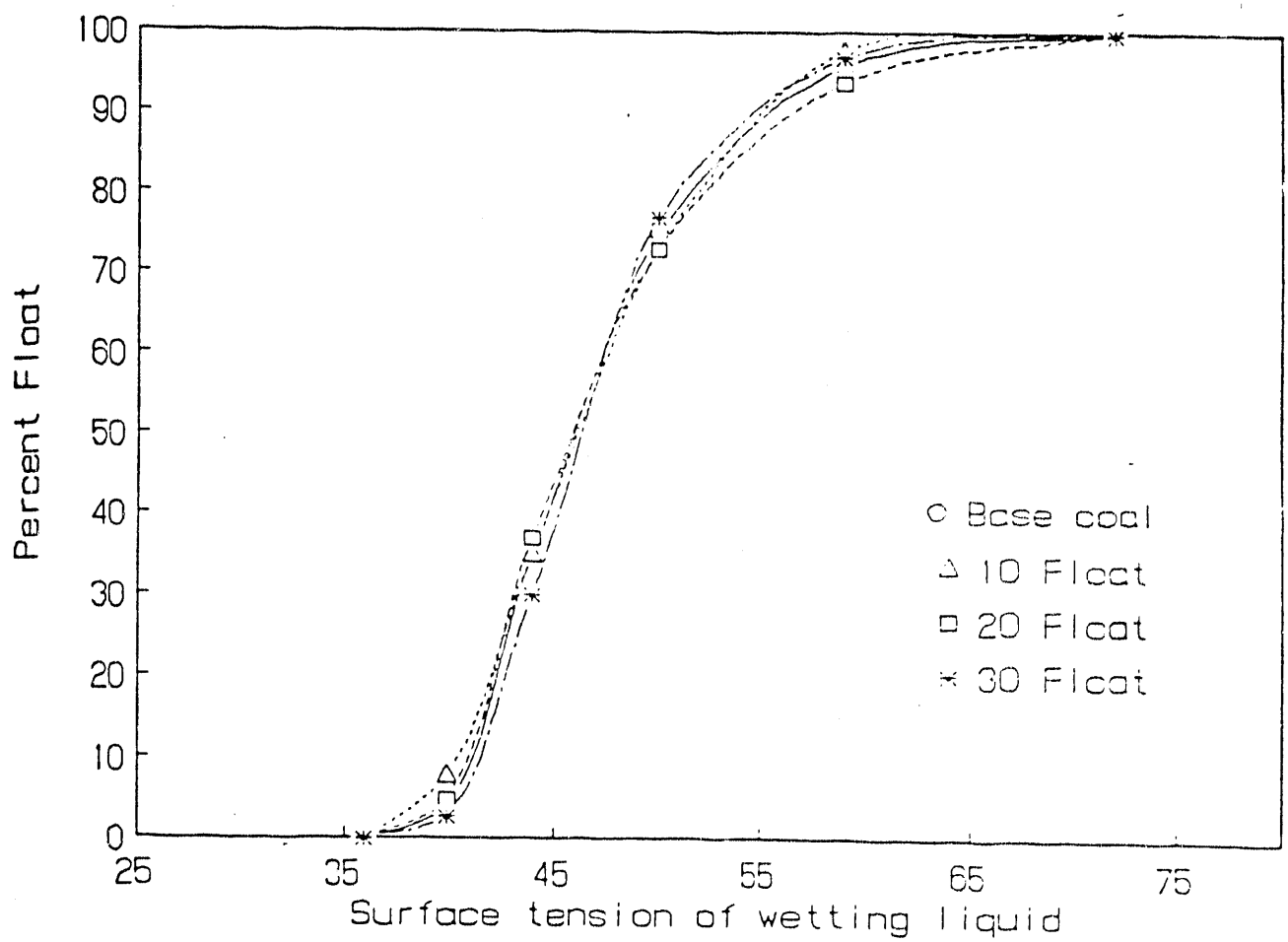

Figure 17: Schematic film flotation partition curves for a population of heterogeneous particles.

The working hypothesis was tested and the results are shown in Figure 18. The data presented in Figure 18 was obtained by doing film flotation experiments using base coal (raw coal), coal samples floating on a 10% vol. methanol-water mixture, those floating on a 20% vol. methanol-water mixture and those floating on a 30% vol. methanol-water mixture. The test itself is described in detail in the experimental section.

Film flotation partition curves provide critical wetting surface tension distributions of particulate samples. Critical wetting surface tension is a measure of the surface energy. Since Figure 18 shows that the heterogeneity of the coal particles is essentially of the second kind (discussed above); i.e. heterogeneous populations in which every particle is heterogeneous, these distributions are representative of the surface energy of individual particles. The surface area distribution is taken to be the same as mass distribution since the process is interfacially controlled (reference [46] provides a sensitivity analysis of the model where it has been established that the interfacial energy contribution to the process is in excess of 85% of the total free energy change). Thus, γ_c partition curves constructed from film flotation data essentially *demonstrate the heterogeneity on the surface of single coal particles* of size -35 +80 mesh.

As an additional test various float fractions from the partition curves were treated with cationic polyacrylamide along with base coal and subjected to film flotation. The results given in Figure 19 show the distribution of energy sites after polymer treatment to be representative of a single particle, since the curves follow the trend indicated in Figure 17.

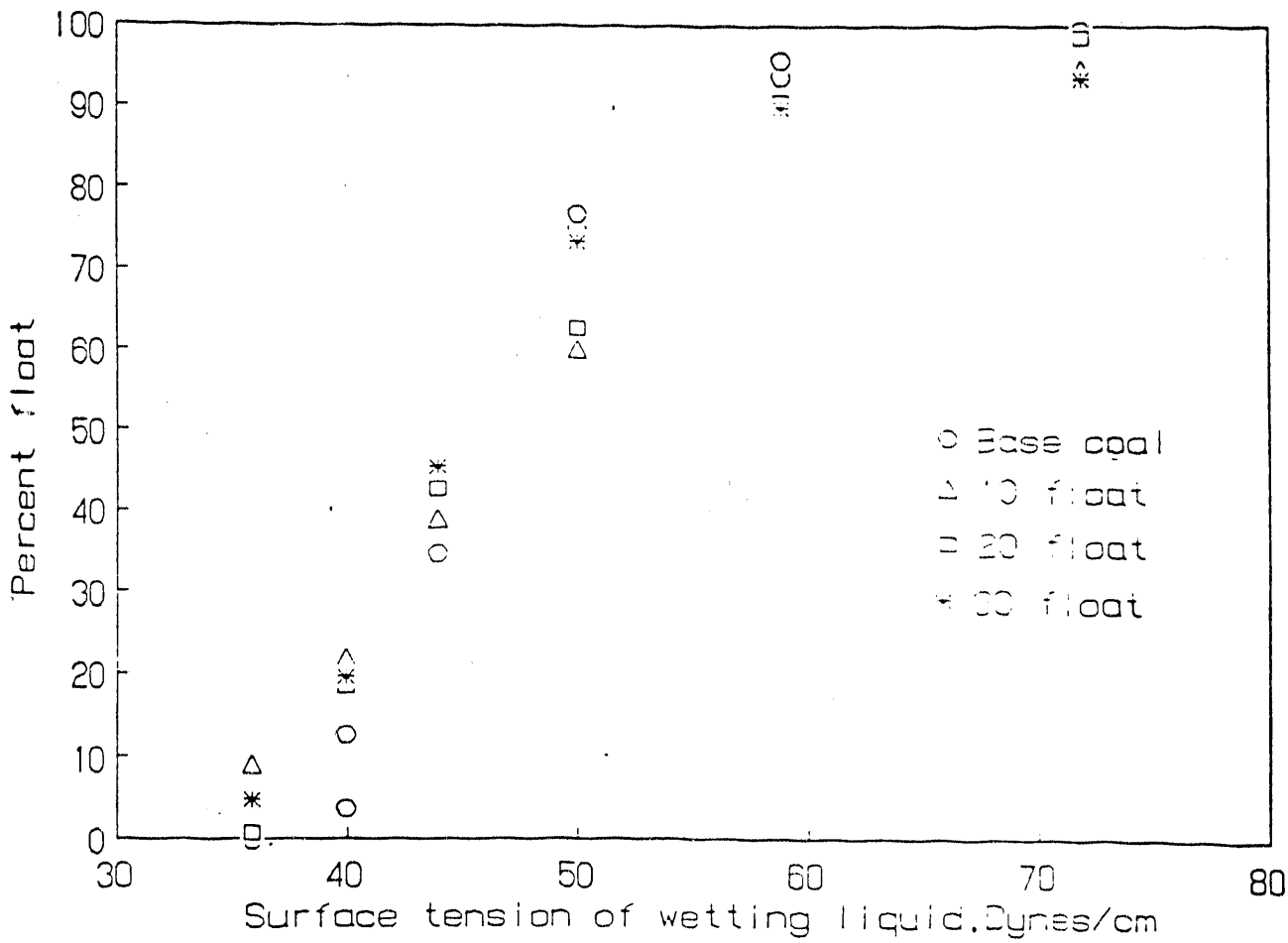

Figure 18: Film flotation partition curves for base coal and various float fractions.

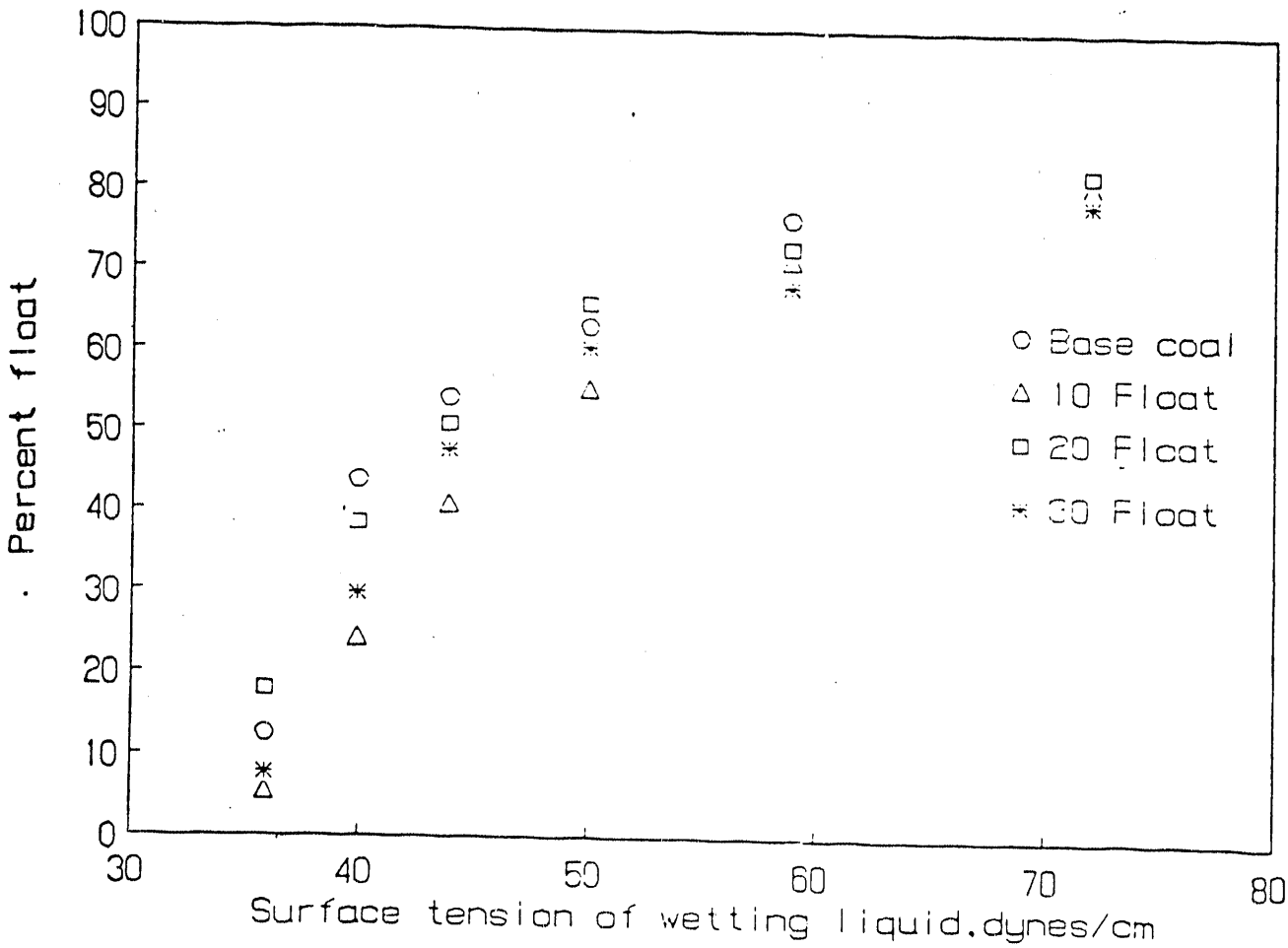

Figure 19: Film flotation partition curves of base coal and float fractions after treatment with 1000 ppm of cationic polyacrylamide for 24 hours

6.3.1 Effect of Oxidation on surface site distributions

The effect of oxidation on the nature of the site distribution curve was examined by heating the coal at 70°C in a convection oven, as a function of time ranging from short periods (in hours; Figure 20) to longer durations (in days; Figure 21). It is observed that the heating of coal results in a marked shift in the site distribution curve towards the region of lower critical surface tension, with the maximum shifting from a γ_c value of around 44 for the base coal to 38 for heated coals. There is also an increase in the area under the peak corresponding to γ_c between 37 and 39, with an increase in the time of heating. The above observations may be explained on the basis of either one or a combination of the three possibilities mentioned below: a) loss of surface volatiles, b) loss of surface moisture and c) change in the structure of adsorbed moisture on coal, after heating.

Experiments were conducted with coal samples subjected to heating in an air heated oven at 70°C and performing film flotation using the hot coal sample, same sample cooled under dessicator and ambient conditions. Experiments were also performed by subjecting a sample which has been heated and cooled to reoxidation at 70°C. Film flotation of coal heated at a temperature of 140°C in a muffle furnace for 24 hours was also performed. Simultaneously base coal smples of coal were placed in a dessicator under vacuum for twenty four hours after which film flotation was performed in order to study the effect of moisture removal on film flotation response.

Film flotation experiments yield information on the percentage of surface area with a particular γ_c value. γ_c values tending towards 72 indicate increased hydrophilicity whereas lower γ_c values indicate increased hydrophobicity. Discussion in the previous paragraph suggested that when coal was heated in air at 70°C for two days the coal surface became more hydrophobic as evidenced by the peak shifts

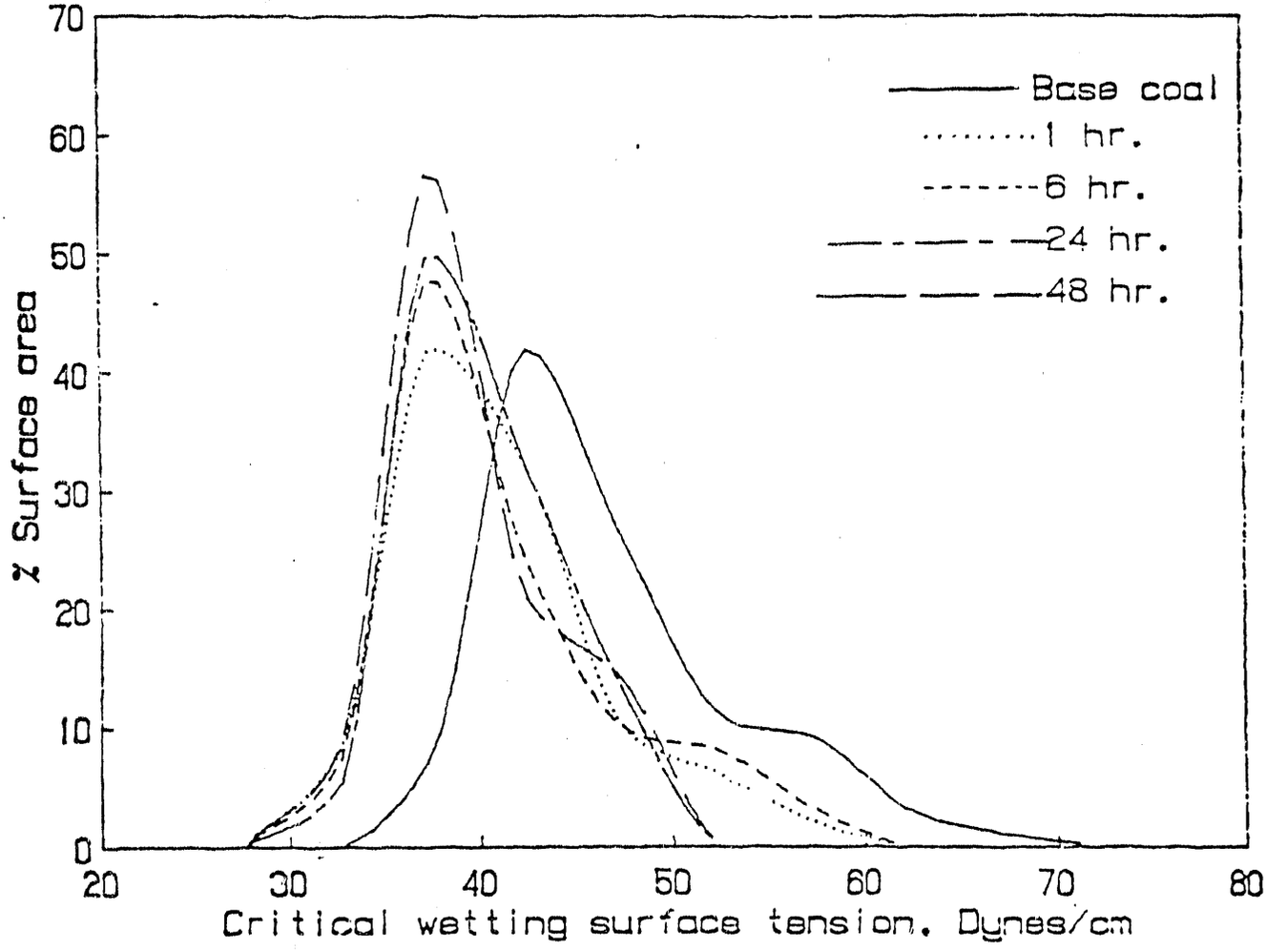

Figure 20: Site distribution curves of base coal and base coal heated at 70°C for different durations (in hours) and cooled under ambient conditions.

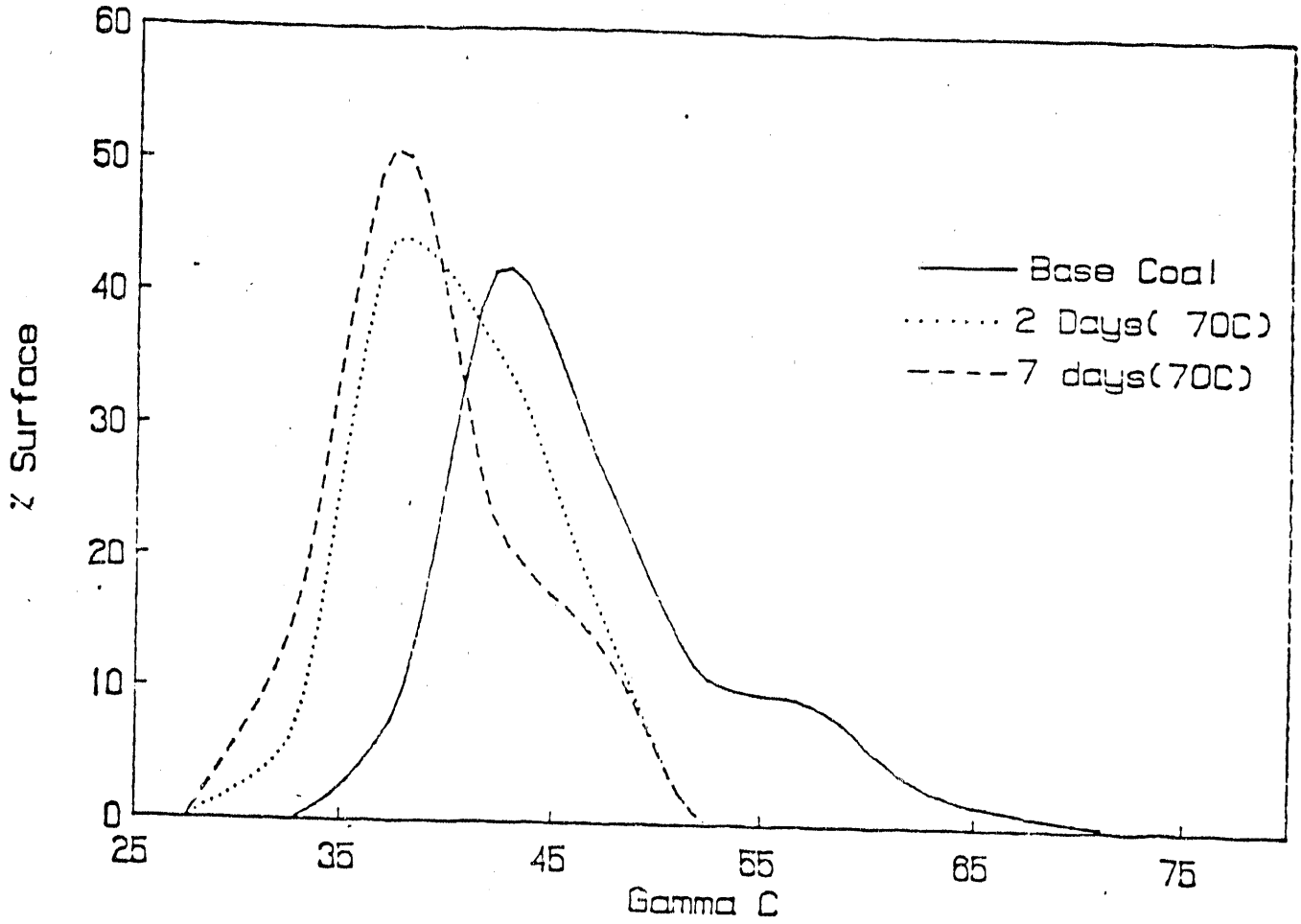

Figure 21: Site distribution curves of base coal and base coal heated at 70°C for different durations (in days) and cooled under ambient conditions.

in the site distribution curves from around 45 γ_c to 36 γ_c. The same trend was noticed upon heating the coal for seven days at 70°C. These curves are reproduced in Figure 22 which also shows the site distribution curve of a coal sample heated in a furnace in air at 140°C for 24 hours. As expected oxidation of the coal renders the coal surface hydrophillic as indicated by the fact that around 12% of the surface area has a γ_c of 72 or more and this surface is spontaneously wetted by water.

It is therefore suggested that 12% of the surface of this sample consists of moieties resembling the structure of water; namely OH groups. An increase in hydroxyl groups on coal surface upon oxidation has already been reported [85]. The site distribution curve of coal oxidized at 140°C shows a wider distribution than the site distribution of base coal or coal heated at 70°C. This wider distribution is indicative of the increase in heterogeneity of this coal surface which is possibly due to difference in the extent of oxidation of the various moieties on the coal surface. Figure 23 shows the site distribution curve for base coal, coal heated to 70°C and cooled under ambient condition and again subjected to 70°C for 2 more days and subsequently cooled (reheated sample). It can be observed that there is no measurable change in the site distribution curves between 26 γ_c and 52 γ_c. This indicates that there is no further increase in hydrophobicity upon reheating. However, there is an increase in the percentage of surface area for γ_c between 52 and 65 indicating the appearance of hydrophilic groups.

It is suggested that the initial heating removes surface moisture and volatiles. During subsequent ambient cooling water adsorbs on the coal. Subsequent reheating removes the adsorbed water and also oxidizes the coal surface renedering it comparatively hydrophilic.

In order to study the effect of inherent surface moisture in coal, samples were placed in a dessicator under vacuum for twenty four hours after which film flotation

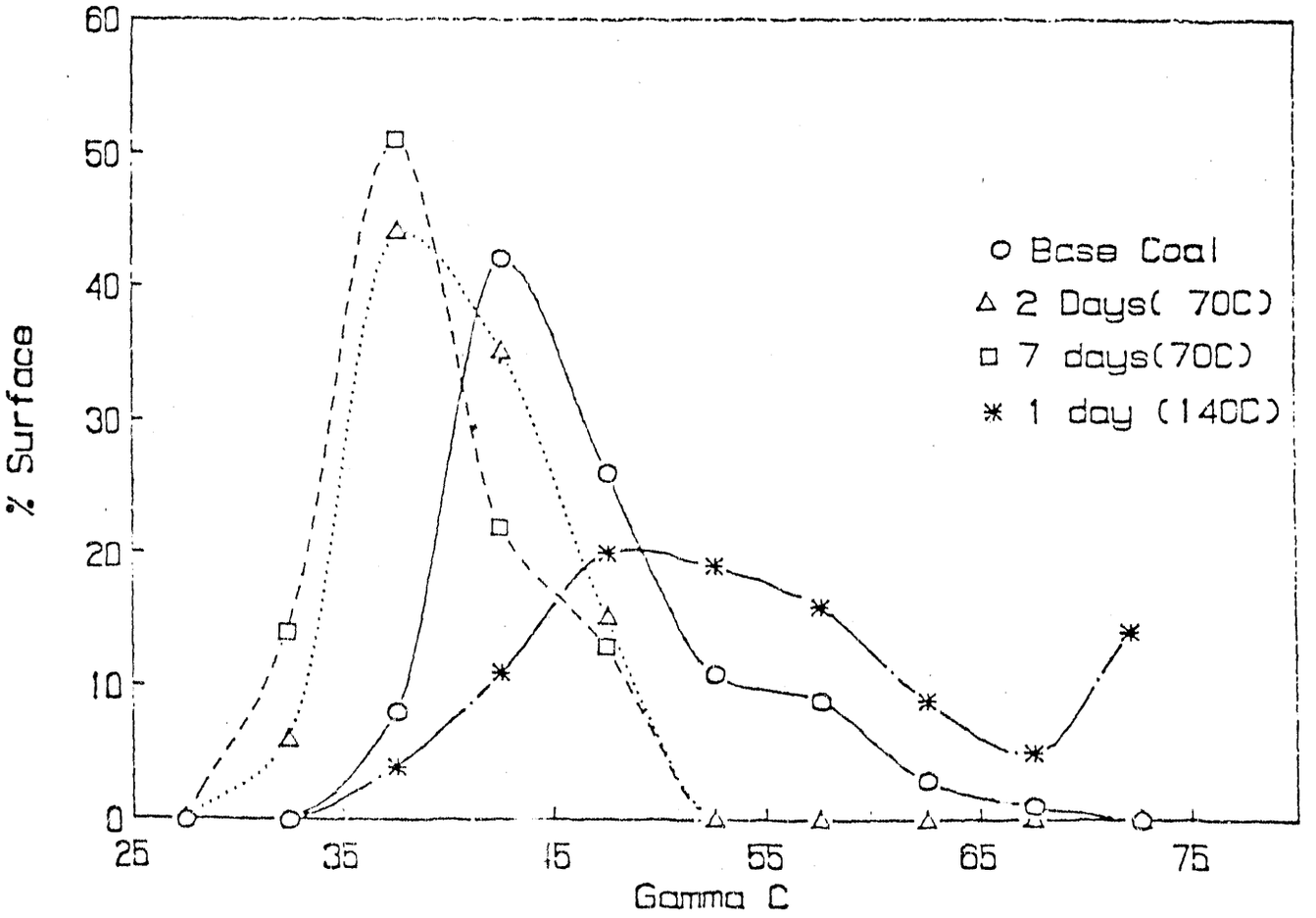

Figure 22: Site distribution curves of base coal and coal heated at 70°C for 2 days and coal heated at 140°C for 24 hours.

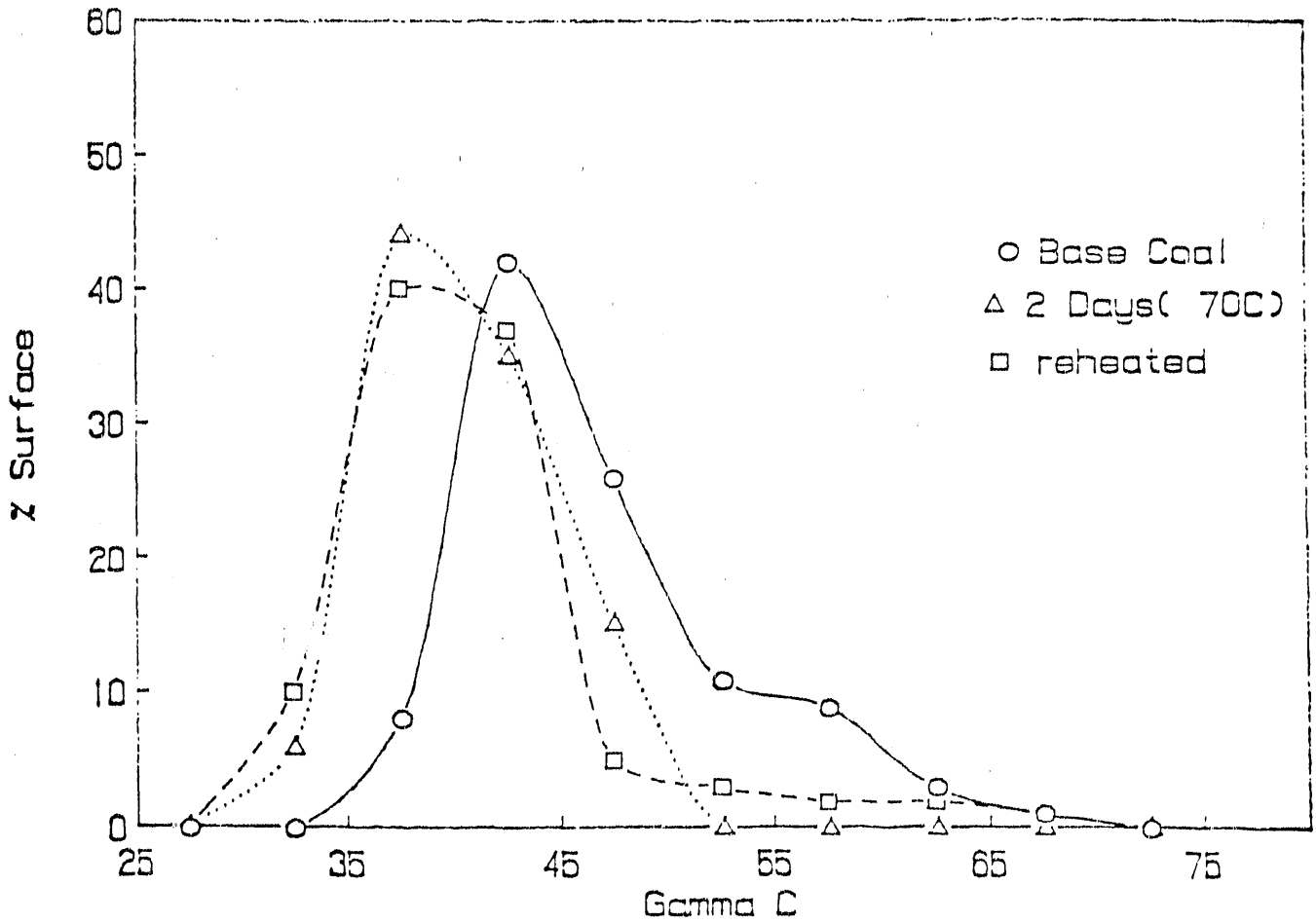

Figure 23: Site distribution curves of coal heated at 70°C for 2 days and cooled under ambient conditions, and the same sample reheated at 70°C for 2 days and cooled under ambient condition.

was performed. The site distribution curve obtained is shown in Figure 24 along with those for base coal. It is noticed that there is no shift in the peak at around 44 γ_c of base coal compared to that for dessicated coal; however, the area under the peak increases in the case of the dessicated sample. This increase is concomitant with the decrease in the area of surface sites with γ_c values between 47 and 72 and can be attributed to removal of water in the dessicator. One would have expected a γ_c of 72 for free moisture resembling water. However, in view of the wide range of γ_c values for inherent surface moisture, it is suggested that the surface moisture is present in a heterogeneous but ordered structural form.

Figure 25 gives the site distribution curve for coal heated to 70°C without cooling, the same sample cooled under ambient condition and in a dessicator, to show the effect of moisture which adsorbs during cooling. The sample cooled in the dessicator shows only a marginal increase in hydrophobicity whereas a significant increase in hydrophobicity is seen for the sample cooled under ambient conditions. This is possible if the adsorbed water exhibits autophobicity possibly due to ordering in the adsorbed water layer. Recent nuclear magnetic resonance (NMR) relaxation studies of moisture in coal indicates a range of heterogeneous water environments to exist rather than a single homogeneous phase [111]. The results presented in this section tend to support this observation and also are indicative of the ability to derive sensitive information from such analyses.

6.3.2 Surface Modification:Polymer Adsorption

Polyacrylamide is used in the flocculation of fine coal particles and was hence used to modify coal surfaces. The properties of coal surface thus modified are discussed in subsequent sections. In this section adsorption of polyacrylamide on coal is discussed. Adsorption isotherm and kinetic data were generated by the depletion

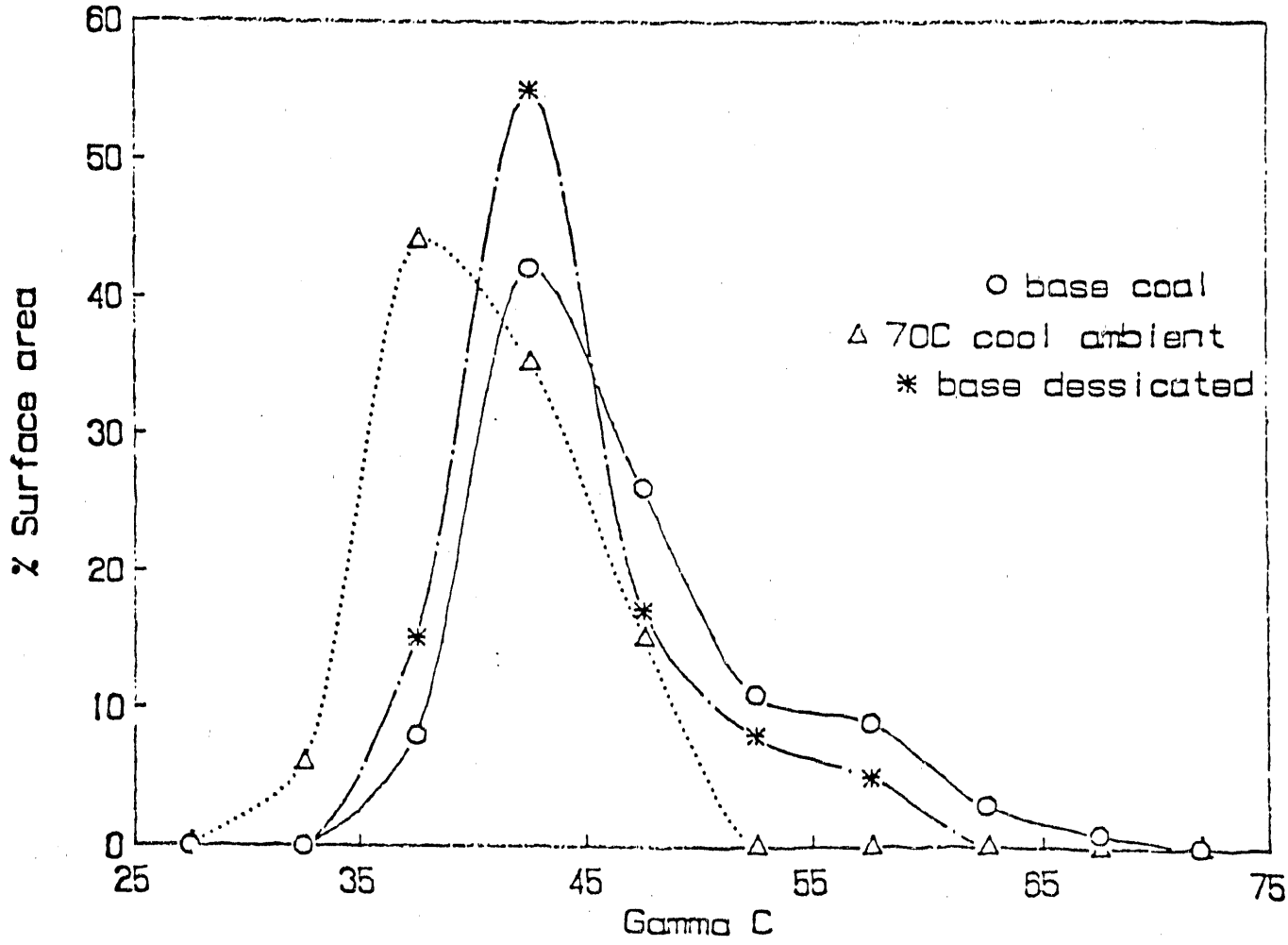

Figure 24: Site distribution curves of coal sample placed in a dessicator under vacuum for 24 hours.

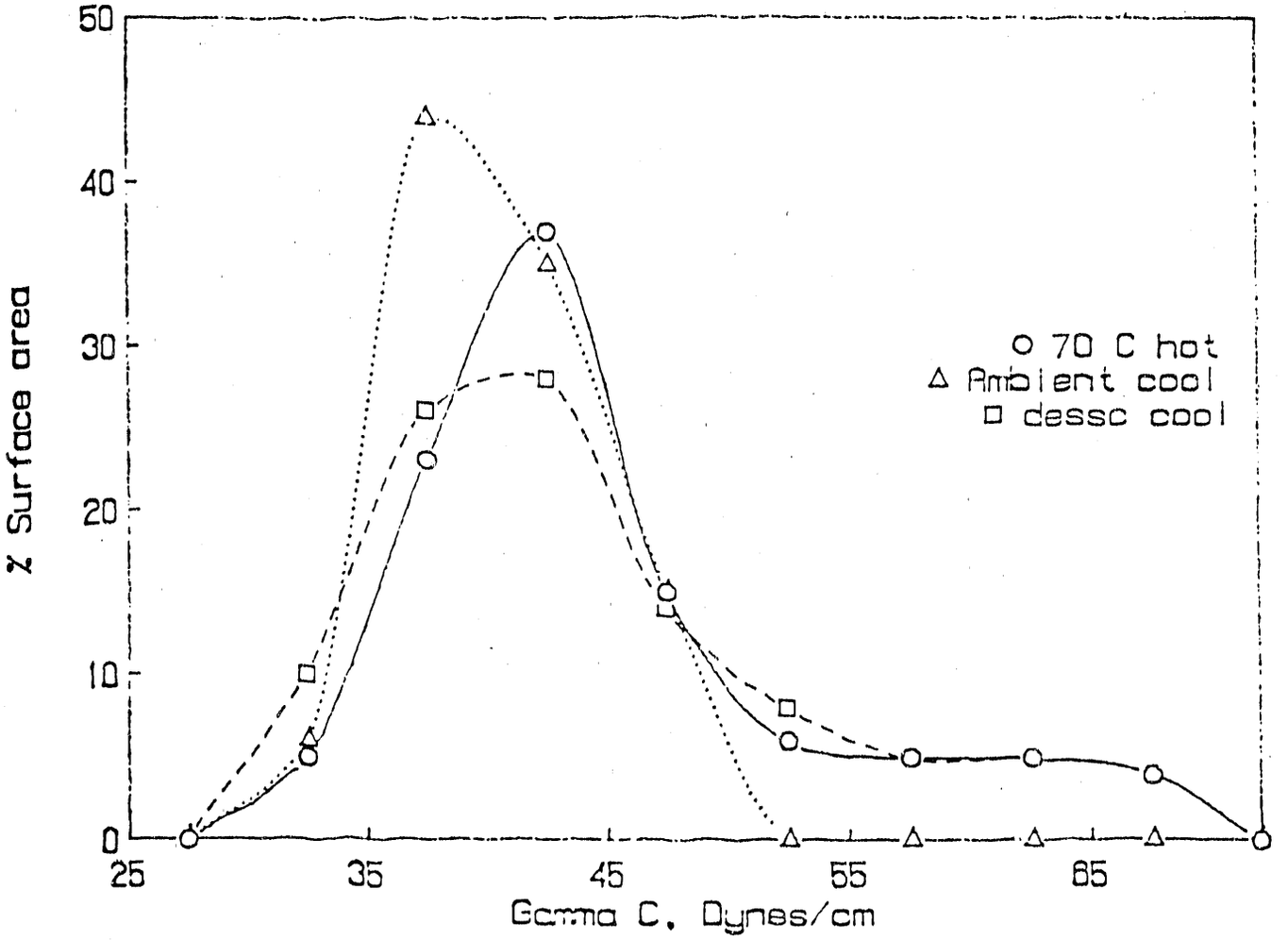

Figure 25: Site distribution curves of coal heated at 70°C for 2 days without cooling, cooled in a dessicator under vacuum and cooled under ambient condition.

technique.

Initially concentration of polyacrylamide (PAM) in the supernatant was determined using a Ubbelohde viscometer. The viscometer was calibrated for the polymer under study and the equation of best fit used to determine residual concentrations. All experiments were done at 25°C in a temperature controlled bath. It was found that Ubbelohde viscometer is unsuitable for determing residual polymer concentrations in the case of PAM of higher cationicity (34%) and anionic PAM (30% anionicity) due to a nonlinear relationship between concentration and drain times, and therefore the adsorption data using this method were obtained only for PAM of 10% cationicity and nonionic PAM.

During the preliminary experiments it was also observed that fines were generated while conditioning on a wrist action shaker. Hence experiments were conducted under static conditions with the vials being gently inverted by hand three times every 24 hours.

Kinetics of adsorption of cationic PAM on coal was examined first and is shown in Figure 26. The results show a large degree of scatter which is probably due to the inherently heterogeneous nature of coal. Previous work in our laboratory on the kinetics of PAM adsorption on oxide minerals has shown equilibrium to reach in 400 minutes [112]. However, in the present case the kinetic study of adsorption of cationic PAM show that equilibrium is reached only in 2000 minutes. In view of the scatter (see Figure 26), residual concentration measurements for obtaining adsorption isotherm were conducted only after 10,000 minutes in order to ensure equilibrium.

Figure 27 shows the adsorption isotherms of cationic polyacrylamide of 10% cationicity and nonionic polyacrylamide on coal. Both the isotherms are of the high affinity type typical of polymer adsorption. Adsorption of nonionic PAM is

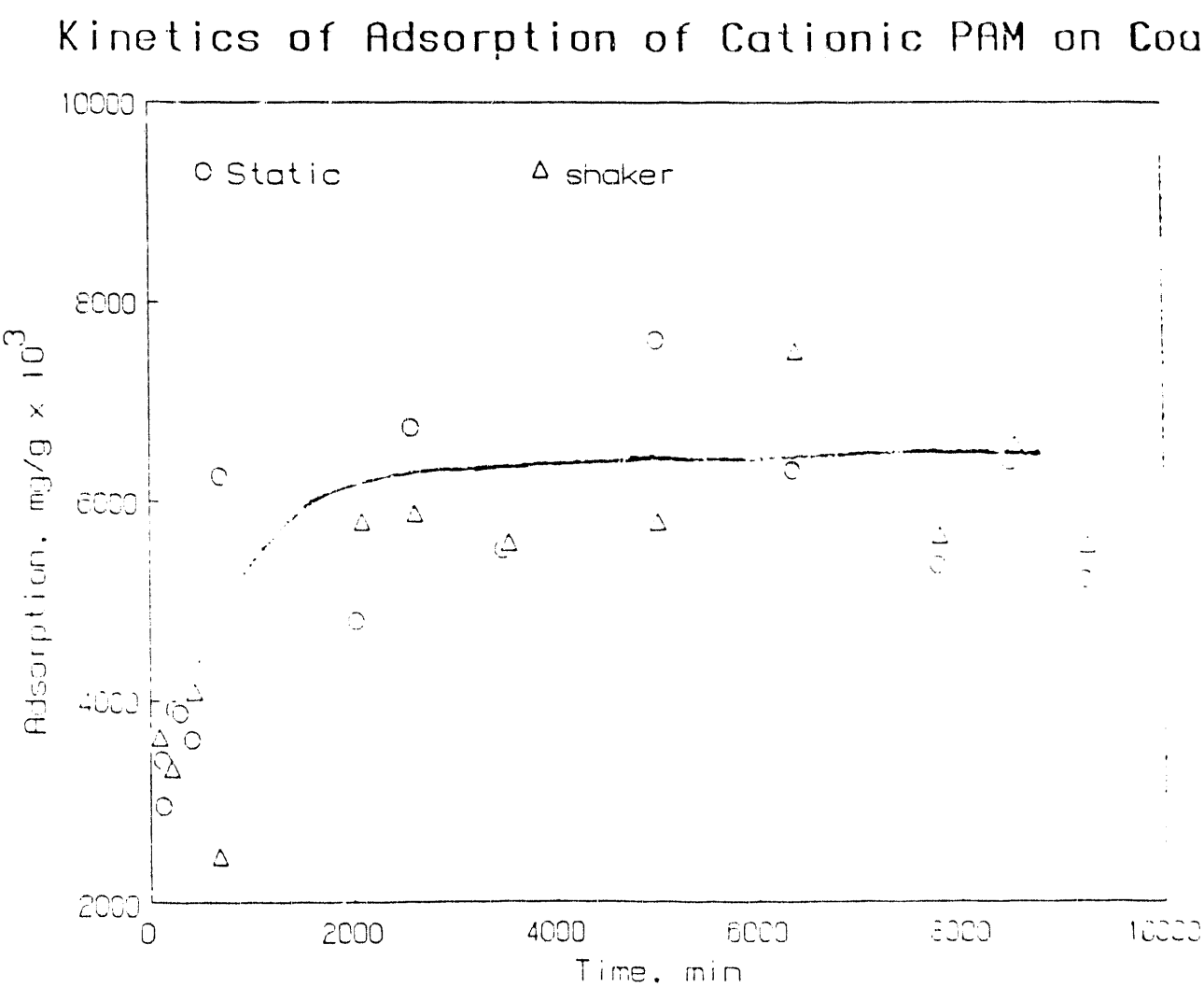

Figure 26: Kinetics of adsorption of cationic polyacrylamide on coal.

essentially by hydrogen bonding as the polymer is not expected to have any residual charge. The adsorption density of cationic PAM in the initial portion of the isotherm continues to rise steeply till a plateau value equal to that of the nonionic PAM isotherm is reached. This indicates that the initial adsorption of polyacrylamide is by hydrogen bonding. In the case of the cationic PAM, the polymer being positively charged adsorbs on the few available negative sites on coal in addition to adsorption by hydrogen bonding. The continuing increase in the adsorption density of cationic PAM is due to possible conformational changes of the polymer adsorbed by hydrogen bonding. Effect of porosity, polydispersity and polymer migration will also contribute to the slow increase in adsorption.

As mentioned earlier residual polymer concentration measurement by Ubbelhode viscometer could not be adopted in the case of polyacrylamide polymers of high charge density. In view of this a Total organic carbon (TOC) analyzer was acquired and since this enables a more accurate determination of residual polymer concentration, adsorption experiments were repeated. Figure 28 shows the adsorption isotherm for nonionic, cationic (10% and 34% cationicity) and anionic polyacrylamides (30% anionicity) in which the adsorption density was calculated from residual polymer concentration obtained using the TOC analyzer.

Comparison of Figure 27 and Figure 28 shows that plateau adsorption values obtained using viscosity measurements are one order of magnitude high . than those obtained using TOC. However, both methods yield typical high affinity type isotherms. The higher values of adsorption using viscosity measurements indicate that there is preferential adsorption of polymer of certain molecular weight components. It is suggested that the higher molecular weight component adsorbs preferentialy under equilibrium conditions used in the present experiments. This leads to a supernatant (after adsorption) containing a larger proportion of low molecular weight components and therefore lower drain times which in turn yields lower cal-

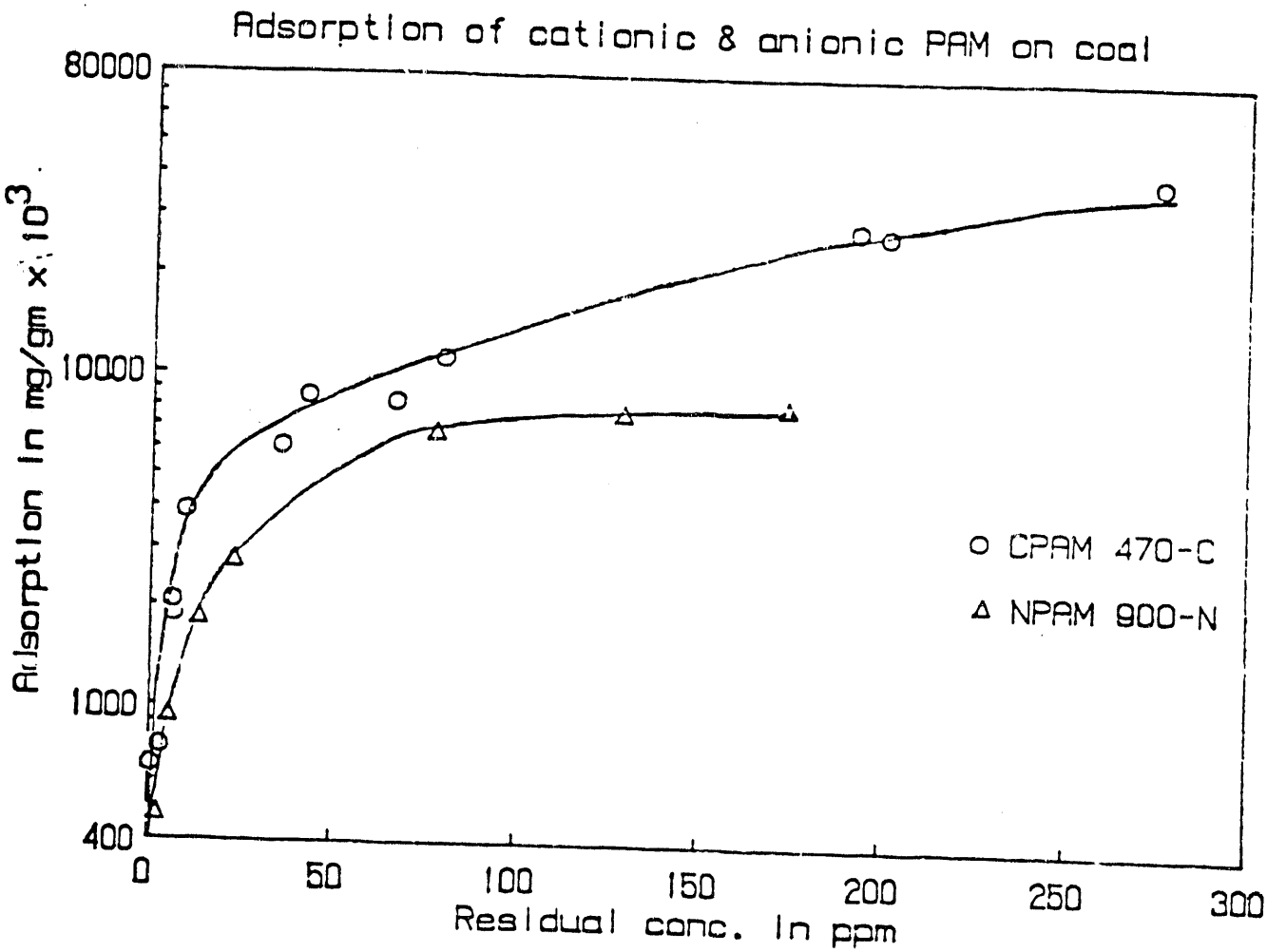

Figure 27: Adsorption isotherm of 10% cationic polyacrylamide and nonionic polyacrylamide on coal based on residual concentrations measued by Ubbelhode viscometer.

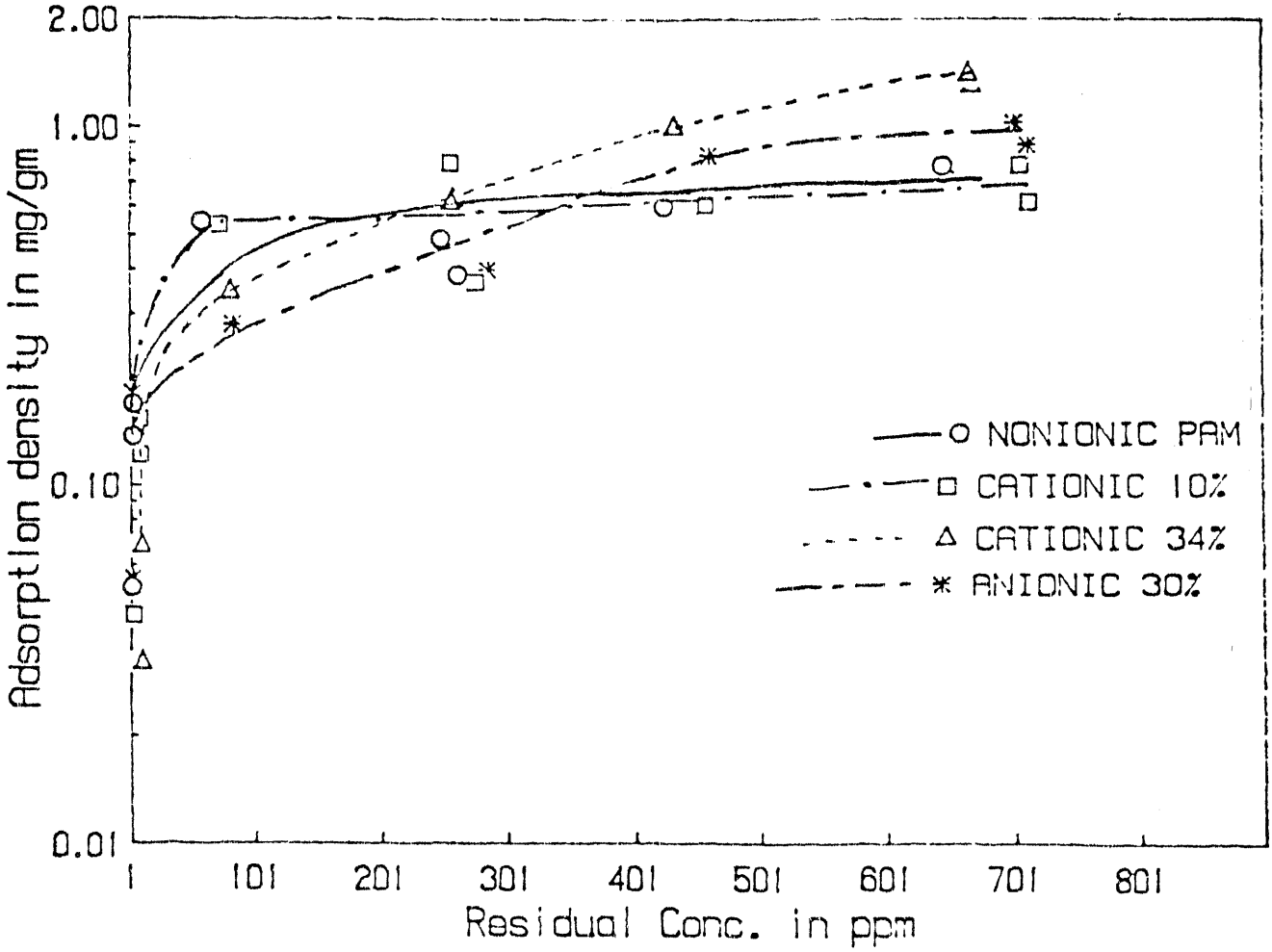

Figure 28: Adsorption isotherms of polyacrylamide of various charge densities on coal based on residual concentration measurement using a Total Organic Carbon analyzer.

culated residual concentration and higher adsorption density. Since the polymers used are of commercial quality, polydispersity is to be expected. Evidently, adsorption data obtained using TOC method will be more representative of the actual adsorption.

The adsorption isotherms for cationic polyacrylamide (34% cationicity) and anionic polyacrylamide (30% anionicity) show continued increase in adsorption density. As mentioned earlier effect of coal porosity, polydispersity and polymer migration and changes in conformation will contribute to the slow increase in adsorption density.

Fluorescence spectroscopy has recently been shown to be a powerful tool to investigate adsorbed layers [113]. Essentialy the technique consists of using a probe molecule (typically pyrene) attached to the polymer of interest and subsequently following the response of the probe molecule to systematic vaiations in the adsorbed layer environment. The fluorescence spectra of pyrene labelled polyacrylamide solution, supernatant of the solution after adsorption and the coal slurry after adsorption are shown in Figures 29, 30, 31 respectively. The presence of an excimer peak at 492 nm in Figure 29 indicates that the polyacrylamide molecules in the solution are in coiled form [113]. The formation of an excimer is due to interaction between an excited and unexcited pyrene on the same molecule. Higher molecular weight components of the polymer are likely to have more intramolecular pyrene than lower molecular weight components. Comparison of Figures 29 and Figure 30 reveals that the excimer intensity of the supernatant is significantly reduced after adsorption. This indicates that the supernatant of the polymer after adsorption has a significantly larger proportion of lower molecular weight components than the original solution suggesting preferential adsorption of higher molecular weight components. These results are in agreement with the above adsorption studies.

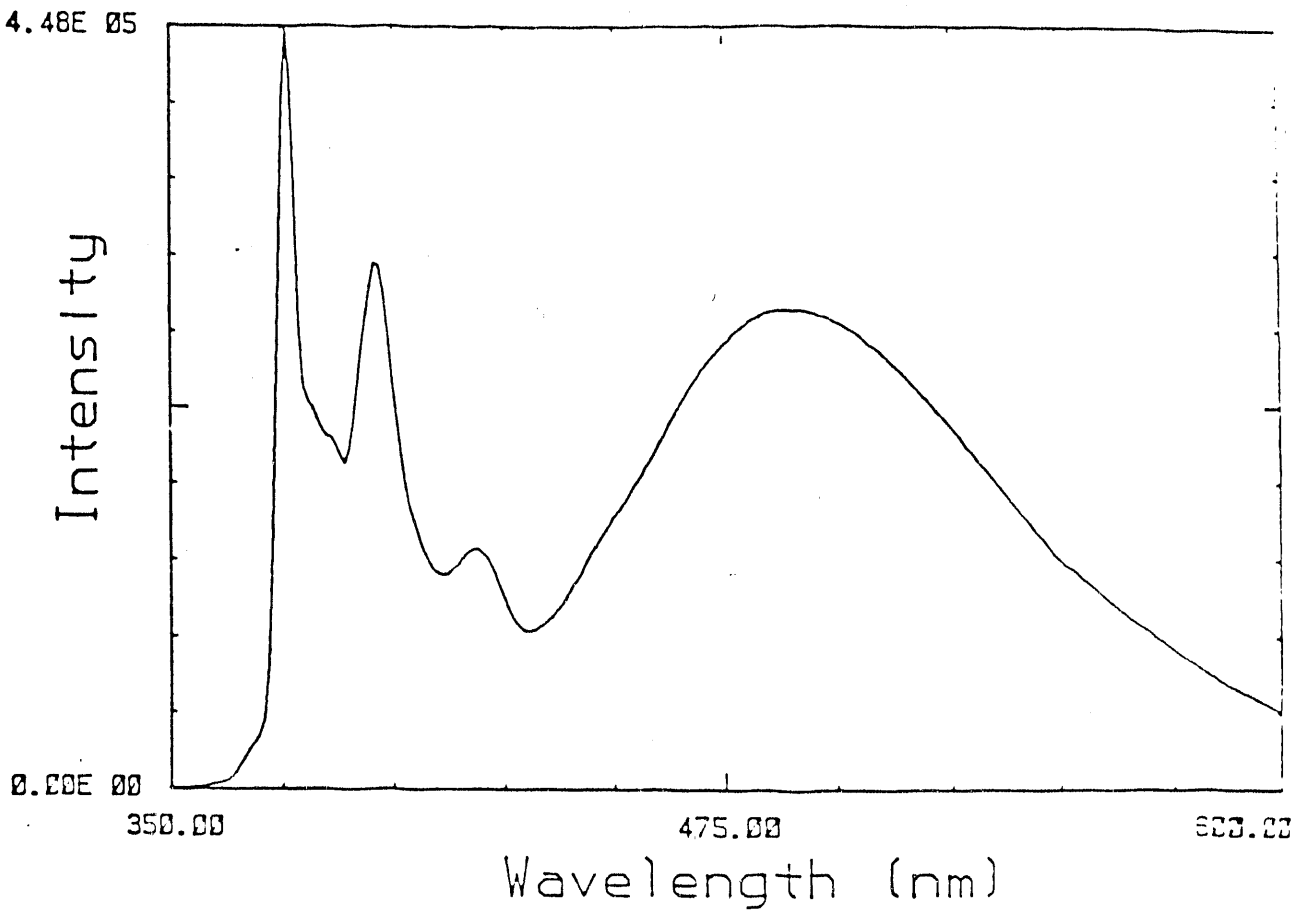

Figure 29: Fluorescence emission spectrum of pyrene labeled polyacrylamide in solution.

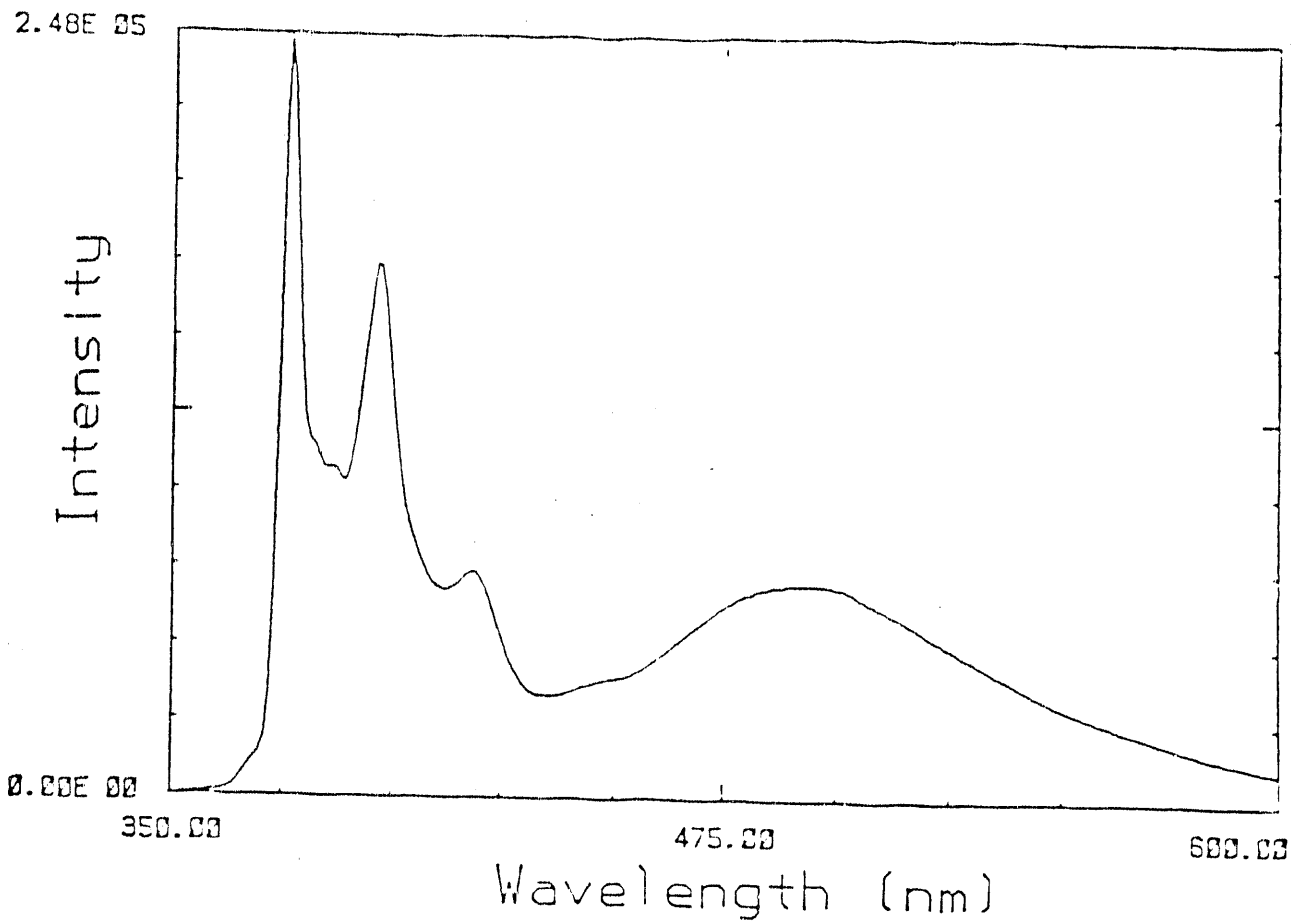

Figure 30: Fluorescence emission spectrum of pyrene labeled polyacrylamide in supernatant after adsorption.

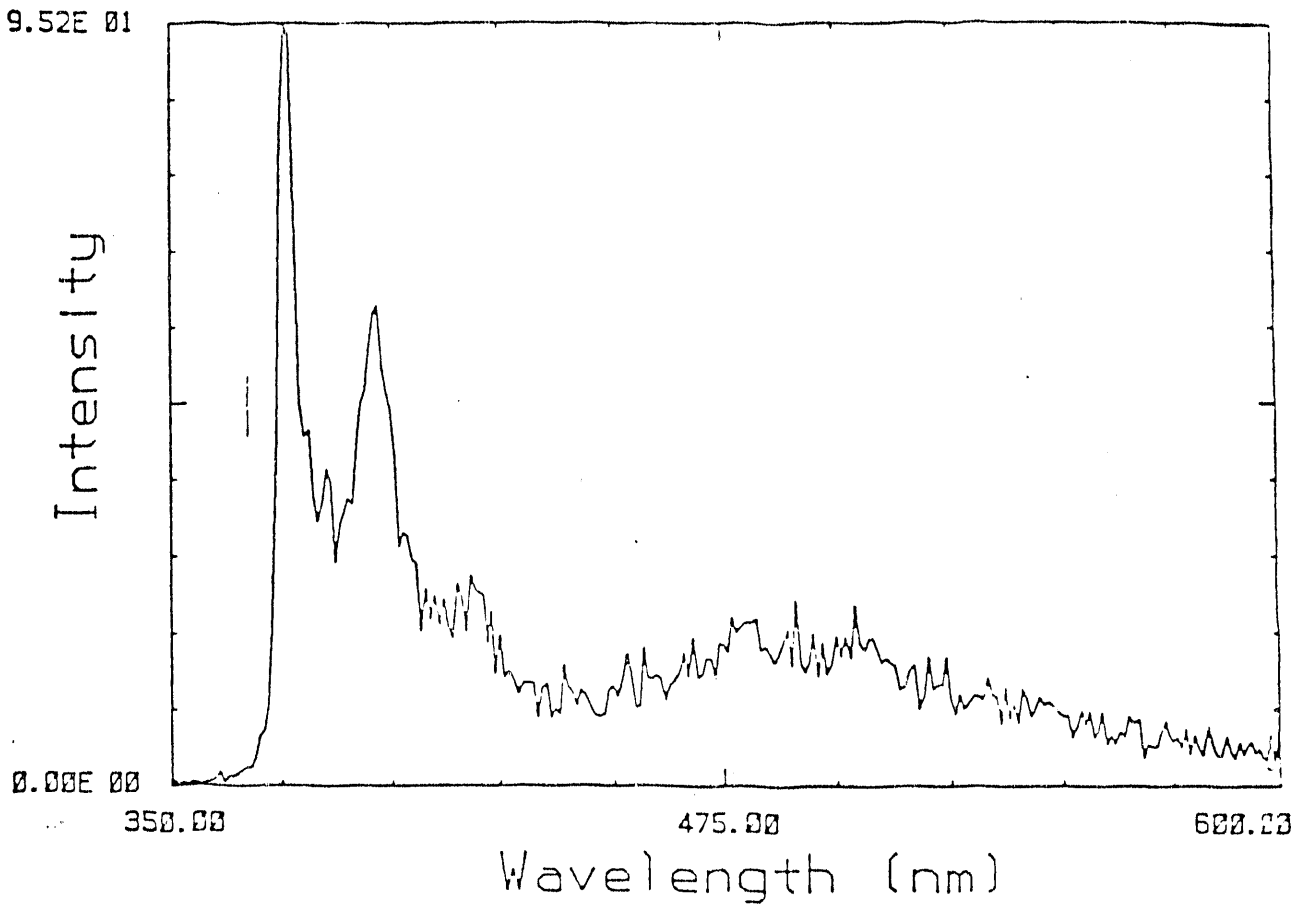

Figure 31: Fluorescence emission spectrum of pyrene labeled polyacrylamide adsorbed on coal.

Wavelength^{-1}	Assignement
3600	OH stretching
3300	N-H stretching and OH (H bonded)
3000 to 2900	Aromatic C-H stretch, Aliphatic C-H stretch
1600	Aromatic ring C = C vibration enhanced by oxygen groups
1460	Aliphatic CH_2 bending
1250	C-O or C-O-C
850	Aromatic C-H out of plane bending

Table 2: Major infrared peak assignments for coal.

As seen from Figure 31, the intensity of the flourescence emmision is extremely low to draw any meaningful conclusion regarding polymer conformation on the coal surface. This low intensity of emission is due to the high absortivity of light by coal.

Diffuse Reflectance Infrared Fourier Transform Spectroscopy (DRIFT) was used to study polymer treated coal surfaces. Figure 32 shows DRIFT spectrum of the coal sample used in the present study.

The spectrum is typical of bituminous coal. The major peaks and their assignments are shown in Table 2 [114].

Figures 33, 34, 35 show the DRIFT spectra of commercial grade nonionic polyacrylamide, and cationic polyacrylamide of 10% and 34% cationicity respectively. All spectra show the characteristic N-H stretching peak at about 3300 cm^{-1}, C-H stretching at 2900 cm^{-1} and a broad peak at 600 cm^{-1} attributed to N-C=O bending [115]. The peaks at 1640 cm^{-1} and 1450 cm^{-1} are assigned to C=O stretching and CH_2 bending vibrations respectively.

In the case of nonionic polyacrylamide a peak at 1300 cm^{-1} is noticed along with a shoulder at 1100 cm^{-1} whereas the spectrum for 10% cationic polyacrylamide shows two distinct peaks at these wavenumbers and in the case of 34% cationic polyacrylamide a broad band is noticed in this region. It appears that the intensity of the peak at 1100 cm^{-1} increases relative to that of the peak at 1300 cm^{-1} as the

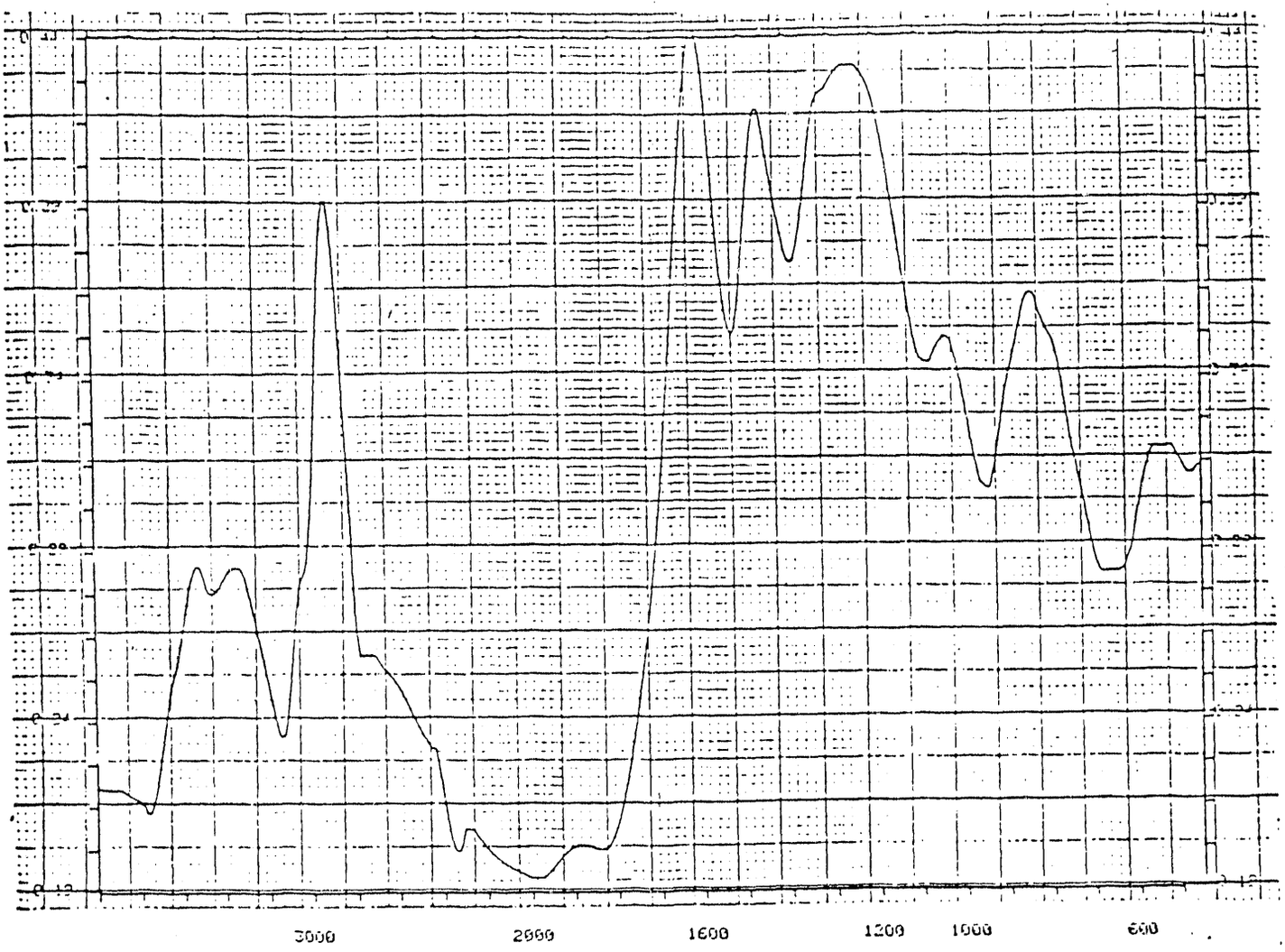

Figure 32: DRIFT spectrum of bituminous coal used in this study.

cationicity increased. Also, a small but recurring peak is noticed at 2100 cm^{-1} in all the spectra.

Figures 36, 37, 38 show the difference spectra of base coal and coal treated with 1000 ppm of polyacrylamide. These spectra are different from the spectra of polyacrylamide crystals shown in Figures 33, 34, 35, indicating that the adsorbed polymer exists in a different state. However, it is seen that in all these cases the difference spectra contain contribution from the coal as well as the polymer. This aspect renders interpretation of the adsorbed state difficult from the IR spectra.

6.3.3 Effect of surface modification on surface site distributions

Film flotation experiments were conducted as described earlier using the base coal and polymer treated samples. The experimental technique involved sprinkling of coal (typically 0.25 gm) on water-methanol mixtures of varying concentrations. The resulting float and sink fractions were separated by decantation and dried under ambient conditions and weighed. The weights recorded were used to construct cummulative site distribution curves. Polymer treated coal samples were obtained by conditioning 2 gms of coal in water for one hour in scintillation vials after which a known concentration of PAM solution was added and further conditioned for 48 hours, followed by filtering and drying of the solids under ambient conditions.

Nature of coal surface upon adsorption of PAM: Figure 39 shows the γ_c distribution curves of base coal and coal treated with nonionic polyacrylamide, cationic polyacrylamide of 10% and 34% cationicity and anionic polyacrylamide of 30% anionicity. An interesting observation is the absence of bound or hydrated water characterized by a γ_c of 72, on the surface of coal treated with the cationic polyacrylamide of 34% cationicity and the anionic polyacrylamide. It appears that

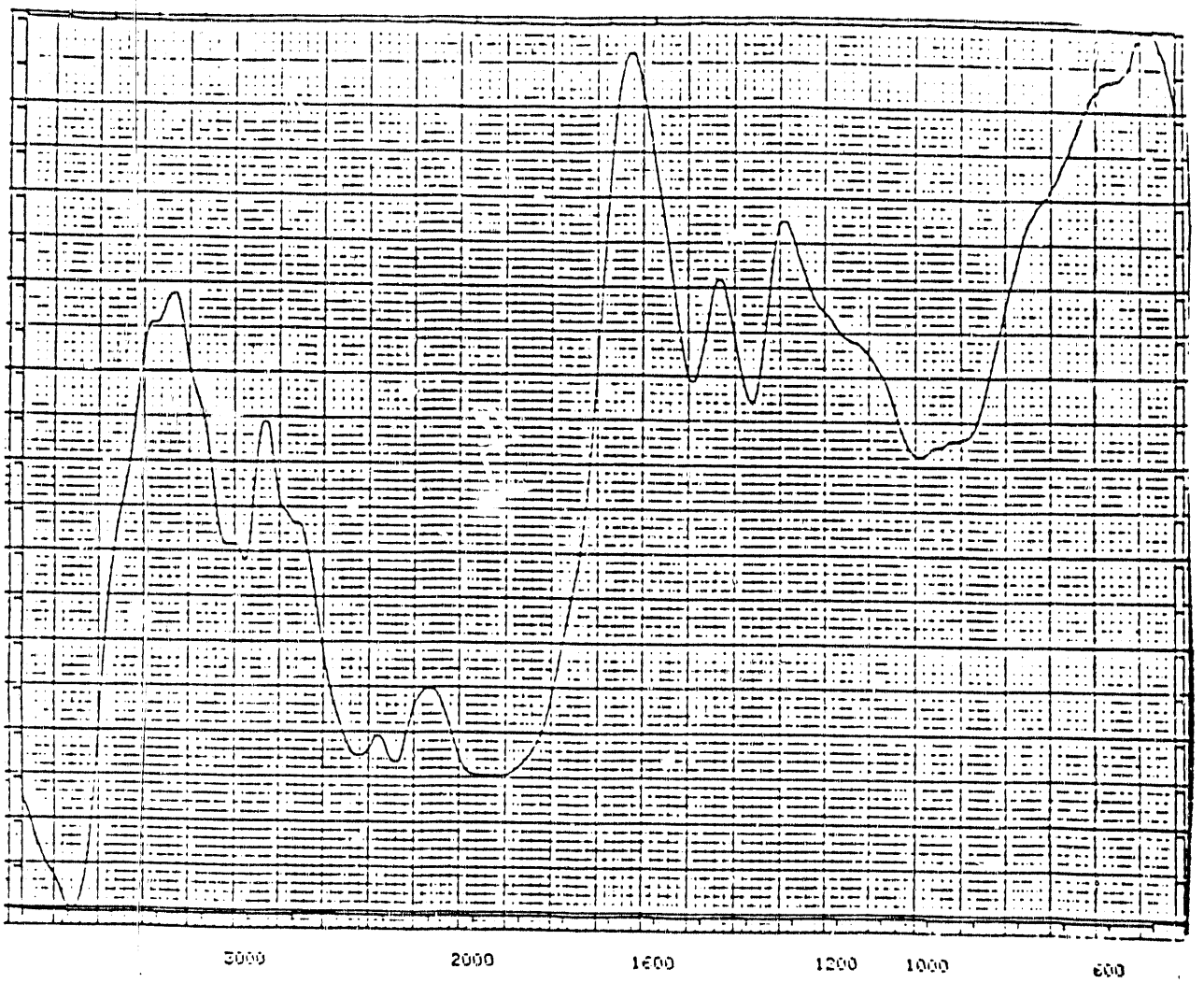

Figure 33: DRIFT spectrum of commercial grade nonionic polyacrylamide

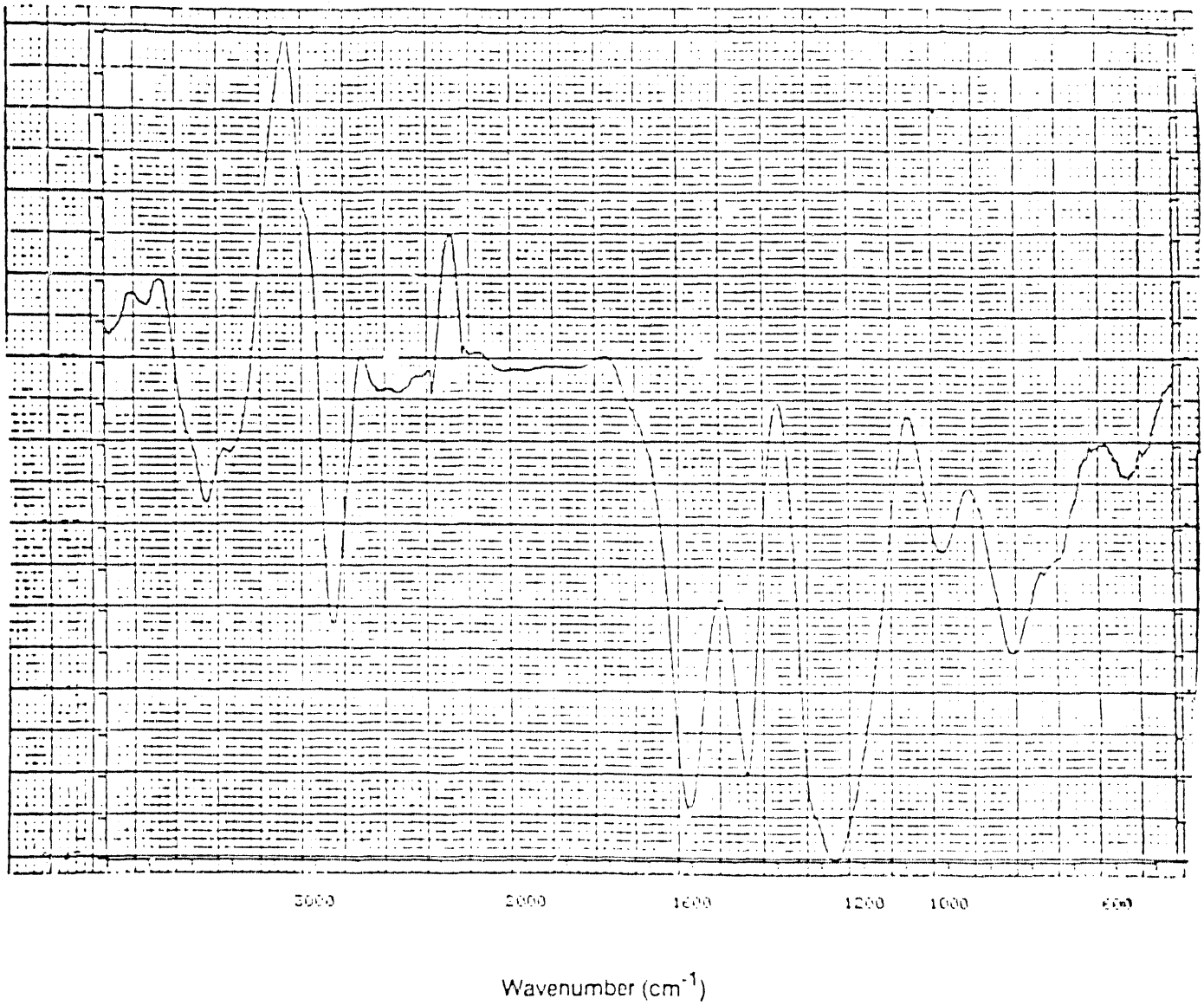

Figure 34: DRIFT spectrum of commercial cationic polyacrylamide (10% cationicity) coal used in this study.

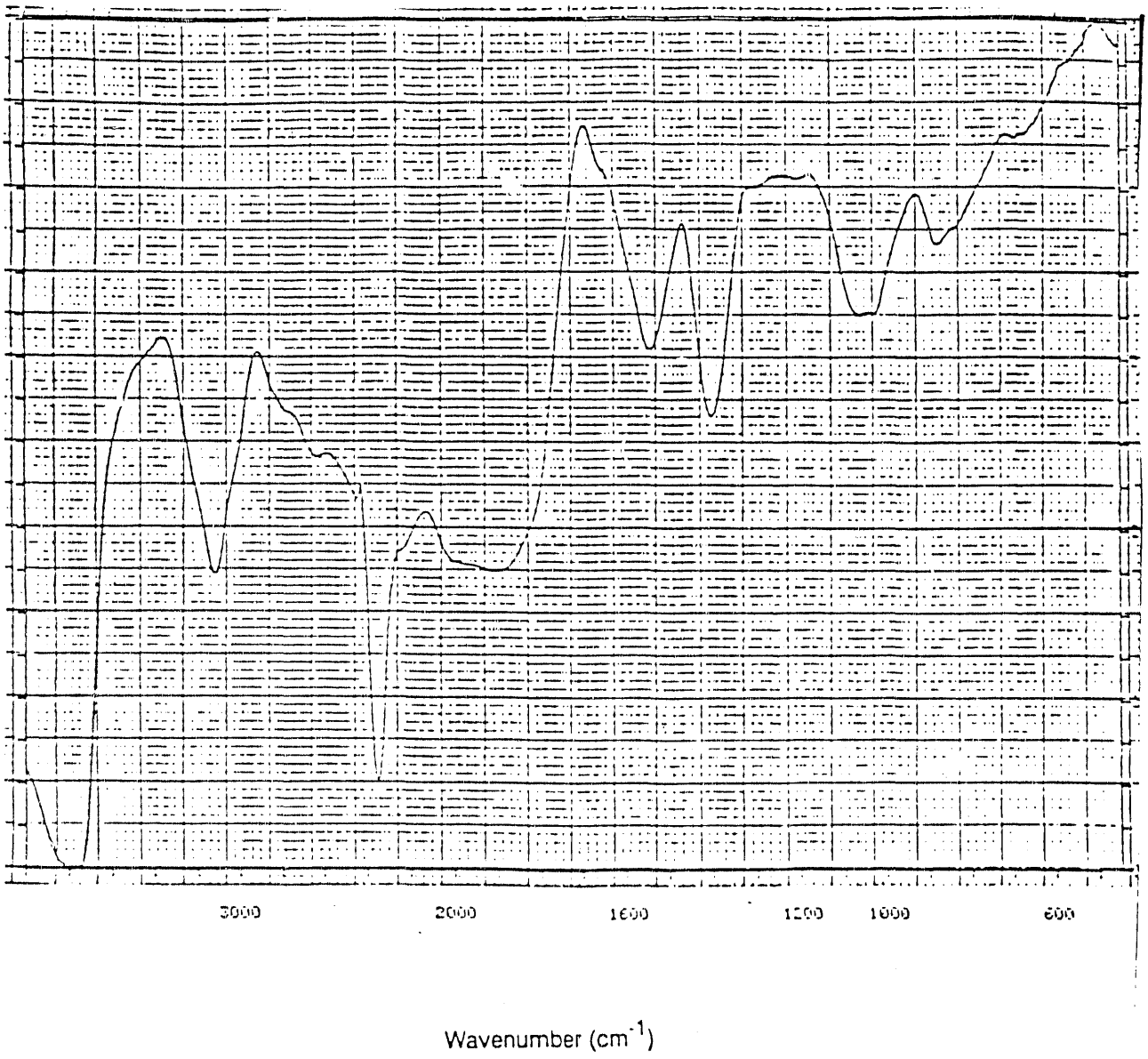

Figure 35: DRIFT spectrum of commercial cationic polyacrylamide (34% cationicity) bituminous coal used in this study.

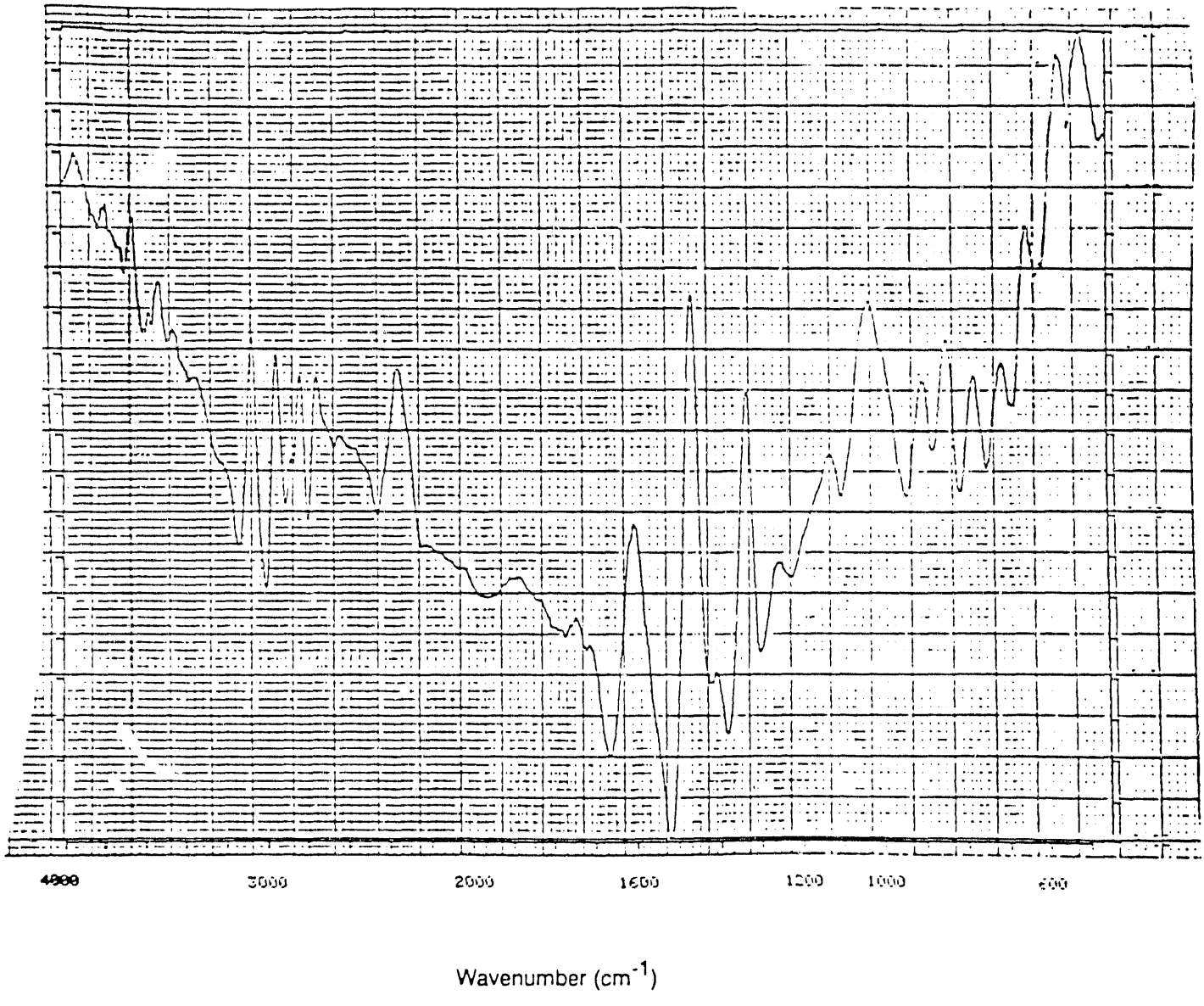

Figure 36: Difference spectrum of base coal and nonionic polyacrylamide.

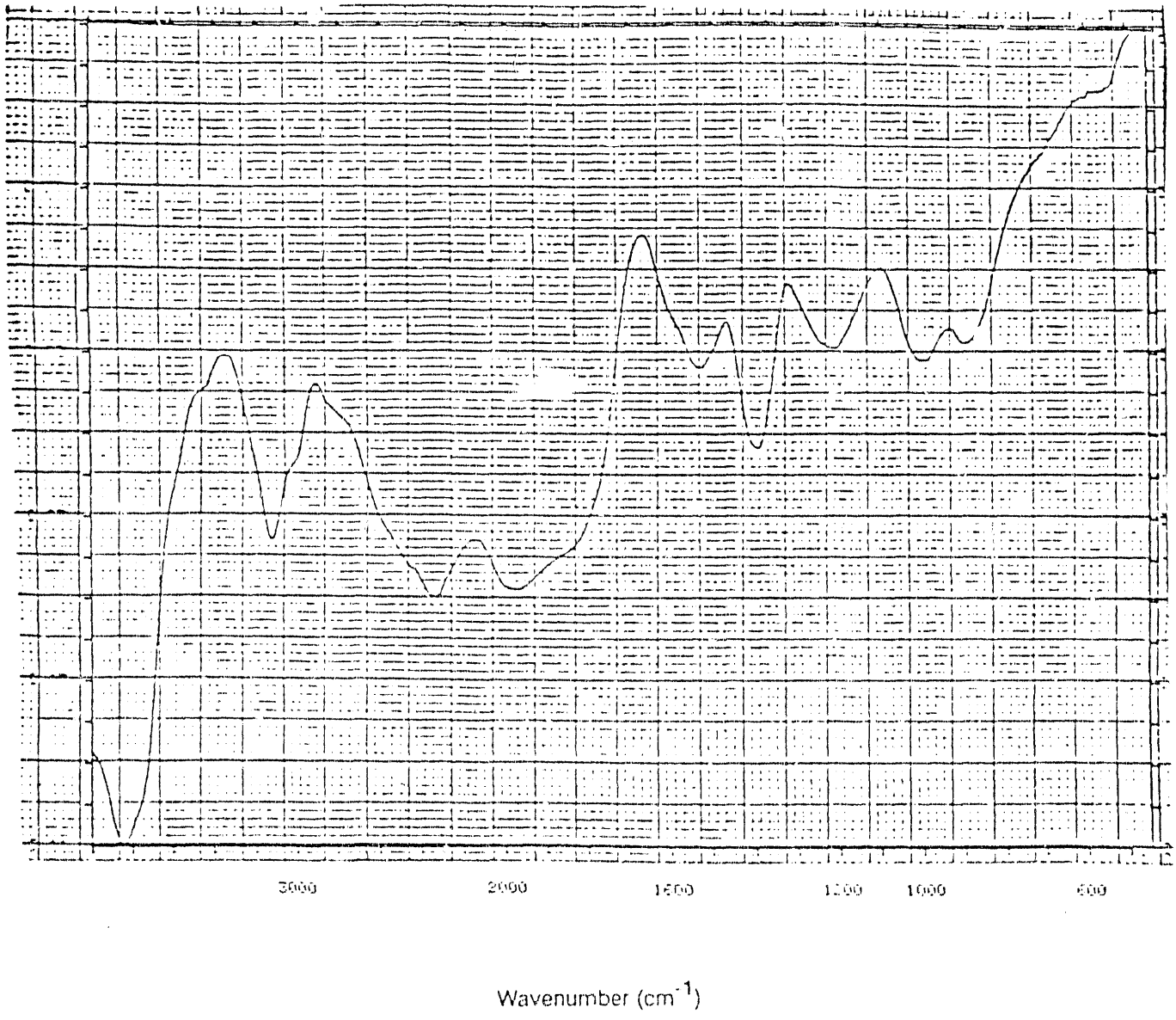

Figure 37: Difference spectrum of base coal and cationic polyacrylamide (10% cationicty).

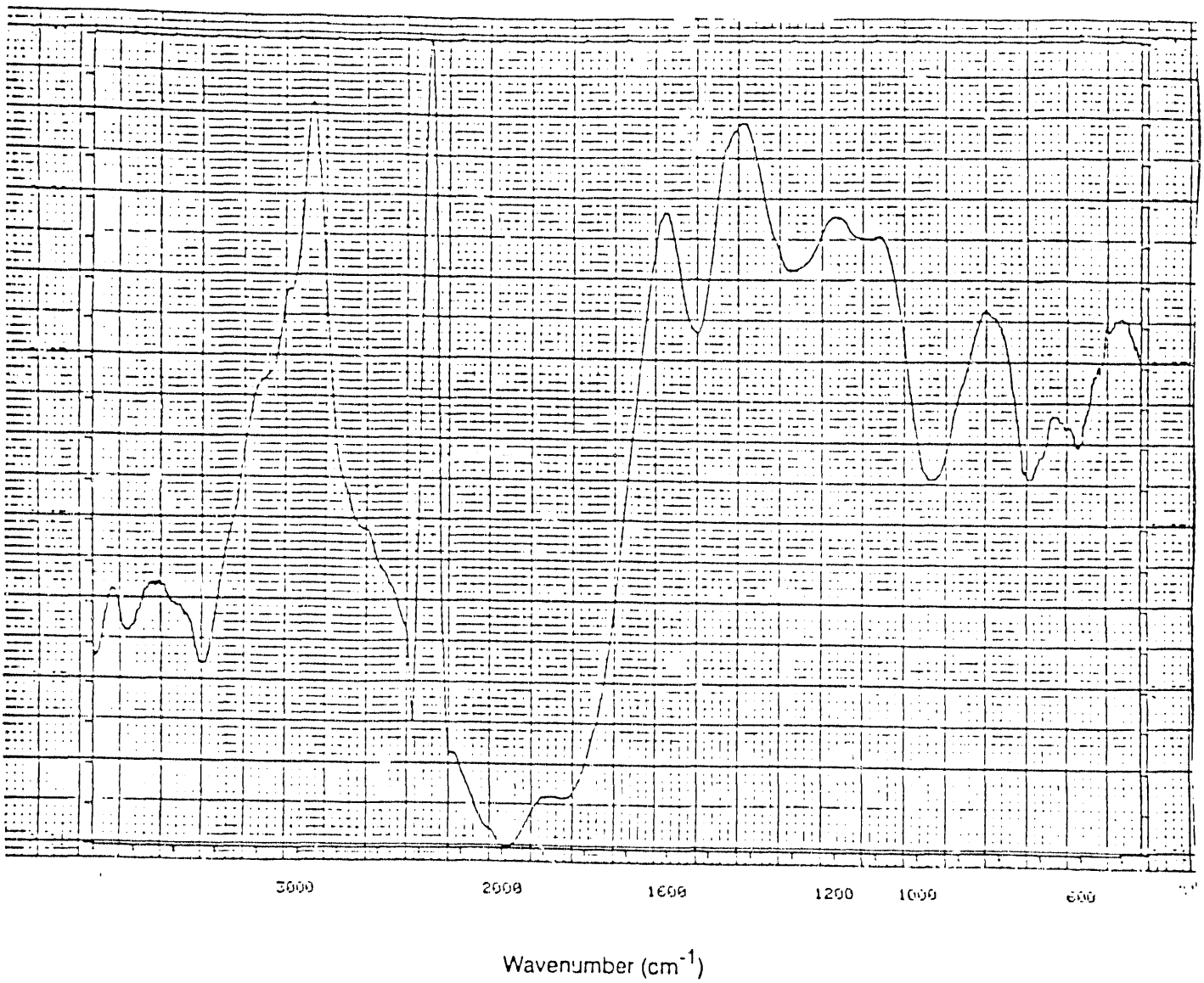

Figure 38: Difference spectrum of base coal and cationic polyacrylamide (34% cationicity).

when the charge density of the polymer is increased the water retention power is reduced. This is plausible since increased charge density would prevent the polymer from adopting a more compact structure and thus cannot hold more solvent water. If the amide groups of the polymer are exposed on the surface, γ_c of 40 can be expected [93]; the peak at γ_c 39 in this study is attributed to the amide group. It is also seen that as the charge density increases the area under the peak at 38 -39 γ_c increases indicating that more of the surface is covered by amide groups. The trend in the case of 30% anionic polyacrylamide and 34% cationic polyacrylamide is reversed; the difference of around 5% in the surface area occupied by amide groups is probably due to artifacts.

Adsorption of the cationic polyacrylamide and the anionic polyacrylamide takes place by the anchoring of the hydrocarbon chain such that the amide groups are pointing towards the surface. In the case of the coal treated with the anionic polyacrylamide the maximum γ_c occurs at 32 suggesting that the adsorption of the anionic polyacrylamide takes place in such a manner that relatively fewer hydrophilic groups are exposed. However, the surface of coal treated with the nonionic polyacrylamide appears more heterogeneous. Around 20% of the area in this case has a γ_c of 38 to 41. It is also evident that there are sites with γ_c ranging from 50 to 68 each occupying an area of around 5 to 10%. These are probably representative of C=O groups of the polymer.

Figure 40 shows the evolution of the site distribution curve as a function of the initial concentration of the cationic polyacrylamide treatment. The area occupied by bound water on the surface characterized by γ_c of around 72, increases from zero for untreated coal to a maximum value of 35% at 750 ppm followed by a decrease to 20% as the cationic PAM concentation is increased to 1000 ppm. The amount of water retained is a function of the degree of coiling of polymer molecule. As the concentration of the polymer is increased, the polymer in the adsorbed layer

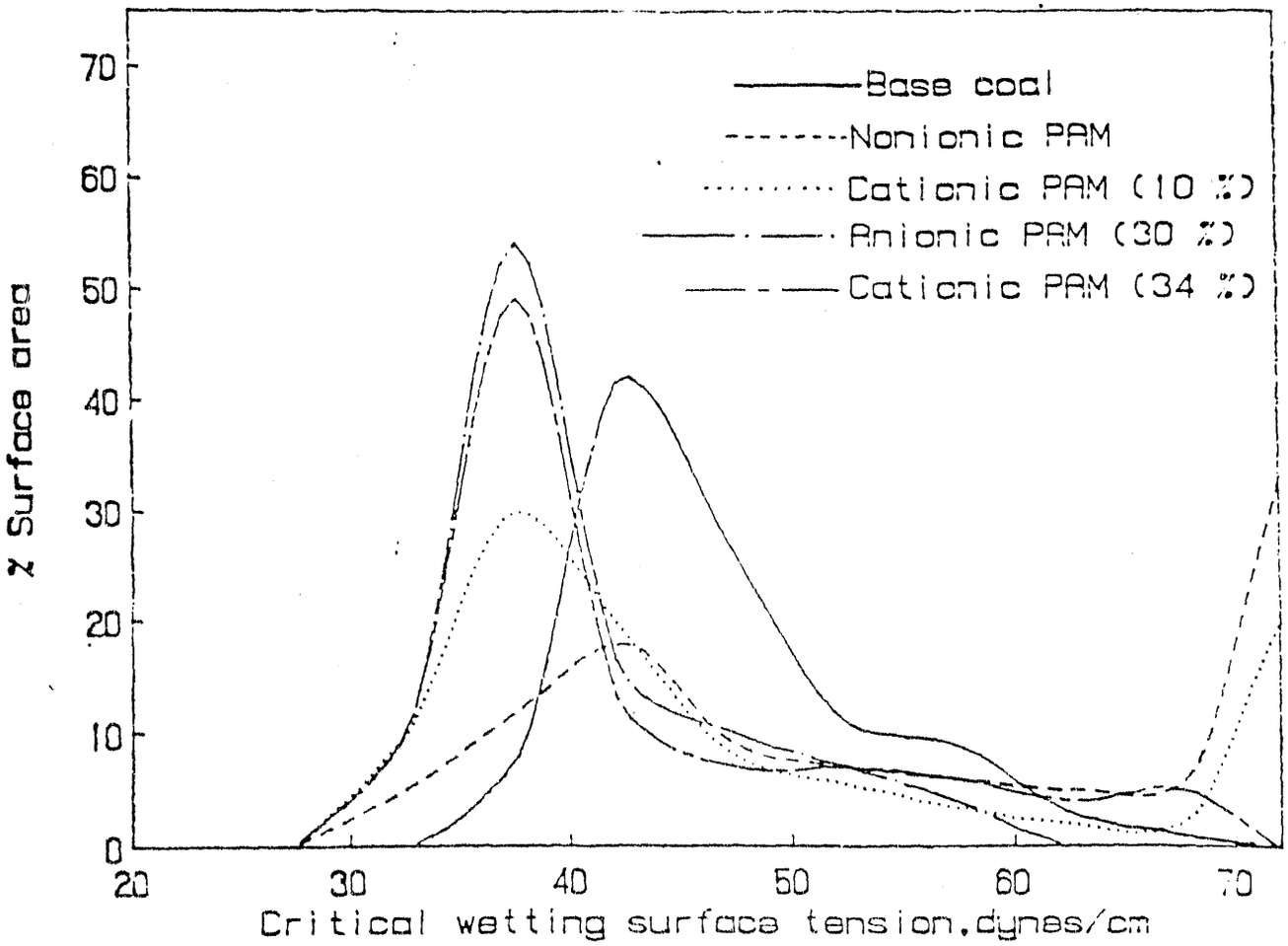

Figure 39: Site distribution curves constructed from film flotation tests for base coal and coal treated with 1000 ppm of various polyacrylamides

can undergo changes in conformation. Also, an absence of shift in the minimum γ_c toward lower values, upon increased polymer adsorption indicates that there is no preferen ial adsorption of polymer on higher energy sites. This behavior suggests that polyacrylamide adsorption on coal surface is entropically driven. A similar observation can also be made when the evolution of site distribution curves as a function of the time of adsorption are analyzed (Figure 41), as would be expected for a entropically driven adsorption process.

Effect of PAM adsorption on low temperature treated coal: As discussed in the earlier section, the low temperature heating of coal resulted in a shift in the distribution of surface sites to lower γ_c values. The adsorption of the polyacrylamide on the surface modified substance would thus be an important variable to study, in order to understand the nature of interaction of the polyacrylamide with various surface sites on coal. The nature of changes in the site distribution curve, upon adsorption of polyacrylamide on low temperature heat treated coal, are shown in Figure 42. It can be seen clearly, in comparision with data in Figure 39, that the adsorbed layer of the polyacrylamide on the oxidized coal surface is different from that of adsorbed polyacrylamide layer on base coal. In the case of the nonionic polyacrylamide, the percentage of sites having a γ_c of 72 has decreased from 30% on base coal to 15% on oxidized coal. This indicates that the adsorbed layer of the nonionic polyacrylamide on oxidized coal exhibits a less dense structure than that of the adsorbed nonionic polyacrylamide layer on base coal. Also, the sites with γ_c in the range of 52 to 62, that dissappeared on heating, reappears upon adsorption of both the nonionic and the anionic polyacrylamides.

In the case of the anionic polyacrylamide an increase of 15% in the area of γ_c in the above range is noticed. Upon adsorption of the nonionic polyacrylamide and the anionic polyacrylamide the percentage of area with a γ_c from 22 to 50 on

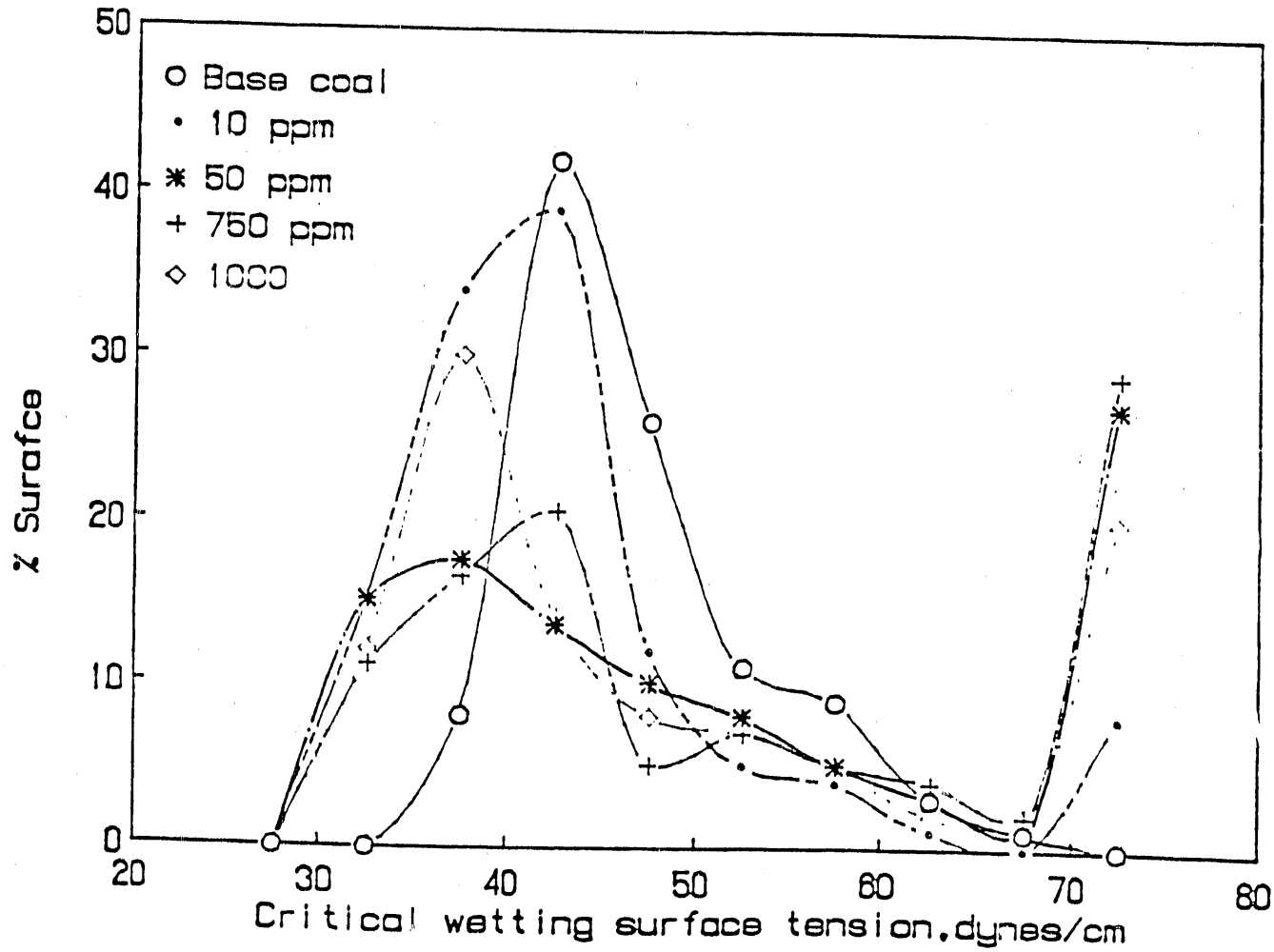

Figure 40: Evolution of site distribution curves constructed from film flotation tests for base coal as a function of the initial concentration of cationic polyacrylamide.

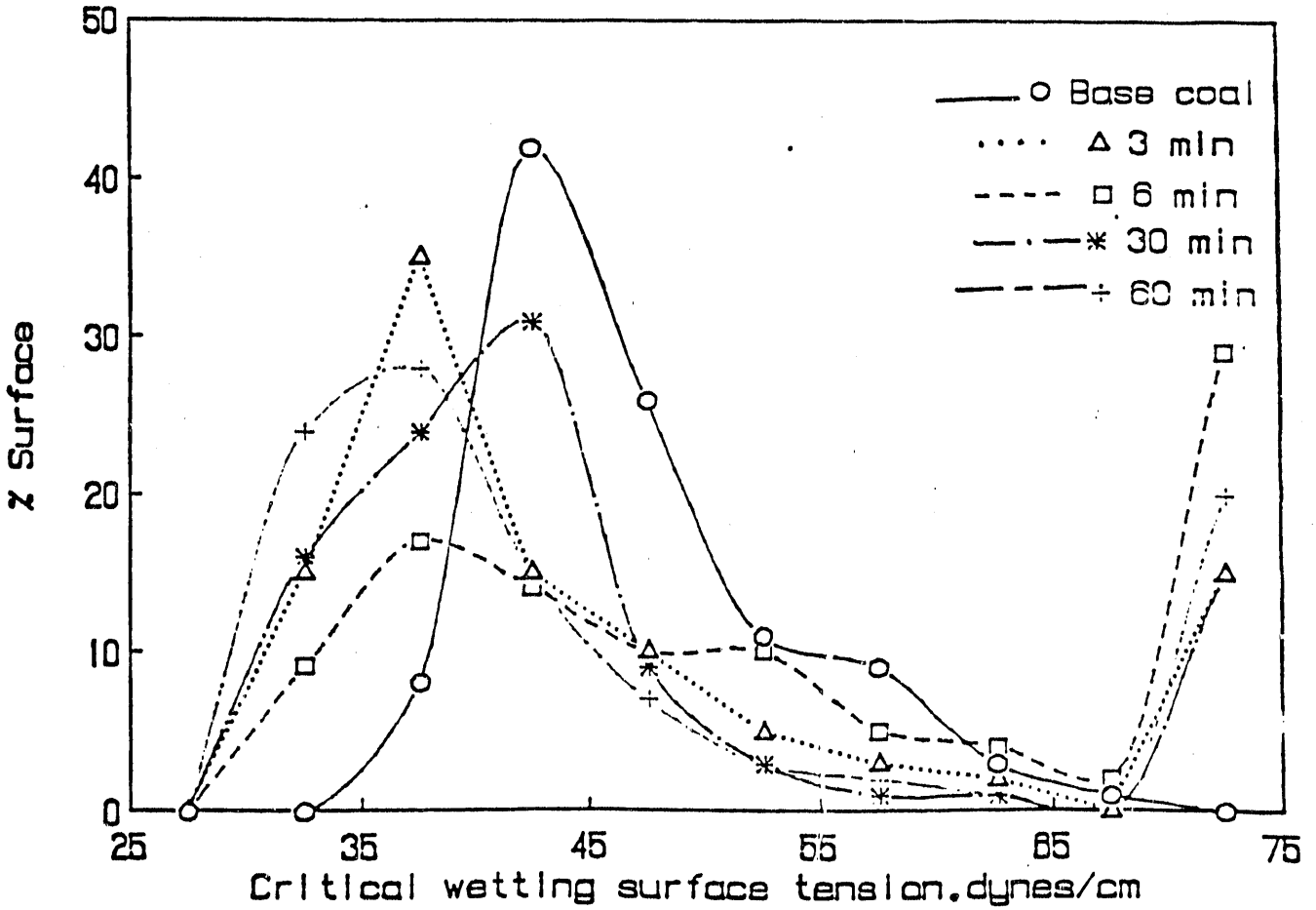

Figure 41: Evolution of site distribution curve as a function of time of treatment with cationic PAM (10% cationicity)

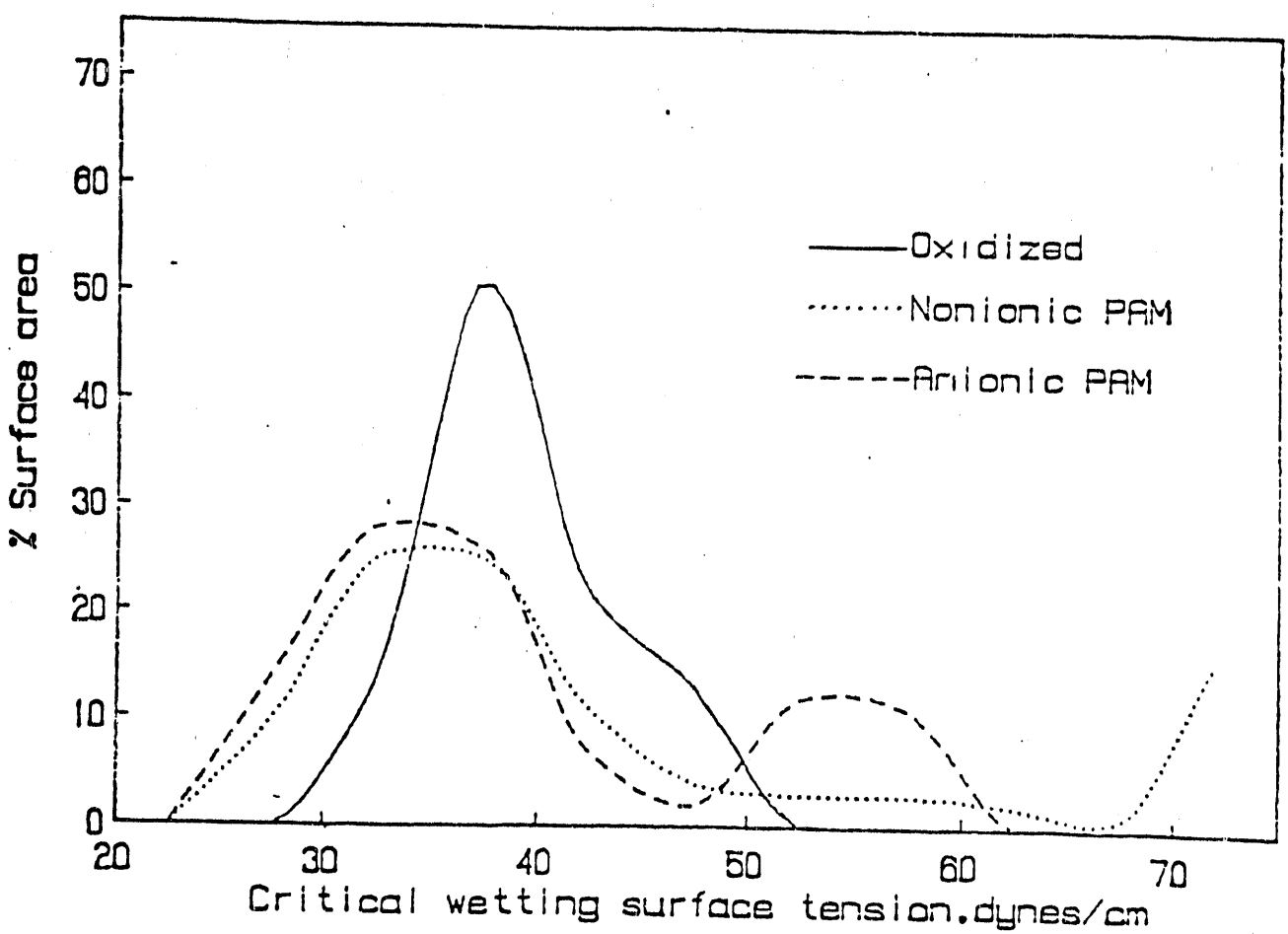

Figure 42: Site distribution curves constructed from film flotation tests of oxidized coal treated with polyacrylamide.

oxidized coal surface is identical, in contrast to the behavior observed with the base coal. More of the hydrocarbon chain of the polymer molecule is apparently exposed compared to that of the amide groups in the case of adsorbed layers on oxidized coal as evidenced by the shift in the curve towards lower γ_c values. The broad peaks are also indicative of the fact that the arrangement of polymers in the adsorbed layer is probably random and guided by entropic considerations, more so in the case of the oxidized coal than the base coal.

Site distribution on coal surface modified by dodecane: Dodecane is a collector often used in coal flotation and the effect of dodecane treatment on coal surface site distribution was studied.

a) Dodecane treatment in Denver cell

A bench scale Denver flotation machine equipped with a Perspex cell was used. Five gram samples of coal (-80 +100 mesh) were conditioned with 900 ml of distilled water for 2 minutes. The speed of the impeller was kept at 1200 rpm. 900 ml of water was added along with the required amount of dodecane and the slurry was further conditioned for 5 minutes. At the end of the period the coal was recovered by filtration, dried under ambient conditions and used in film flotation experiments. The experiment was conducted at two different levels of dodecane viz. 7 microliter and 80 microliter. The lower limit corresponds to a dosage of 1.7 kg/ton which is a typical amount used in coal froth flotation.

b) Dodecane treatment in a Waring blender

A commercial Waring blender with seven speed settings and equipped with a 2500 ml stainless steel jar was used in these tests. Waring blender was chosen in view of the higher speeds achievable which in turn will presumably enable a finer dispersion of oil in water to be obtained. The variables employed and the conditions

used during these experiments are given below. In all cases the weight of the coal (5 grams), amount of water (500 ml) and the dodecane dosage (7 micro liter) were kept constant. The numbers after the word speed corresponds to the speed setting in the Waring blender and progressively increasing speeds are indicated by higher numbers. After treatment, the coal was recovered by filtration, dried in ambient atmosphere and used in film flotation experiments. The various experimental conditions and the corresponding nomenclature are given below.

WB-1	Water and dodecane mixed at speed 1 for 1 minute, weighed amount of coal added and further conditioned for 1 minute at speed 1.
WB-2	Water and dodecane mixed at speed 2 for 1 minute, weighed amount of coal added and further conditioned for 1 minute at speed 1.
WB-3	Water and dodecane mixed at speed 5 for 1 minute, weighed amount of coal added and further conditioned for 1 minute at speed 1.
	In all the above tests, dry coal was added to the oil-water dispersion. In order to determine the effect of pre-wetting the coal on modification of its surface characteristics by n-dodecane the tests mentioned below were conducted.
WB-4	Coal was conditioned with water at speed 1 for 1 minute, dodecane added and slurry further conditioned for 1 minute at speed 2.

WB-5 Coal was conditioned with water at speed 1 for 1 minute, dodecane added and slurry further conditioned for 1 minute at speed 6.

In order to produce maximum modification of the coal surface oil agglomeration experiments were conducted. In these tests, 100 ml of dodecane was added to 5 grams of coal in 100 ml of water. The entire coal sample was immediately transferred to the oil phase when agglomeration was noticed as expected. The coal was recovered by filtration, washing and drying. The dried coal was used in film flotation experiments.

The cumulative partition curves obtained from film flotation data for the base coal (untreated coal) and the oil agglomerated coal is shown in Figure 43. The curve corresponding to the oil agglomerated sample indicates that the surface of coal which has undergone oil agglomeration is more homogeneous than that of the base coal.

Figure 44 shows the cumulative partition curves of coal samples modified by dodecane in a Denver flotation cell. An increase in the dodecane dosage shifts the curve to regions of lower γ_c indicative of a more hydrophobic surface. Figure 45 illustrates the cumulative partition curves for coal surfaces modified by dodecane in a commercial Waring blender. All the curves in Figure 45 can be considered to fall in a broad band with the exception of the curve corresponding to sample WB1. The latter indicates that the surface of particles in sample WB1 has more higher energy sites than those of other samples.

As dodecane is insoluble in aqueous medium modification of the coal surface by dodecane can be expected to be controlled by the probability of collision of the oil drops and the coal particles. In order to analyze the information contained in Figures 43 to 45 and to compare the distribution of sites, frequency distribution

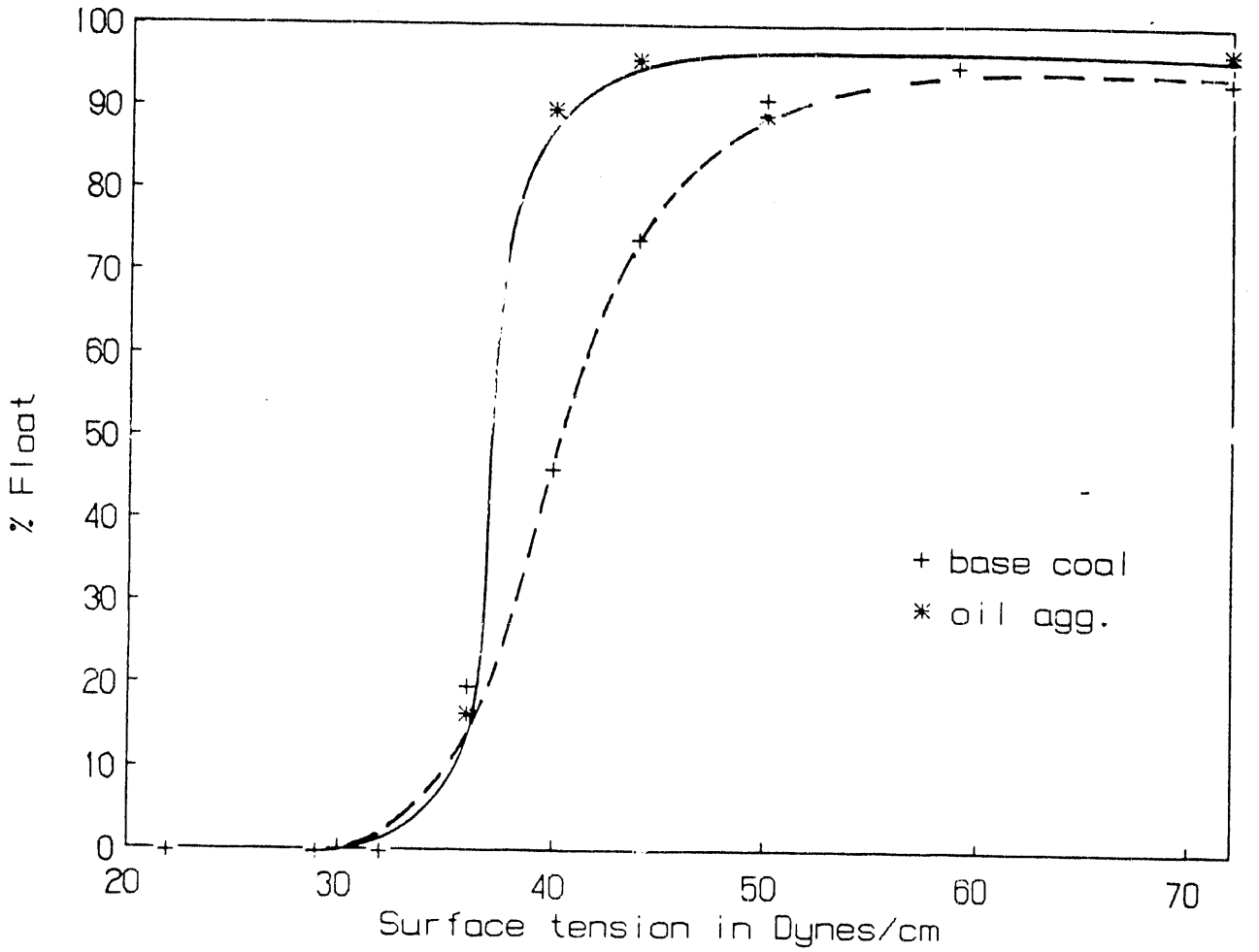

Figure 43: Cumulative partition curves for the base coal and oil agglomerated coal.

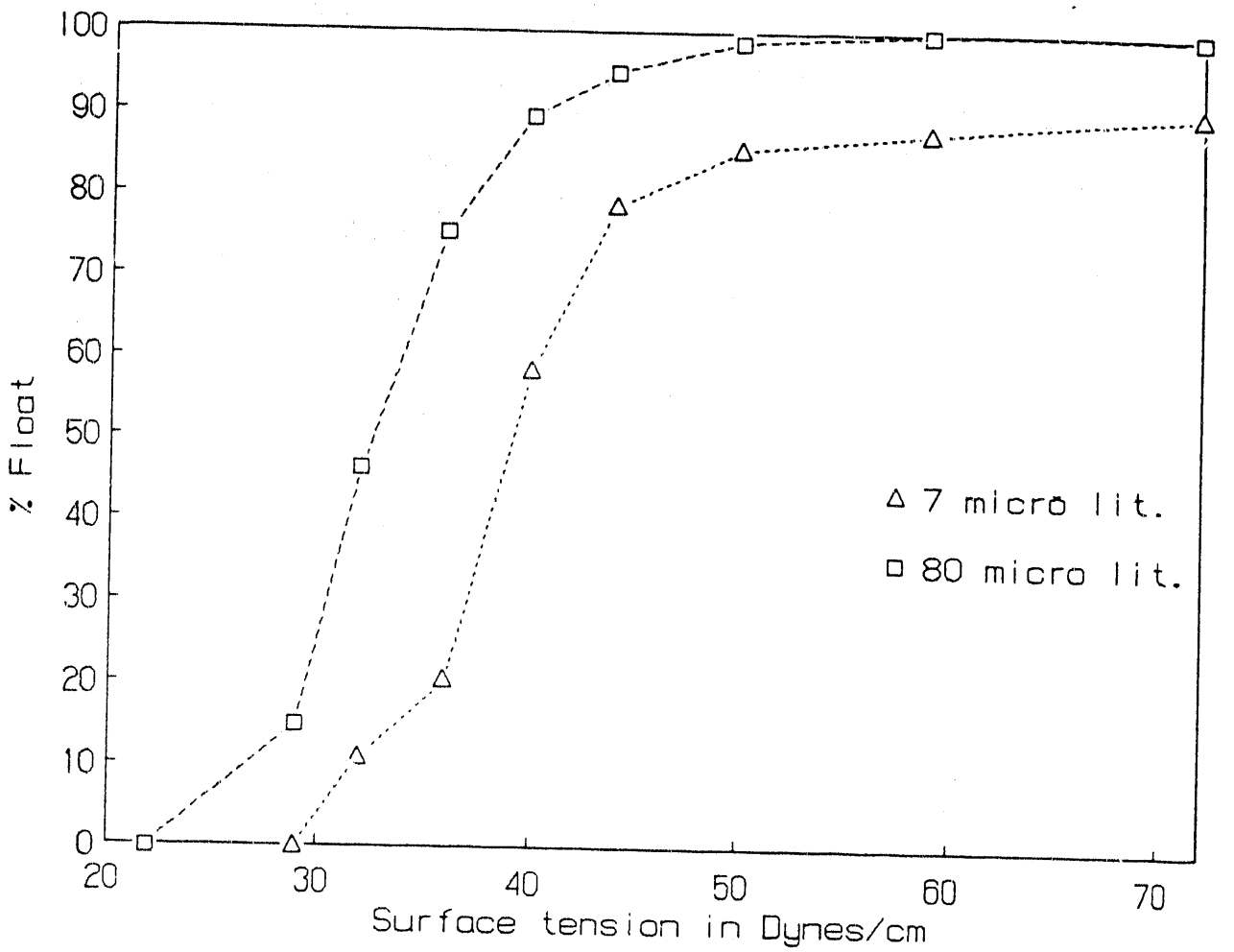

Figure 44: Cumulative partition curves for coal samples treated with n-dodecane in a denver cell (the amounts in the figure represent microlitres of n-decane per 5 gms of coal).

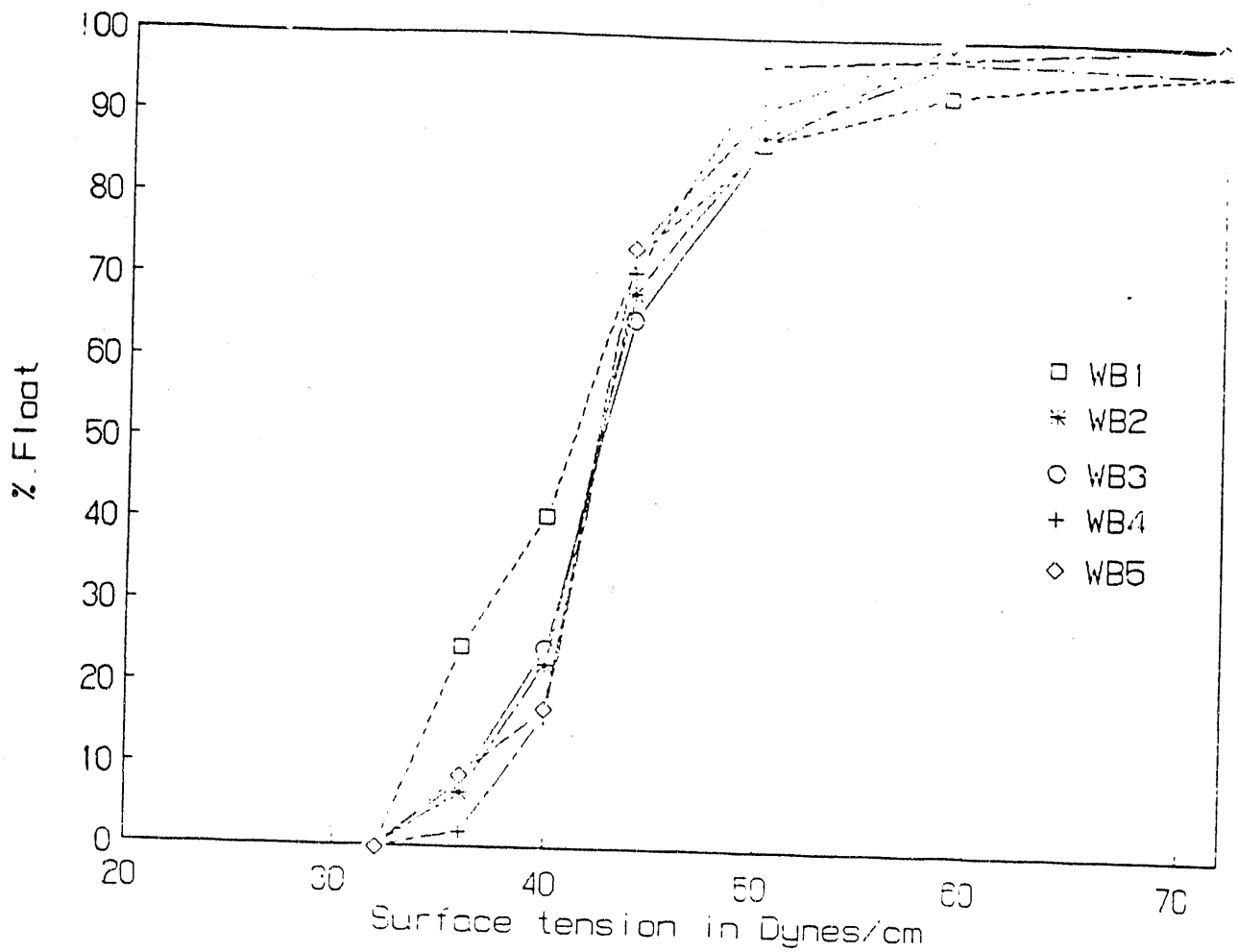

WB1, WB2 and WB3: Dodecane dispersed in water for 1 minute at speeds 1 (WB1), 2 (WB2) and 3 (WB3); coal added to the emulsion and the slurry conditioned for 1 minute

WB4 and WB5: Coal dispersed in water at speed 1 for 1 minute; dodecane added and the slurry conditioned for 1 minute at speeds 2 (WB4) and 6 (WB5)

Figure 45: Cumulative partition curves for coal samples treated with dodecane in a waring blender.

plots are required; such a typical plot is shown in Figure 46. For convenience in deriving trends the frequency plots were reconstructed as distribution curves. Figure 47 shows the site distribution curves of base coal, oil agglomerated coal and coal treated with dodecane in a Denver cell.

The mean value of γ_c for base coal is around 42 dynes/cm. After treatment with 7 micro liters of dodecane the mean value shifts to around 39 dynes/cm while the percentage of surface area with γ_c values between 25 and 38 increases. This trend is more pronounced when the dodecane dosage level is increased.

It can be seen from Figure 47 that 75 percent of the surface of oil agglomerated coal has a γ_c of around 38 dynes/cm as compared to 30 percent of the surface with a γ_c of 30 dynes/cm for the coal treated with 80 microliters of dodecane. It should be noted that sites with lower energies (or γ_c) are relatively more hydrophobic than those with higher energies (or γ_c). Interestingly this evidence translates to the fact that the oil agglomerated coal has a lot more high energy sites while the surface of the sample treated with 80 microliters of dodecane has lesser proportion of sites of lower energy. Since the oil agglomerated coal is completely hydrophobic (the entire sample was in the oil phase, the aqueous phase being devoid of any particles) it appears that *macroscopic properties of hydrophobicity and hydrophilicity of particulate matter are governed not only by the magnitude of the surface energies but also by the amount of surface with various energies*. Site distribution curve of coal treated with 7 microliters (corresponding to 1.7 kg/ton, which is a typical dosage in coal froth flotation) shows that there is a 10 percent increase in the surface area with a 38-40 γ_c. Concomitantly there is a 10 percent increase in the area of sites with γ_c less than 30 dynes/cm (low energy sites). These changes are probably responsible for the increased hydrophobicity and flotability of the coal during flotation using dodecane as the collector.

Figure 48 shows the site distribution curves for coal samples after surface

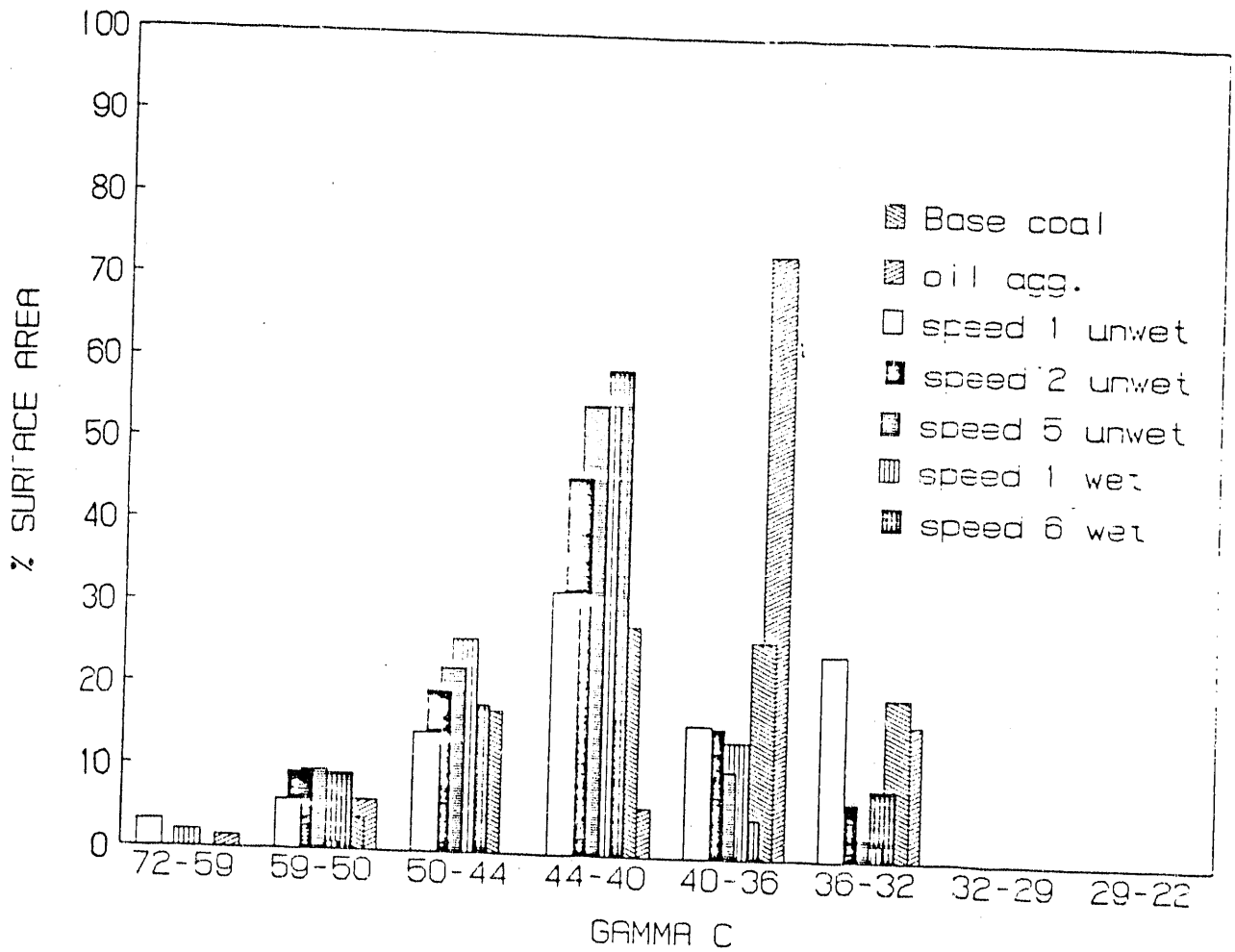

Figure 46: Frequency distribution of γ_c for base coal, oil agglomerated coal and coal samples treatred with dodecane in a Waring blender.

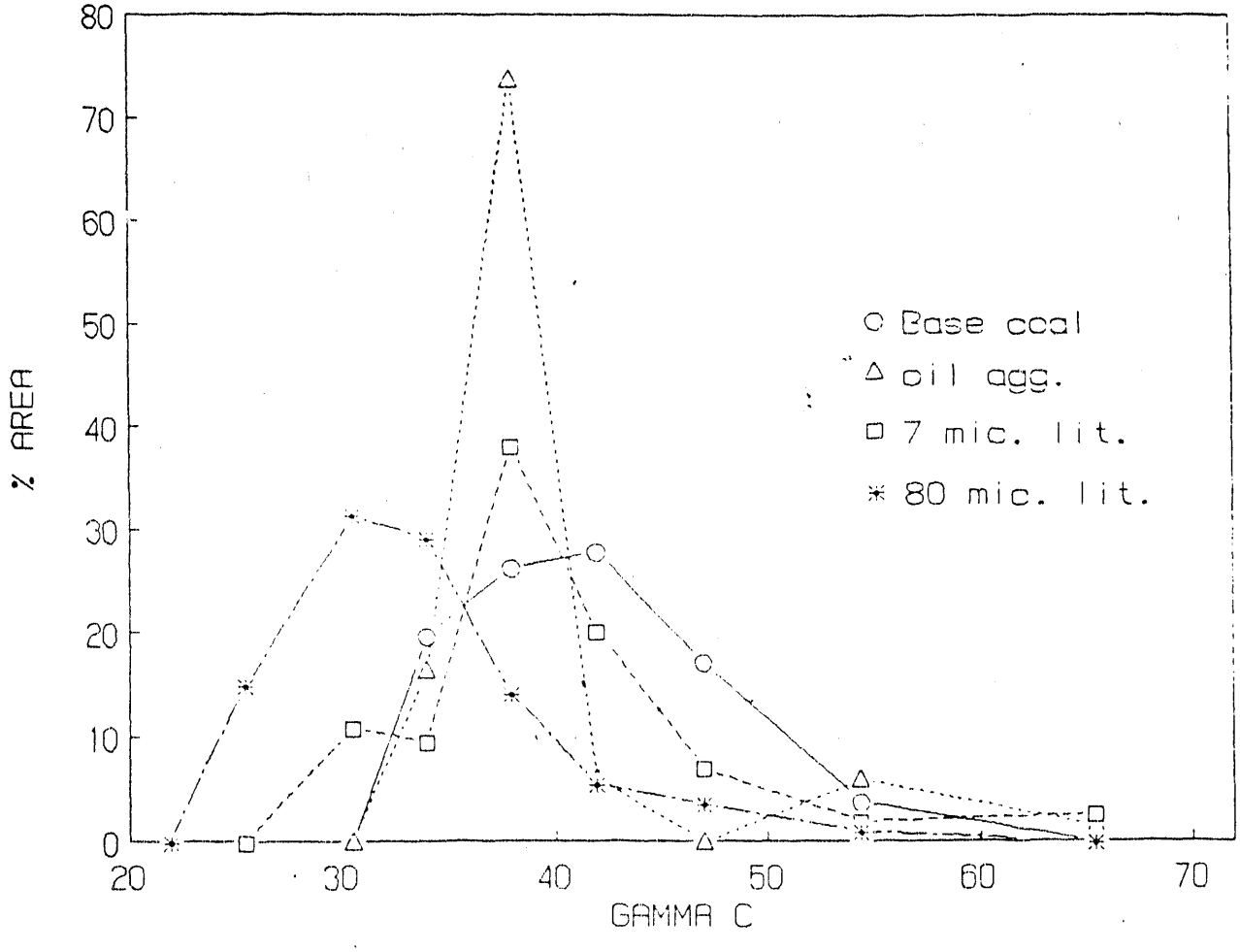

Figure 47: Site distribution curves for base coal, oil agglomerated coal and coal samples treated with dodecane in a denver cell.

modification by dodecane (7 microliters) in a Waring blender at various speeds and conditions mentioned earlier. The dark line indicates the site distribution curve for the base coal. It can be seen that an increase in blender speed increases the percentage of sites with 42 γ_c from 30 percent in the case of base coal to 60 percent in the case of coal samples conditioned at high speeds. This indicates that samples conditioned at higher speeds are more hydrophobic. Since the rate of collision of oil drops with the coal surface is expected to control the amount of coating and since an increase in the agitation speeds will improve the collision probability, higher agitation speeds are expected to increase the amount of coal surface coated by dodecane.

In coal froth flotation it has been observed [116] that an increase in the dosage of dodecane above 1.72 kg/ton (corresponding to 7 microliters for 5 grams of coal) does not have any effect on the grade or recovery of coals similar to the one used in this study. In fact a phenomenon known as "over oiling" has been noticed in industrial coal flotation circuits where excessive addition of oil decreases the flotation performance [117]. The results obtained in our study indicate that an increase in the dosage of dodecane above a critical value renders the coal surface relatively less hydrophobic. Also the degree of dispersion of dodecane in water does enhance the hydrophobicity as can be seen from the site distribution curves for coal sample treated with 7 microliters of dodecane in the Denver cell and Waring blender. In the former case, 30% of the surface has a 40 γ_c while 50 to 60 percent of the surface of the latter possesses $\approx 43\gamma_c$. However, an increase in the speed at which the agitation is conducted, above a critical value, does not have any effect on the site distributions of dodecane treated coal. It has been observed that an increase in the impeller speed above 1200 rpm in the Denver flotation cell does not increase the recovery or grade of coal during coal froth flotation [116]. This implies the existence of an upper limit to probability of collision between oil drops and coal

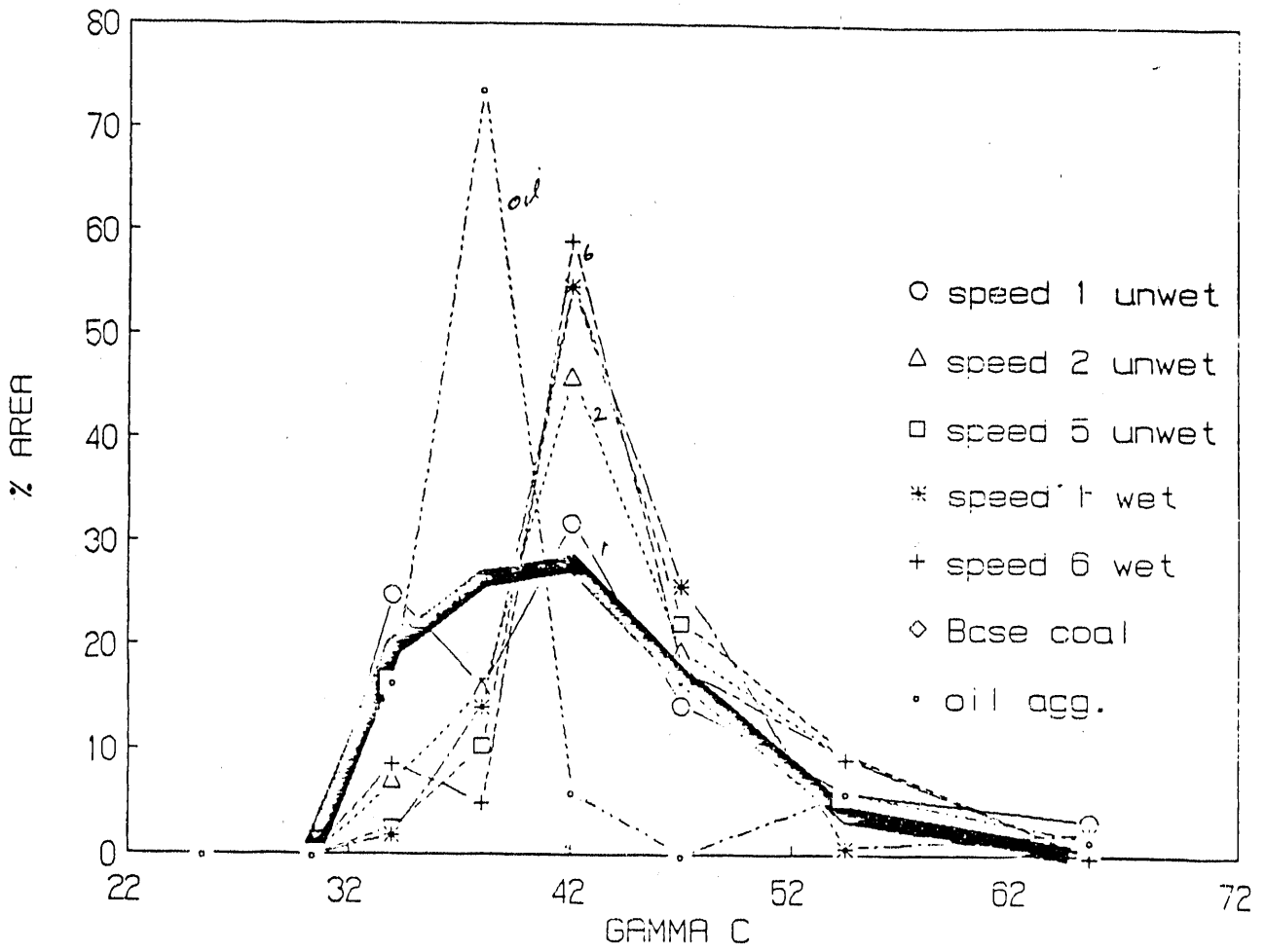

Figure 48: Site distribution curves for base coal, oil agglomerated coal and coal samples treated with dodecane in a Waring blender.

surface which is dictated by the flotation cell hydrodynamics.

6.4 CONTACT ANGLE DISTRIBUTIONS

The γ_c (critical wetting surface tension) distribution curves for the base coal sample which were discussed in the previuos sections can be converted to contact angle distributions. Contact angle ***distribution*** is a more meaningful description of the surface property of a heterogeneous substance like coal than average contact angle values. Neumann et al [118] have developed an equation of state which allows the surface tension of low energy solids to be determined from a single contact angle formed by a liquid whose surface tension is known. These researchers have published results of their analyses based on a computer program in the form of a table [119].

γ_c is equal to the surface energy if one assumes a value of unity for the interaction parameter (a parameter that is dependent on the nature of cohesive and adhesive forces) which is valid in the case of hydrophobic solids [120]. On this basis the contact angle which would be formed by water drops, whose surface tension was assumed to be 72 mN/m was obtained from the above table for various values of γ_c of the base coal used in this study. The resulting distribution of the contact angle is shown in Figure 49. It is evident from this figure that there exists a wide range of contact angles *on a single coal particle* ranging from around 80° to 20°. About 42% of the surface area has a contact angle of around 67°. It is not clear if the observed macroscopic contact angle (of pellets made from particulate samples) is the mean, median or mode of the actual contact angle distribution on coal particles.

The implications of the presence of sites with high and low contact angles on the same surface lead to complex wetting behavior and is discussed below.

Dettre and Johnson's classical studies [121,122,123] on contact angle hysteresis have resulted in the diagram shown in Figure 50, in which advancing, equilibrium

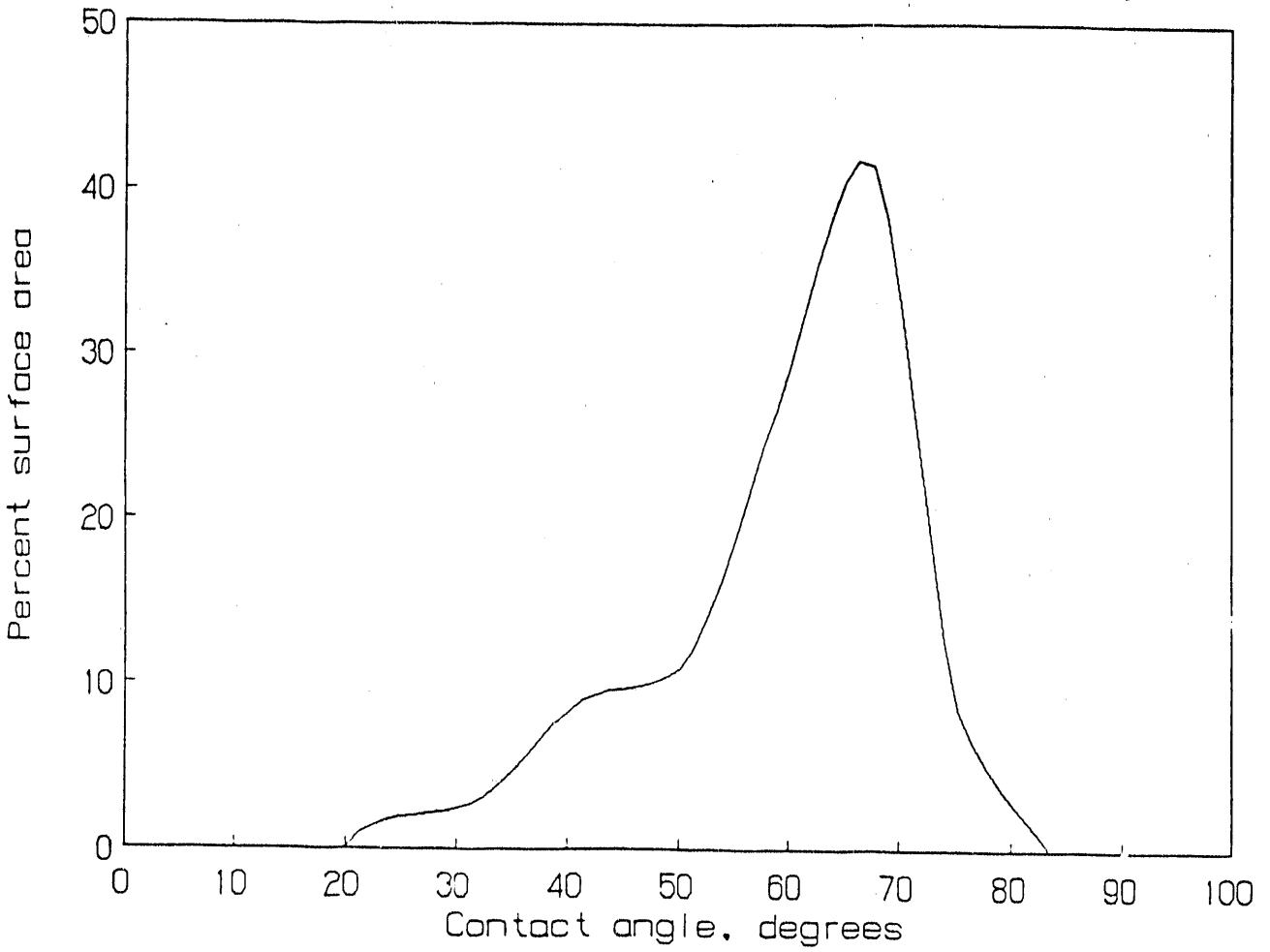

Figure 49: Distribution of contact angle on coal surface as calculated from γ_c distributions and Neumann's equation of state.

and receeding contact angles are plotted against the percentage of total surface with higher energy sites. From the discussion in the previous section we observe that the fraction of high energy (polar) sites is relatively low. This implies that a small change in the amount of polar sites on the coal surface will lead to large changes in the receding contact angle, while not affecting the advancing angle much.

A decrease in the receding angle with a decrease in the surface concentration of hydrophilic groups is not unexpected. The constancy of advancing angles as the surface composition changes is however not self evident, but has been supported by other researchers also [100]. The advancing contact angle has been regarded not merely as a measure of wettability but also as an indicator of the surface composition that can be used for determining fundamental surface properties of solids. The fact that the advancing contact angle is constant over a wide range of hydrophilic / hydrophobic ratios supports coal surface studies in which a constant value of γ_c has been observed [21]. However it should be noted that in these studies only the average γ_c was calculated using a Zisman's plot of advancing contact angles.

In flotation the receding contact angles govern the probability of attachment of particle to a bubble and advancing contact angles govern the probability of detachment. For a *homogeneous* hydrophobic surface a small change in the surface composition can lead to drastic changes in the receding angle while not affecting the advancing angle. For a hydrophobic substance like coal which shows a distribution of contact angles, a complex interplay between advancing and receding angles can be expected to affect the flotation process.

The spatial distribution of sites is a critical parameter in the wetting process. From Figure 50 it is clear that even though a surface may be grossly hydrophobic, the presence of small variations in hydrophilic sites can lead to a uniform advancing angle over the entire surface along with high as well as low receding angles for

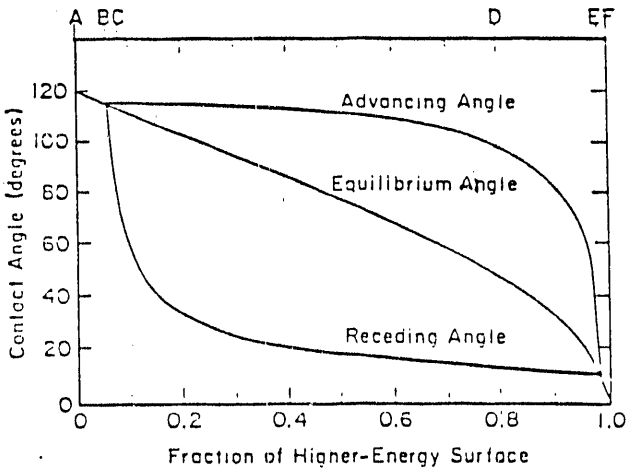

Figure 50: Contact angles *vs* surface composition: After Dettre and Johnson, (1964).

neighbouring microdomains. If such microdomains are situated within the area of contact of a bubble, then the system can be expected to be complex. Studies of contact angle *distributions* together with the *distributions* of the forces of attachment and detachment is likely to aid in developing a comprehensive model of the flotation process for such solids.

For a solid surface consisting of many macroscopic domains, the intrinsic contact angles with respect to a given liquid being θ_1,θ_2,θ_3... etc., Cassie obtained [124] the equilibrium contact angle θ for a heterogeneous surface as

$$\cos\theta = f_1 \cos\theta_1 + f_2 \cos\theta_2 + ..., (f_1 + f_2.... = 1) \qquad (15)$$

where f_1, f_2 ... are fractional areas of various domains. Recently Israelachvilli and Gee [125] derived a similar relationship

$$(1 + \cos\theta)^2 = f_1(1 + \cos\theta_1)^2 + f_2(1 + \cos\theta_2)^2 + ..., (f_1 + f_2.... = 1) \qquad (16)$$

which replaces the Cassie equation whenever the heterogeneity is of molecular dimensions. A test of these equations requires that areas of various domains and their contact angles be available.

Both the above equations were used in this study to calculate the equilibrium $\cos\theta$ value from the theta distribution shown in Figure 49. It was found that the equilibrium contact angle given by the Cassie equation was 60.47°, whereas the modified equation yields a value of 59.95°. In view of the sample preparation procedures currently employed for contact angle studies such as making pellets and polishing the surface, it is doubtful whether a 0.5° difference in measured angles would lead to any meaningful prediction of the spatial distribution of the sites.

However, accurate contact angle measurements on coal particles (not pellets) may provide useful results regarding spatial distributions.

6.5 THERMODYNAMIC APPROACH TO SURFACE SITE DISTRIBUTION

6.5.1 Gas adsorption

The thermodynamic approach to the study of surface site distributions involves determination of the heats of adsorption as a function of the amount adsorbed. The scientific principle on which this approach is based is that if an adsorbent surface is uniform then the heat of adsorption for every incremental amount adsorbed will be constant. In the case of a heterogeneous substrate, adsorption will initially occur on the higher energy sites and then subsequently on the lower energy sites as adsorption proceeds towards monolayer coverage. In general, the heterogeneity of the adsorbent will lead to a decrease in the heat of adsorption as adsorption proceeds. Two different techniques are used to obtain the heat of adsorption viz. immersional calorimetry and gas adsorption. The former provides data on the integral heat of adsorption and the later provides the isosteric heat of adsorption. Gas adsorption data also enables the calculation of the surface area of the coal sample under investigation (Bruceton mines, hand picked, HVAB).

In general, hydrophobic solids are characterized by higher heat values for immersion in organic liquids than for immersion in water, whereas the reverse is true for hydrophilic solids [45]. Similarly the heat of wetting of hydrophobic solids is greater in polar liquids than in nonpolar liquids [45,128]. Methanol was used as an adsorbate in the present study. Methanol is the first member of the homologous series of monohydric alcohols. It is similar to water in structure; one might view methanol as the methyl derivative of water. As such it has a low surface activity

at the solution-gas interface and is extremely polar. Though water, possessing two OH groups, is more polar, this tends to primarily to cause water molecules to be attracted to one another rather than to other groups. A methanol molecule possesses only one OH group, so that it is easily attracted to another polar group rather than to a second methanol molecule. Furthermore, the polar group is joined to the smallest possible hydrocarbon group, so that its effect is weakened and, in fact, the nonpolar group is advantageous since it permits easier wetting or attachment to carbonaceous surfaces. This unique position of methanol is shown by the fact that even ethanol is limited by steric hindrance of its larger hydrocarbon group e.g. the heat of wetting of coal is liberated more slowly in it compared to that in methanol [129]. Therefore ability of methanol to wet the coal surface completely and its propensity to adsorb at both hydrophobic and relatively hydrophilic sites on coal prompted its choice as the adsorbate in this study.

The adsorption isotherm of methanol vapor on coal is shown in Figure 51. Following the classification introduced by Brunauer et al [130] the isotherm corresponds to type II. Assuming a value of 17.9 $\AA^2$ for the adsorbed methanol molecule [131], BET analysis yields the surface area of the coal sample to be 111 m^2/g. Anderson et al in a study conducted in 1956 had obtained a value of 113 m^2/g for the same coal as that used in this study [132].

Figure 52 shows the adsorption isotherm of methanol on coal at two different temperatures of 30°C and 11°C plotted as the amount adsorbed at various pressures of the adsorbate. This plot was used to derive the pressures at the two different temperatures at constant adsorption density. Using these values in the integrated form of the Classius-Clapeyron equation

$$\Delta H = \frac{R T_1 T_2}{T_1 - T_2} \times \ln(p_1/p_2) \qquad (17)$$

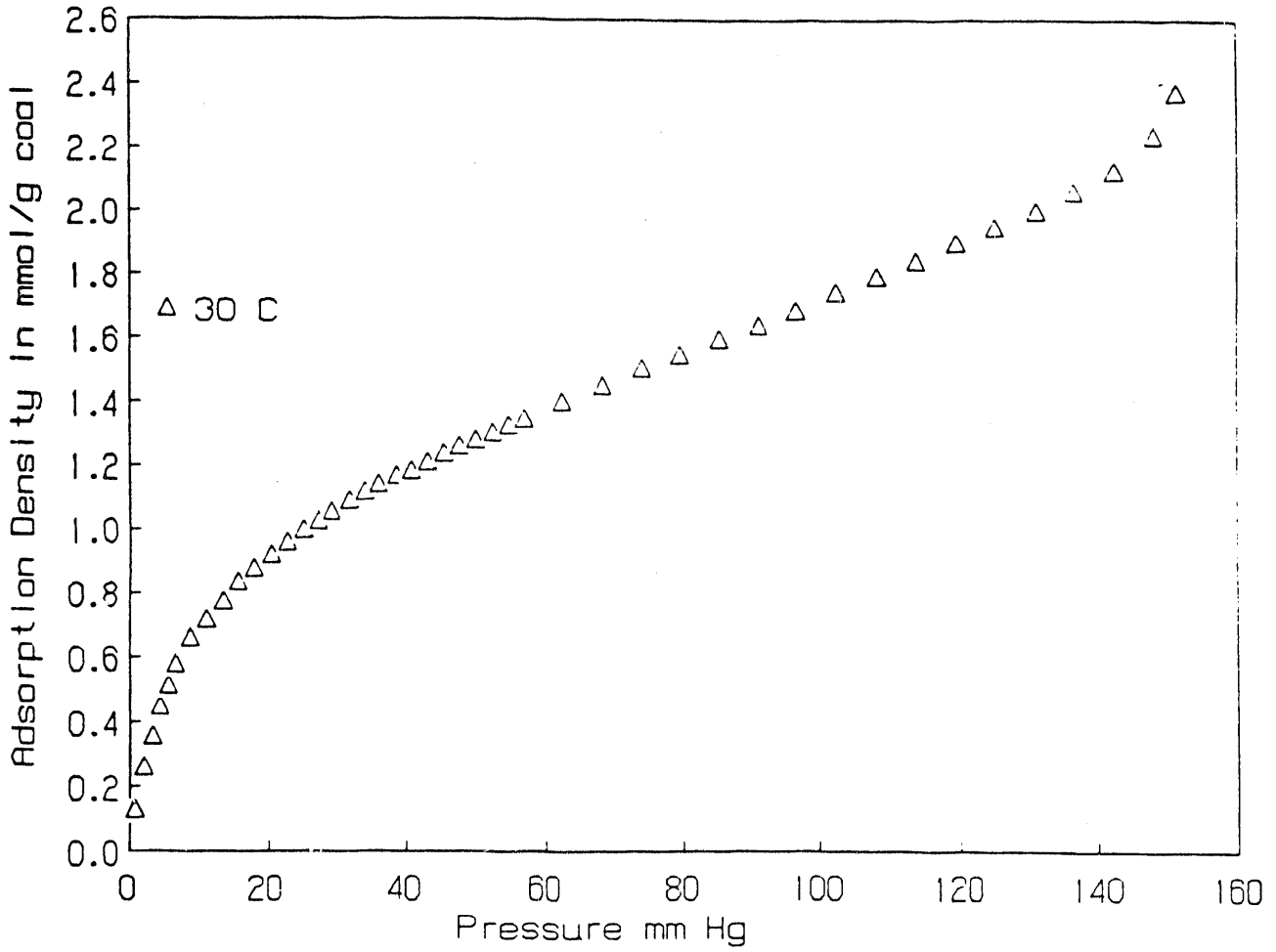

Figure 51: Adsorption isotherm of methanol vapor on coal at 30°C plotted as a function of partial pressure of methanol.

the heat of adsorption ΔH is obtained. Since the procedure is essentially based on the differential heat that can be obtained directly from adsorption isosteres the heat of adsorption calculated in this manner is called isosteric heat of adsorption and is a differential heat.

Figure 53 shows the computed isosteric heat of adsorption as a function of the amount adsorbed. It can be immediately discerned that the heat of adsorption falls below the heat of liquefaction of methanol. Such situations where heats of adsorption fall below the heat of liquefaction are very rare. In fact only a few systems showing such behavior have been reported in the literature [132,133]. In order to cross check this observation the isotherms at 30°C and 11°C were plotted as a function of the relative pressure and it was indeed observed that these isotherms do cross over. The lower portion of the isotherms (at low relative pressures) is shown on an expanded scale in Figure 54. It can be seen that the isotherms cross over at θ = 0.28 and θ = 0.98 (θ is statistical fractional coverage). These coverages correspond to those where the isosteric heat of adsorption crosses the heat of liquefaction of methanol.

The initial drop in the isosteric heat of adsorption from 44 KJ/mol to 38 KJ/mol as coverage increases can be attributed to the heterogeneity of the higher energy sites. The heat of liquefaction of methanol is around 38 KJ/mol. The decrease in the isosteric heat beyond θ = 0.28 to values lower than the heat of liquefaction indicates that adsorbed layer under these conditions is in a less condensed state than that of liquid methanol. The rise in the heat of adsorption beyond θ = 0.5 is probably indicative of the later stages in the adsorption wherein contribution from lateral interactions is expected. As we approach monolayer coverage the heat of adsorption once again rises above the heat of liquefaction and approaches its initial value. This can be construed as indicative of the fact that the energy involved in the adsorption of the initial molecules on highest energy sites is the same as that

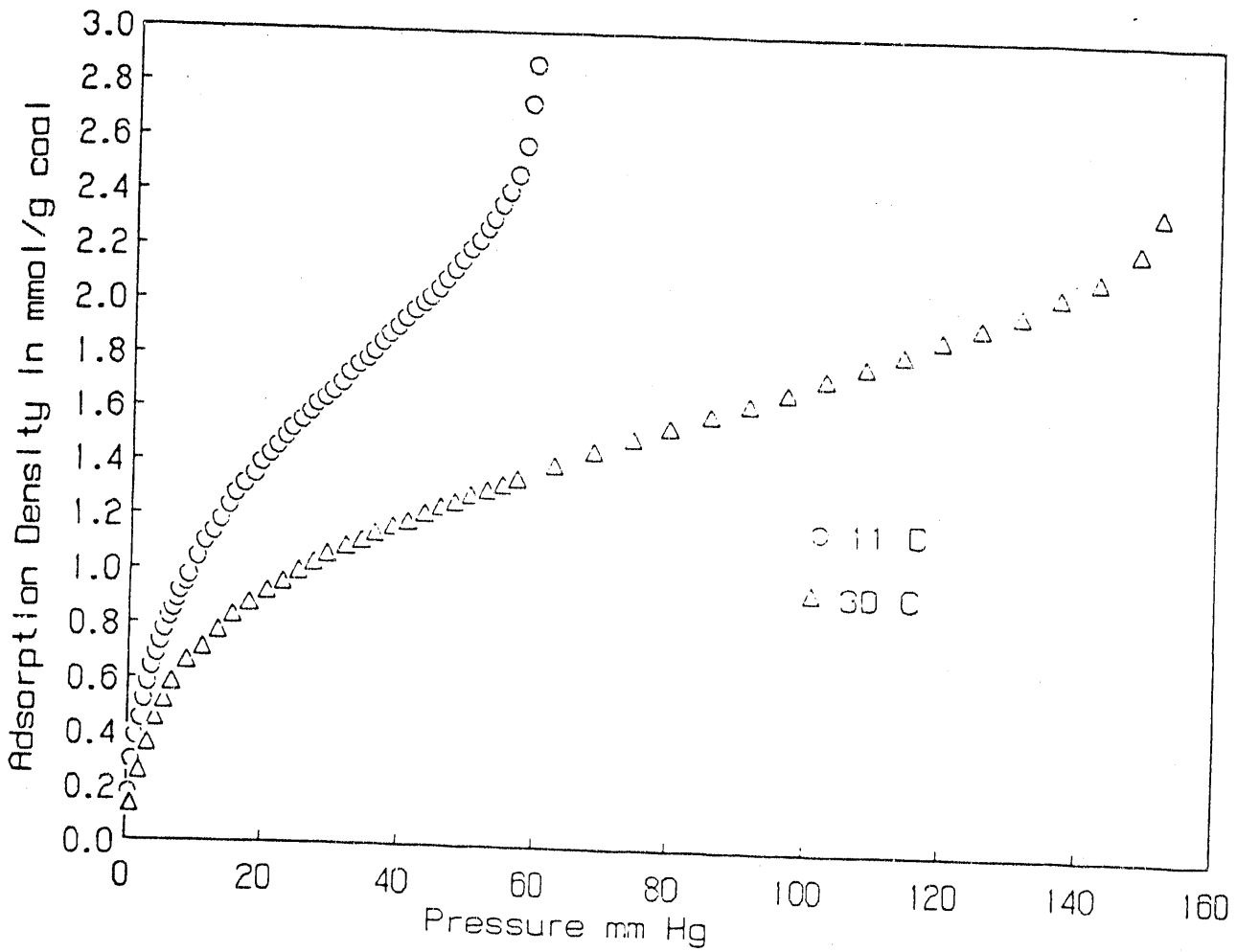

Figure 52: Adsorption isotherm of methanol vapor on coal at 30°C and at 11°C plotted as a function of partial pressure of methanol.

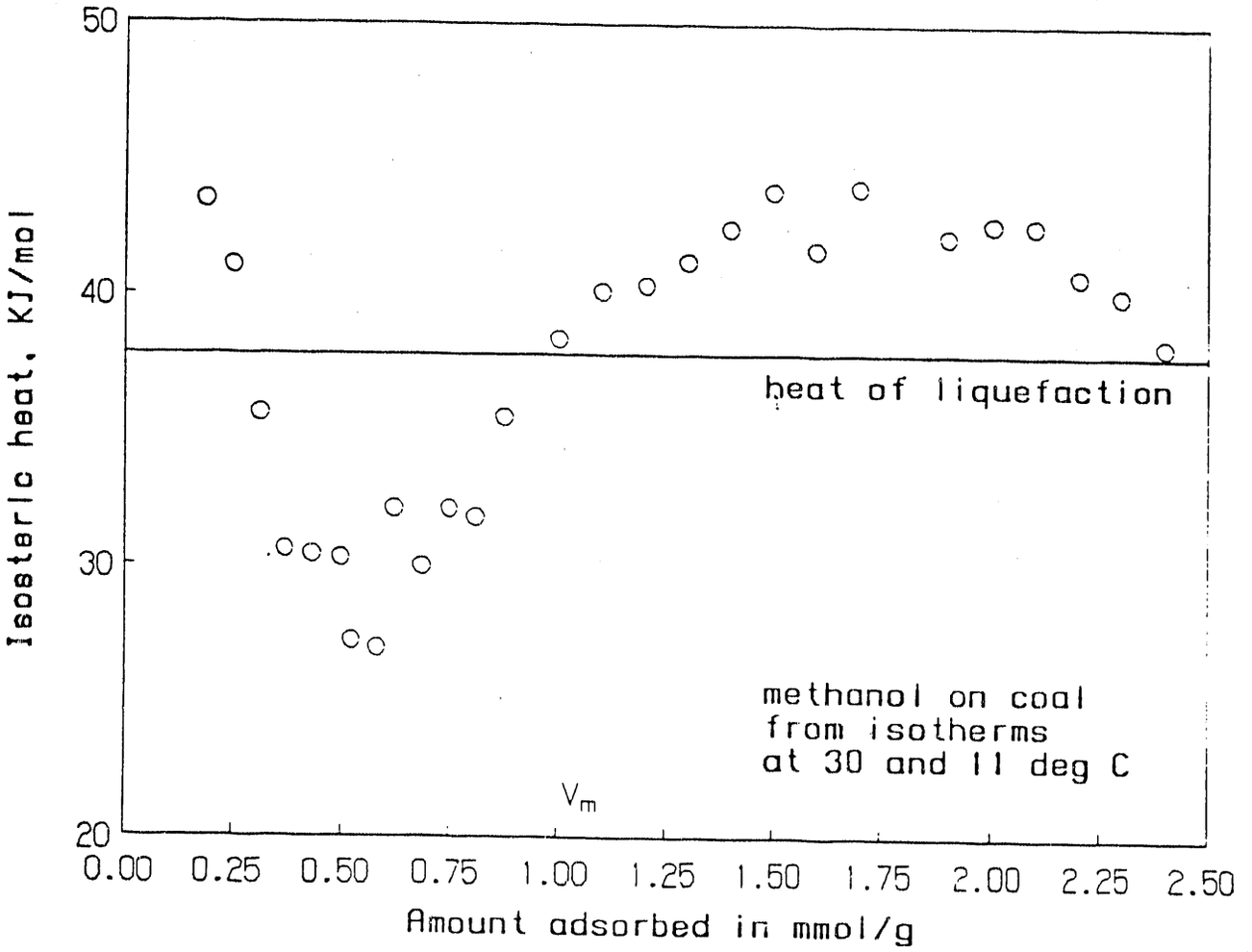

Figure 53: Isosteric heat of adsorption of methanol vapor on coal.

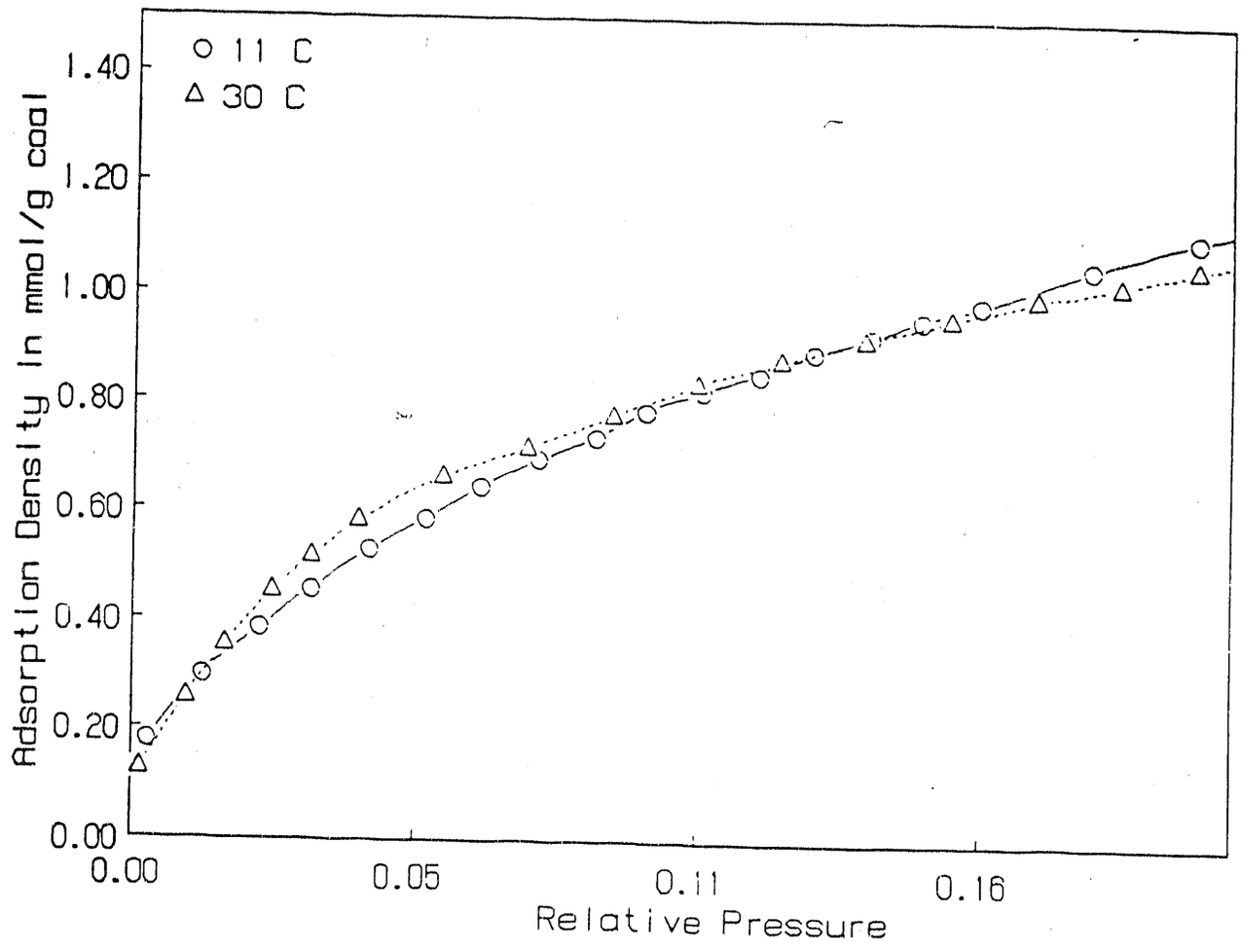

Figure 54: Low pressure region of the adsorption isotherm of methanol on coal at 11 degrees C and 30 degrees C plotted as a function of the relative pressure.

of the adsorption in the second layer. It therefore appears that the higher energy sites on coal are clustered densely leading to an adsorbed layer which is in a highly condensed state, whereas the lower energy sites are sparsely distributed with the result that individual adsorbed molecules are in a state less condensed than that of the liquid state. As a corollary, the adsorbed layer in the latter state is probably mobile.

6.5.2 Enthalpy of immersion

The heat of immersion of coal as a function of precoverage of methanol is shown in Figure 55. In order to obtain experimental data at low coverages (less than $\theta = 0.5$) the methanol vapor source used to precover the coal surface had to be maintained at minus 30°C, and experimental difficulties were encountered under such conditions.

Heat of immersion experiments as a function of precoverage of the adsorbate provides information on the composite nature of a solid surface. As pointed out by Zettlemoyer, "too often the values of the heat of immersion of a solid into a variety of liquids are compared directly when additional knowledge of the value of the heat of immersion at various precoverages of the wetting liquid is necessary for proper interpretation of wetting phenomena." This aspect is particularly important in coal science and to our knowledge there exists no published information on the study of heat of immersion of coal as a function of the precoverage of the wetting liquid. It is also felt that the experimental techniques and the skill required to conduct these experiments are presently unavialable in U.S. universities.

The heat of immersion is directly related to the integral heat of adsorption $H_{ads(i)}$ as follows;

$$H_{ads(i)} = [h_{I(SL)} - h_{I(SJL)}] + \Gamma H_L \qquad (18)$$

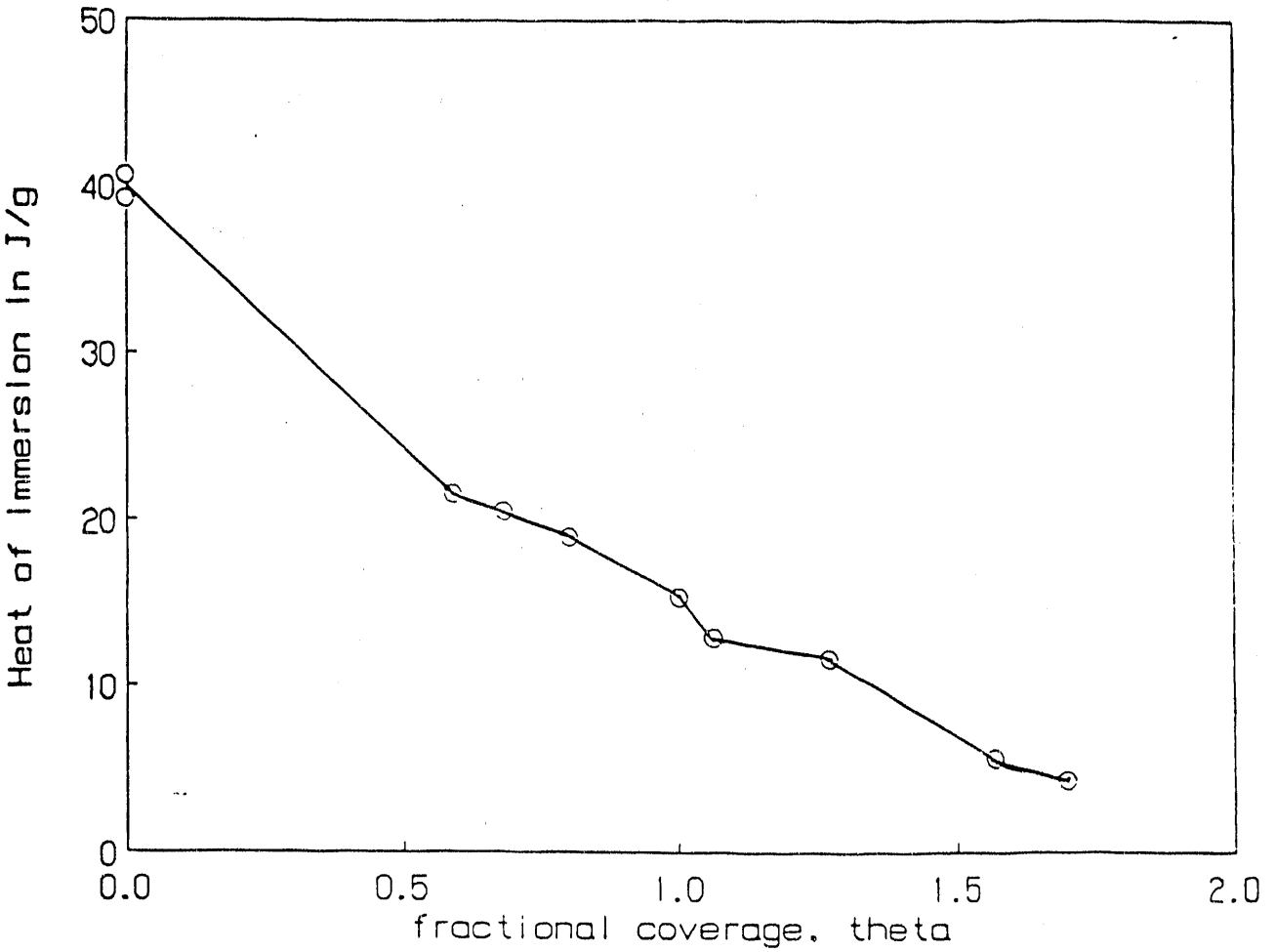

Figure 55: Heat of immersion of coal in methanol as a function of preadsorbed methanol.

where $h_{I(SL)}$ is the heat of immersion of the bare surface, $h_{I(SfL)}$ is the heat of immersion of the solid precovered with N adsorbed molecules (Γ is the adsorption density) and H_L is the heat of liquefaction.

The integral heat of adsorption derived from the experimental data in Figure 55 is shown in Figure 56. Differentiation of the integral heat of immersion curve provides a measure of the differential heat of adsorption. The classical work of Beebe and coworkers [134,135] had earlier demonstrated that in the case of homogeneous surfaces the differential heat of adsorption is constant as a function of precoverage of the adsorbate.

Heterogeneous surfaces are characterized by a steady drop in the differential heat of adsorption as a function of precoverage. Zettelmoyer and co-workers [136] have used this approach wherein the slope of the differential heat of adsorption as a function of precoverage was used to obtain a quantitative measure of the surface site distributions for attapulgite. The theoretical treatment of the surface site distribution function has been provided by Drain and Morrison [137]; briefly a site distribution function $g(\epsilon)$ can be defined so that the sites with energy between ϵ and $\epsilon + \delta(\epsilon)$ can accomodate $g(\epsilon)\delta\epsilon$ moles at STP of adsorbed gas;

$$g(\epsilon) = \frac{dN}{d(\Delta H_d)} \tag{19}$$

where N is the amount adsorbed. It should be appreciated that the double differentiation necessary to obtain the site distribution function is not sufficiently accurate to show up minor variations. Nevertheless, the heat of immersion curve, the differential heat curve and the distribution curve serve to give representative picture of the distribution of sites and more importantly this procedure provides a *quantitative measure of the heterogeneity in terms of the site distribution function.*

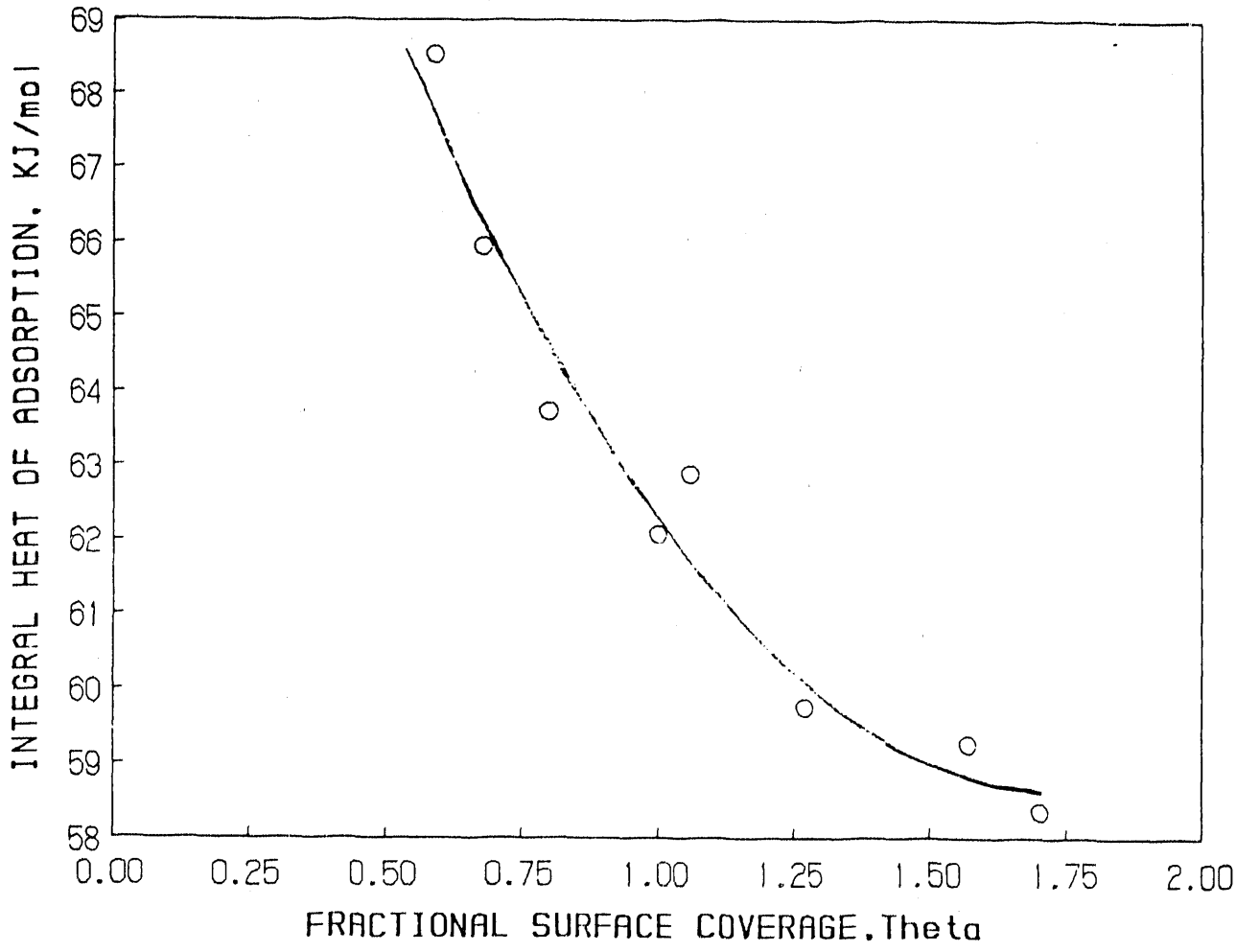

Figure 56: Integral heat of adsorption of methanol on coal as a function of preadsorbed methanol.

6.6 Spectroscopic investigations

Spectroscopic techniques have been widely used for characterizing surfaces and adsorbed layers. In this project different spectroscopies was employed on the same coal to obtain complementary surface chemical information.

6.6.1 DRIFT

Diffuse Reflectance Infrared Fourier Transform (DRIFT) spectroscopy was used to investigate the differences in functional groups of float and sink fractions obtained from film flotation experiments.

Float and sink fractions from film flotation experiments conducted with 30 weight percent methanol were collected. Particles in the float fraction were found to have a critical wetting surface tension (γ_c) value between 72 and 44 mN/m (they are not wetted by the 30 weight percent methanol-water mixture which has a surface tension of 44 mN/m). Similarly particles belonging to the sink fraction have γ_c values between 44 and 32 mN/m. This difference in the γ_c range for the float and sink fractions could only be due to the nature of the surface functional groups (polar or nonpolar) and their distribution. This aspect was investigated using DRIFT spectroscopy.

DRIFT spectroscopy has been used to study coal surfaces in recent years [138]. Most of the work in this area is concerned with the elucidation of coal oxidation mechanisms [139,140] where sequential changes in the peaks corresponding to polar groups are monitored. Oxidation has been shown to affect wettability and flotation [21,141]. It was felt that the DRIFT spectra of the above float and sink fraction would reveal the role of surface functional groups in determining the distribution of γ_c values for coal samples. Figure 57 shows the DRIFT spectrum of base coal and is similar to the spectrum reported earlier. Figure 58 through Figure 60 show

the spectra of the base coal, float and sink fractions together with the difference spectrum, plotted in the same scale. The difference spectrum reveals that the samples have identical spectral features, at least as far as the major coal peaks (listed in Table 2) are concerned.

Laser Microprobe Mass Analyzer (LAMMA) spectra (discussed below) have indicated the possibility that the average structural unit in coal is greater than 4 microns. Film flotation results yield a γ_c distribution on each particle of coal. Therefore, spot analyses by DRIFT would not be sensitive to the differences in average properties and would yield only information on the local salient features. This also implies that all particles in the population have a similar distribution of surface sites (in magnitude). In these cases it would be expected that the differences in the DRIFT spectra of the float and sinl fractions would be undetectable, and this was indeed experimentaly observed here. The surfaces of the float and sink fractions are certainly different; this diffrence could be due to the spatial distribution of the surface sites. DRIFT spectra features would be unable to distinguish differences in spatial distribution, and would therefore yield similar spectra for both float and sink fractions.

In a separate series of experiments DRIFT spectra of a sample of Upper Freeport coal and Pittsburgh No.8 coal showed no detectable difference in major peaks. However, flotation results showed that Pittsburgh coal is more hydrophobic than Upper Freeport coal.

The above results and observations indicate that DRIFT spectroscopy is insensitive to the changes in functional groups which determine the range of γ_c values of heterogeneous particles. It is recogonized that this insensitivity may be due to the differences in the concentrations of the functional groups being below the detection level of the instrument. However, in view of the fact that all particles in a

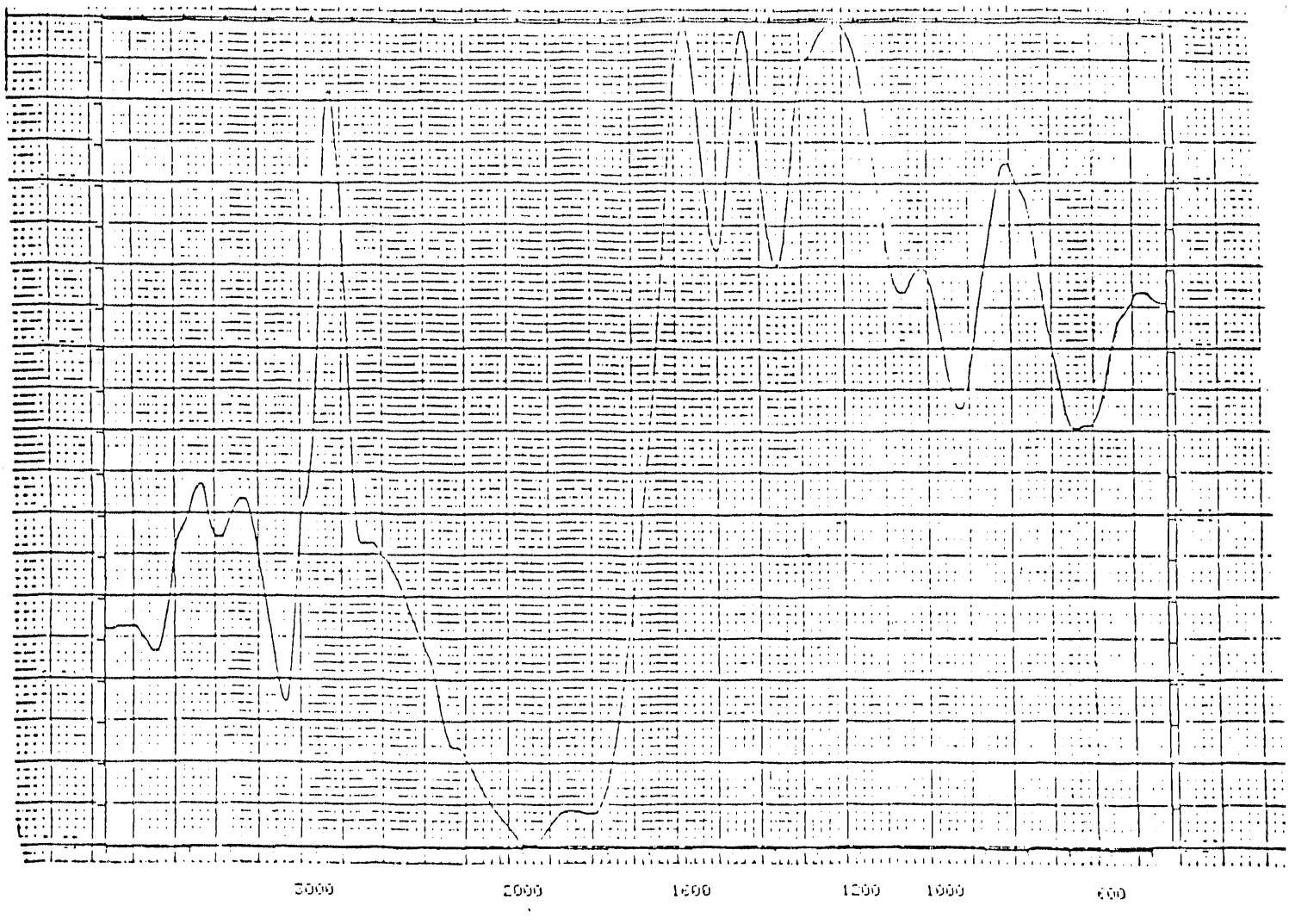

Figure 57: DRIFT absorbance spectrum of base coal.

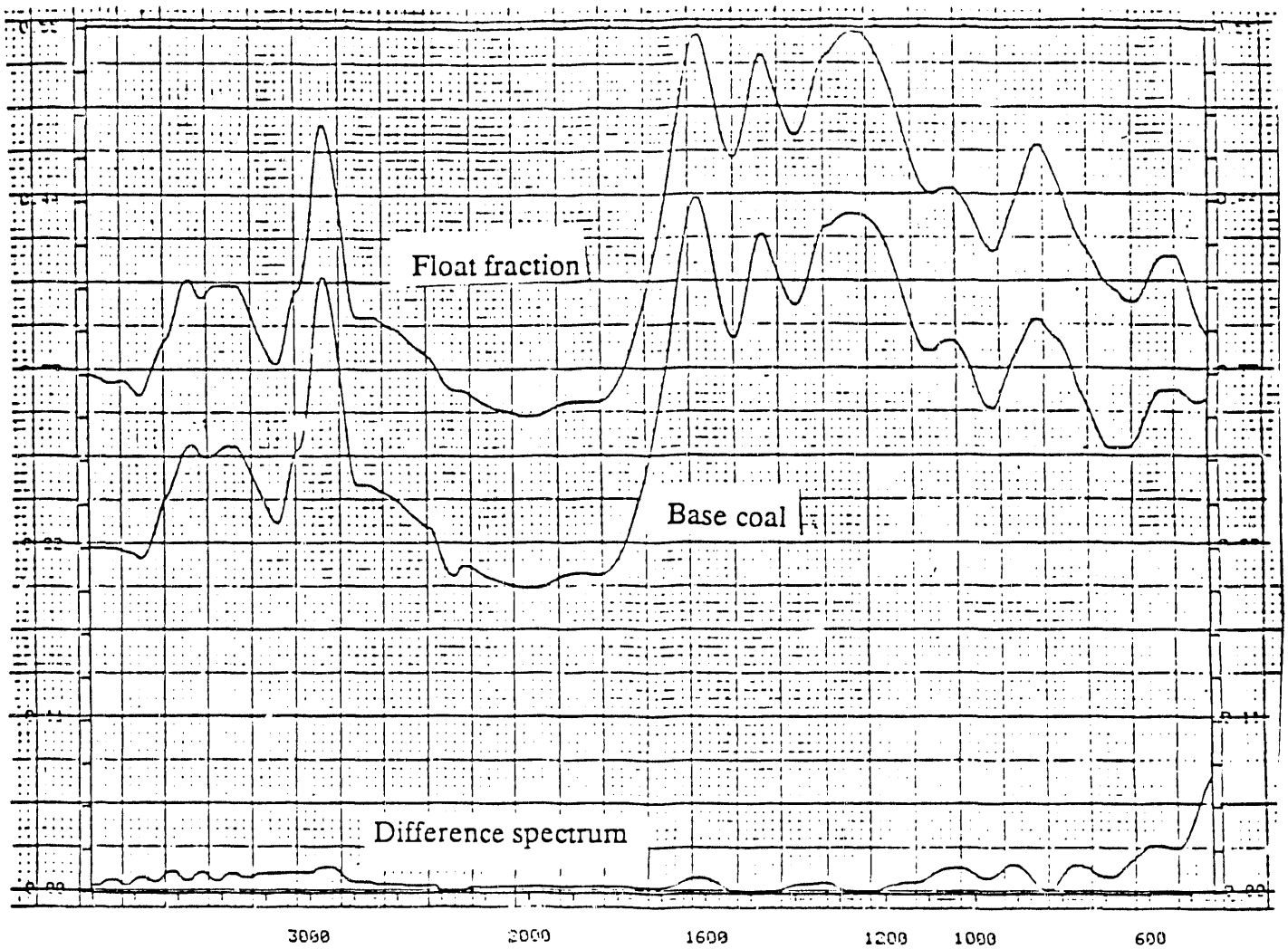

Figure 58: DRIFT absorbance spectra of base coal and float fraction obtained from film flotation and the corresponding difference spectrum.

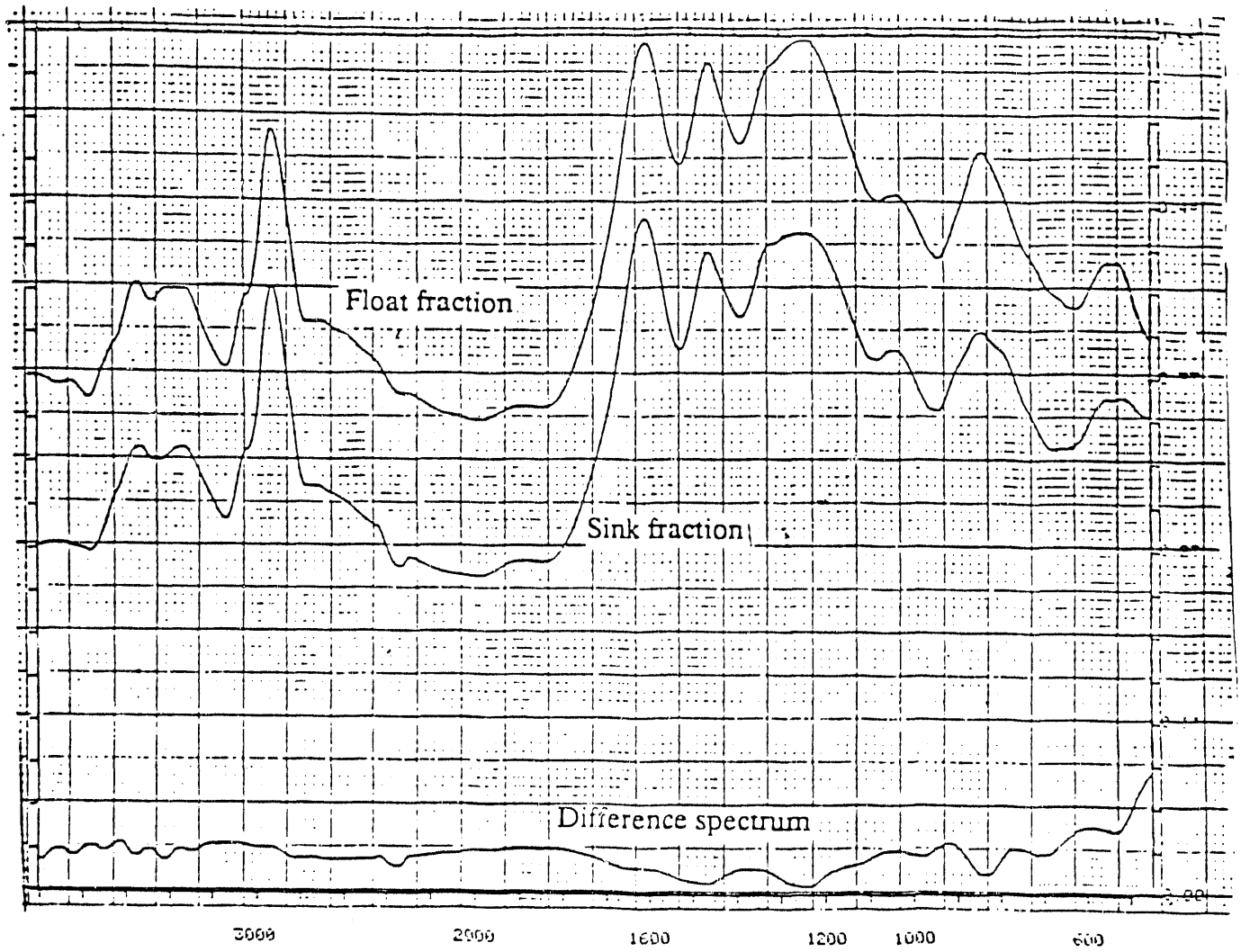

Figure 59: DRIFT absorbance spectra of float and sink fraction obtained from film flotation and the corresponding difference spectrum.

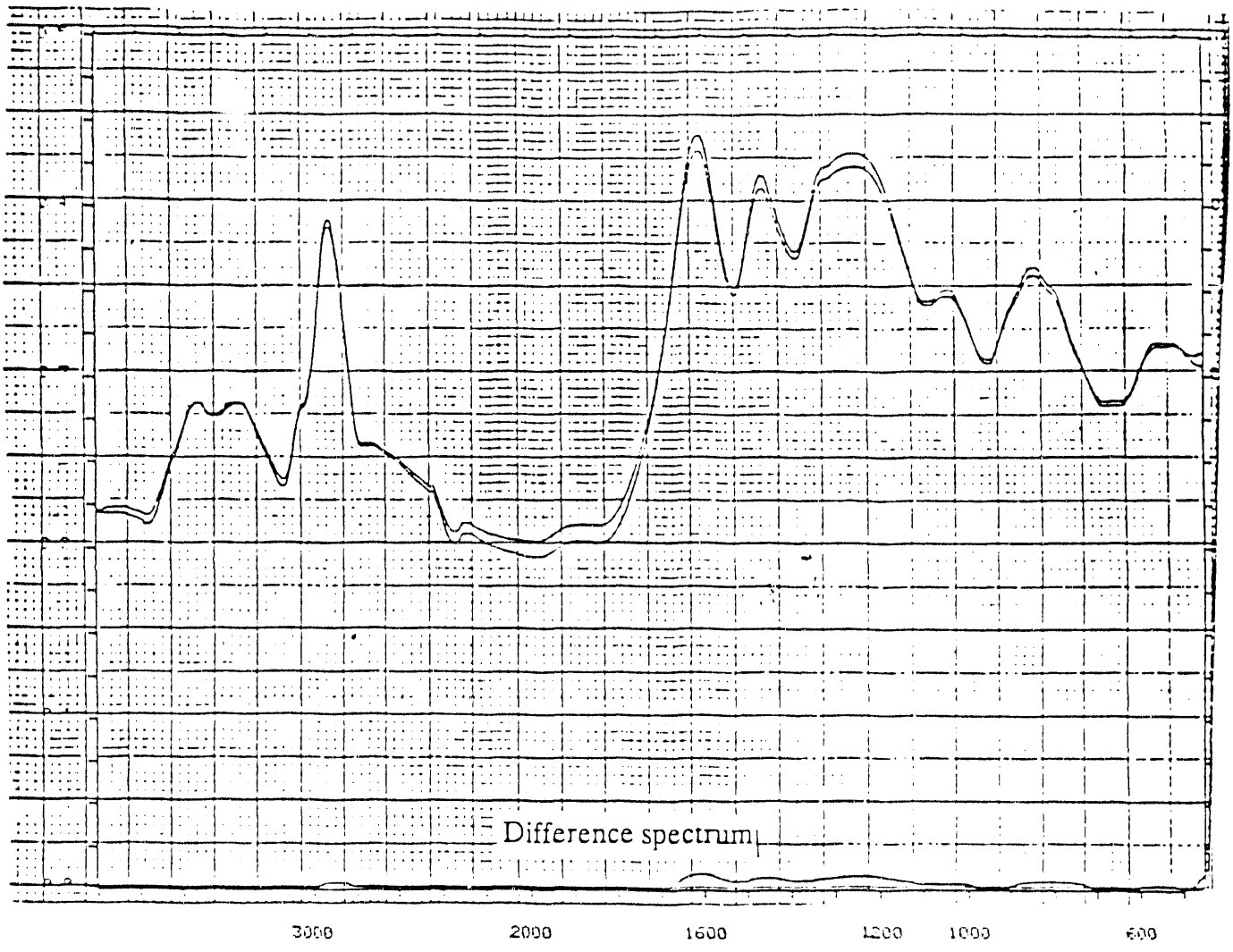

Figure 60: DRIFT absorbance spectra of base coal and sink fraction obtained from film flotation and the corresponding difference spectrum.

population have a similar γ_c distribution (in magnitude), it appears that the spatial distribution of sites is more important in governing wetting behavior than the absolute number of the sites of various surface energies.

6.6.2 LAMMA

Laser Microprobe Mass Analyzer (LAMMA) line scan spectra of coal were obtained. LAMMA is a state of the art surface analytical technique ideally suited for advanced research on a heterogeneous organic material like coal. LAMMA has already proven very useful in the investigation of the fragmentation of polymeric substances with a view to the identification of organic inhomogeneities. Gardella et al [142] were able to demonstrate using one of the first generation laser microprobes that polymer side chains yield characteristic fragmentation patterns. It has also been possible to detect carbazoles in polyethelyene [143] and triphenyl arsenic in polyvinyl butarate [144]. These researches clearly demonstrate the utility of this equipment in coal research since coal is a heterogeneous mixture of polymeric sub-units.

The LAMMA spectra (both the positive and negative ion spectra) are enclosed in Appendix C. Spectra are spot analysis at intervals of 4 microns. Normal data consists of spectral plots of mass versus intensity. Interpretation of the spectra is based on the mass number, isotopic pattern and fragmentation patterns. Spatial variation in both the relative intensity and fragmentation pattern is illustrated in the reduced positive ion spectral line scan profile at intervals of 4 microns in Figure 61. For any given species the variation in the fragmentation pattern is quite evident along the linescan. This variation in fragmentation pattern shows the microheterogeneity of the coal.

Inhomogeneity in the distribution of inorganic elements can be noticed even at 4 micron levels. For example in Figure 61, sodium and aluminum are noticed

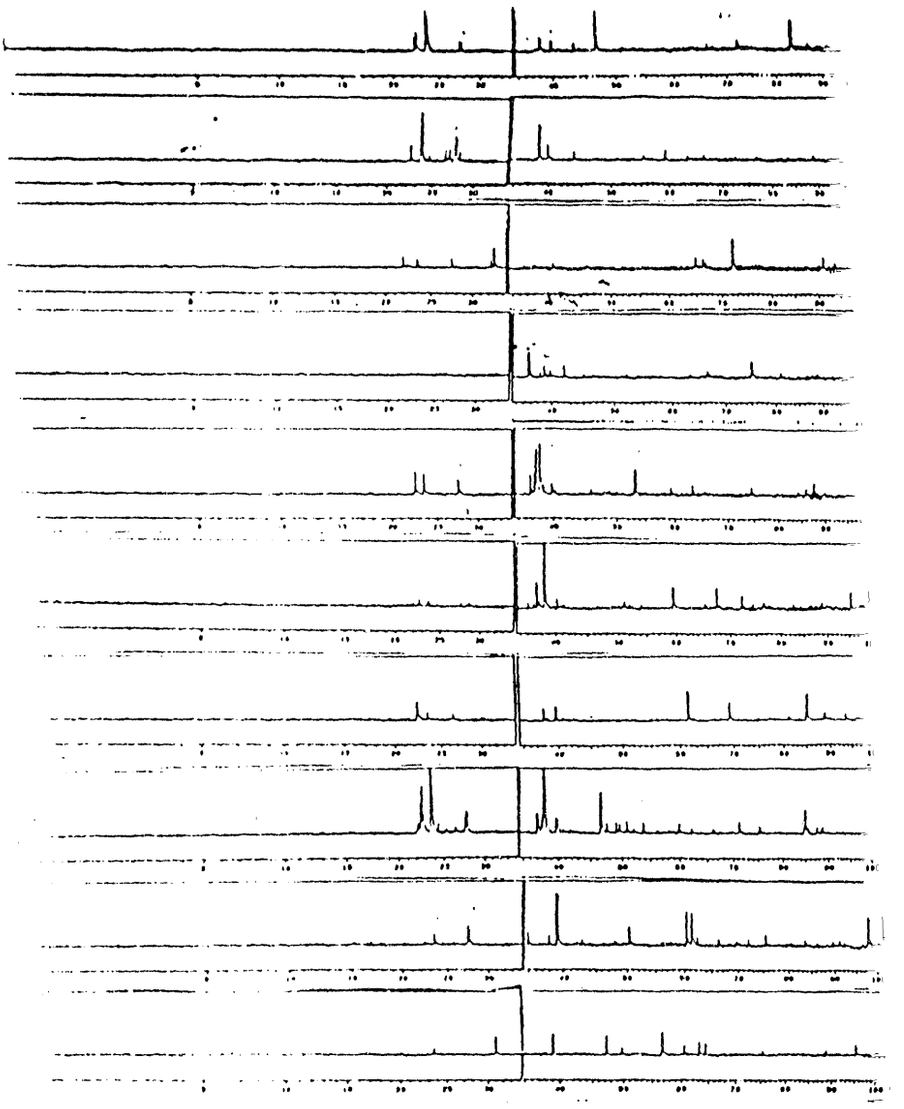

Figure 61: Positive

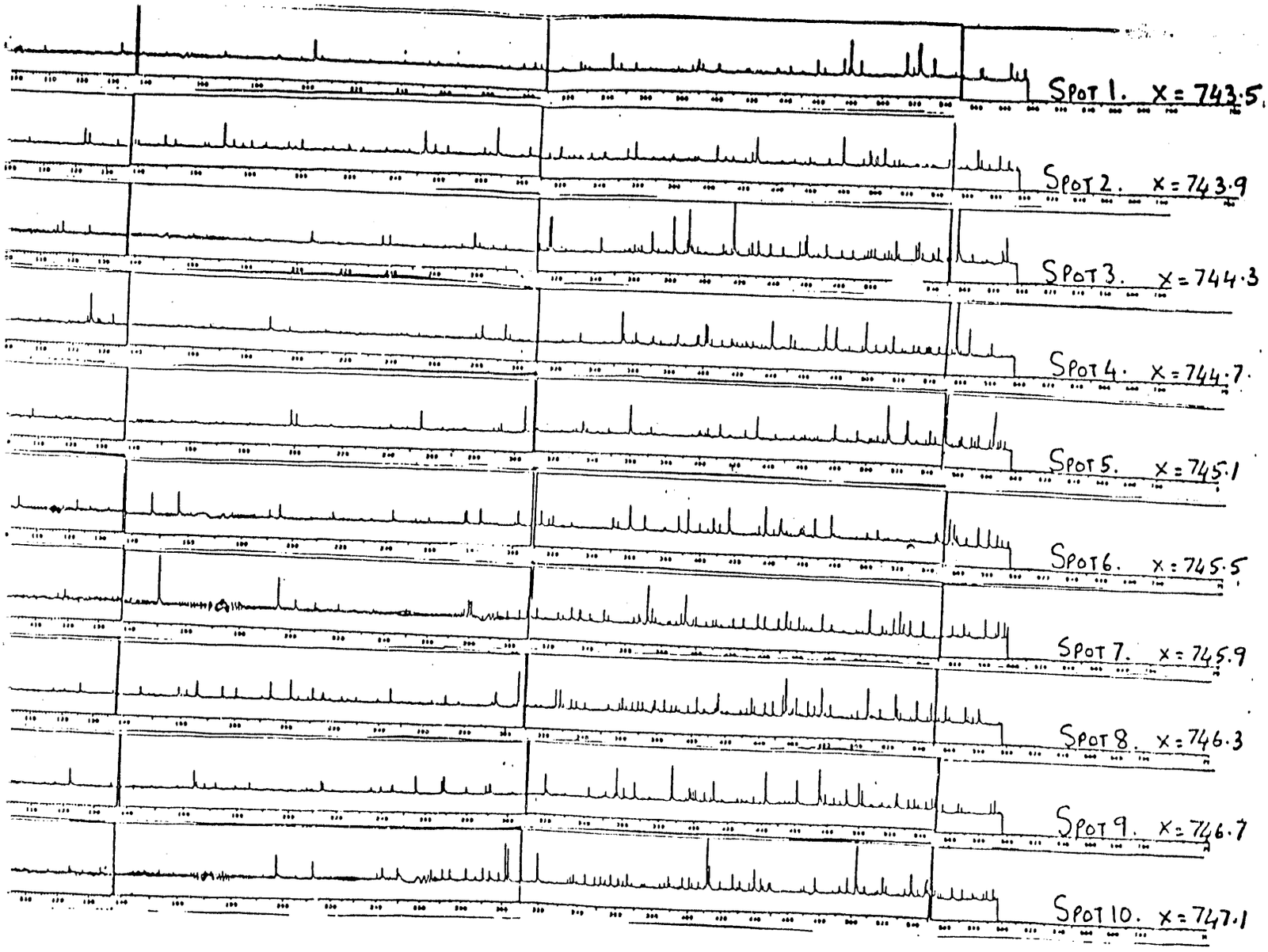

ion LAMMA spectral line scan profiles at intervals of 4 microns.

in spots 1, 2, 3 and 5, but are absent in spots 4 and 6. This shows that inorganic matter in coals are finely dissemenated. Pottasium, Chromium, Manganese and Cobalt are also noticed. The presence of these inorganic species are in line with SEM/EDX studies discussed earlier.

A study conducted with LAMMA previously [145] describes the laser desorption processes and illustrates the methodology for peak assignments. The coal macromolecular system shows major peaks at $(B + X_n)$ in both the positive and negative ion spectra, where B represents the hydrocarbon nucleus and X represents groups typically H, OH, O, CN, and CO.

Both the positive and negative spectra show a characteristic pattern of peaks that concentrate around multiples of 12. This aspect appears more intense on the negative spectra than on positive spectra. However the negative spectra are less intense than the positive spectra. The smaller fragment peaks found in the neighborhood of the multiples of 12 peaks can be attributed to moieties of the C_nH_m type. This is probably indicative of the high aromaticity of the coal sample. The coal sample is high volatile bituminous type with around 80% carbon and has a high degree of lusture indicative of vitrinite. The sample is also hydrophobic. These facts are also indicative of high aromaticity. Oxygenated fragments are also discernable as evidenced by peaks at atomic mass units (AMU) of 47,67, and 83 in the positive spectra attributed to $CHOOH$, C_4H_2O and C_4HOOH. Peaks occuring at intervals of 8 in the region 320 to 540 (AMU) in the case of positive spectra can similarly arise from moieties like $(B+O)$ or $(B+O_2)$ where B is the parent fragment. Microheterogeneity of organic species is also evident, for example in Figure 61, the region 140 to 160 AMU the spectrum at the spot X = 745.9 shows a peak at 150 AMU which is absent at other spots. The peak at 360 AMU appears in all the spectra except in the case of spectra at spots X = 745.9 and X = 743.5.

Positive ion spectra in the 40 to 300 AMU range of the fragmentation pattern

show a high degree of inhomogeneity as can be seen by the variation in the pattern and in the appearance of various peaks. The 320 to 600 amu region is seen to be densely populated and indicates that the major desorbable components fall in this category. However, even in this region there is no similarity in the fragmentation pattern along the linescan. Microheterogeneity is also evident as can be seen by the fragmentation pattern at 4 micron intervals in the case of the negative ion spectra, given in Appendix C.

Based on the present LAMMA study and the site distribution studies it is evident that the organic heterogeneity exists on every single coal particle. This heterogeneity is probably due to the distribution of various organic moieties spatially as seen from LAMMA results. There appears no trend in the fragmentation patterns at 4 micron intervals along a 40 micron line scan. This is possibly an indication that the spatial distribution of moieties is random at this micron level. A major conclusion that is evident from the LAMMA study is that the coal "molecule" or average repeatable structural unit, if it exists, is larger than 4 microns.

6.6.3 D - ESCA

Since surface characterization is an important aspect in this project, ESCA (Electron Spectroscopy for Chemical Analysis) study of the coal surface was conducted. Surface derivatization, a technique often used in the preparation of organic compounds for gas-liquid chromatography, uses site specific molecular "tags" that bond to key chemical groups on the surface. The molecular tags contain atoms that are not part of the surface, however; they increase the sensitivity of detection by ESCA by over an order of magnitude. Surface derivatization is especially useful for tagging functional groups that are not directly resolvable by ESCA, such as phenolic OH and carboxyl. Application of derivatization in conjunction with ESCA is a relatively new technique for quantifying functional groups on the surface which has not

Element	Atom percent
Carbon	84.0
Oxygen	11.0
Aluminum	0.8
Silicon	1.3
Nitrogen	2.3
Sulfur	0.3

Table 3: Elemental composition data measured from the coal surface ($\approx 100\mathring{A}$).

been possible till now. To our knowledge there exists no published literature on the absolute amount of various functional groups on the surface of coals. For the first time quantitative information on specific functional groups on the coal surface has been obtained by surface derivitization procedure and is reported here.

The surface elemental composition as infered from the survey spectrum (Spectrum 1) is shown in Table 3 and the corresponding chemical binding states obtained from the high resolution spectra taken over the C(1s), S(2p), O(1s) and N(1s) photoelectron signal regions (Spectrum 1a, 1b, 1c, 1d) are given in Table 4. The C(1s) spectrum (Spectrum 1) exhibits an asymmetric line shape which is characteristic for polynuclear aromatic compounds [146].

Sulfur was found in elemental form and as a sulphate. Interestingly two components of the N(1s) signal (Spectrum 1d) were observed. The lower binding energy component most likely corresponds to a nitrogen atom in an aromatic structure. The higher binding energy component possibly corresponds to an aliphatic type of nitrogen. The mean γ_c of the base coal sample is 44 dynes/cm. Values of γ_c close to 44 dynes/cm are found for many functional groups with nitrogen in them, for example urea and amides. Silicon appears to be the major inorganic component on the surface.

In order to estimate the number of surface hydroxyl, carbonyl and carboxylic groups, the samples were submitted to site specific reactions resulting in the in-

X-Ray Power: _____ Flood Gun: 7.0 Operator: GB Spot: 1000 u Resolution: 4

VERTICAL SCALE

4000

COUNTS/INCH

ESCA SPECTRUM

CURSOR BINDING ENERGY

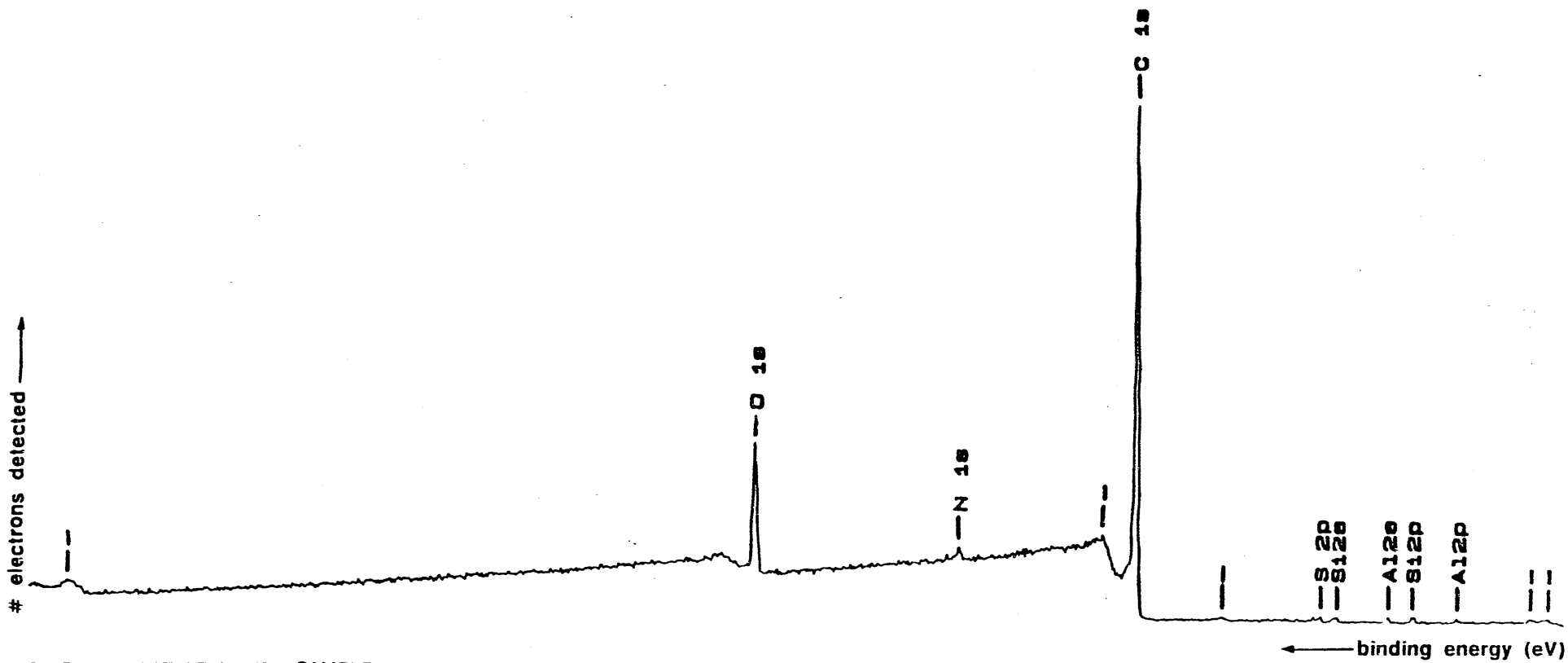

1000.0

UPPER BINDING ENERGY (eV)

SAMPLE: _____

COMMENTS: _____ Disc: HARD

DATA FILE #: GB9002A

Region 1

0.0

LOWER BINDING ENERGY (eV)

SAMPLE B

AS REC

2 # SCANS

Spectrum #: 1

138A

X-Ray Power: _____ Flood Gun: 7.0 Operator: GB Spot: 600 u Resolution: 2

VERTICAL SCALE

1000

COUNTS/INCH

ESCA SPECTRUM

CURSOR BINDING ENERGY

Energy	Width	Area	%	Delta BE
278.80	1.82	64238	80.4	0.00
280.17	1.65	10765	13.5	1.37
282.38	1.02	1168	1.5	3.58
283.82	1.40	1927	2.4	5.02
285.42	1.72	1805	2.3	6.62

80% Gaussian
Last chi-square: 1.671

C(1s)

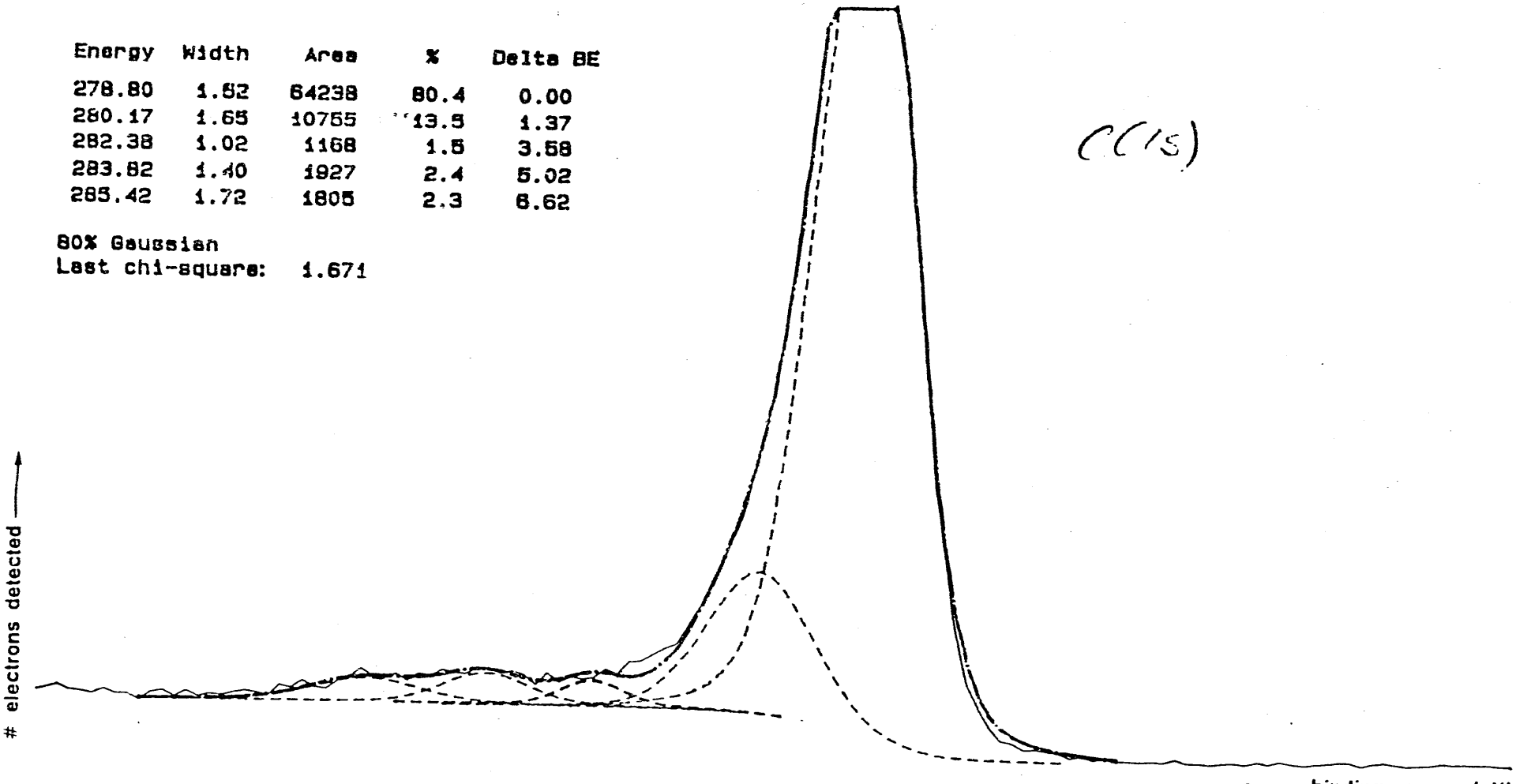

290.0
UPPER BINDING ENERGY (eV)

SAMPLE:

COMMENTS:

Disc: HARD

DATA FILE # GB9002B
Region 1

270.0
LOWER BINDING ENERGY (eV)

SAMPLE B
AS REC

5
SCANS

Spectrum #: ____ 1a

138B

X-Ray Power: _____ Flood Gun: 7.0 Operator: GB Spot: 600 u Resolution: 2

VERTICAL SCALE

40

COUNTS/INCH

ESCA SPECTRUM

CURSOR BINDING ENERGY

Energy	Width	Area	%	Delta BE
158.44	1.90	1552	66.2	0.00
162.98	1.98	792	33.8	4.84

80% Gaussian
Last chi-square: 2.787

5(2p)

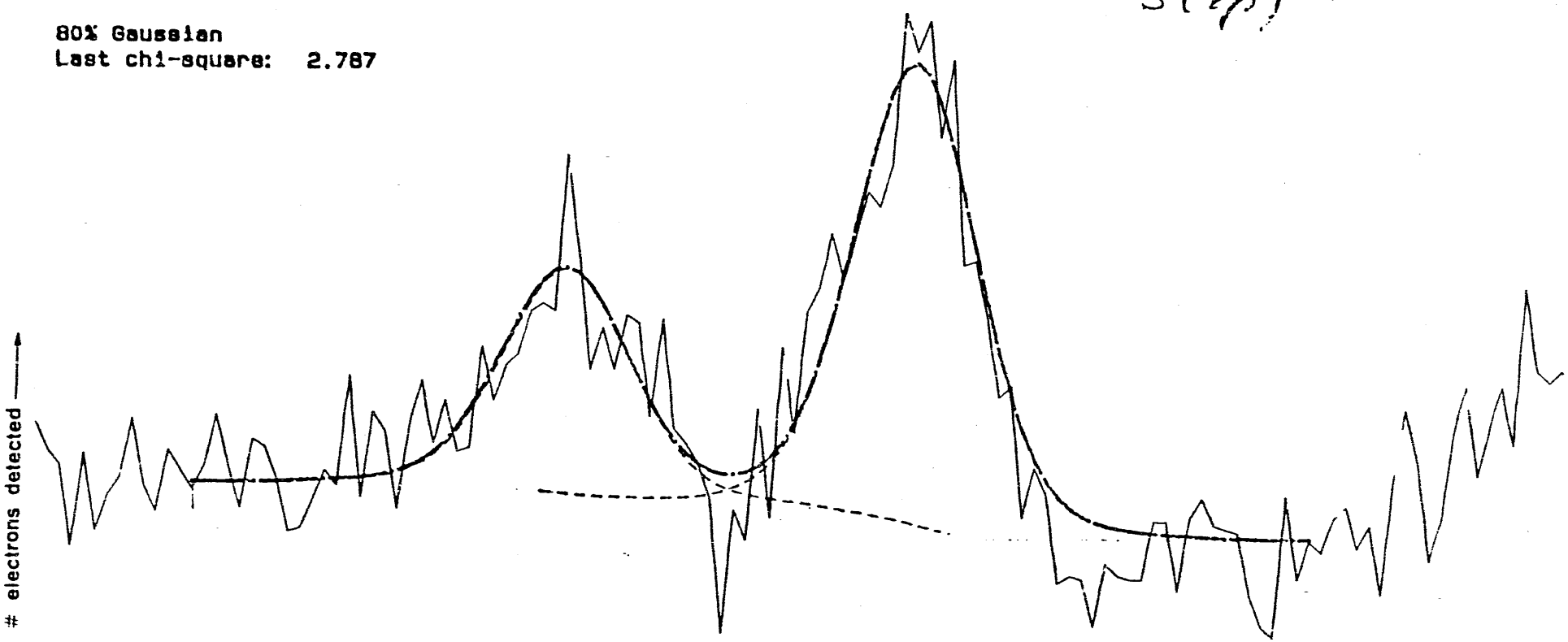

170.0
UPPER BINDING ENERGY (eV)

SAMPLE:
COMMENTS:
SAMPLE B
AS REC

Disc: HARD

DATA FILE #: 6B90028
Region 3

150.0
LOWER BINDING ENERGY (eV)

10
SCANS

Spectrum #: 16

138C

X-Ray Power: _____ Flood Gun: 7.0 Operator: GB Spot: 600 u Resolution: 2

VERTICAL SCALE

400

COUNTS/INCH

ESCA SPECTRUM

CURSOR BINDING ENERGY

Energy	Width	Area	%	Delta BE
526.01	1.77	10141	36.5	0.00
527.53	1.82	17671	63.5	1.52

80% Gaussian
Last chi-square: 1.845

O(1s)

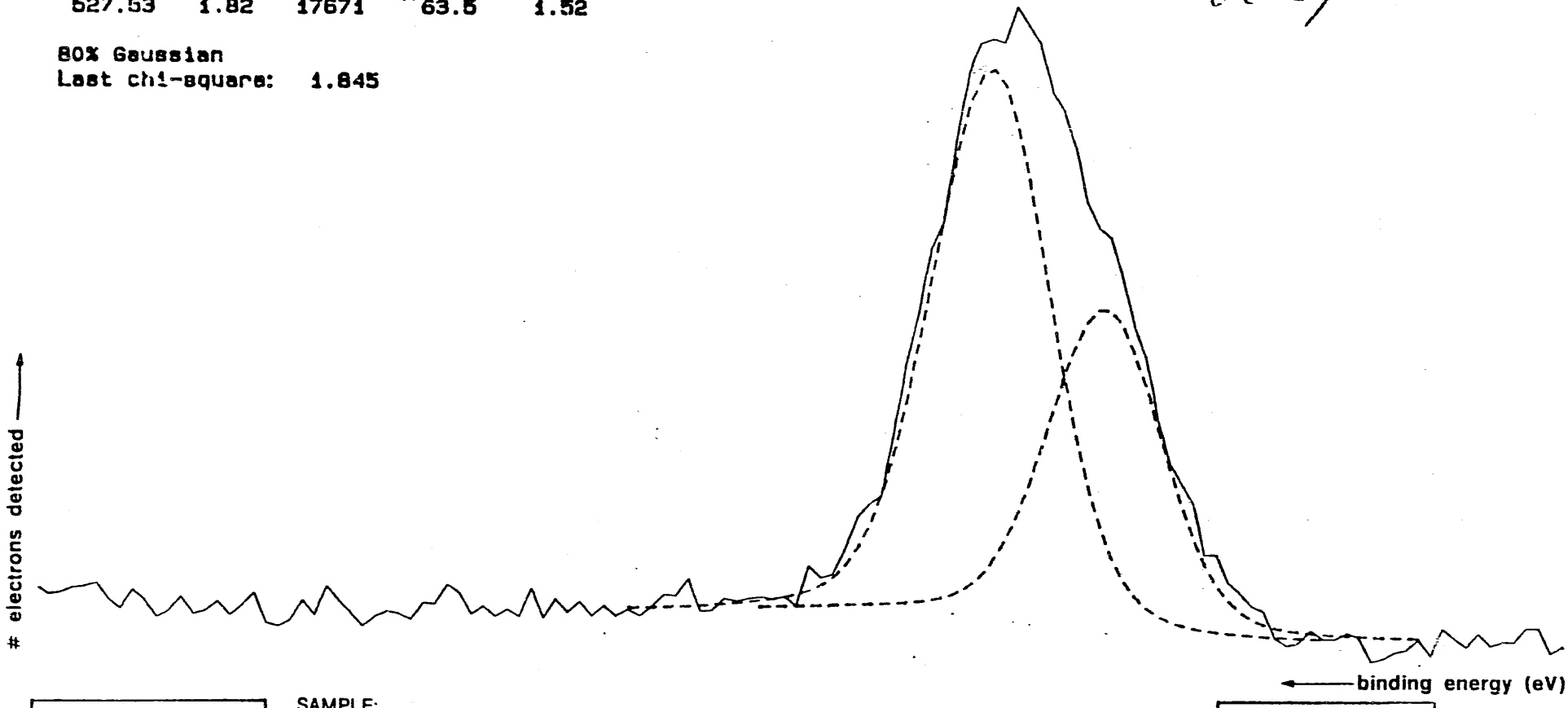

540.0
UPPER BINDING ENERGY (eV)

SAMPLE:
COMMENTS:

Disc: HARD

DATA FILE # GB9002B
Region 2

520.0
LOWER BINDING ENERGY (eV)

SAMPLE B
AS REC

5
SCANS

Spectrum #: 1c

138D

X-Ray Power: _____ Flood Gun: 7.0 Operator: GB Spot: 600 u Resolution: 2

VERTICAL SCALE

100

COUNTS/INCH

ESCA SPECTRUM

CURSOR BINDING ENERGY

Energy	Width	Area	%	Delta BE
392.57	2.08	1961	38.7	0.00
394.44	1.81	3090	61.3	1.87

80% Gaussian
Last chi-square: 3.992

N(1s)

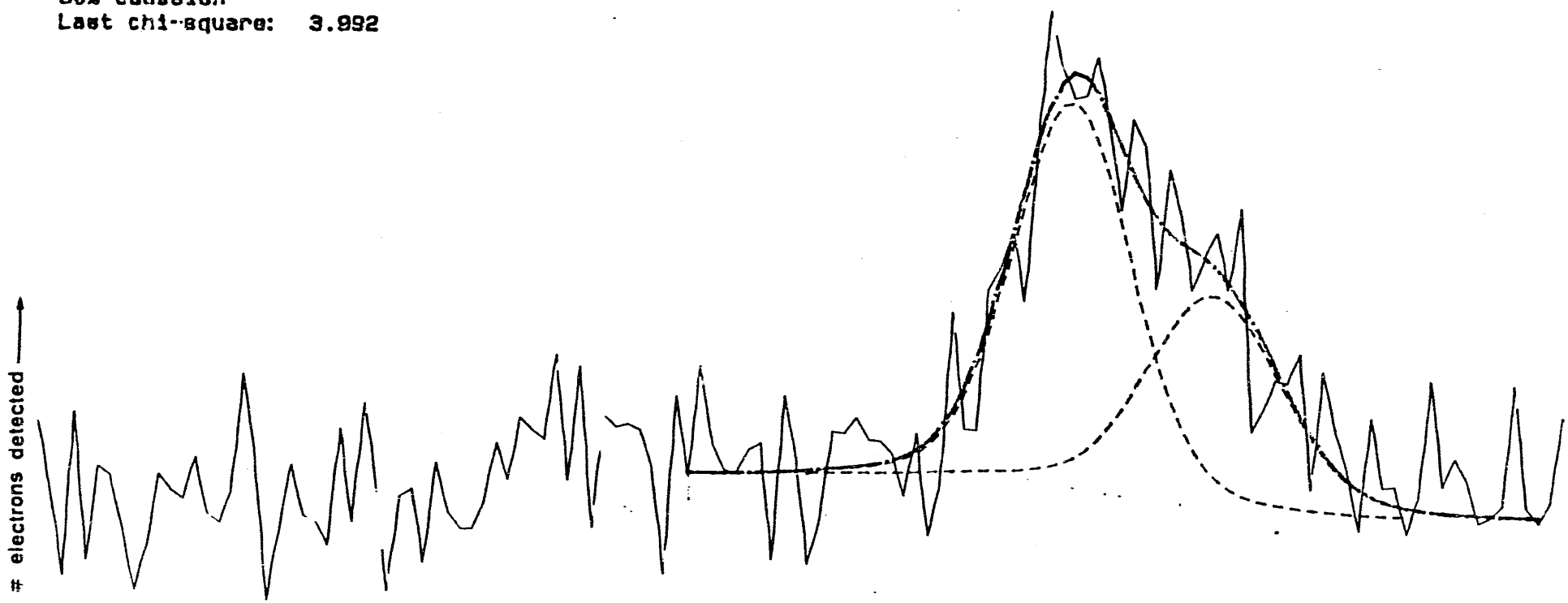

←binding energy (eV)

408.0
UPPER BINDING ENERGY (eV)

388.0
LOWER BINDING ENERGY (eV)

SAMPLE:
COMMENTS:
SAMPLE B
AS REC

Disc: HARD

DATA FILE #: GB9002B
Region 4

10 # SCANS

Spectrum #: 1d

139E

Peak assignments(R=CH)	Binding energy (eV)	Atom percent
C-R	284.6	68.0
C-OR	286	11.0
O=C-OR	288.2	1.3
C4(shake-up)	290	2.0
C5(shake-up)	291.2	1.9
Elemental sulfur	164.2	0.2
Sulfate sulfur	168.8	0.1
C=O	531.8	4.0
C-O	533.3	7.0
-N=	398.4	0.9
N aliphatic	400.2	1.4

Table 4: High resolution D-ESCA data: binding energies, atom percentages and peak assignments.

corporation of fluorine. Ordinary ESCA analysis is not sensitive to the hydrogen present in organic substances.

Since polar groups invariably contain hydrogen, an accurate estimation of polar groups can only be obtained indirectly by the derivatization procedure. The survey spectra taken from the derivatized samples are shown in Spectrum 2 to 4. The number of functional groups per 100 atoms are shown in Table 4(the numbers were calculated by dividing the atom percent fluorine by the number of fluorine atoms in the tag molecule). The three functional groups i.e. -OH, C=O and COOH are present in approximately equal amounts. The number of these functional groups per 100 atoms is between 1 and 2. From previous film flotation studies it is known that this sample of coal is not wetted spontaneously by water. Evidently the amount of polar groups present on the surface of this sample of coal is insufficient to cause complete wetting.

Based only on the high resolution spectra and the binding states one would normally infer more polar groups on the surface than is actually the case. The amount of polar groups is unambigously available from the derivatized ESCA. It is

X-Ray Power: _____ Flood Gun: 5.0 Operator: GB Spot: 1000 u Resolution: 4

VERTICAL SCALE

2000

COUNTS/INCH

ESCA SPECTRUM

CURSOR BINDING ENERGY

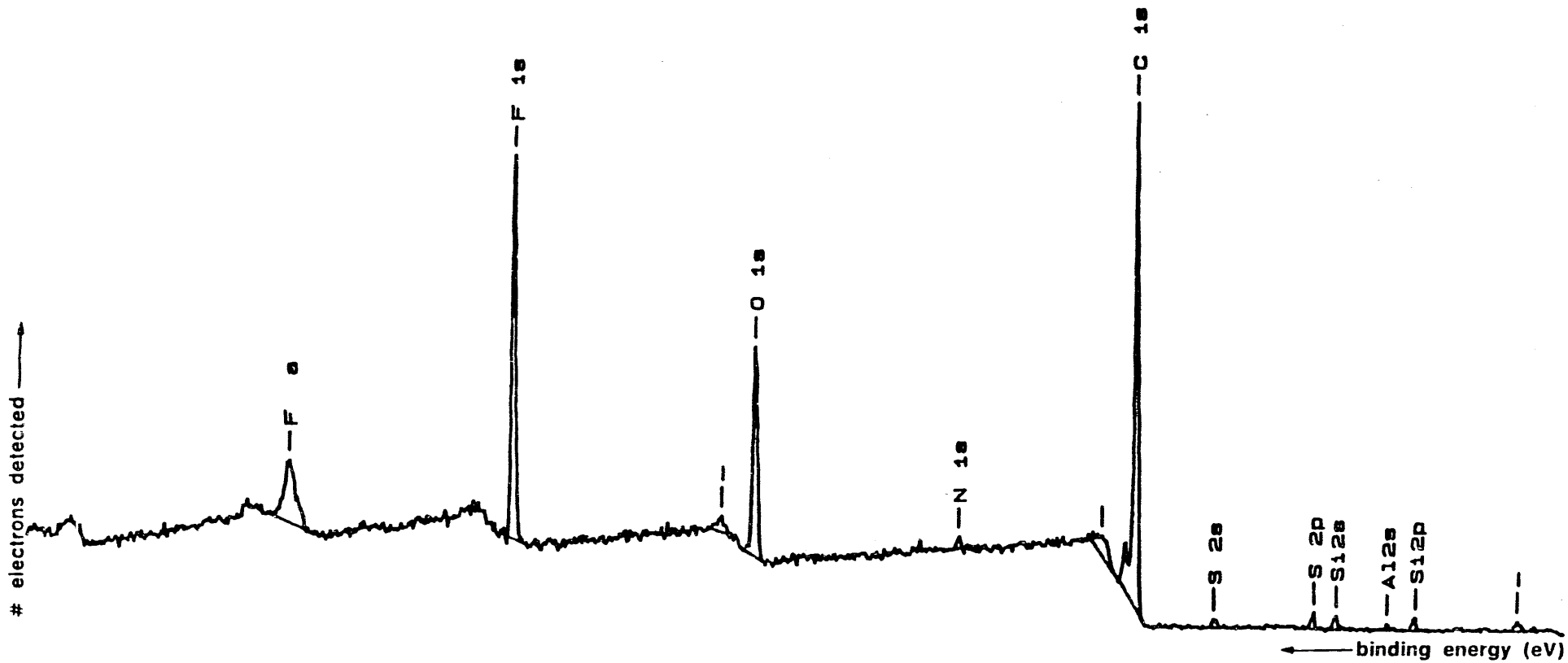

1000.0
UPPER BINDING ENERGY (eV)

SAMPLE:

COMMENTS: Disc: (1) 124 DATA FILE #6B9002B

Region 1

0.0
LOWER BINDING ENERGY (eV)

SAMPLE B

OH DERIVATIVE

2 # SCANS

Spectrum #: 2

139B

X-Ray Power: _____ Flood Gun: 10.0 Operator: GB Spot: 1000 u Resolution: 4

VERTICAL SCALE

4000

COUNTS/INCH

ESCA SPECTRUM

CURSOR BINDING ENERGY

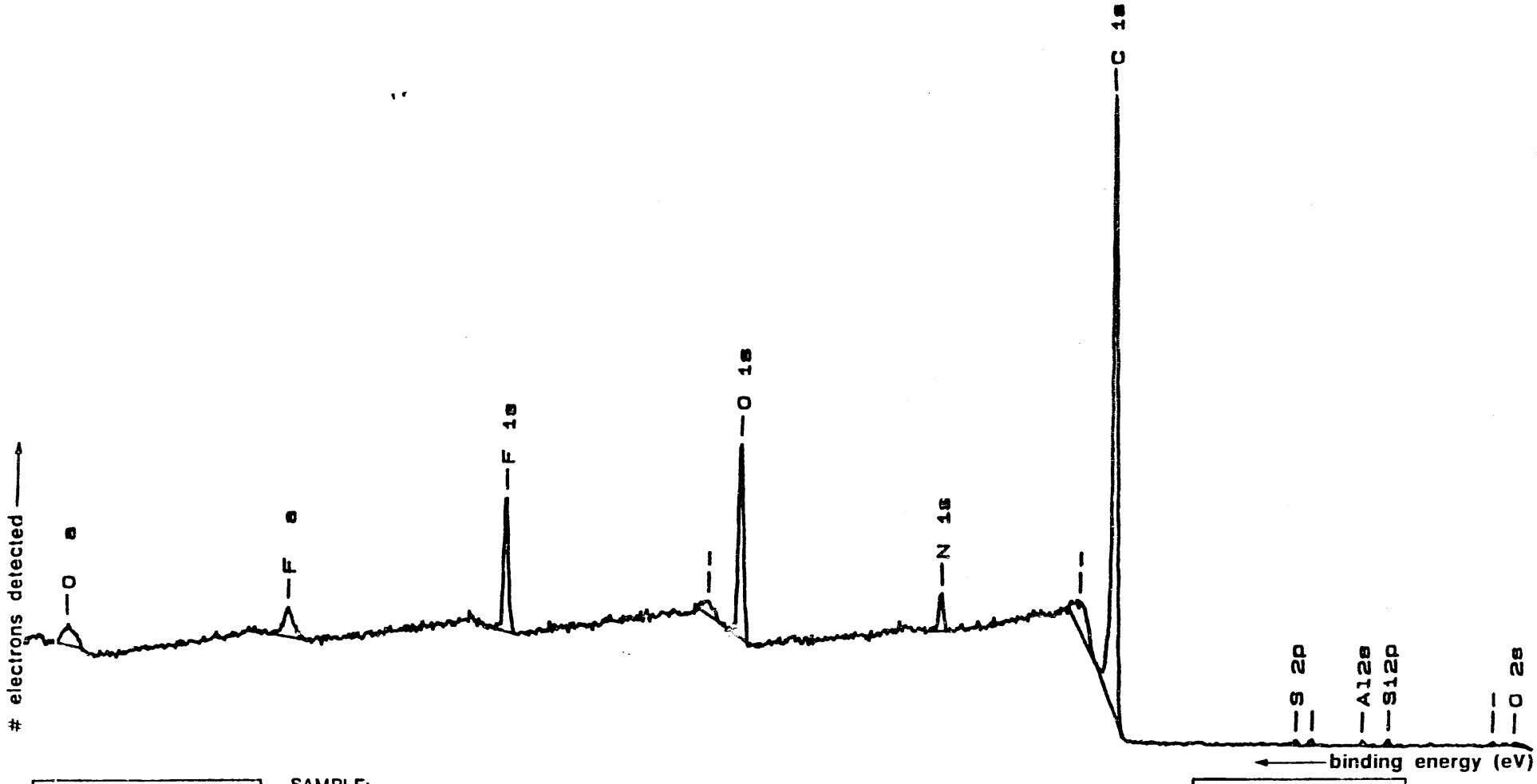

1000.0
UPPER BINDING ENERGY (eV)

SAMPLE:

COMMENTS: Disc: (1) 124 DATA FILE #GB9002C

Region 1

0.0
LOWER BINDING ENERGY (eV)

SAMPLE B

C=O DERIVATIVE

2
SCANS

Spectrum #:

139C

X-Ray Power: _____ Flood Gun: 10.0 _____ Operator: GB _____ Spot: 1000 u Resolution: 4

VERTICAL SCALE

4000

COUNTS/INCH

ESCA SPECTRUM

CURSOR BINDING ENERGY

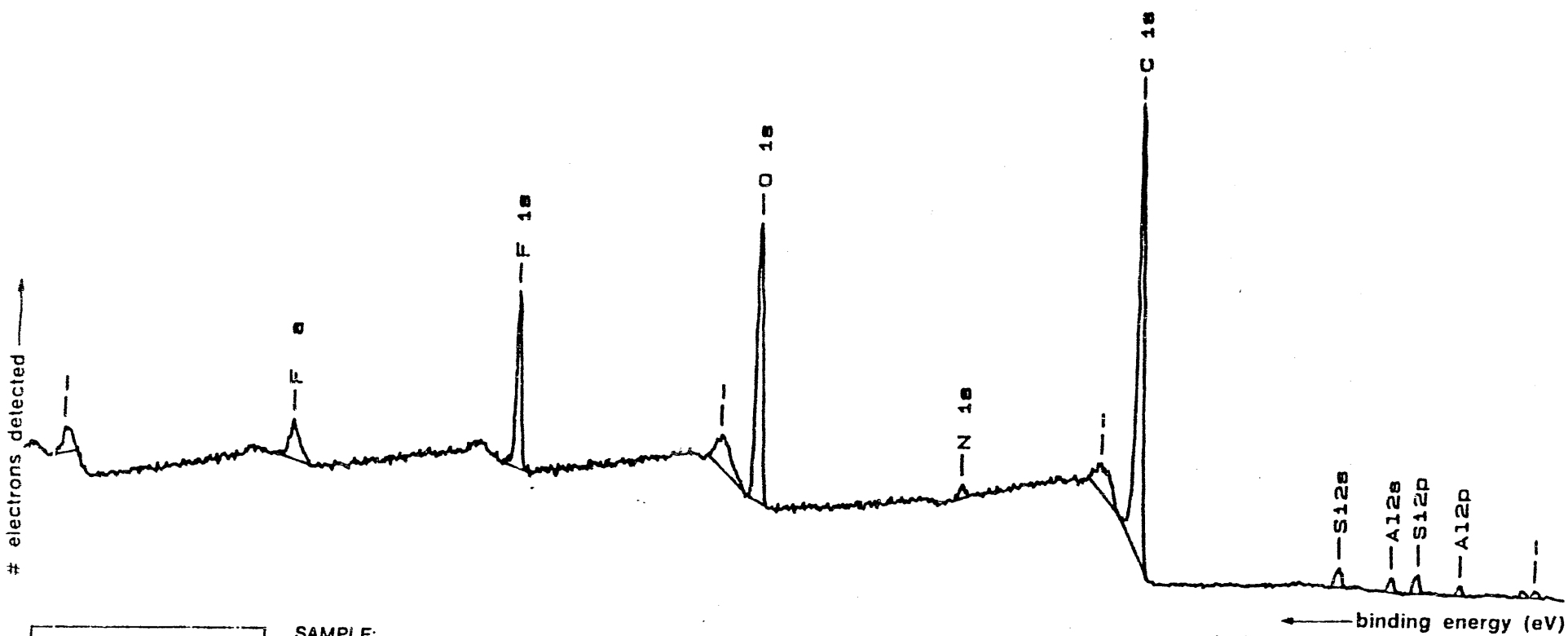

1000.0
UPPER BINDING ENERGY (eV)

SAMPLE:

COMMENTS: Disc: {1} 124 DATA FILE #GB9002D

Region 1

0.0
LOWER BINDING ENERGY (eV)

SAMPLE B

COOH DERIVATIVE

2 # SCANS

Spectrum #: 4

139D

felt that derivatized ESCA will provide information on the polar / nonpolar groups on coal surface and can in turn be used to monitor the effect of oxidation and such alterations on the hydrohpobicity or flotation of coal in a more quantitaive way than has been possible till now.

6.7 Other distributions

During the course of this research we identified potential techniques which will give further complimentary information regarding distribution of surface properties of coal particulates and these techniques are briefly mentioned below.

Recently an instrument is available in the market which provides a distribution in the electrophoretic mobilities of particulate populations (Penkem 3000). In classical studies involving electrophoretic mobilities and zeta potential only an average value characterizes these properties. However as mentioned earlier such average values seldom provide an accurate measure of the interfacial properties. Use of this instument in coal surface science to measure zeta potential distributions will provide more accurate representation of interfacial properties. Zeta potential studies using this instrument have been recently reported in the literature [147,148]

Induction times provide a measure of the bubble particle attachment probability. Usually, induction time is reported to be the value of a particular contact time at which 50% of the tests results in bubble-particle attachment (average value). Recently however, it has been shown that the distribution of attachment frequency is, in fact, a more accurate description of the hydrophobic character of a particulate population [149]. In this study observed flotation results could not be correlated with *average values* of contact angle or induction time. Analysis of induction time distributions revealed that, though the average induction are the same, there existed a difference in the induction time distributions.

Induction time distributions provide a measure of the probability distribution of bubble particle attachment. Centrifugal immersion experiments discussed earlier provide a probability distribution of bubble particle detachment. A combination of these experimentaly determined probability distributions will aid in the development of a flotation model.

Recently Wittkopf [93] has developed a model to calculate the desorption energy distribution of adsorbed water based on mass spectroscopic data. . Such energy distributions were obtained even for persumably homogeneous glass spheres. A typical energy distribution spectrum is shown in Figure 62.

7 CONCLUDING REMARKS

It is well known that coal is a heterogeneous substance. The concept of critical wetting surface tension can be effectively used to characterize this heterogeneity both qualitatively and quantitatively. A new approach for determining the *distribution* in surface properties of coal particles was developed in this study and various techniques capable of providing such information were identified. Distributions in surface energy, contact angle and wettability were obtained using novel techniques such as centrifugal immersion which was developed during the course of this project and film flotation. Changes in these distributions upon oxidation and surface modifications were monitored and discussed. Results from centrifugal immersion and film flotation and have confirmed the existance of surface sites of various energies, and site distribution curves based on these techniques have be obtained.

1. Using the approach developed in this study, it has also been shown for the first time that the observed heterogeneity of a mass of coal particles reflects the heterogeneity of each single particle. In essence it has been possible to

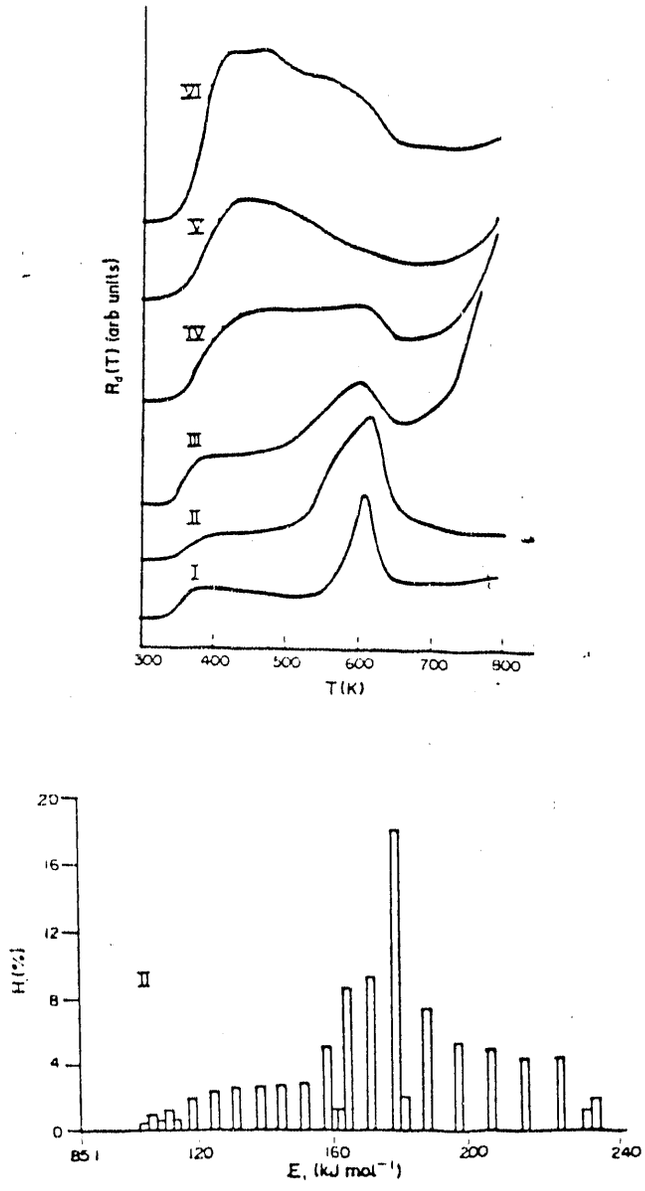

Figure 62: Water desorption spectra from silicate glass samples recorded by a mass spectrometer (top) and the energy distribution calculated from the spectra for sample II.

obtain a psuedo map of the surface of coal and of coal surfaces after various modifications.

2. The inherent surface moisture in coal is probably present as a heterogeneous ordered structure as opposed to free moisture. Low temperature (70°C) heating of coal increases the hydrophobicity of high rank bituminous coal due to the removal of the inherent moisture and possibly surface volatiles. Coal samples with adsorbed moisture were more hydrophobic than those without it, indicating an autophobic behavior. Adsorbed moisture is probably present as an ordered structure and could be responsible for the observed autophobic phenemenon.

3. Based on the changes in the surface site distribution curve on treatment with polyacrylamide (PAM) polymers it is shown that PAM adsorption on coal is essentially a entropically driven process and more so in the case of coal heated to 70°C. In the case of base coal it appears that adsorption of charged PAM takes place by the anchoring of the polymer hydrocarbon chain such that amide groups are pointing towards the surface. As the charge density increases the area occupied by amide groups increases from around 30% for 10% charge density to around 50% for 30% charge density. The adsorbed layer in the case of nonionic PAM presents a comparatively heterogeneous surface indicating a random mode of adsorption. The adsorbed layer of cationic PAM of 10% cationicity and nonionic PAM presents a more dense and compact structure as compared to anionic PAM and PAM of higher cationicity.

4. Heating of coal at 70°C in air decreased the average value of critical wetting tension indicating the formation of a more hydrophobic surface. In the case of adsorbed layers of the nonionic and the anionic polymer on coal heated at 70°C, more of the hydrocarbon chain of the polymer is apparently exposed

compared to the amide groups . 75% of the area of both polymer layers exhibit a similar surface energy distribution. The adsorbed layer of the nonionic PAM on heat treated coal exhibits a less dense structure.

5. A relatively fast and accurate technique to measure polymer concentration at the ppm levels was developed using Total Organic Carbon (TOC) analyzer. TOC was used to measure residual polymer concentrations after adsorption. Adsorption data obtained from TOC is more representative of the actual adsorption than data obtained by nephelometry or titration. Higher values of adsorption density were obtained earlier using viscosity technique employed for concentration determination and this is suggested to be due to preferential adsorption of higher molecular weight components resulting in lower viscosity and hence lower "apparent" residual concentrations.

6. Flourescence spectroscopic studies using pyrene labelled polyacrylamide polymers supported our earlier conclusions on the preferential adsorption of higher molecular weight components on coal.

7. Hydrophobicity of dodecane treated coal is governed by both the amount of sites and the magnitude of the surface energy of these sites. It appears that there exists a critical dosage of the reagent above which the coal surface is grossly less hydrophobic. This is possibly the reason for the "over oiling" noticed in industrial coal flotation. An increase in the speed of the impeller employed to disperse the dodecane in water increases the degree of coating of the dodecane on coal surface. However continued increase in the speed produces no detectable difference in the degree of coating indicative of the role of hydrodynamic factors.

8. DRIFT spectroscopy could not distinguish the surface functional groups responsible for the distribution of sites that determine critical wetting surface

tension of coal. This observation lends support to the conclusion that individual coal particles in a sample (-35 mesh +80 mesh) exhibit similar distribution of sites. It also appears that wetting is governed by spatial distribution of sites with various energies.

9. The frequency distribution of the force required to detach coal particles from the liquid-air interface obtained from centrifugal immersion experiments depends both on the surface chemistry and the shape of the particles. In the case of oxidized coal particles (with a predominately hydrophilic surface) the frequency distribution curve represents the distribution of surface moieties. In the case of hydrophobic coal particles, the curve is a collective manifestation of the distribution of the shapes of the particles and the dynamics of the detachment process.

10. Centrifugal immersion technique is a powerful tool for studying the relative wetting behavior of irregularly shaped hydrophobic particles, including the stability (probability of detachment) of such particles at the liquid-air interface. In contrast to other techniques, this technique takes into account the dynamics of spreading, surface heterogeneity, and shape effects and therefore provides an accurate characterization of the wetting behavior as encountered in practical situations.

11. Wettability distribution curves constructed from centrifugal immersion data as a function of the liquid phase shows a complex and as yet undetermined relationship between the shape, surface tension and the force required to detach heterogeneous coal particles from the liquid-vapor interface. It appears that the series of wettability distribution curves as a function of surface tension of the liquid phase will be sensitive to the surface properties of coal particles in cases where a single wettability distribution curve is not sensitive.

12. Based on the LAMMA study and our previous site distribution studies it is evident that the organic heterogeneity exists on every single coal particle. This heterogeneity is probably due to the distribution of various organic moieties spatially as seen from LAMMA results. There was no trend in the LAMMA fragmentation patterns at 4 micron intervals along a 40 micron line scan. This indicates that the distribution of moieties on the surface is random at the 40 micron spatial level. A major conclusion that is evident from the LAMMA study is that the coal "molecule" or average repeatable structural unit, if it exists, is larger than 4 microns.

13. The absolute amounts of phenolic, carboxylic and carbonyl groups on the surface of coal was obtained using derivatized ESCA which is a new technique. The polar functional groups are present in approximately equal quantities and range between 1 and 2 functional groups per 100 atoms. Surface elemental analysis and information on the binding states of the elements were also obtained. Aromatic and aliphatic nitrogen were detected. The amount of aliphatic nitrogen is approximately the same as the amount of polar groups.

14. Using the γ_c distribution and Neumann's equation of state for calculating surface tensions, a contact angle distribution on the surface of coal particles was calculated. Contact angles on coal particles range from 80° to 20°. About 40 percent of the surface has a contact angle of about 68°. The existence of sites with different contact angles is likely to lead to a very complex interplay between the advancing and receeding angle distributions in coal flotation systems.

15. A thermodynamic approach to study coal surface heterogeneity was developed and is illustrated along with experimental results. A qualitative picture of the distribution of sites on the coal surface can be obtained from the isosteric

heat of adsorption as a function of the amount adsorbed. Heat of immersion provides a quantitative measue of the heterogeneity in terms of the site distribution function. It appears that the more hydrophobic sites on coal surface are densely clustered whereas, the more hydrophilic (or relatively less hydrophobic) sites are distributed sparsely. To our knowledge this is the first time heats of adsorption have been measured as a function of coverage on coal and also where both calorimetric and isosteric heats for the same system are presented.

16. A multi-pronged approach consisting of centrifugal immersion, film flotation, gas adsorption, calorimetry and different spectroscopies is used to elucidate the heterogeneous nature of the distribution of surface sites on coal and changes in the distribution upon chemical and thermal treatment. Other type of distributions and techniques to study them are also discussed briefly.

The present work is a contribution to our understanding of the fundamental nature of the complex coal surface.

7.1 Impact of study on advaced physical coal beneficiation processes

The results of this research project is of practical importance in the area of clean coal technology where surface based beneficiation projects are employed for better utilization of coal. A fundamental knowledge of the *distribution* of surface sites on coal and effect of treatments on the distribution should help to control these processes efficiently since often only a small fraction of the surface need to possess have a given property to bring about the desired effect.

For example it is conceivable that a particle whose surface consists of predominantly hydrophilic sites (say unliberated mineral matter) can float if the bubble

attaches to a hydrophobic patch. However the density of this particle will also determine if the surface tension and bouyancy forces are sufficient for the particle to float. One ultimate objective in fine coal flotation is to relate the density of locked coal-pyrite particle to its flotability. This in turn requires knowledge of the ***distribution of relatively hydrophobic and hydrophilic sites*** and effect of chemical treatment on it. Such knowledge will help in designing optimum operation and control of precleaning circuits and thereby in enhancing the efficiency of advanced physical beneficiation processes.

In the area of spherical agglomeration and flotation surface heterogeneity plays an imporatnt role. Its important to note that wettability is a macroscopic concept which is related on a microscale to the distribution of wettable and non wettable sites on the surface.The relative distribution of hydrophilic and hydrophobic sites will govern the absolute wetting of the surface. More specifically, it the rate at which the leading edge of a spreading liquid moves that will deterimine if the wetting medium will overide a patch of nonwettable region. If the nonwettable region is "small" then it is conceivable that the liquid will overide the region and vice versa. Thus the spatial distribution of sites and its scale is an important and a fundamental varaible which determines the wetting behavior of heterogeneous surfaces. These aspects are directly related to the study of dynamic contact angles and kinetics of wetting, published information on which are scarce. The effeciency with which the spherical agglomeration process is able to selectively beneficiate coal is directly related to these issues.

References

[1] The Presidents commision on Coal, 1980

[2] "Facts about Coal - 1988", National Coal Association Publication

[3] Aplan, F. F., "Fine coal preperation - its present status and future" in Fine Coal Processing, S.K. Mishra and R.R. Klimpel (eds), Noyes Publication (1983)

[4] Keystone Manual, 1984

[5] U.S. D.O.E., DOE/EIA-C118, (1984)

[6] Bluck, W. V. and McMorris, W. L., "Effect of coal preparation on power plant fuel cost measured at busbar", Mining Enginnering, Vol 37, No. 9, (1985), 1135-40.

[7] Sehgal, R. S. and Clifford, K. L., "Where are we going with fine coal", Paper presented at the SME-AIME Fall meeting, Minneapolis, MN, Oct 1980

[8] Farley, W. and Colebank, M., "How chemically promoted flotation boosts fines recovery", Coal Mining and Processing, Vol 20, No.5, (1983), 48-51

[9] see Ref (3) page 12

[10] Harris, C. C., Personal communication, 1989

[11] de Gennes, P. G., "Wetting: Statics and Dynamics" Reviews of modern physics, Vol 57, No.3, Part I, (1985)

[12] Cazabat, A. M. and Cohen Stuart, M. A., "Dynamics of wetting on smooth and rough surfaces", Progr. Colloid and Polymer Sci., 74, (1987), 69-75

[13] Brady, G. A. and Gauger, A. W., "Properties of coal surfaces", Ind. Eng. Chem., Vol. 32, No.12, (1940), 1599-1604

[14] Horsely, R. M. and Smith, H. G., "Principles of coal flotation", Fuel, Vol 30, No.3, (1951), 54-63

[15] Brown, D. J., " Coal Flotation", in Froth Flotation - 50 th Anniversery Volume, Fuerstenau, D. W., ed., AIME, NY 1962, 518-538

[16] Sun, S. C., " Hypotheses for different flotabilities of coals, Carbon and Hydrocarbon Minerals", Trans. AIME, Vol 199, (1954), 67-75

[17] Rosenbaum, J. M., " Characterization, flotation and selective agglomeration of western coals", Ph.d. thesis, University of California, Berkely, Dec 1981

[18] Aplan, F. F., " Estimating western coal flotability" in Gold, Silver, Uranium and Coal - Geology, Mining, Extraction and Environment, Fuerstenau, M. C. and Palmer, B. R., eds., AIME, NY 1980, 380-398

[19] Parekh, B. K. and Aplan, F. F., " The critical surface tension of wetting of coal", in Recent Developments in Surface Science, Li, N. N., ed. CRC press (1978), 107-113

[20] Gayle, J. B. and Smelly, A. G., " Effects of temperature variation on contact angles for coal and related substances", USBM Report of Investigation 5585, (1960), 16

[21] Gutierrez-Rodriguez, J. A. and Aplan, F. F., " Effect of oxygen on the hydrophobicity and floatability of coal", Colloids and Surfaces, Vol 12, No.1-2, (1984), 27-51

[22] Neumann, A. W. and Good, R. J., " Techniques of measuring contact angles" in Surface and Colloid Science, Vol II- Experimental methods, Good,

R. J. and Stromberg, R. R., eds , Plenum 1979, 31-91

[23] Laskowski, J., " Surface properties of coals in relation to their flotation", Proc. 8th Int. Min. Proc. Cong., Lenningrad, (1968)

[24] Walker, P. L., Jr., Peterson, E. E. and Wright, C. C., " Surface active agent phenomena in dust abatement", Ind. Eng. Chem., Vol 44, (1952), 2389-2393

[25] Fox, H. W. and Zisman, W. A., " The spreading of liquids on low energy surfaces, I. Polytetrafluoroethylene", Journal of Colloid science, Vol 5, (1950), 514-531

[26] Bernett, M. K. and Zisman W. A., " Relation of wettability by aqueous solutions to the surface constitution of low energy solids", Journal of Physical Chemistry, Vol 63, (1959), 1241-1246

[27] Zisman, W. A., " Relation of equlibrium contact angle to liquid and solid constitution" in Contact Angle, Wettability and Adhesion, Gould, R. F., ed., Advances in chemistry series, No. 43, (1964), 1-51

[28] Zisman, W. A., " Surface energetics of wetting, spreading and adhesion", Journal of paint technology, Vol 44, No.564, (1972), 41-57

[29] Shaffrin, E. G. and Zisman, W. A., " Constitutive relation in the wetting of low energy sur ces and retraction method of preparing monolayers", Journal of Physical Chemistry, Vol 64, (1960), 519-524

[30] Shaffrin, E. G., " Critical surface tension of polymers" in Polymer Handbook, 2nd Edition, Brandrup, J. and Immergut, E. H., eds., III-221

[31] Lucassen-Reynders, E. H., " Contact angle and adsorption on solids", Journal of Physical Chemistry, Vol 67, (1963), 467-472

[32] Bergeman, D. and van Voorst Vader, F., " Effect of surfactants on contact angle at nonpolar solids", Journal of Colloid and Interface Science, Vol 42, No.3, (1973), 467-472

[33] Kelebek, S., Smith, G. W., Finch, J. A. and Yoruk, S., " Critical surface tension of wetting and flotation seperation of hydrophobic solids", Sep. Sci. Tech., Vol 22, No. (6), (1987), 1527-1546

[34] Kelebek, S., " Wetting behavior, polar characteristic and flotation of inherently hydrophobic minerals", Trans. Inst. Min. Metall. (Section C: Mineral Proc., Extr. Metall.), June 1987, 96

[35] Hornsby, D. T. and Leja, J., " Critical surface tension and flotation of inherently hydrophobic solids" Colloids and Surfaces, Vol 1, (1980), 425-429

[36] Finch, J. A. and Smith, G. W., " Bubble solid attachment as a function of bubble surface tension"

[37] Yarar, B. and Kaoma, J., " The critical surface tension of wetting of sulfide minerals", SME-AIME, Trans., 276, (1984), 1875-1878

[38] Hemphill, G. P. and Yarar, B., " Use of critical wetting surface tension in the beneficiation of oil shales", in Energy Developments: New Forms, Renewables and Conservation, Allen, F., ed.,Pergamon (1984), 111-116

[39] Kaoma, J. and Yarar, B., " Correlation of the critical surface tension of wetting and the non-stochiometric composition of MoS_2" in Chemistry and Uses of Molybdenum, Proc. IV Int. Conf., Barry, H. F. and Mitchell, P. C. H., eds., Ann Arbor, Michigan (1982), 117-122

[40] Yang, G. C., Ph.D. Thesis, University of California, Berkely, (1983)

[41] Good, R. J., " Surface free energy of solids and liquids: Thermodynamics, Molecular forces and Structure", Journal of Colloid and Interface science, Vol 59, No.3, (1977),1-55

[42] Bangham, D. H. and Razouk, R. I., Trans. Farad. Soc. 33, (1937), 1459

[43] See ref [9], page 830

[44] Fuerstenau, D. W., " Characterization of coal surfaces - Final report", DOE/PC/70776 (1985)

[45] Chessik, J. J. and Zettlemoyer A. C., " Immersional heats and the nature of solid surfaces", Advances in Catalysis, Vol 11 (1959), 263-299

[46] Marsh, H., " The determination of surface areas of coal - Some physico-chemical considerations", Fuel, Vol 44 (1965), 253-268

[47] Sunberg, D. G., Abadi, M. J. and Giroux, M. S., " Surface properties of coal", ORNL/MIT - 264, Dec 1977

[48] Alger, M. M., Chow, O. K. and Khan, M. Z., " Surface properties and reactions of coal", ORNL/MIT - 266, Mar 1978

[49] Field, L. A., Papadopoulos, A. J. and Wang, R. D., " Surface properties and reactions of coal, Part 2 ", ORNL/MIT - 270, Mar 1978

[50] Fuller, E. L., Jr., " Structure and chemistry of coals: Calorimetric analyses", Journal of Colloid and Interface Science, Vol 75, No.2 (1980), 577-583

[51] Nordon, P. and Bainbridge, N. W., " Heat of wetting of a bituminous coal", Fuel, Vol 62 (1983), 619-621

[52] Glanville, J. O. and Wightman, J. P., " Wetting of powdered coals by alkanol-water solutions and other liquids" Fuel, Vol 59 (1980), 557-562

[53] Allen, T and Burevski, D., " Applications of the flow microcalorimeter to heats of adsorption measurements at gas-solid interfaces", Powder Technology, Vol 17 (1977), 265-271

[54] Medalia, A. I. and Di Rivin, " Carbon blacks " in Characterization of Powder Surfaces, G. D. Parfitt and K. S. W. Sing (eds), Academic press, 279-351

[55] Day, R. E., Greenwood, F. G. and Parfitt, G. D., " Effect of heat treatment on the adsorption of sodium dodecyl sulphate from aqueous solutions on Spheron 6", Proc. IV Int. Cong. on Surface active substances, Belgium (1967), 1005-1013

[56] Young, D. M. and Crowell, A. P., "Physical adsorption of gases", Butterworth, (1962).

[57] Tamamushi, B. in Adsorption from Solutions, Ottewill, R. H., Rochester, C. H. and Smith, A. L., eds., Academic press (1983), 79

[58] Abram, J. C. and Bennett, M. C., " Carbon blacks as model porous adsorbents", Journal of Colloid and Interface Science, Vol 27, No.1, (1968)

[59] Saleeb, F. Z. and Kitchner, J. A., " The effects of graphatization on the adsorption of surfactants by carbon blacks" Journal of Chemical Society, 167, (1965), 911-917

[60] Zettlemoyer, A. C. and Narayan, K. S., in Proc. IV Inter. Cong. on surface activity, Vol 2, Brussels (1964)

[61] Weber, W.J., Jr., and Morris, J.C., " Equilibria and capacities for adsorption on carbon ", Journal of Sanitary Engineering, Div. Proc. Am. Soc. Civil Engnrs, SA 3, (1964), 79

[62] You, Y., " The interfacial chemistry of coal and its relation to coal flotation ", Ph.D. Thesis, University of California, Berkely, (1983)

[63] Blaschke, W., " Beneficiation of coal fines by selective flocculation", VII Int. Coal Preparation Congress, Paper F2, Sydney, (1976)

[64] Hucko, R., " Beneficiation of coal by selective flocculation, A laboratory study", USBM Report of Investigation 8234, Bureau of Mines, Washington D.C.

[65] Brooks, G. F., Littlefair, M. J., Spencer, L. and Abdelrahman, A. A., " Selective flocculation of Coal/shale mixtures using commercial and modified polyacrylamide polymers", Proc. XIV Int. Min. Proc. Cong., Toranto, 7.1-7.17

[66] Krishnan, S. V., " Selective flocculation of fine coal", in Fine Coal Processing, Mishra, S. K. and Klimpel, R. R., eds., Noyes publication (1987)

[67] Moudgil, B. M., " Effect of polyacrylamide and polyethylene oxide polymers on coal flotation", Colloids and Surfaces, Vol 8, No.2, (1983), 225-229

[68] Horsely, R. M., " Oily collectors in coal flotation", Trans. Inst. of Min. Eng., Vol 111, (1951-52), 886-900

[69] Wen, W. W., " Electrokinetic behavior and flotation of oxidized coal", Ph.D. Thesis, The Pennsylvania State University, (1978)

[70] Mishra, S. K., " Improved recovery of fine coal by flotation frocess", in Fine Coal Processing, Mishra, S. K. and Klimpel, R. R., eds., Noyes publication (1987)

[71] Osaka, A. S. K., " The mechanism of frother interactions with coal", Ph.D. Thesis, University of California, Berkely, (1983)

[72] Diaz, J. M. and Hernanz, J. F., "Flotation and Sulfur Selectivity of Bituminuos Coal with Different Degrees of Oxidation", Fuel, Vol. 63, No. 10, 1466-1468.

[73] S. C. Tsai, Fundamentals of Coal Beneficiation and Utilization, Coal Science and Technology 2, Elsevier, Amsterdam (1982).

[74] N. Berkowitz, An Introduction to Coal Technology, Academic Press, New York (1979).

[75] Speight, J. G., Analytical Methods for Coal and Coal Products, Vol. II, Academic Press, New York (1979).

[76] Gethner, J. S., "The Mechanism of the Low Temperature Oxidation of Coal by Oxygen: Observation and Separation of Simultaneous Reactions Using In-situ FTIR Difference Spectroscopy", Applied Spectroscopy, Vol. 41, (1987), 50-63

[77] Federicks, P. M. and Moxon, N. T., "Differentiation of In-situ oxidized and Fresh Coal Using FTIR Techniques", Fuel, Vol. 65, No. 11, (1986), 1532-1538

[78] Huffman, G. P., Huggins, F. E., Dunmyre, G. R., Pignocco, A.J. and Lin, M. C., "Comparative Sensitivity of Various Analytical Techniques to the Low Temperature oxidation of Coal", Fuel, Vol. 64, No. 6, (1985), 848-856

[79] Brooks, J. D. and Sternhell, S., Aust. J. Appl. Sci., Vol. 8, (1957), 206-221

[80] Schafer, H. N. S., Fuel, Vol. 39, (1970), 197-213

[81] Schafer, H. N. S., Fuel, Vol. 39, (1970), 271-280

[82] Celik, M. S. and Somasundaran, P., Colloids and Surfaces, Vol. 1, (1980), 121-124

[83] Fuerstenau, D. W., Rosenbaum, J. M. and Laskowski, J., Colloids and Surfaces, Vol. 8, (1983), 153-174

[84] Laskowski, J., Sirois, L. I. and Moon, K. S., Coal Preparation, Vol. 3(3), (1986), 1-21

[85] Savage, R. H. in Ann. N.Y. Acad. Sci., 53, (1951), 862

[86] Zettlemoyer, A. C., Tcheurekdjian, N. and Hosler, C. L., Journal Appl. Math. Phys., 14, (1963), 496

[87] Reilly, C. N. and Everhart, D.S., " ESCA analysis of functional groups on modified polymer surfaces", Appl.Elec.Spec.for Chem.Anal., Wiley & Sons 1982, 105

[88] Briggs, D. and Kendall, C. R., " Derivatization of discharge treated LDPE: An extension of XPS analysis and a probe of specific interactions in adhesion", Int.J.Adhesion and Adhesives,13, (1982)

[89] Coal Science, Gorbaty, M. L., Larsen, J. W. and Wender, I., eds., Academic press (1982)

[90] Nutt, C. W., Chem. Eng. Sci., 12, (1960), 133

[91] Somasundaran, P., Varbanov, R., Tchaliovska, S., Nishkov, I., " Ensemble effects in the detachment of floating microspheres", Submitted for publication in Colloids and Surfaces.

[92] Jarvis, N. L., Fox, R. B. and Zisman, W. A., " Surface activity at organic liquid-air interface, V. The effect of partially fluorinated additives on the wettability of solid polymers" in Contact angle, Wettability and Adhesion, ACS 43,(1964), 317-331

[93] Wittkopf, H., " Calculation of desorption energy distribution applied to temperature programmed H2O desorption from Silicate glass surface", Vacuum, Vol 37, No.11-12, (1987), 819-823,

[94] Rouquerol, J. and Davy, L. " Automatic gravimetric apparatus for recording the adsorption isotherms of gases or vapors onto solids", Thermochimica Acta, 24 (1978), 391-397.

[95] Poirier, J. E., Francois, M., Cases, J. M. and Rouquerol, J., "Study of water adsorption on Na montmorillonite: new data owing to the use of a continuous procedure", Proc. of the II Engg. Fdn. Conf. on Fundamentals of Adsorption, AICHE publication (1987).

[96] Isabelle Fournel, "Etude des caracteristiques et des conditions d'utilization d'un appareil de gravimetrie d'adsorption d'eau et de thermo-analyse" Master's Thesis, Institut national polytechnique de lorraine, Oct 1985.

[97] Partyka, S., Rouquerol, F. and Rouquerol, J., " Calorimetric determination of surface Areas: Possibilities of a modified harkins and Jura Procedure", Journal of colloidal and Interface Science, Vol 68, No. 1, (1979), 21-31.

[98] Letoquart, C., Rouquerol, F. and Rouquerol, J., J. Chim. Phys., 70, (1973), 559.

[99] Schulze, H. J., Int. Journal of Mineral Processing, 4, 241, (1977).

[100] Neummman, A. W., Advances in Colloid and Interface Science, vol 4, 105-191, 1974.

[101] Rapacchietta, A. V., Neumann, A. W., and Omenyi, S. N., Journal of Colloid and Interface Science, vol 59, 541-554, 1977.

[102] Rapacchietta, A. V., Neumann, A. W., and Omenyi, S. N., Journal of Colloid and Interface Science, vol 59, 555-567, 1977.

[103] Somasundaran, P., Varbanov, R., Tchaliovska, S., Nishkov, I., "Ensemble effects in the detachment of floating microspheres", Colloids and Surfaces, to appear.

[104] Fuerstenau, D. W., Williams, M. C., "Characterization of the lyophobicity of particles by film flotation",Colloids and Surfaces, 22, 87, (1987).

[105] Marmur, A., Chen, W., Zografi, G. J., Journal of Colloid and Interface Science, 113, 114, (1986).

[106] Nutt, C. W., "Froth Flotation: The adhesion of solid particles to flat interfaces and bubbles", Chemical Engineering Science, 12, 133, 1960.

[107] Oliver, J. F., Huh, C. and Mason, S. G., "Resistance to spreading of liquids by sharp edges", Journal of Colloid and Interface Science, vol 59, No 3, 568-581, 1978.

[108] Ablett, R., Phil. Mag. [6], 46, 244, (1923)

[109] Hoffman, R., J. Colloid and Interface. Sci., 50, 228, (1975).

[110] Schulze, H. J., Wahl, B. and Gottschalk, G., "Determination of adhesive strength within the liquid-gas interface in flotation by means of a centrifuge method", Journal of Colloid and Interface Science, Vol. 128, No. 1, 57, (1989).

[111] Unsworth, John F., Fowler, C.J., Heard, N.A., Weldon, V.L., and McBrierty, V.J., " Moisture in coal - 1. Differentiation between forms of moisture by NMR and microwave attenuation techniques ", Fuel, vol 67, (1988), 1111-1119.

[112] Lee, L.T., " Adsorption of Polyacrylamide on Oxide Minerals ", D.E.Sc. Thesis, Columbia University, (1986).

[113] Chandar, P., Somasundaran, P., Turro, N.J., Waterman, K.C.," Excimer fluorescence of solid-liquid interfacial pyrene-labeled poly(acrylic acid) conformation", Langmuir, 3, (1987), 298-300.

[114] Tsai, S. C. Fundamentals of Coal Beneficiation and Utilization, Elsevier, (1982), 41.

[115] Handbook of Chemistry and Physics, CRC press, 67 edition, (1988), F-207.

[116] Liu, D., Vasudevan, T. V. and Somasundaran, P., Unpublished results (1989)

[117] Harris, C. C. personal communications, 1990

[118] Neumann, A. W., Good, R. J., Hope, C. J. and Sejpal, M. "An equation of state approach to determine surface tensionsof low energy solids from contact angles ", Journal of Colloid and Interface Science, Vol 49, No. 2,(1974), 291.

[119] Neumann, A. W., Absolom, D. R., Frances, D. W., van Oss, C. J., " Conversion tables of contact angles to surface tension", Seperation and Purification methods, 9 (1), (1980), 69-163.

[120] Becher, P., " Interaction parameter calculations from contact angle data", Journal of Colloid and Interface Science, Vol 59, No. 3, (1977), 429.

[121] Johnson, Jr., R. E., Dettre, R. H., Advances in Chemistry Series, 43, (1964), 112.

[122] Johnson, R. E., Jr., Dettre, R. H., Journal of Physical Chemistry, 68, (1964), 1744.

[123] Johnson, Jr., R. E., Dettre, R. H., Advances in Chemistry Series, 43, (1964), 136.

[124] Johnson, Jr., R. E., Dettre, R. H., Journal of Physical Chemistry, 69, (1965), 1507.

[125] Herzberg, W. J., Manan, J. D. and Vermeulan, T., " The receeding contact angle ", Journal of Colloid and Interface Science, Vol 33, No. 1, (9170), 164.

[126] Cassie, A. B. D., Discuusions of the Faraday Society, 3, (1948), 11.

[127] Israelachvilli, J. N., and Gee, M. L., " Contact angles on chemically heterogeneous surfaces ", Langmuir, 5, (1989), 288-289.

[128] Robert, L. and Brusset, H., " Heat of immersion of Carbon Products", Presented at the Vth International Conference on Coal Science, Cheltenham, 28-30 May 1963.

[129] Le R. Malherbe, P. and Carman, P. C., " Swelling of coals by methanol and its significance", Fuel vol 31,(1951), 210-219.

[130] Brunauer, S., Deming, L. S., Deming, W. E. and Teller, E., Journal of the American Chemical Society, 62, (1940), 1723.

[131] Emmett, P. H. and Brunauer, S., Journal of the American Chemical Society, 59, (1937), 1553

[132] Anderson, R. B., Hall, W. K., Lecky, J. A., and Stein, K. C., "Sorption Studies on American coals", Journal of Physical Chemistry, 60, (1956), 1548.

[133] Deitz, V. R., "Bibliography of solid adsorbents, 1900 to 1942", Bone Char Research Project Inc., Charlestown, Mass and ."Bibliography of solid ad-

sorbents, 1942 to 1953", National Bureau of Standards, Circular 566, Washington, D.C.

[134] Beebe, R. A. and Young, D. M., Journal of Physical Chemistry, 58, (1954), 93.

[135] Amberg, C. H., Spencer, W. B. and Beebe, R. A., Canadian Journal of Chemistry,33, (1955), 305.

[136] Chessick, J. J. and Zettlemoyer, A. C., " Study of silicate minerals. V. A quantitative determination of the acid strength of exchange sites on Attapulgite", Journal of Physical Chemistry, 62, (1958), 1217.

[137] Drain, L. E. and Morrison, J. A., Trans. Faraday Society., 48, (1952), 316.

[138] Fuller, Jr., E. L., and Smyrl, N. R., "Chemistry and structure of coals - Diffuse reflectance IR spectroscopy equipment and techniques", Fuel, vol 64, (1985), 1143-1150.

[139] Calemma, V., Rausa, R., Margaret, R. and Girardi, E., "FTIR study of coal oxidation at low temperatures", Fuel, vol 67, (1988), 764-770.

[140] Gethner, Jon S., "Mechanism of low temperature oxidation of coal - Observation and separation of simultaneous reactions using insitu FTIR difference spectroscopy", Applied Spectroscopy, vol 41, No 1, (1988), 50-63.

[141] Somasundaran, P. and Roberts, Jr. C. E., "Aging and Benificiation" in Sample Selection, Aging and Reactivity of Coal, Eds, Ralph Klien and Robert Wellek, Chapter 7, (1989).

[142] Gardella, J. A., Hercules, D. M. and Heinen H. J. "Mass spectrometry of molecular solids: Laser microprobe mass analysis of selected polymers" Spectroscopy letters, 13(6),(1980), 347-360.

[143] Heinen, H. J.," On ion formation in laser desorption mass spectrometry with LAMMA", Int. J. Mass Spectrom. Ion Phys. 38, (1981), 309-322.

[144] Ollmann, G., Kupka,K. D., Hillenkamp, F. "Detection of metalorganic complexes out of an organic matrix by laser micromass spectrometry", Int. J. Mass. Spectrom. Ion Phys., (1983), 47:31-34.

[145] Vanderborgh, N. E. and Ronald Jones, C. E., "Laser Microprobe Analysis on Coal and Shale Samples", Analytical Chemistry, 55, (1983), 527-532.

[146] Cheung, W., Journal of Applied Physics, 55, (1984), 1388.

[147] Marganski, R. E. and Rowell, R. L., " Electrophoretic mobility distribution in aqueous dispersions of bituminious coal and residual hydrocarbon materials ", Journal of Energy and Fuels, 2, (1988), 132.

[148] Angle, C. W., Donini, J. C. and Hamza, H. A.," The effect of ultrasonication on the surface properties, ionic composition and electrphoretic mobility of an aqueous coal suspension" Colloids and Surfaces, 30, (1988), 373-385.

[149] Ye, Y., Kandhrika, S. M., Miller, J. D.,"Induction time measurements at a particle bed ",Int. Journal of Mineral Proc., 25, (1989), 221.

A SEM-EDX PHOTOMICROGRAPHS

Fig 1 [figure numbers refer to accompanying photomicrographs] shows an inclusion in a +8 mesh fraction coal particle. Elemental analysis of the overall inclusion indicates that the inclusion is a clay particle coated with gypsum. The presence of iron together with sulphur shows that pyrite is also present. Fig 2 shows a pyrite particle located in a fissure of the inclusion matrix. The presence of calcium indicates that the pyrite particle is coated with calcium sulphate. Fig 3 is a micrograph of a

medium bright particle in the inclusion shown in Fig 1. Though the morphology of the particle indicates it to be clayey particle or a carbonate, the elemental analysis shows predominately iron based compound with Zn, Na, Al and K in the form of chlorides or sulphates. This clearly shows that inorganic impurities are very finely disseminated.

Fig 4 & 5 are secondary and back scattered micrographs of particles marked 1D & 1E embedded in a coal particle. Fig 4 illustrates the high topography of the coal surface and similar morphological characteristics of 1D & 1E. The back scattered image in Fig 5 clearly illustrates the difference in chemical composition of the two particles. It can be observed that particle 1E is coated with coal on its edges and fissures. Elemental analysis reveals that particle 1D is calcium aluminum silicate. Particle 1E is a pyrite particle. These pictures show the intimate nature of association of the clay and pyrite particles with each other and the coal matrix.

Fig 6 is a micrograph of an inclusion in a +8 mesh particle. The elemental analysis of this particle shows it to be composed of compounds involving Na, Ca, Si, P, Al, Fe, S and Cl. It appears that this particle is a polydispersed clay associated with pyrite and salts of chlorides and sulphates. Fig 7 shows another inclusion in a similar sized particle as being composed of pyrite and calcium aluminum silicates. This picture demonstrates the extent of clay and pyrite association. It is also possible that gypsum is present in particles shown in Fig 6 & 7.

Fig 8 shows a back scattered micrograph of a pyrite vein in a +8 mesh particle. The elemental analysis of this vein also shows presence of Al and Si and hence associated clayey matter. Fig 9 & 10 are secondary and back scattered pictures of two particles marked A & B at another point on the surface vein at higher magnification. Particle B is a free pyrite crystal. Particle A is an aluminum silicate compound associated with calcium sulphate and iron.

Fig 1 to 10 discussed above are all +8 mesh fraction coal samples. In order to understand the association of mineral matter in coal better, the analysis was extended to particles in the +100, +200, +635 mesh fractions and are discussed below.

Fig 11 & 12 show the +100 mesh particles in the secondary and back scattered mode. The bottom left corner of Fig 12 shows a classic instance of pyrite encrustations on coal. Other bright particles in the area were scanned and generally found to be of clayey nature or pyrites. Areas marked 1, 2 and 3 in Fig 12 were enlarged and analyzed.

Fig 13 & 14 show the enlarged secondary and back scattered micrographs of the pyrite encrustation marked 1 in Fig 12. Fig 13 illustrates the high topography of the surface. The porous nature of the encrustations is also visible. Fig 14 indicates the disposition of the particles on the coal surface. Areas where coal has smeared the surface of bright particles are evident. The elemental analysis of particle 1 in Fig 14 shows it to be of pyritic nature. Trace amount of Mg is also noted.

The magnified secondary and back scattered images of particles 2 & 3 of Fig 12 are shown in Figs 15, 16, 17 and 18. The elemental analysis reveals particle 2 to be an altered form of feldspar probably cerisite. The difference in relative brightness og this particle is due to the layered structure. Traces of Ti is noted. Particle 3 is a pyrite; a small sand grain is associated with it.

Fig 19 & 20 are micrographs of +200 mesh fraction in the secondary and back scattered modes respectively. The particle in the center of Fig 20 shows bright inclusions intimately associated with coal. Areas marked 1 and 2 on this particle along with another bright inclusion marked 3 were analyzed.

Fig 21 & 22 are enlarged views of particle 1 in Fig 20. The back scattered image in Fig 22 shows the inclusions to be coated with coal (gray areas). The

elemental analysis indicates the inclusion to be aluminum silicates. Free iron is noted; the sulphur is probably due to the coal matrix. Fig 23 & 24 are enlarged micrographs of particle 2 in Fig 20. The elemental analysis indicates the particle to be pyritic. The back scattered image in Fig 24 shows a ring of black particles around the pyrite encrustation. Analysis of this region as indicated in the spectrum reveals the black particles to be aluminum silicates. Elemental sulphur in comparitively large quantities are noticed. These indicate that the clayey matter is coated with coal dust and that coal matrix near pyrites is rich in sulphur.

Fig 25 & 26 show typical aluminum silicate particles. Fig 27 shows a secondary image of +625 mesh coal particles. Fig 28 shows the corresponding back scattered image. It is evident that at these fine size ranges liberation of mineral matter is maximum. Three bright inclusions marked 1, 2 and 3 in Fig 28 were magnified and analyzed as below. Fig 29 & 30 are the magnified secondary and back scattered images of particle 1. Elemental analysis indicates this particle to be a pyrite crystal. Fig 29 demonstrates the coating of pyrite surface with coal.

Fig 31 & 32 show the magnified micrographs of particle 2. This particle is an altered form of feldspar similar to particle 2 in Fig 16. Here also Ti is noticed in close association with the modified feldspar Fig 33 & 34 are magnified micrographs of particle 3 showing a single liberated grain in the +635 mesh fraction. Elemental analysis of this grain indicates it to be a complex substance composed of iron oxide with magnesium aluminosilicate and smaller quantities of calcium sulphate, calcium fluoride and possibly calcium carbonate. Manganese is also present probably as an oxide.

Figure 2

Figure 1

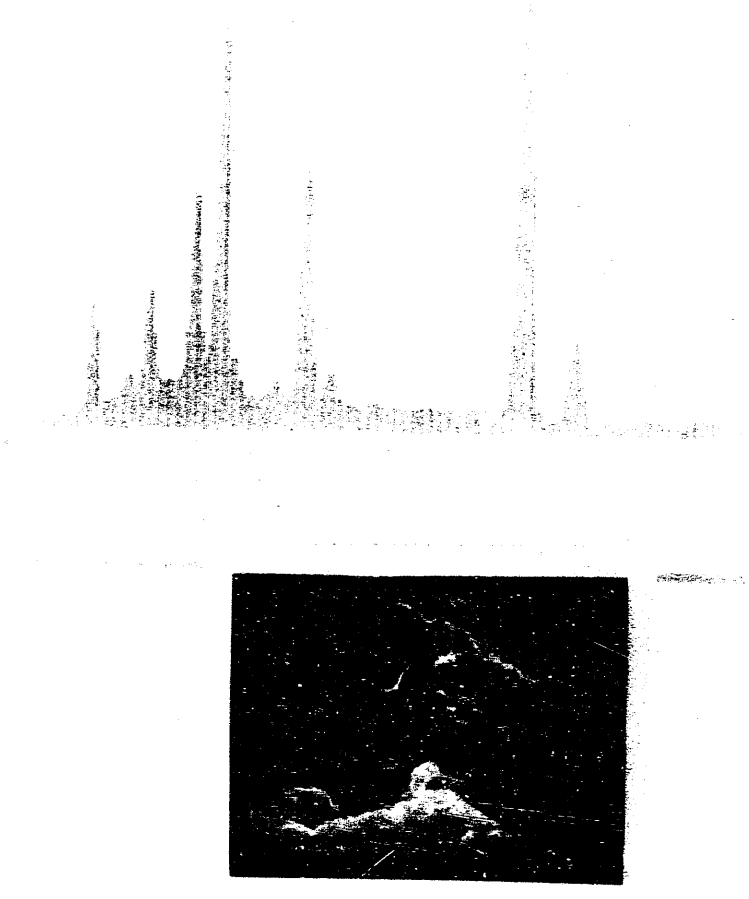

Figure 3

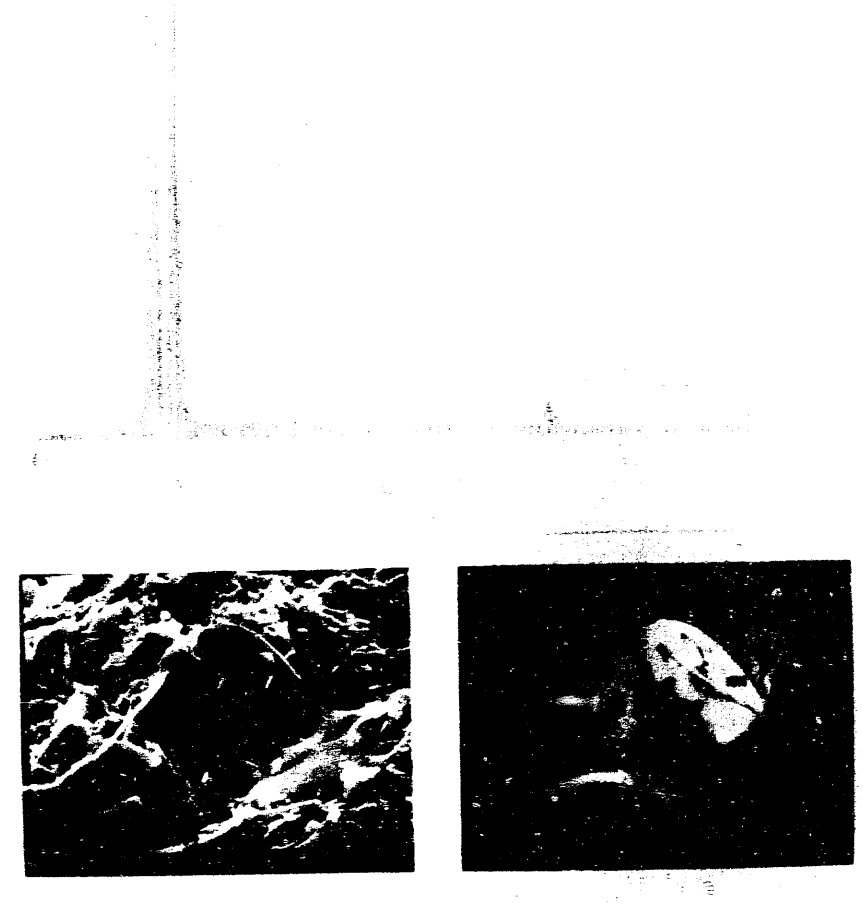

Figure 4

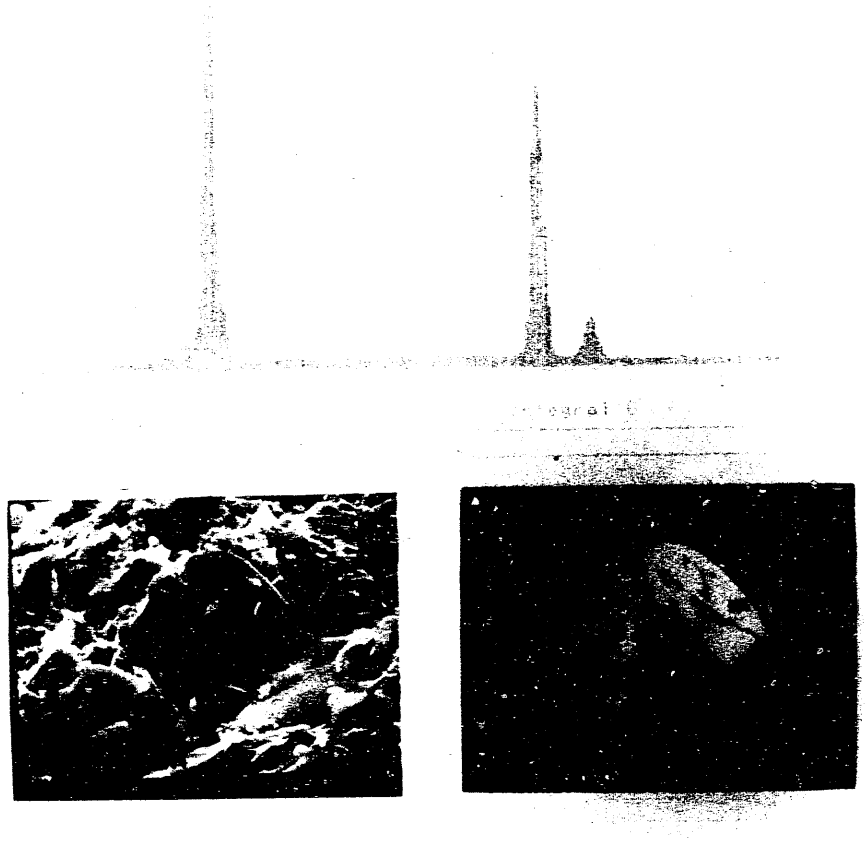

Figure 5

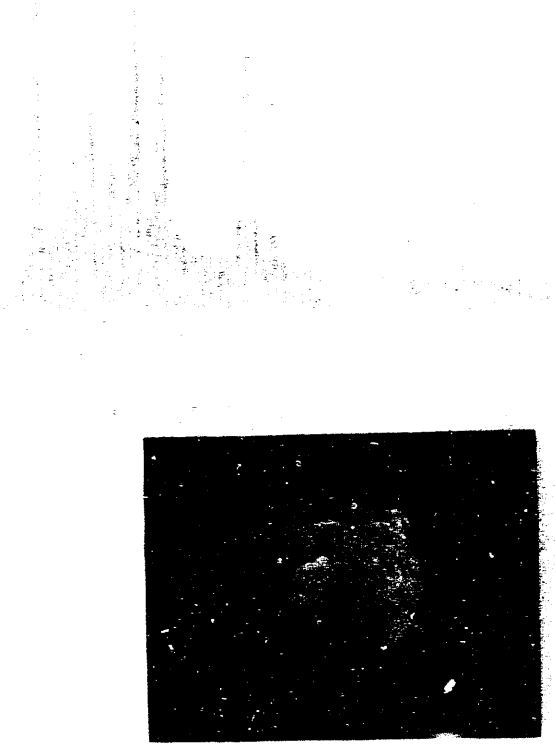

Figure 6

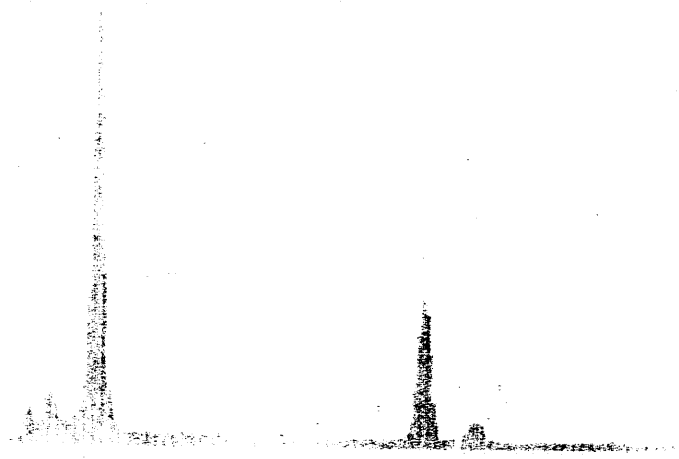

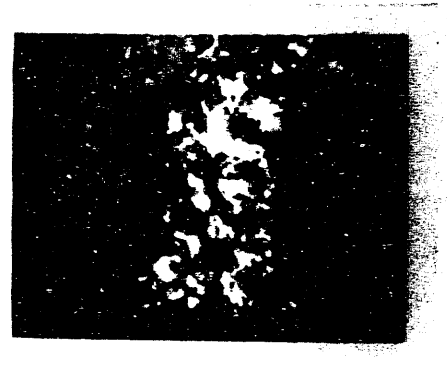

Figure 8

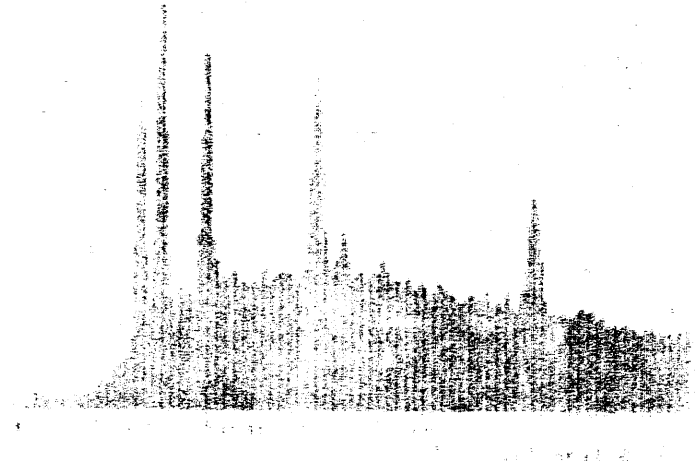

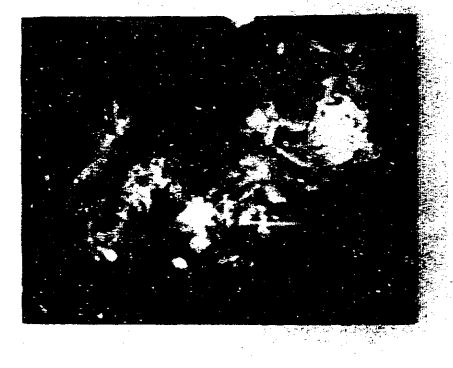

Figure 7

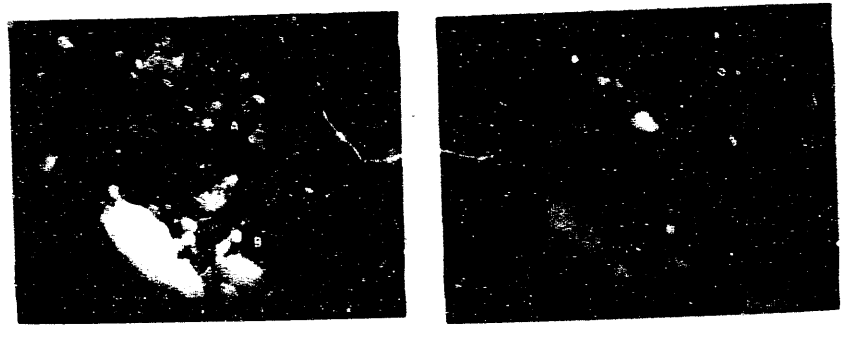

Figure 10

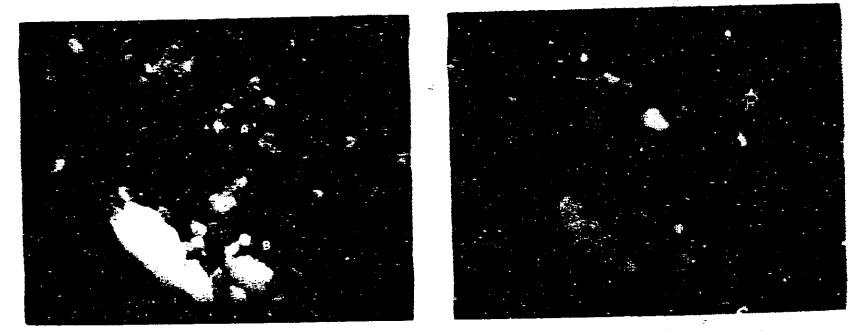

Figure 9

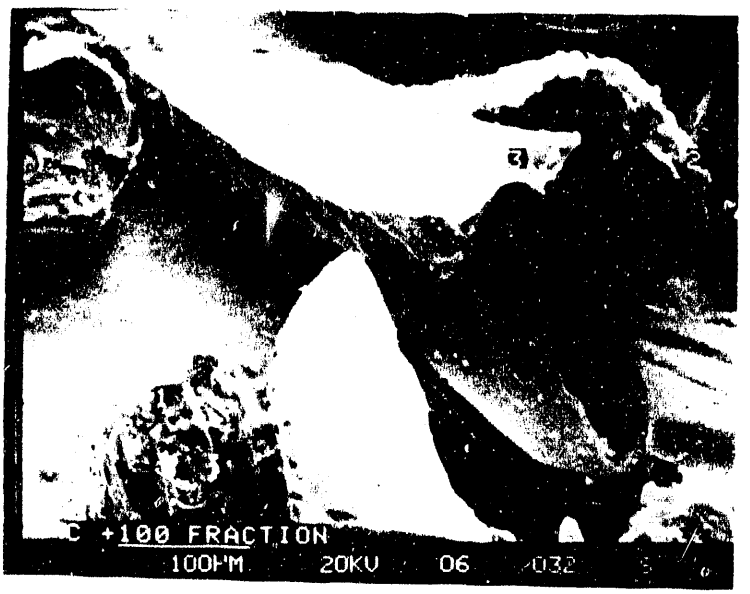

Figure 11

Figure 12

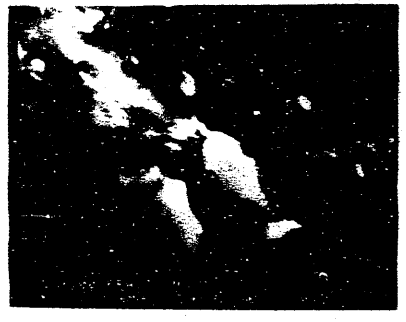

Figure 16

Figure 15

Figure 14

Figure 13

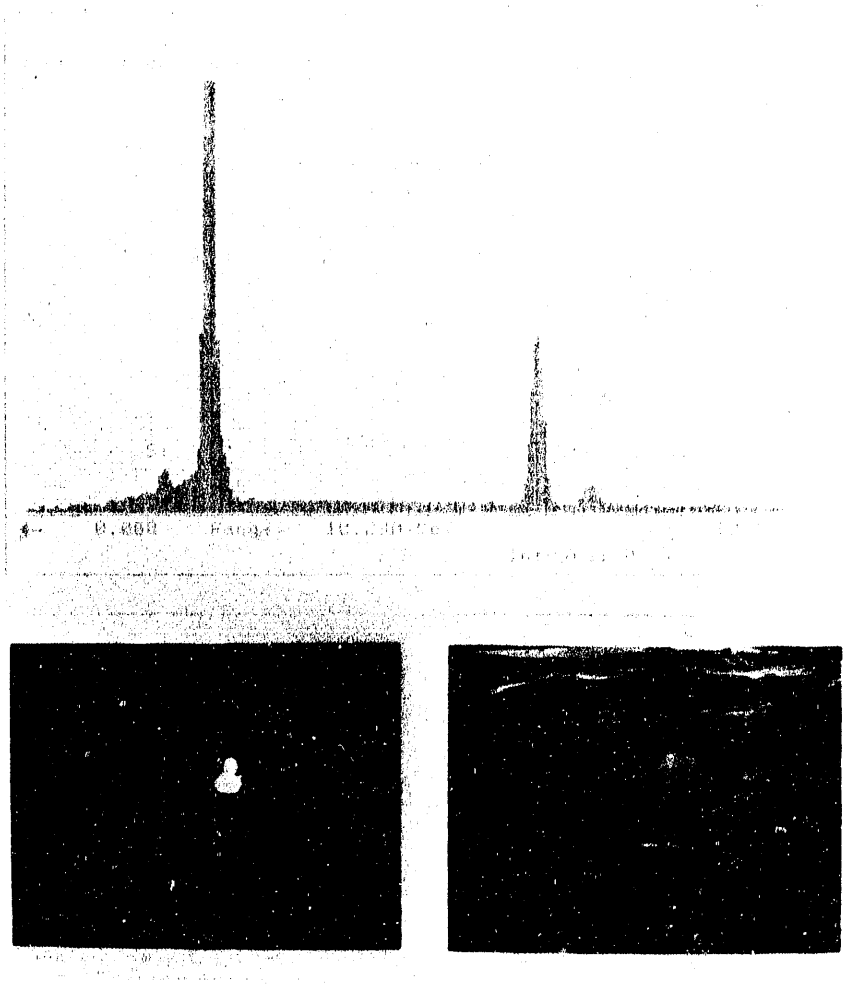

Figure 18

Figure 17

Figure 19

Figure 20

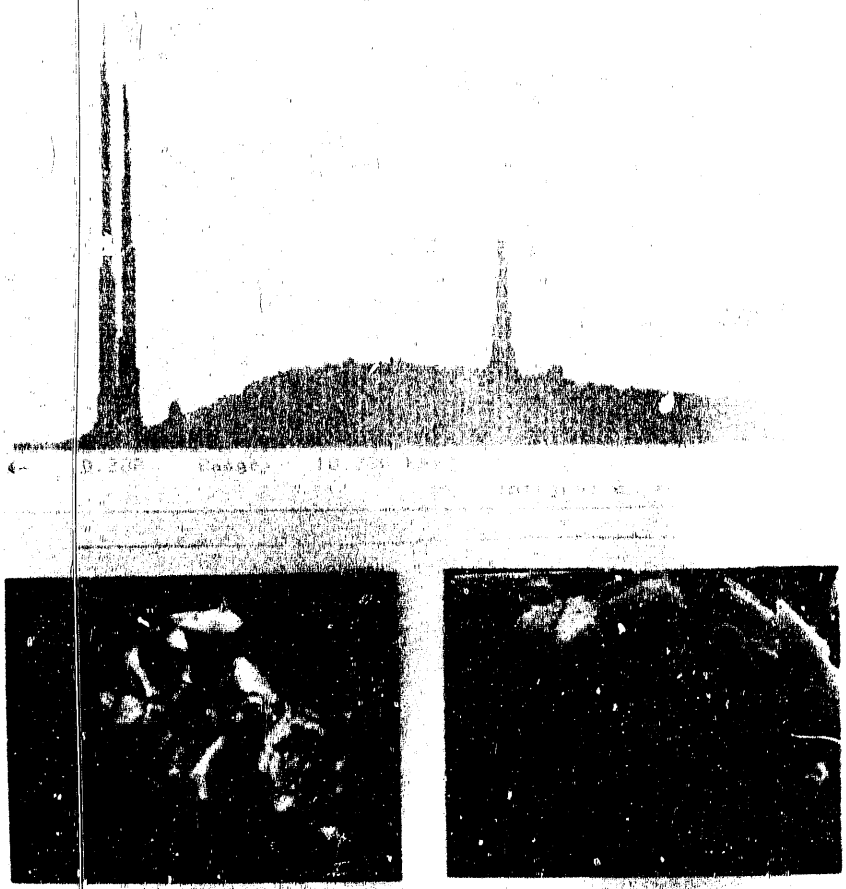

Figure 22

Figure 21

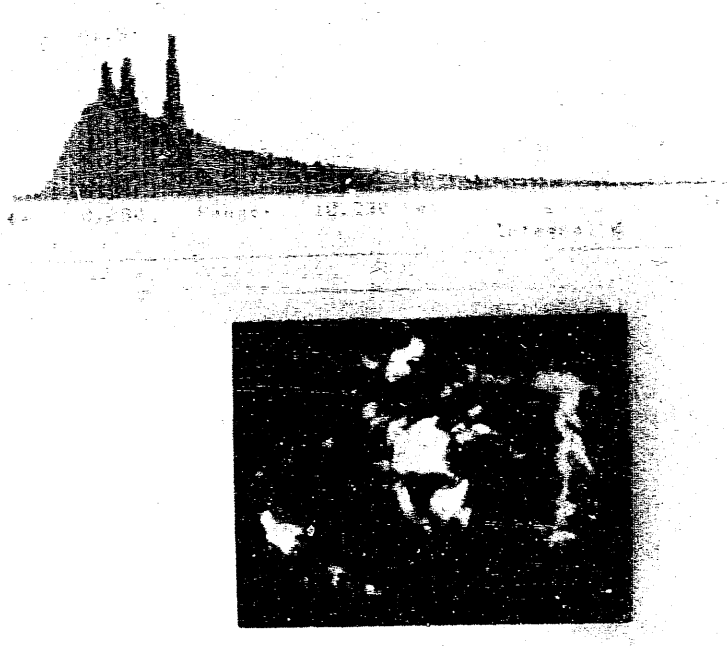

Figure 24

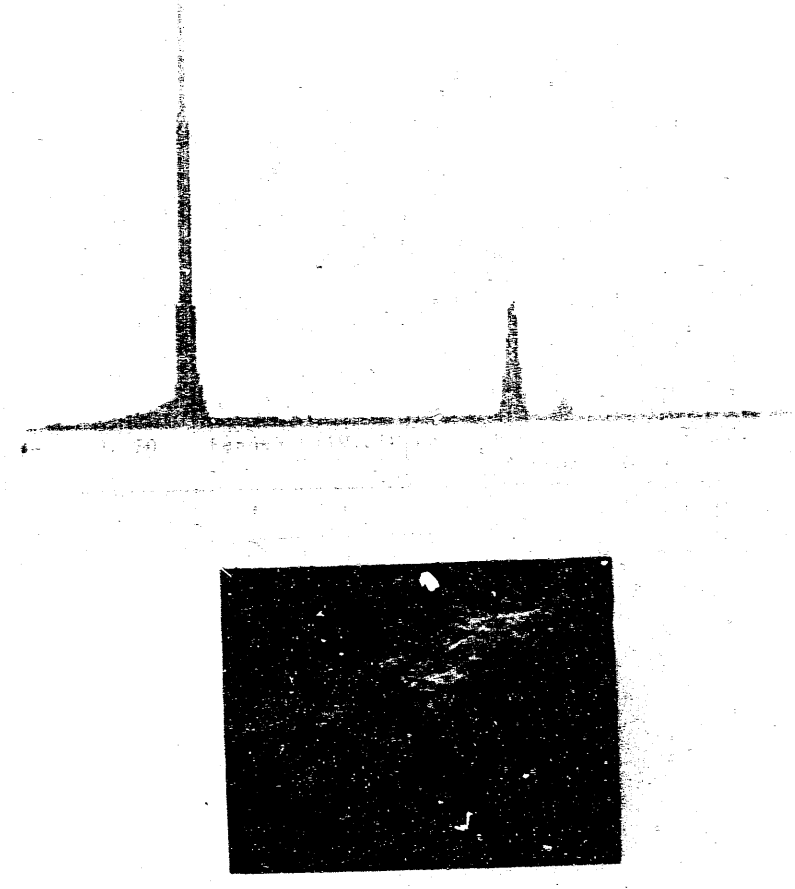

Figure 23

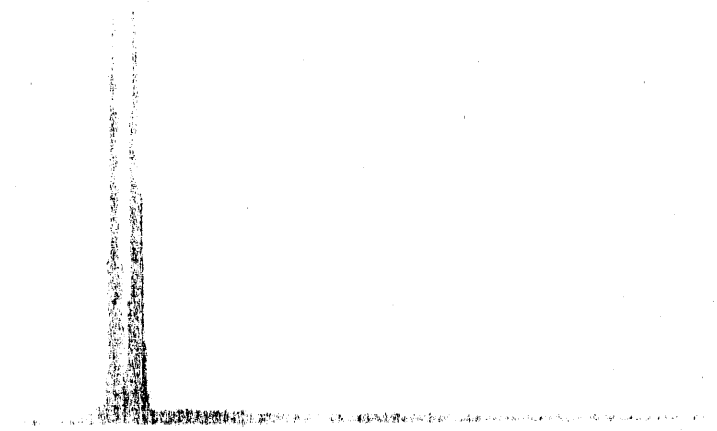

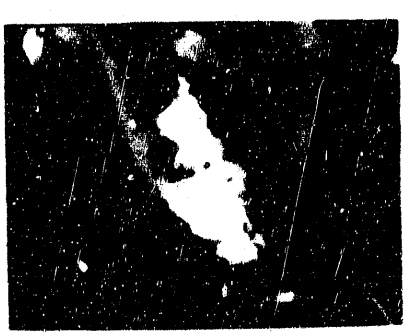

Figure 25

Figure 26

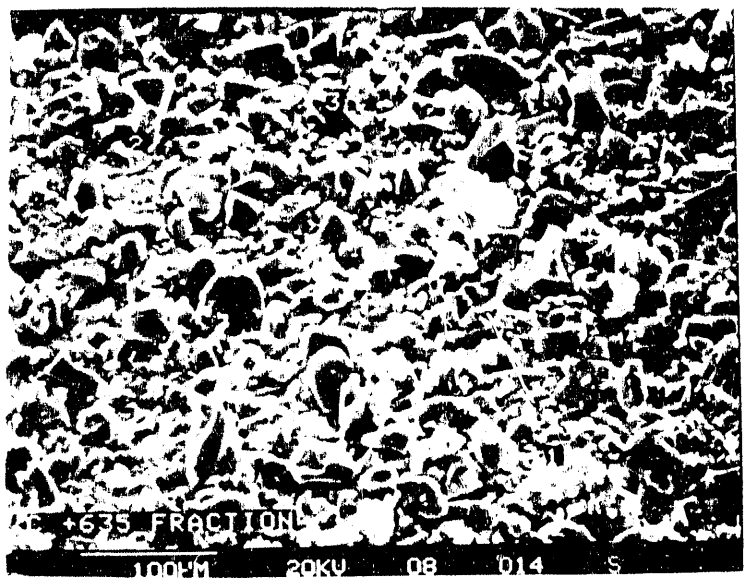

Figure 27

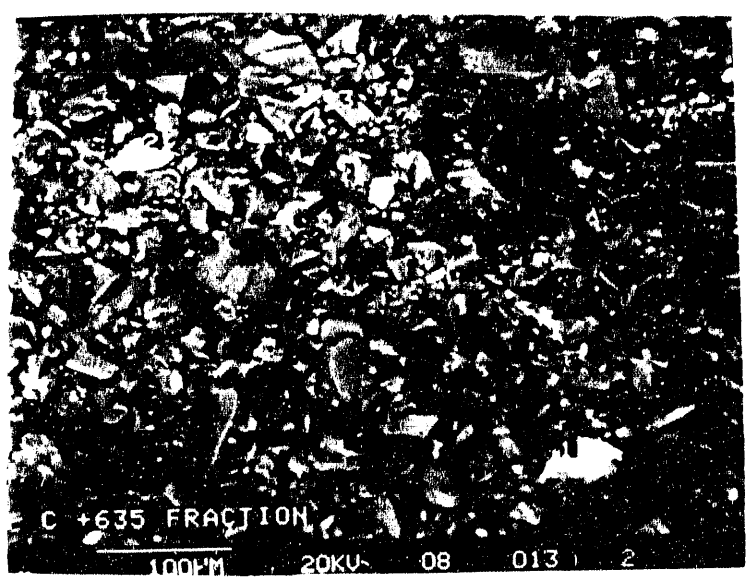

Figure 28

Figure 29

Figure 30

Figure 31

Figure 32

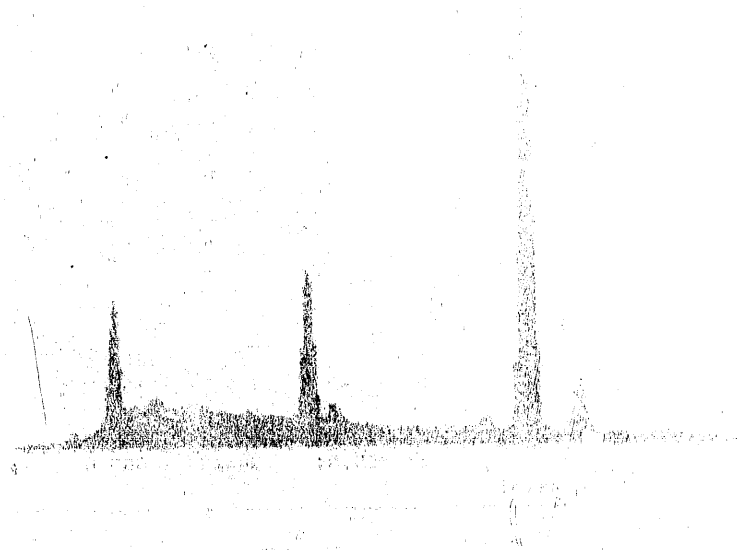

Figure 33

Figure 34

B LASER MICROPROBE MASS ANALYZER

The Laser Microprobe Mass Analyzer (LAMMA) consists of four modules: the laser generating and corresponding optics system, a smple manipulator and chamber and a time of flight mass spectrometer. In addition it includes the high vacuum system, an optical microscope and data acquisition and control system. The data handling system includes a dedicated software for analysis of results and monitoring the equipment performance. A schematic diagram of the system is shown in the accompanying figure. The laser microprobe uses two lasers; a helium-neon laser for sample alignment and a YAG laser for ablatement. The main ablating laser, helium spotting laser and optical viewing system all use the same objective lens to ensure accuracy in sample alignment during scanning and analysis.

Q-switched Nd-YAG laser system provides laser pulses of 20 nanoseconds duration. These laser pulses are then frequency quadrupled to produce the required wavelength. The laser beam is focussed to a diameter of less than 1 micron. The amount of optical energy directed upon the sample is continously controllable from zero to full output by a set of cross-polarized filters. The laser beam ablates the sample from a microvolume of less than 3×10^{-14} cm^3 and produces a vapor plume which is partially ionized. The area of the sample on which the laser is focussed, as viewed through the optical system can be continuously scanned and analyzed by computer control. A laser post-ionization facility which is a unique feature of LAMMA, provides increased sensitivity. This is achieved by ionization of neutral atoms / ion fragments in the vapor plume produced by primary (ablating) laser pulse followed by a second high power (ionizing) laser pulse. This feature also allows the flexibility of using less intensity in the primary (ablating) laser beam which produces the least disruption of the surface as compared to other normal laser microprobes which produce three micron diameter craters.

Little sample handling is necessary. Solid pieces, powders and vacuum stable liquids like oils and fats can be routinely analyzed. Typical samples are mounted on metal supports which is inserted rapidly through an all metal sample inlet port to the sample stage. The sample stage is a high resolution and highly stable device capable of motion in all three dimensions. The stage can carry eight samples. A vacuum of 1×10^{-9} torr can be achieved in the main chamber. The analysis of ions in the post-ionized plume is conducted using a time of flight mass spectrometer over a 2.5 meter flight path. A reflectron with second order energy focussing, ion detection system for positive and negative ions and extraction optics are also included. The output yields a spectrum ranging from 1 to 10,000 atomic mass units and their corresponding intensities with each laser pulse. The resolution of the system is around 1 AMU.

The operation of the system essentially consists of sample loading, evacuation, scanning, laser ablation and acquiring the spectrum and data analysis. In the analysis chamber the sampling area is chosen by a XYZ manipulator while the sample is viewed through the laser optical microscope. The laser energy is set at the desired level and the sample ablated and the spectrum of the resulting fragments recorded. Spectra can also be acquired at constant laser irradiation conditions of various microareas. Operation in this mode should reflect the sample heterogeneity.

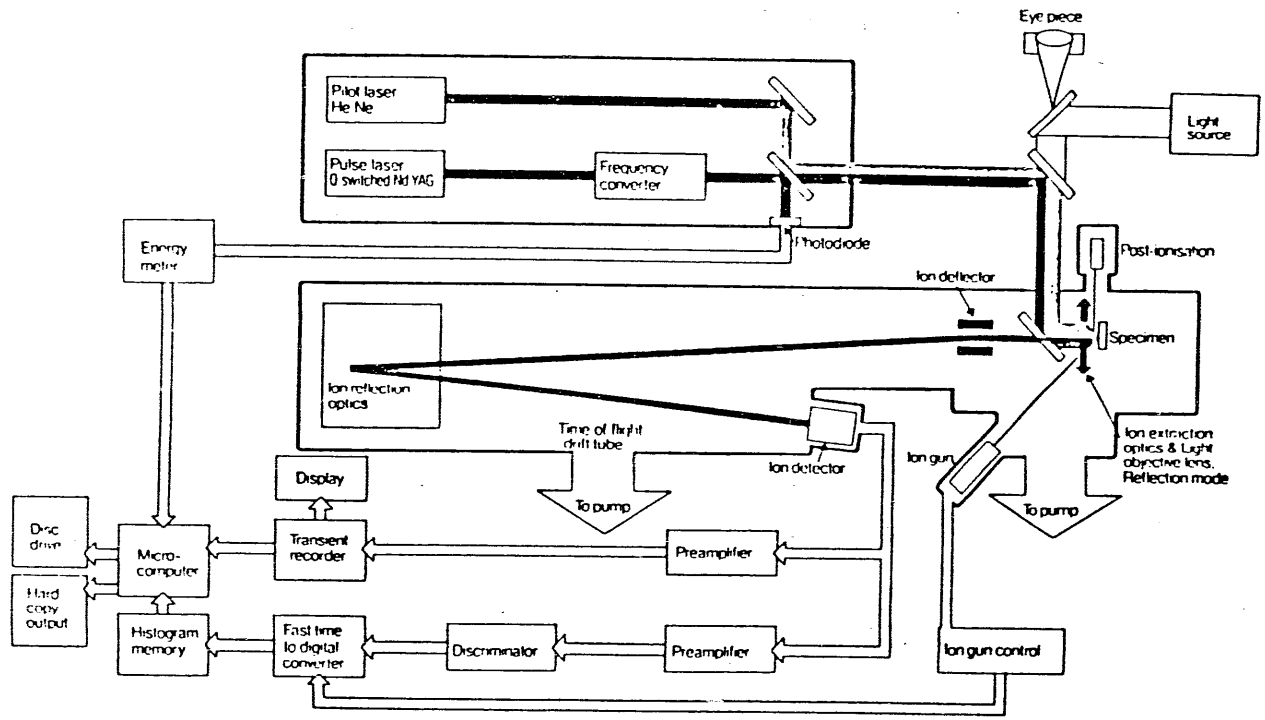

Fig II a. Schematic illustration of the Laser microprobe mass analyzer (LAMMA).

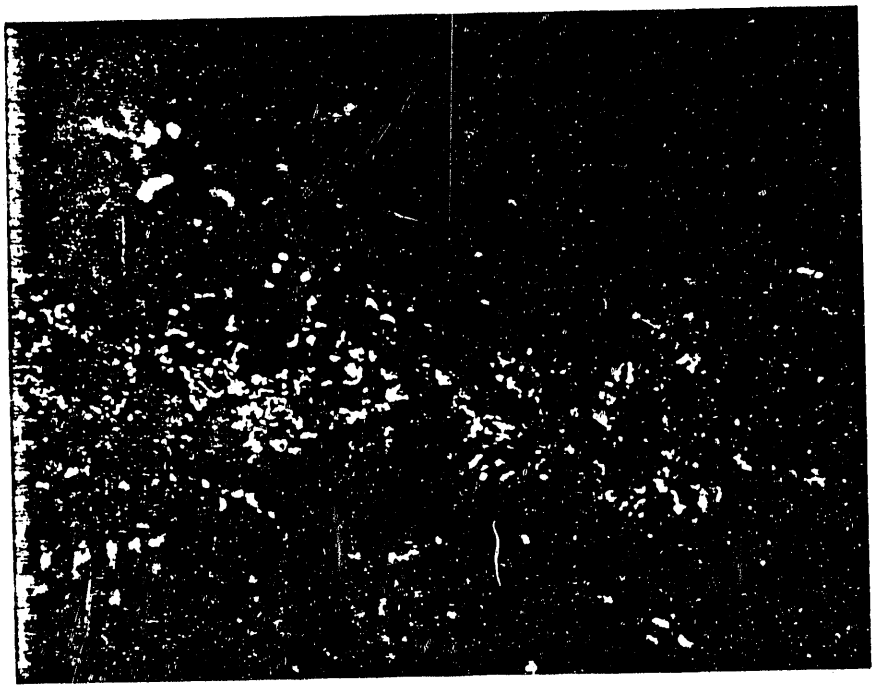

Fig. III a. Photomicrograph of the location on the + 8 mesh coal sample on which the LAMMA analysis was conducted.

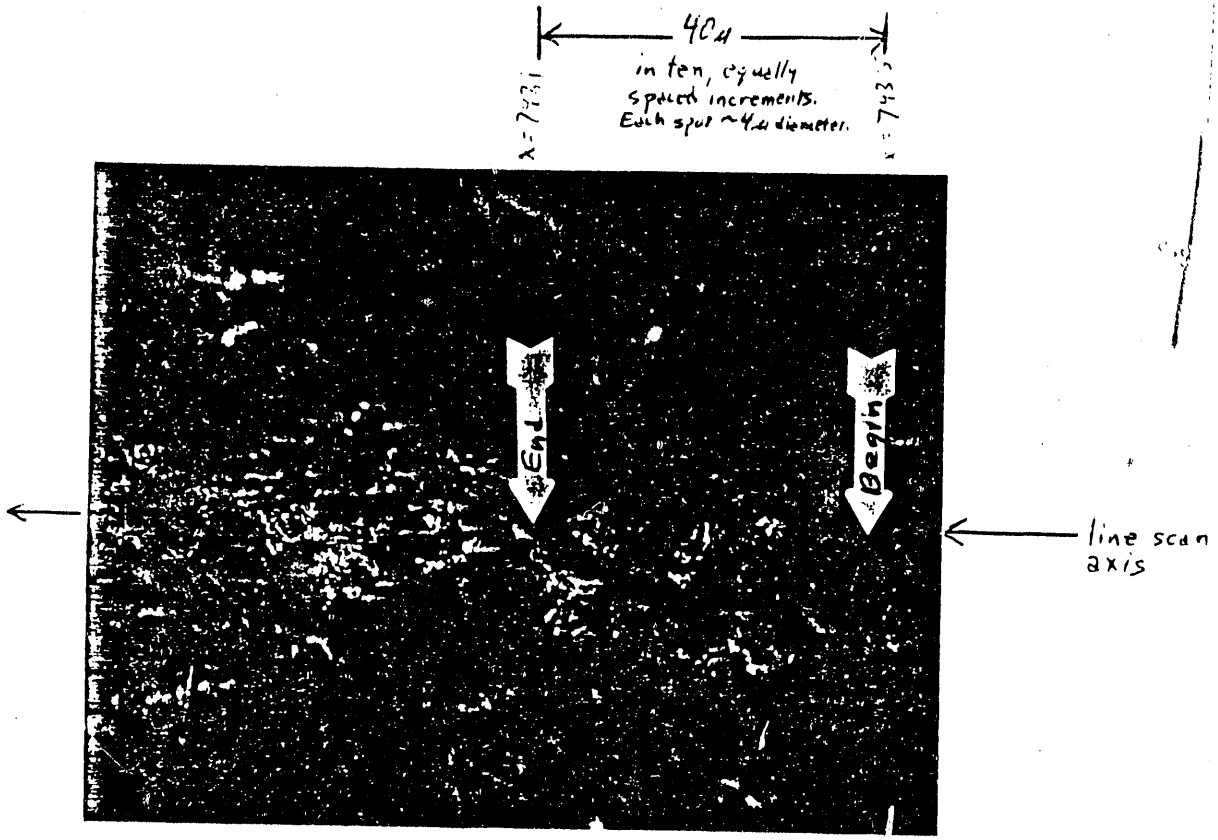

Fig. III b. LAMMA line scan axis end points spanning 40 microns containing 10 equally spaced spots where analysis was conducted.

SSL# 3915-1188 Spectrum 1A
X=743.5, COAL SAMP B, FOC=-1.0 ATT=0.25%, 0.6UJ
COLUMBIA U

SPEKTRUM 7000
POLARITY +
RANGE .16 V

21/12/1988
LASER .590uJ

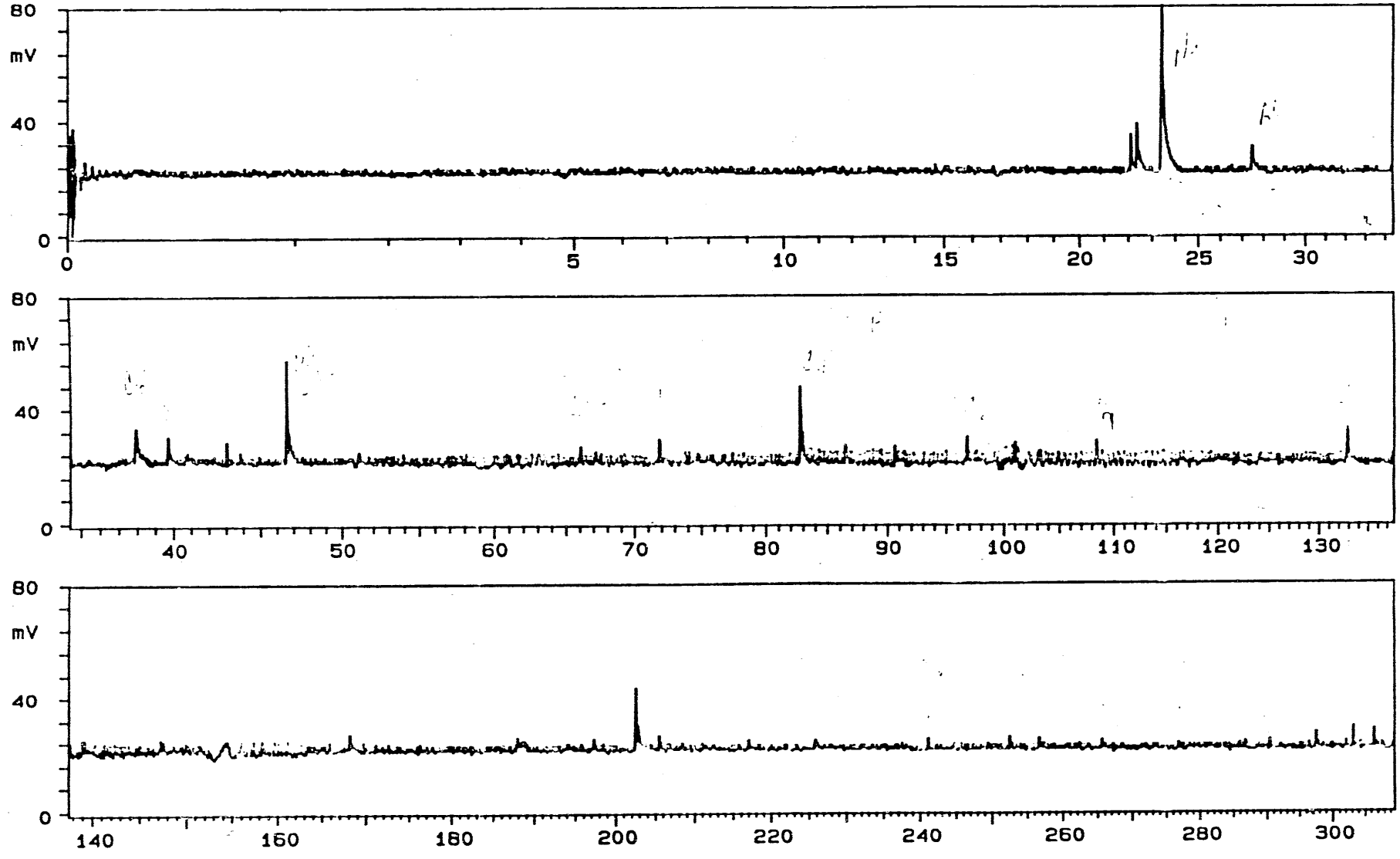

SSL# 3915-1188 Spectrum 1A'
X=743.5, COAL SAMP B, FOC=-1.0 ATT=0.25%, 0.6UJ
COLUMBIA U

SPEKTRUM 7000
POLARITY +
RANGE .16 V

21/12/1988
LASER .590uJ

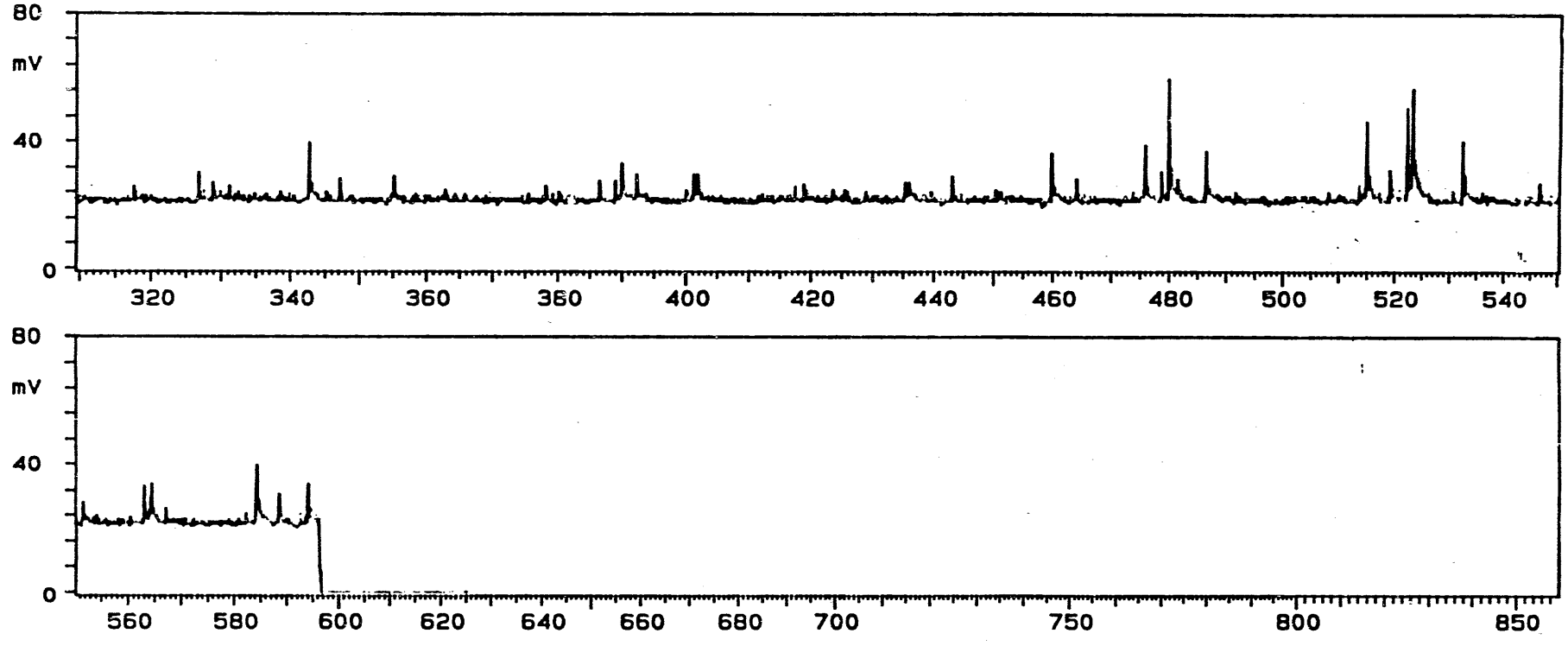

SSL# 3915-1188 Spectrum 2A
X=743.8, COAL SAMP B, FOC=-1.0 ATT=0.25%, 0.6UJ
COLUMBIA U

SPEKTRUM 7060
POLARITY +
RANGE .16 V

21/12/1988
LASER .600uJ

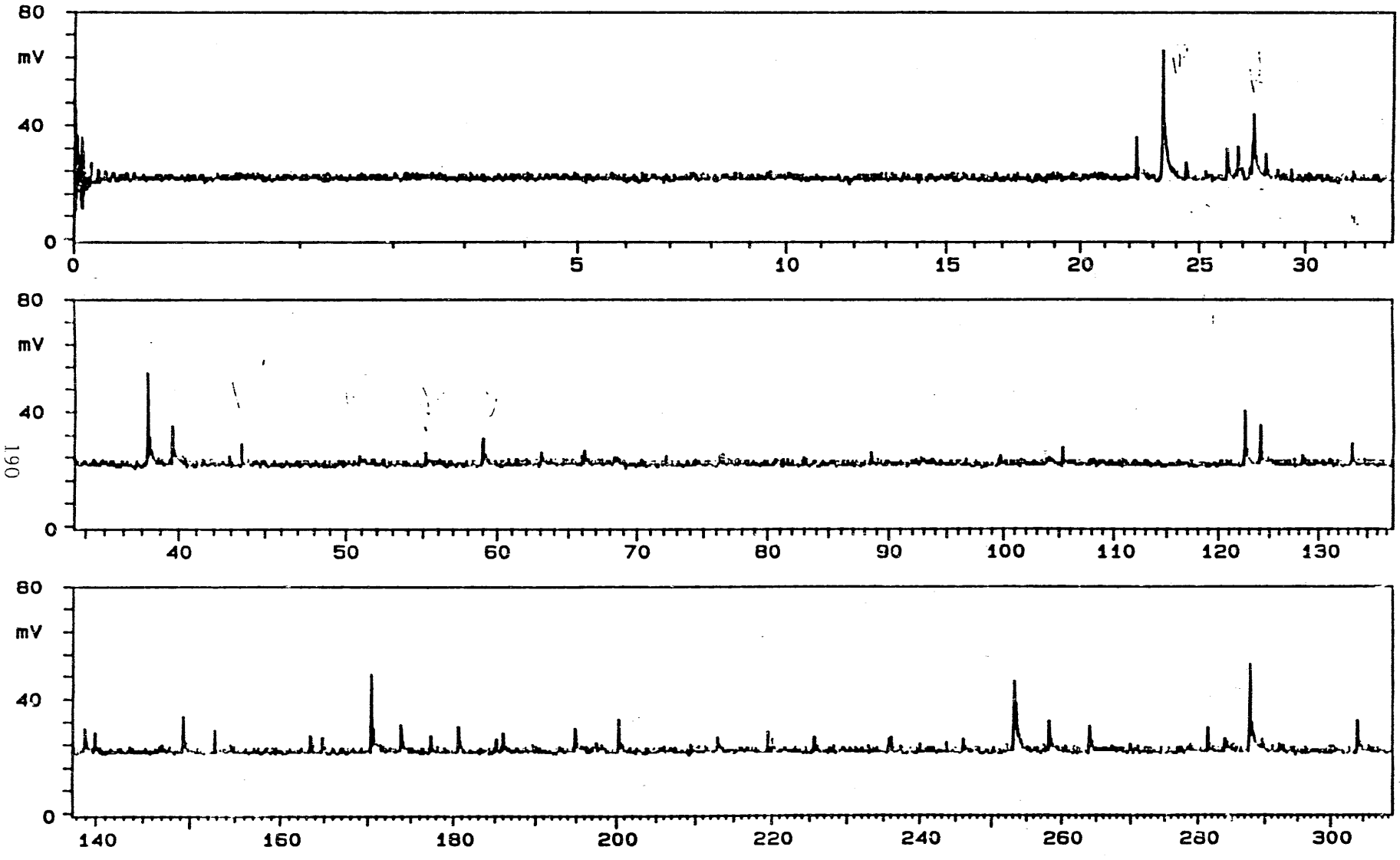

Spectrum 2A'

SSL# 3915-1188
X=743.9, COAL SAMP B, FOC=-1.0 ATT=0.25%, 0.6UJ
COLUMBIA U

SPEKTRUM 7060
POLARITY +
RANGE .16 V

21/12/1988
LASER .600uJ

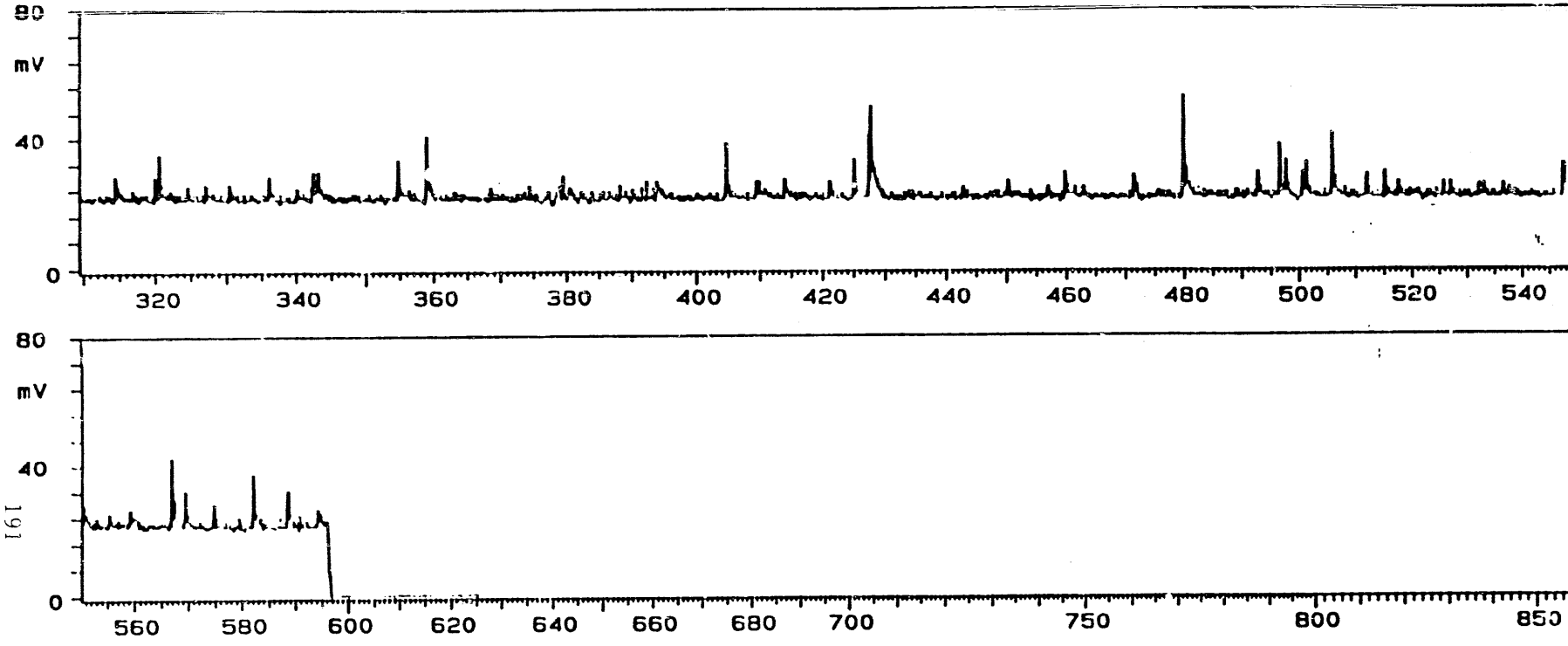

SSL# 3915-11R8 Spectrum 3A
X=744.3, COAL SAMP B, FOC=-1.0 ATT=0.25%, 0.6UJ
COLUMBIA U

SPEKTRUM 7120
POLARITY +
RANGE .16 V

21/12/1988
LASER .620mJ

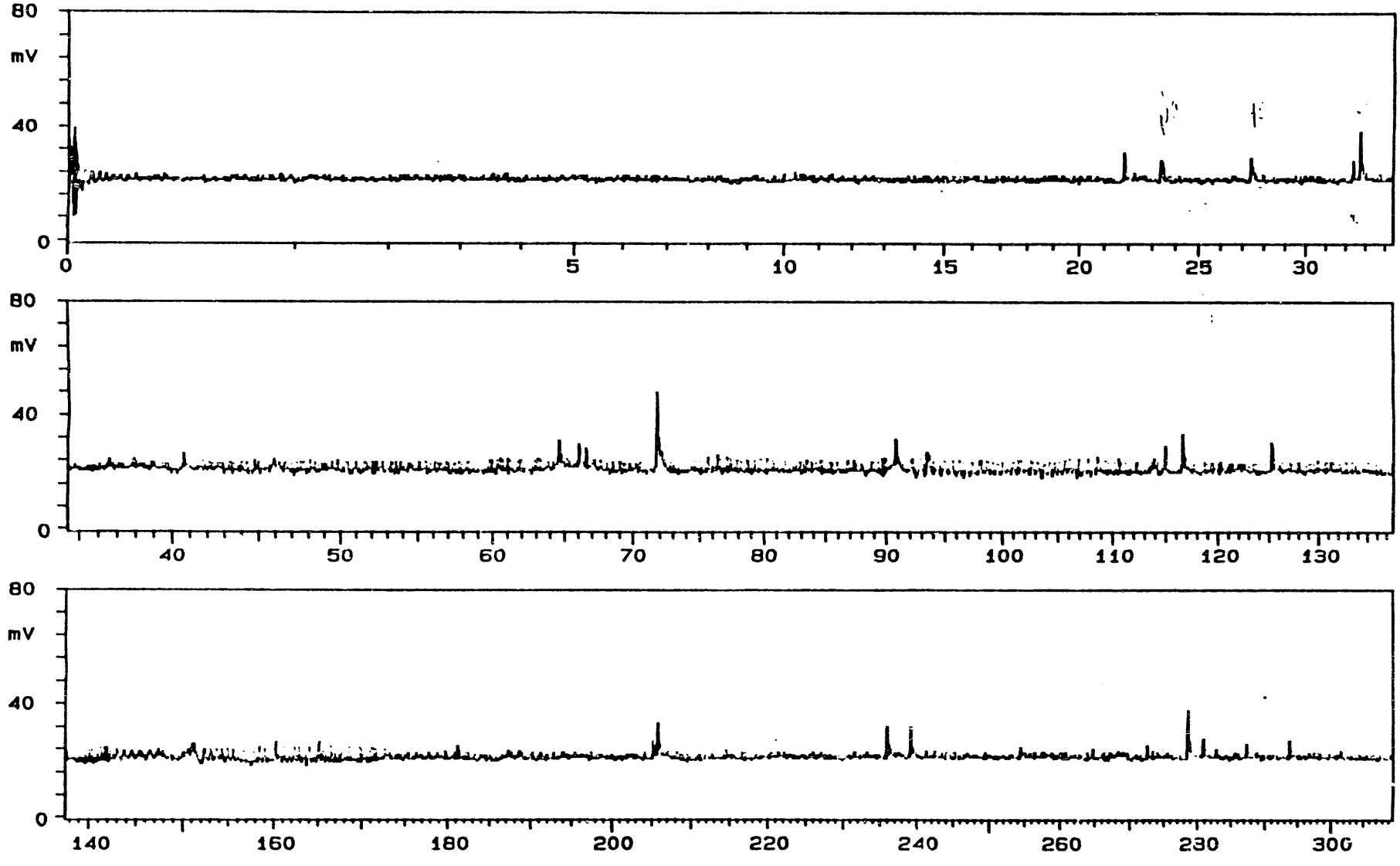

SSL# 3915-1188 Spectrum 3A'
X=744.3, COAL SAMP B, FOC=-1.0 ATT=0.25%, 0.6UJ
COLUMBIA U

SPEKTRUM 7120
POLARITY +
RANGE .16 V

21/12/1988
LASER .620uJ

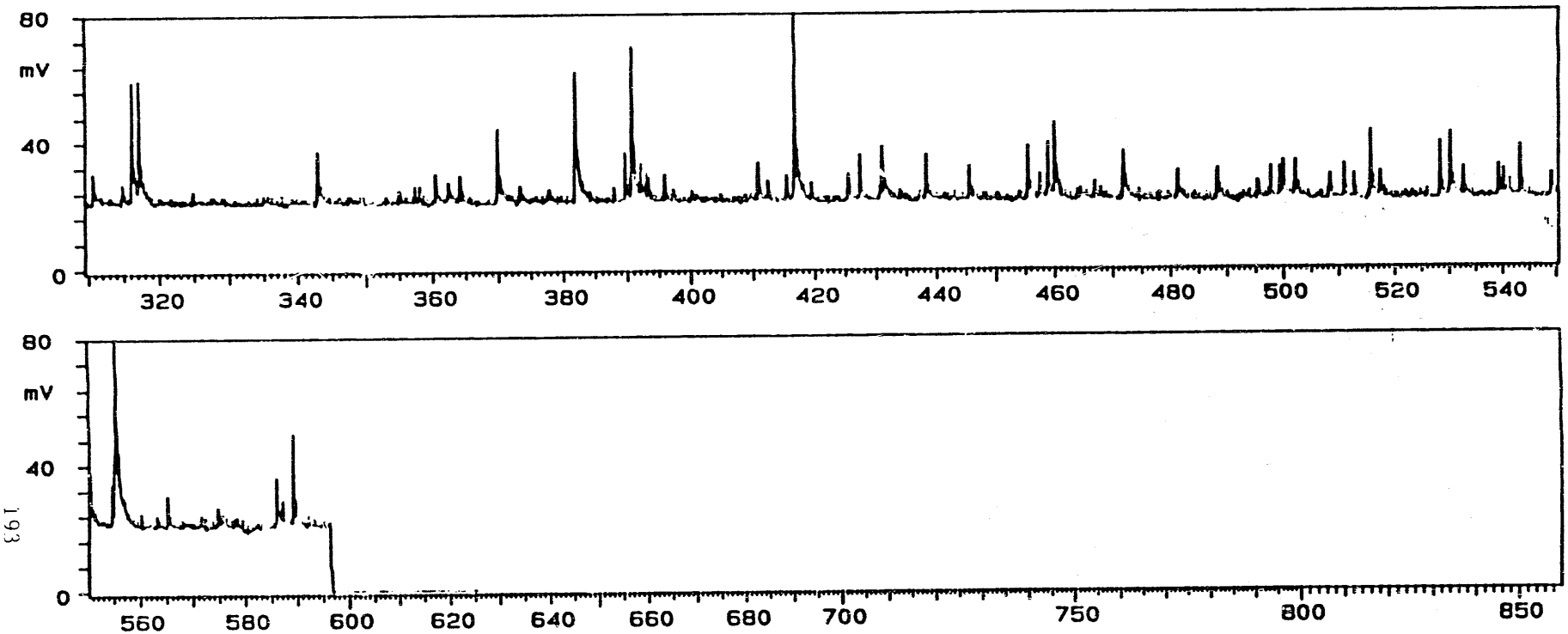

SSL# 3915-1188 Spectrum 4A

X=744.7, COAL SAMP B, FOC=-1.0 ATT=0.25%, 0.6UJ

COLUMBIA U

SPEKTRUM 7180

POLARITY +

RANGE .16 V

21/12/1988

LASER .580uJ

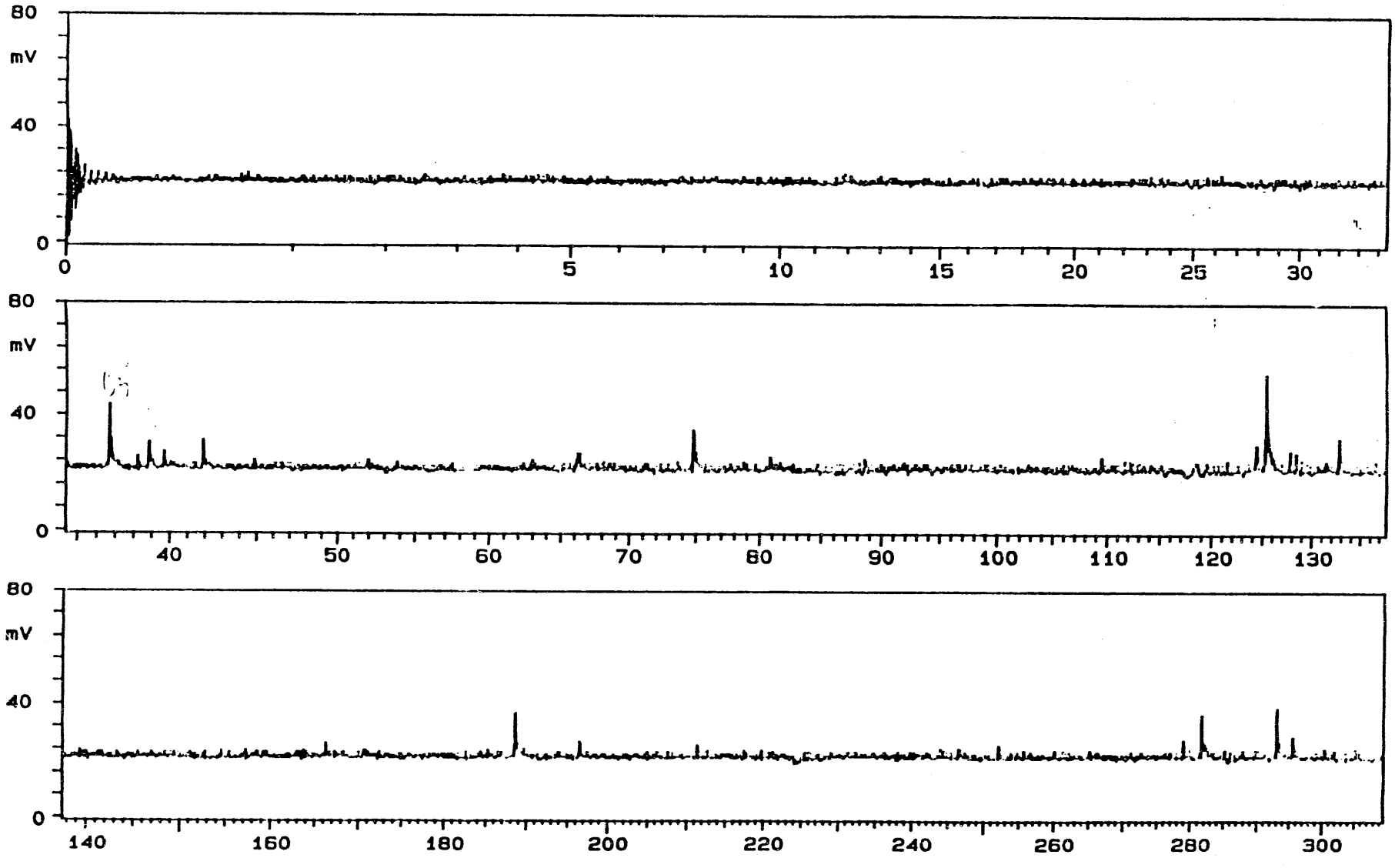

SSL# 3915-1188 Spectrum 4A'
X=744.7, COAL SAMP B, FOC=-1.0 ATT=0.25%, 0.6UJ
COLUMBIA U

SPEKTRUM 7180
POLARITY +
RANGE .16 V

21/12/1988
LASER .580uJ

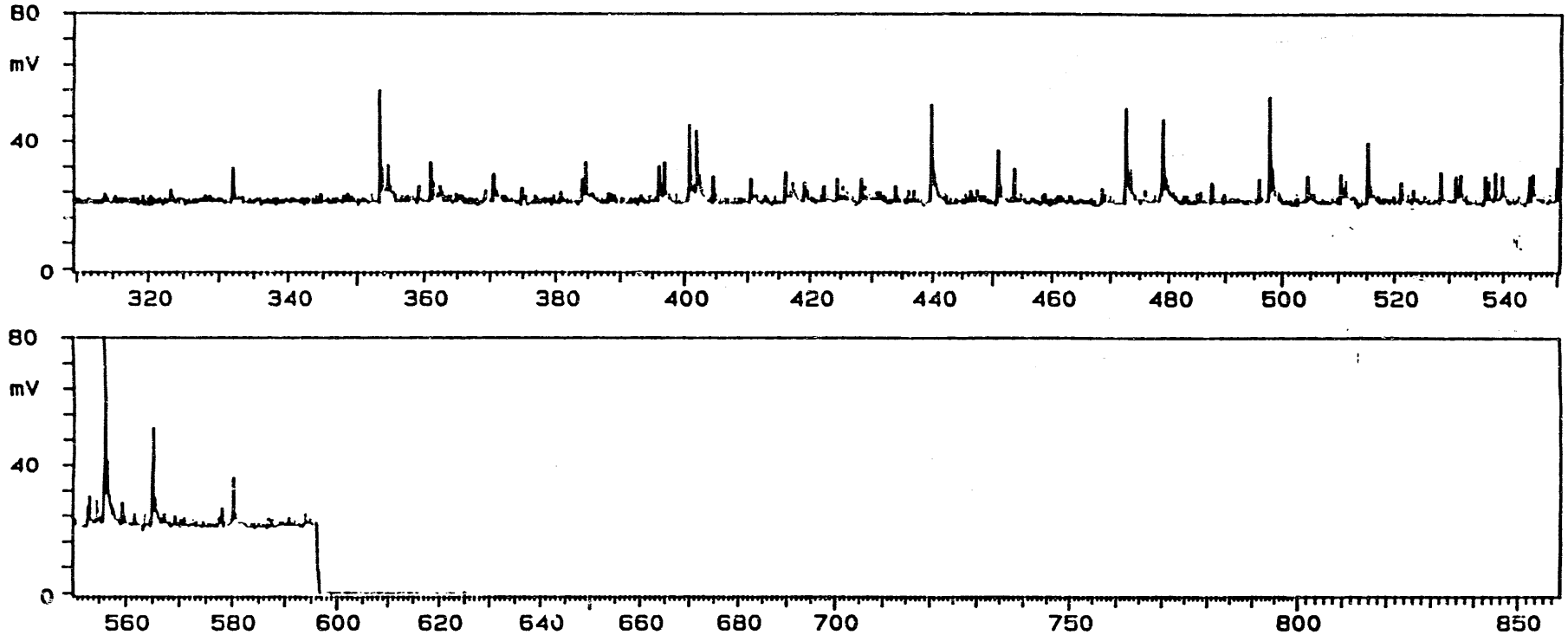

SSL# 3915-1188 Spectrum 5A
X=745.1, COAL SAMP B, FOC=-1.0 ATT=0.25%, 0.6UJ
COLUMBIA U

SPEKTRUM 7240
POLARITY +
RANGE .16 V

21/12/1988
LASER .590uJ

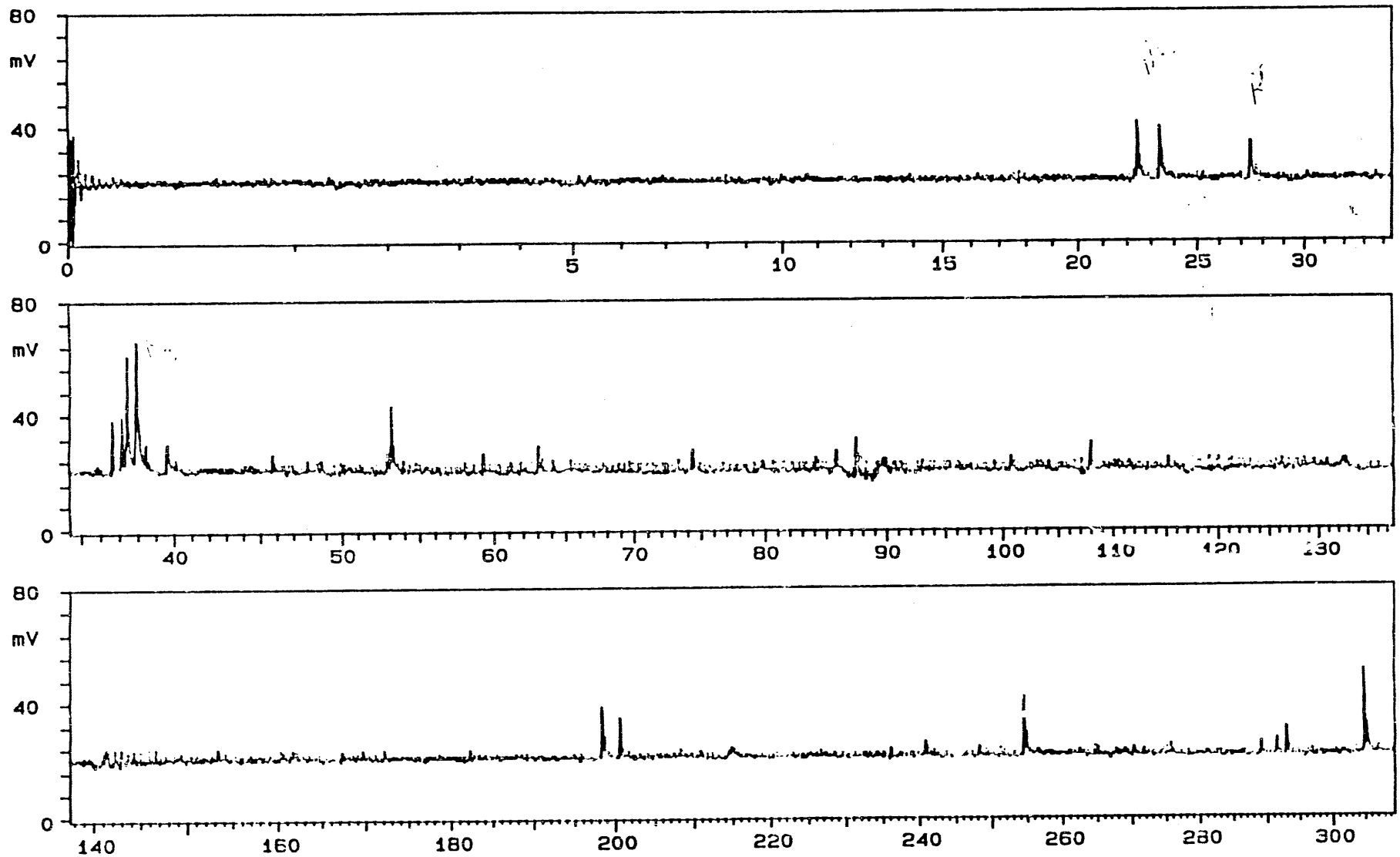

SSL# 3915-1188 Spectrum 5A'
X=745.1, COAL SAMP B, FOC=-1.0 ATT=0.25%, 0.6UJ
COLUMBIA U

SPEKTRUM 7240
POLARITY +
RANGE .16 V

21/12/1988
LASER .600uJ

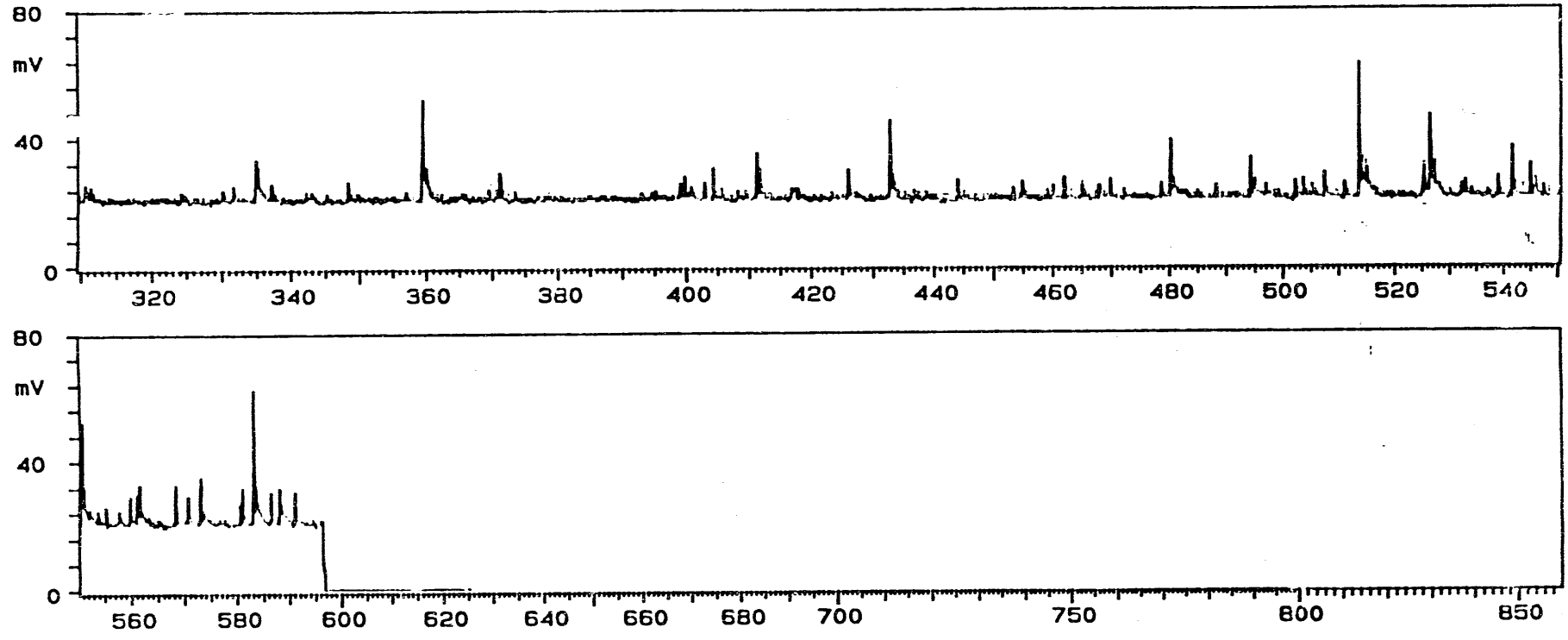

SSL# 3915-1188 Spectrum 6A
X=745.5, COAL SAMP B, FOC=-1.0 ATT=0.25%, 0.6UJ
COLUMBIA U

SPEKTRUM 7300
POLARITY +
RANGE .16 V

21/12/1988
LASER .620uJ

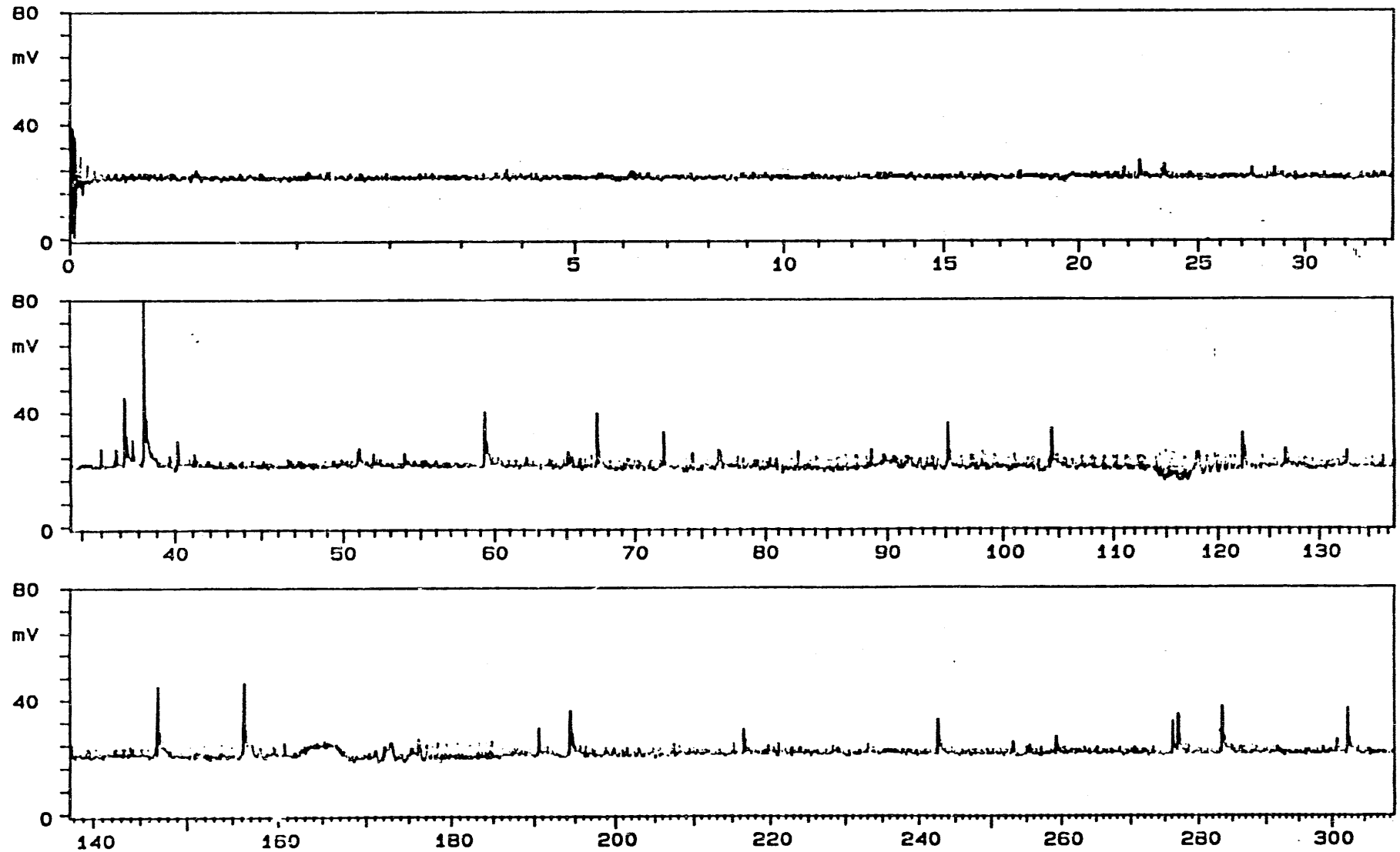

SSL# 3915-1188 Spectrum 6A'
X=745.5, COAL SAMP B, FOC=-1.0 ATT=0.25%, 0.6UJ
COLUMBIA U

SPEKTRUM 7300
POLARITY +
RANGE .16 V

21/12/1988
LASER .620UJ

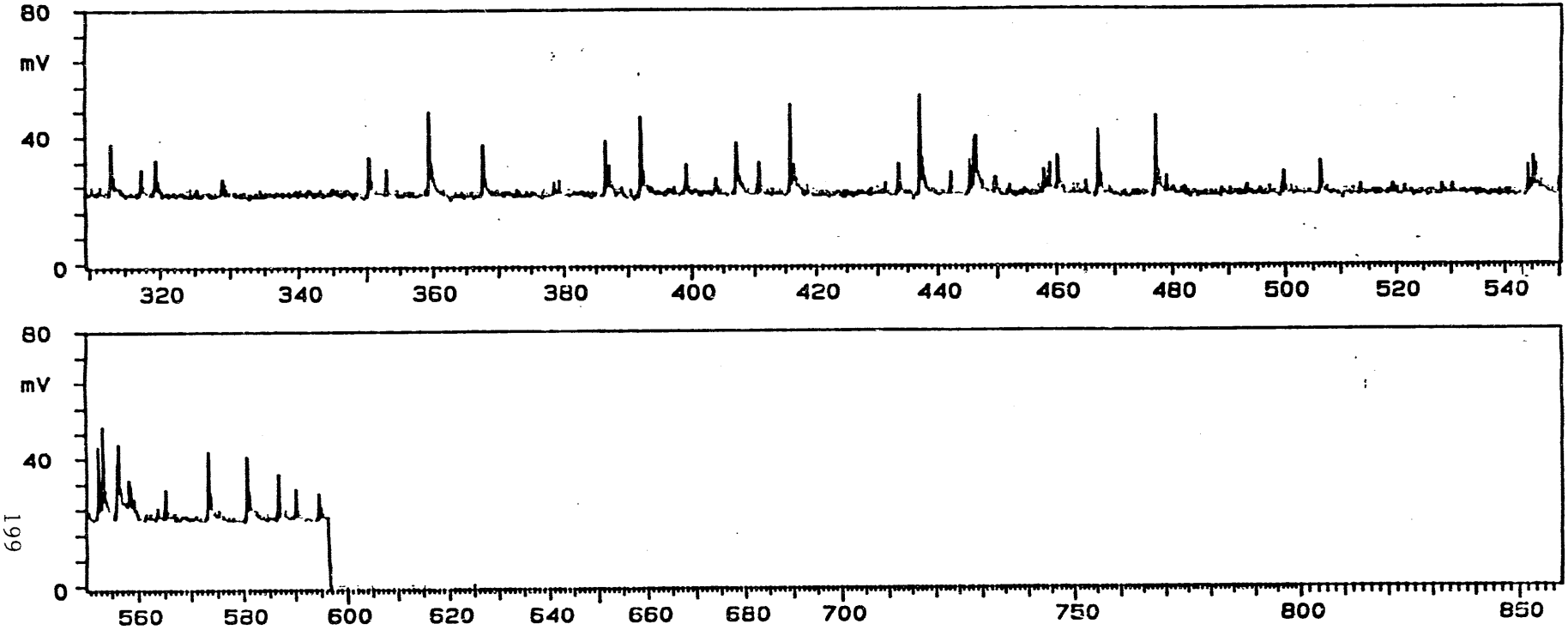

SSL# 3915-1188 Spectrum 7A
X=745.9, COAL SAMP B, FOC=-1.0 ATT=0.25%, 0.6UJ
COLUMBIA U

SPEKTRUM 7360
POLARITY +
RANGE .16 V

21/12/1988
LASER .600uJ

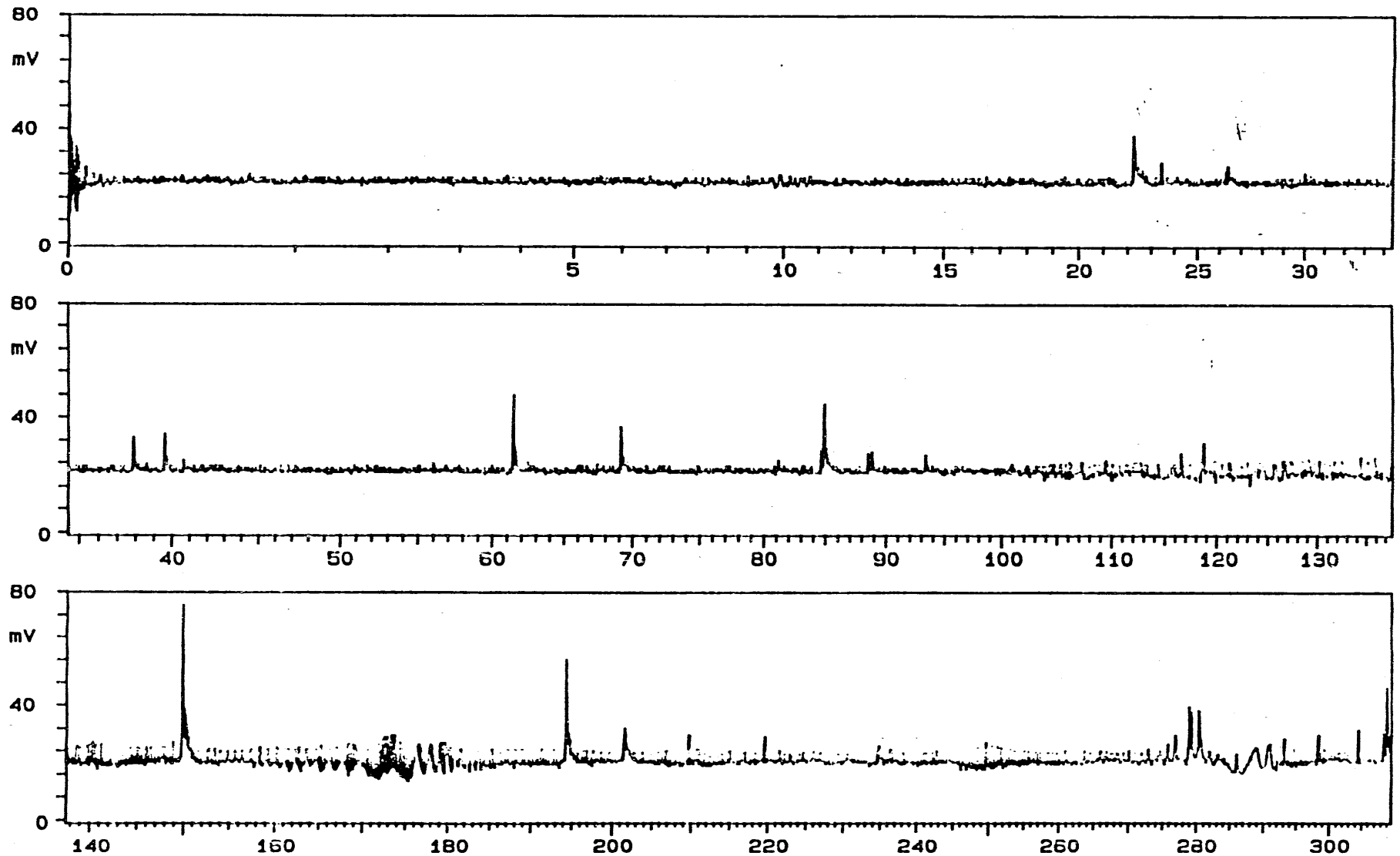

SSL# 3915-1188 Spectrum 7A'

X=745.9, COAL SAMP B, FOC=-1.0 ATT=0.25%, 0.6UJ

COLUMBIA U

SPEKTRUM 7360

POLARITY +

RANGE .16 V

21/12/1988

LASER .600uJ

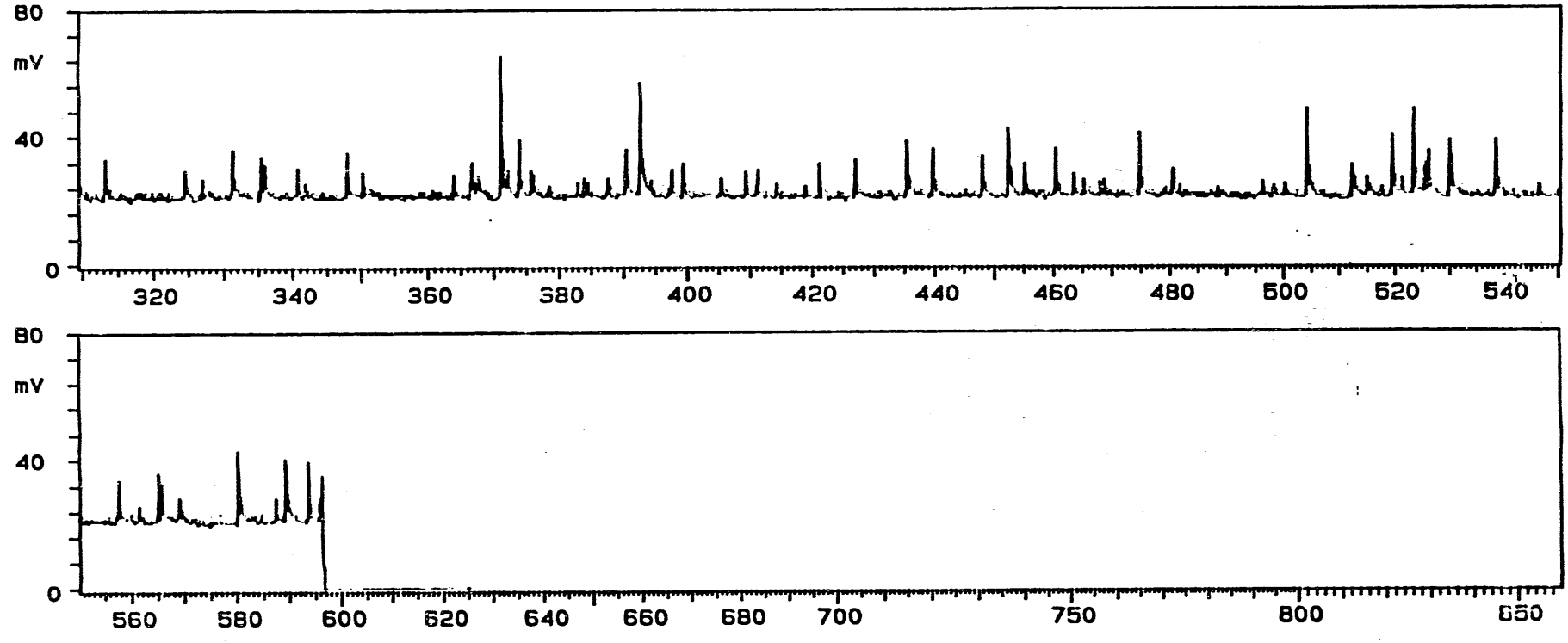

SSL# 3915-1188 Spectrum 8A
X=746.3, COAL SAMP B, FOC=-1.0 ATT=0.25%, 0.6UJ
COLUMBIA U

SPEKTRUM 7420
POLARITY +
RANGE .16 V

21/12/1988
LASER .620uJ

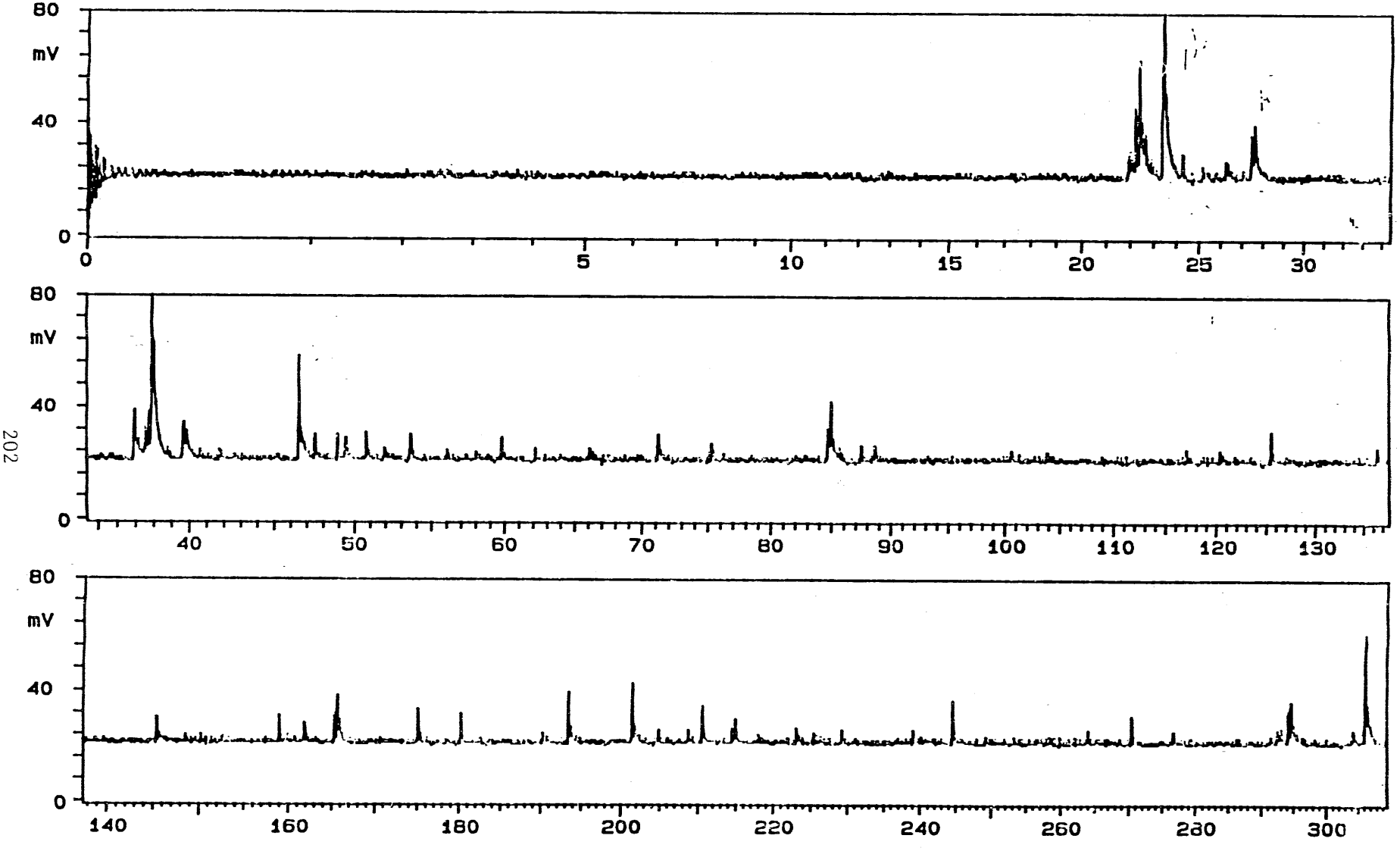

Spectrum 8A'

SSL# 3915-1188
X=746.3, COAL SAMP B, FOC=-1.0 ATT=0.25%, 0.6UJ
COLUMBIA U

SPEKTRUM 7420
POLARITY +
RANGE .16 V

21/12/1988
LASER .620UJ

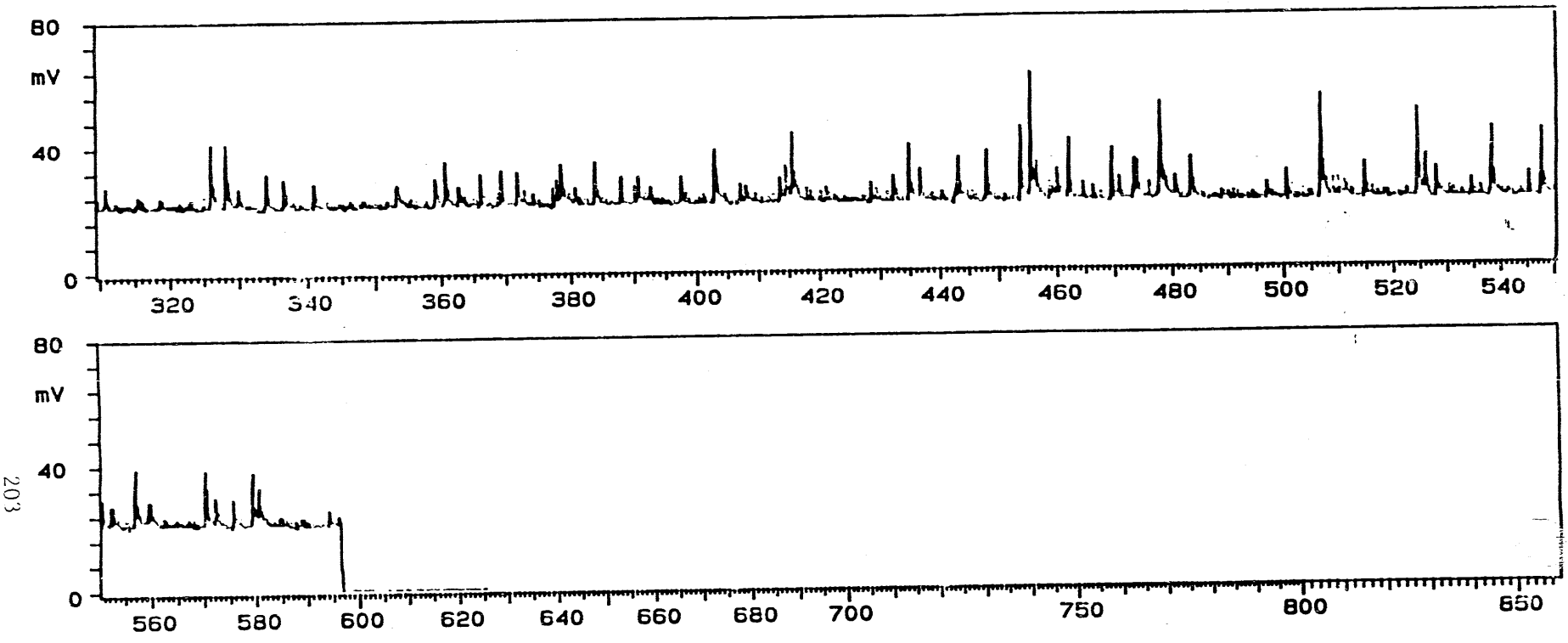

SSL# 3915-1188 Spectrum 91

X=746.7. COAL SAMP B. FOC=-1.0 ATT=0.25%. 0.6UU

COLUMBIA U

SPEKTRUM 74[illegible]

POLARITY +

RANGE .16 V

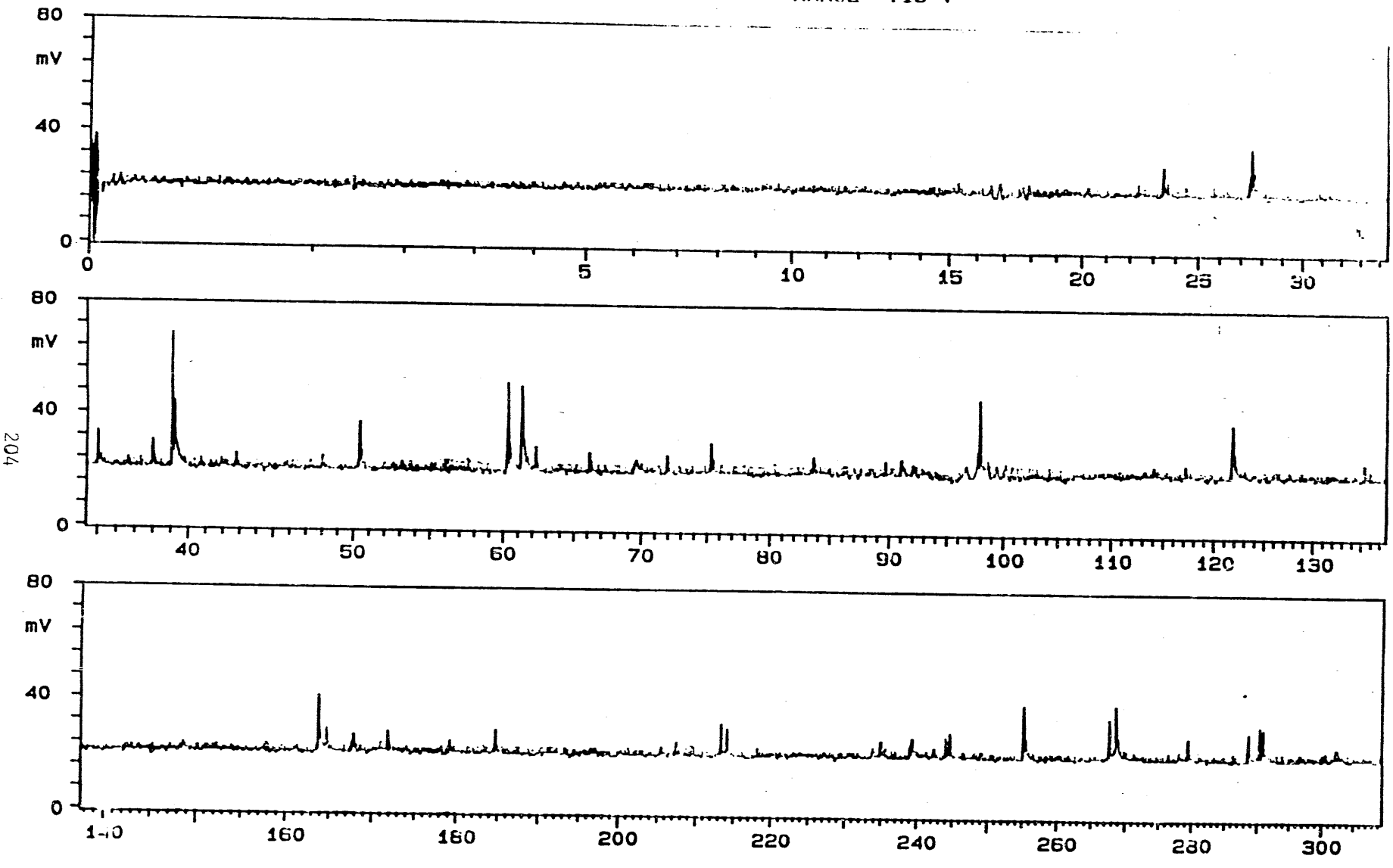

SSL# 3915-1188 Spectrum 9A'
X=746.7, COAL SAMP B, FOC=-1.0 ATT=0.25%, 0.6UJ
COLUMBIA U

SPEKTRUM 7480
POLARITY +
RANGE .16 V

21/12/1988
LASER .600UJ

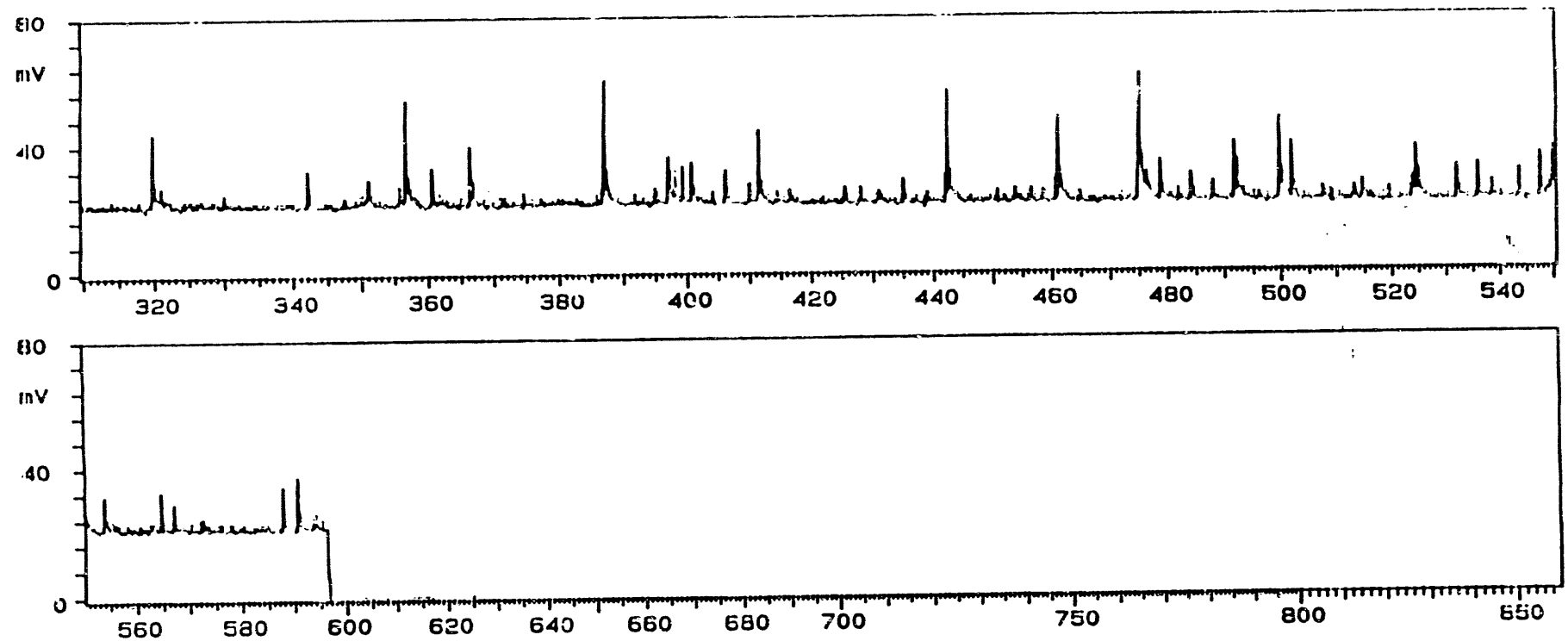

SSL# 3915-1168 Spectrum 10A

X=747.1, COAL SAMP B, FOC=-1.0 ATT=0.25%, 0.6UJ

COLUMBIA U

SPEKTRUM 7540

POLARITY +

RANGE .16 V

21/12/1988

LASER .600uJ

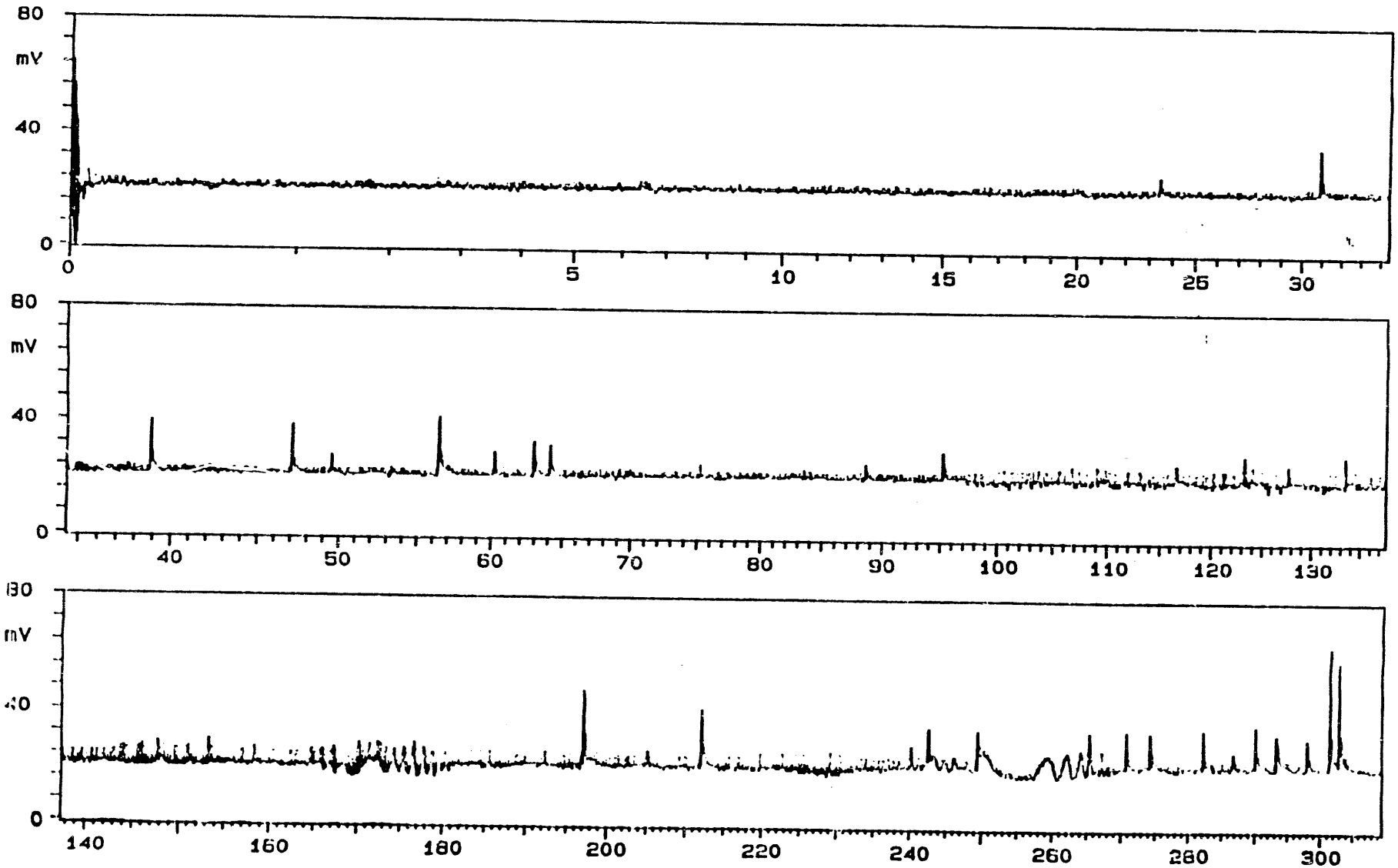

SSL# 3915-1188 Spectrum 104'
X=747.1. COAL SAMP B. FOC=-1.0 ATT=0.25%. 0.6UJ
COLUMBIA U

SPEKTRUM 7540
POLARITY +
RANGE .16 V

21/12/1988
LASER .600uJ

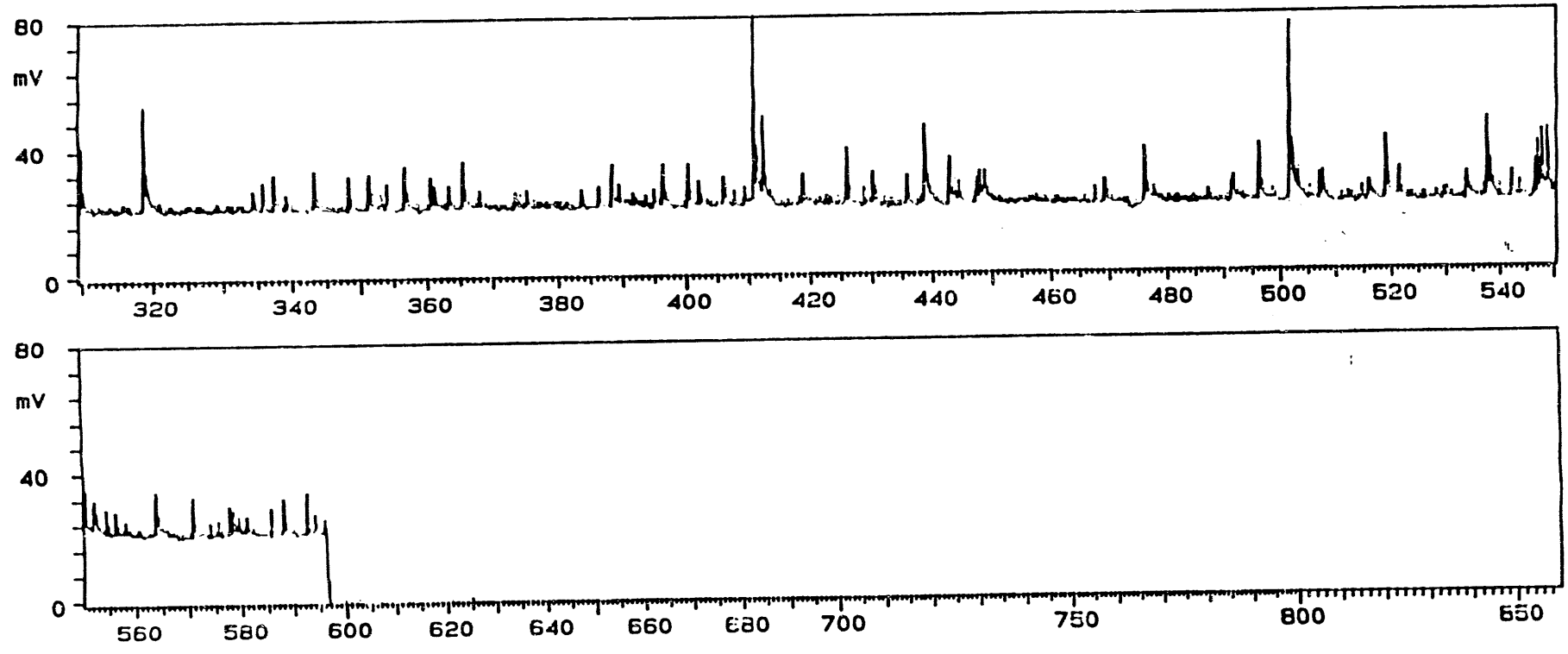

SSL# 3915-1188 Spectrum 11

X-747.1, COAL SAMP B, FOC=-1.0 ATT=0.25%, 0.6UJ

COLUMBIA U : REPEAT SAME LOCATION, DEPTH 2

SPEKTRUM 7640

POLARITY +

RANGE .16 V

21/12/1988

LASER .610uJ

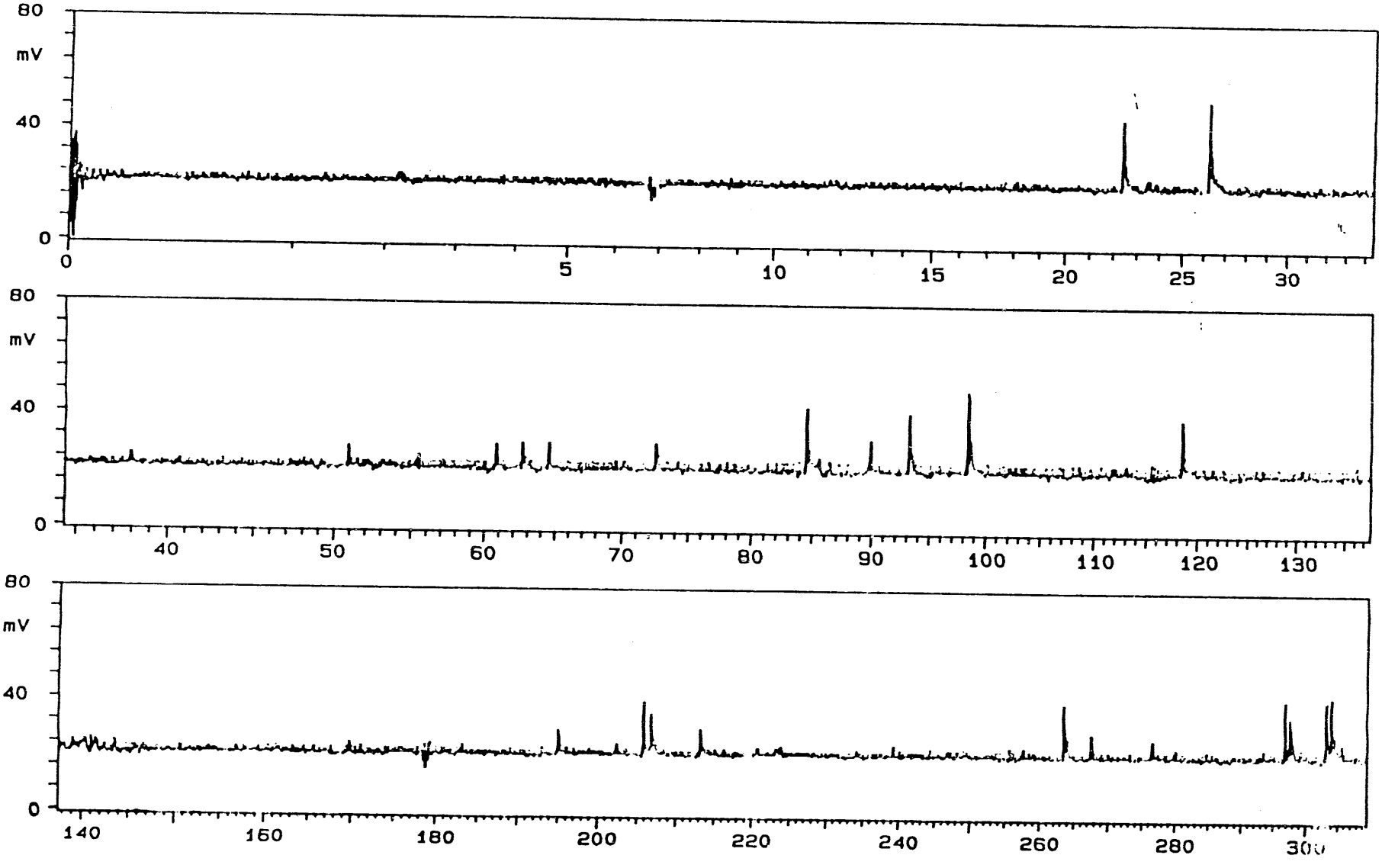

SSL# 3915-1188 Spectrum 11A'

SPEKTRUM 7640

21/12/1988

X=747.1, COAL SAMP B, FOC=-1.0 ATT=0.25%, 0.6UJ

POLARITY +

LASER .610uJ

COLUMBIA U : REPEAT SAME LOCATION, DEPTH 2

RANGE .16 V

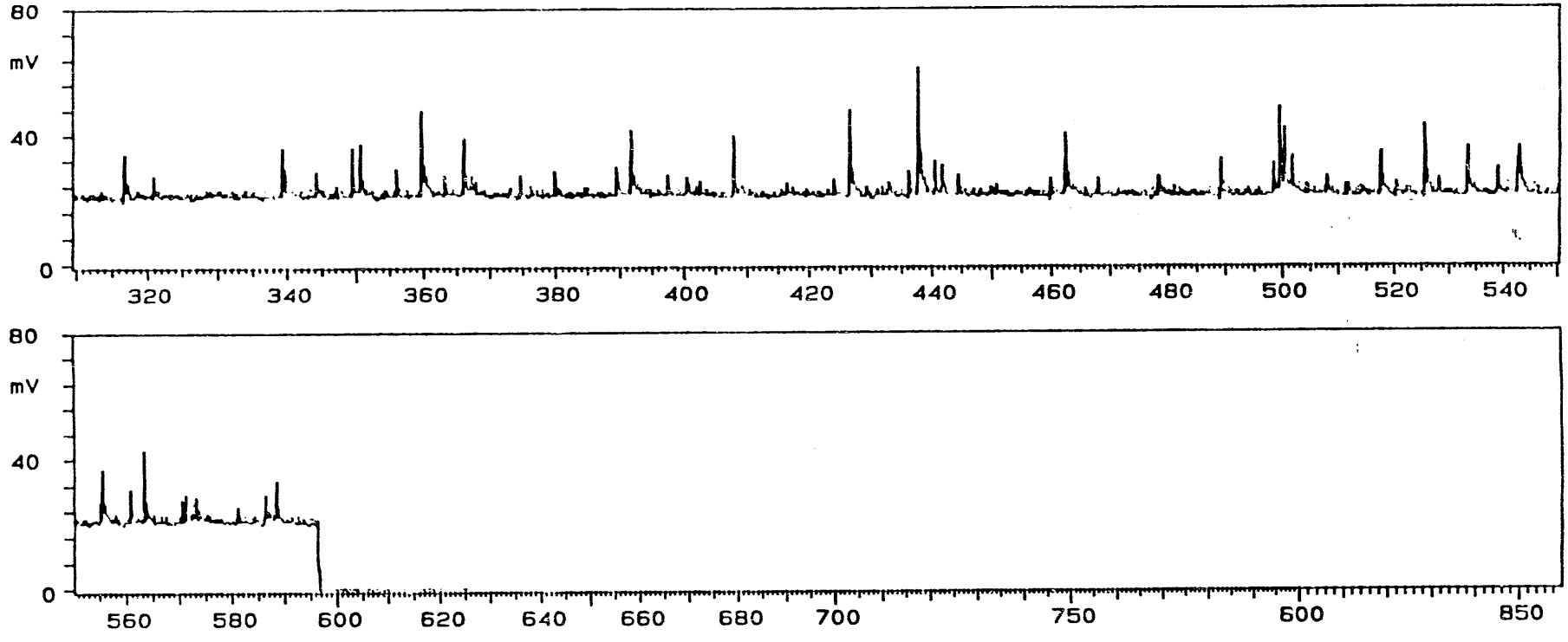

SSL# 3915-1188 Spectrum 1B
X=743.5, COAL SAMP B, FOC=-1.0 ATT=0.25%, 0.6UJ
COLUMBIA U

SPEKTRUM 6970
POLARITY -
RANGE .16 V

21/12/1988
LASER .550uJ

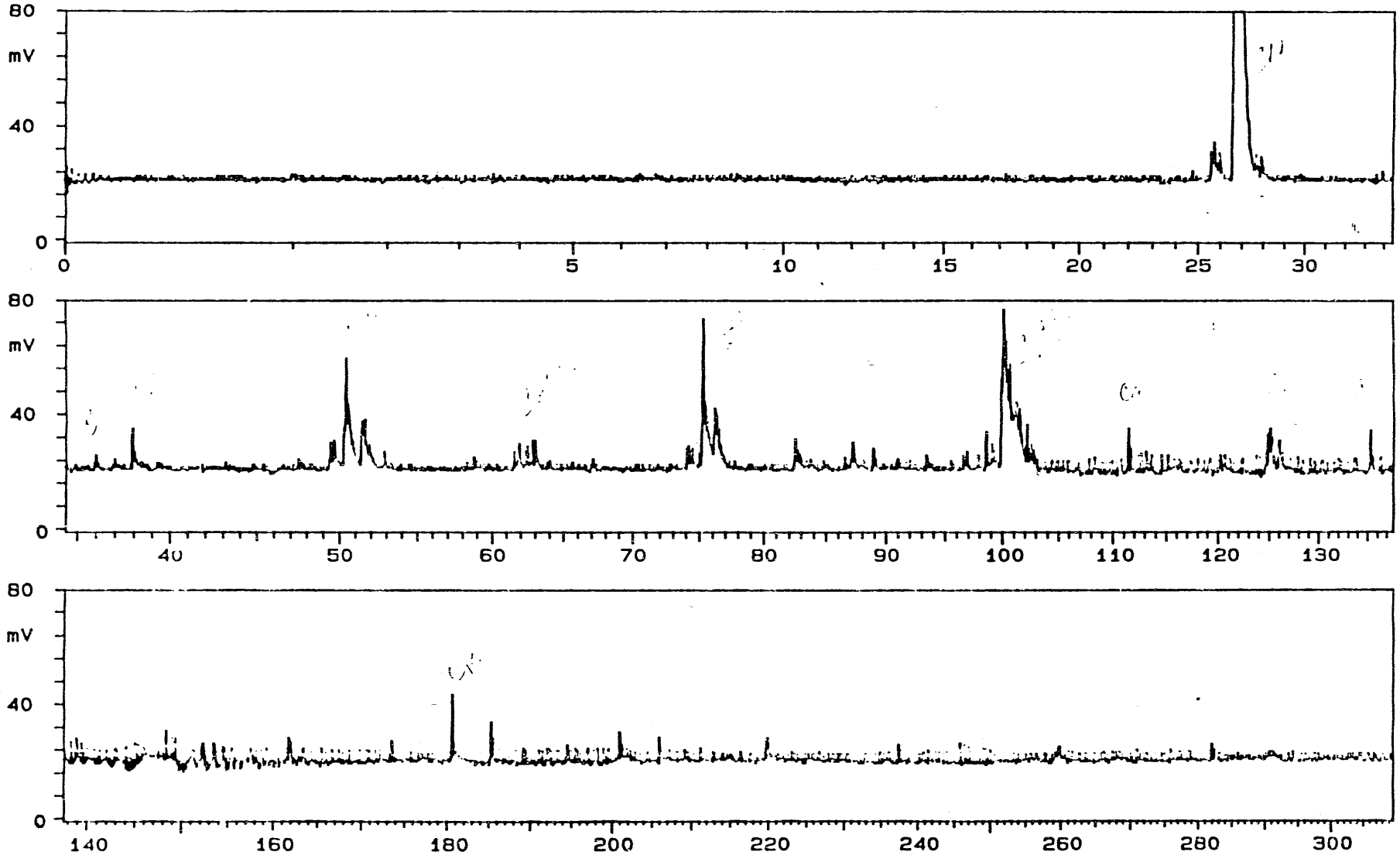

SSL# 3915-1188 Spectrum 18'
X=743.5. COAL SAMP B. FOC=-1.0 ATT=0.25%. 0.6UJ
COLUMBIA U

SPEKTRUM 6970
POLARITY -
RANGE .16 V

21/12/1988
LASER .550uJ

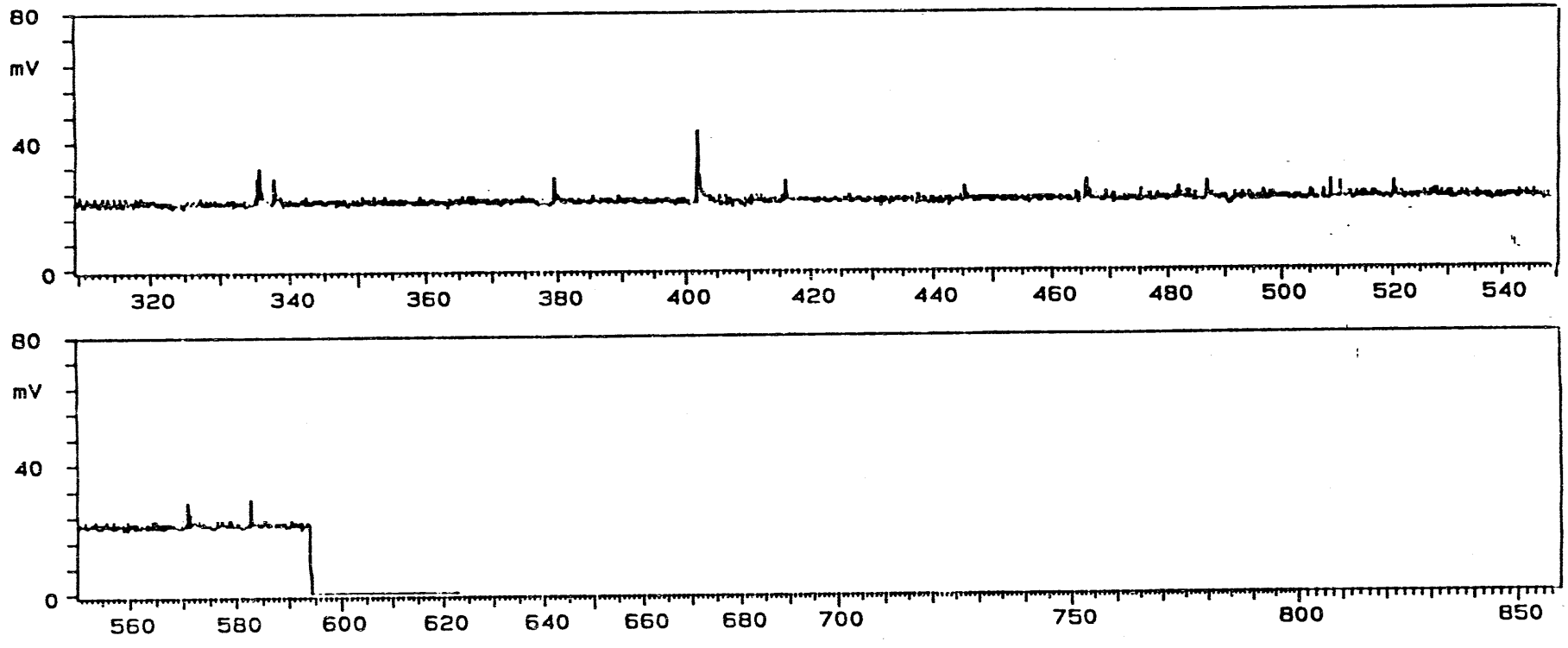

Spectrum 2B

SSL# 3915-1188
X-743.9, COAL SAMP B, FOC=-1.0 ATT=0.25%, 0.6UJ
COLUMBIA U

SPEKTRUM 7030
POLARITY -
RANGE .16 V

21/12/1988
LASER .610uJ

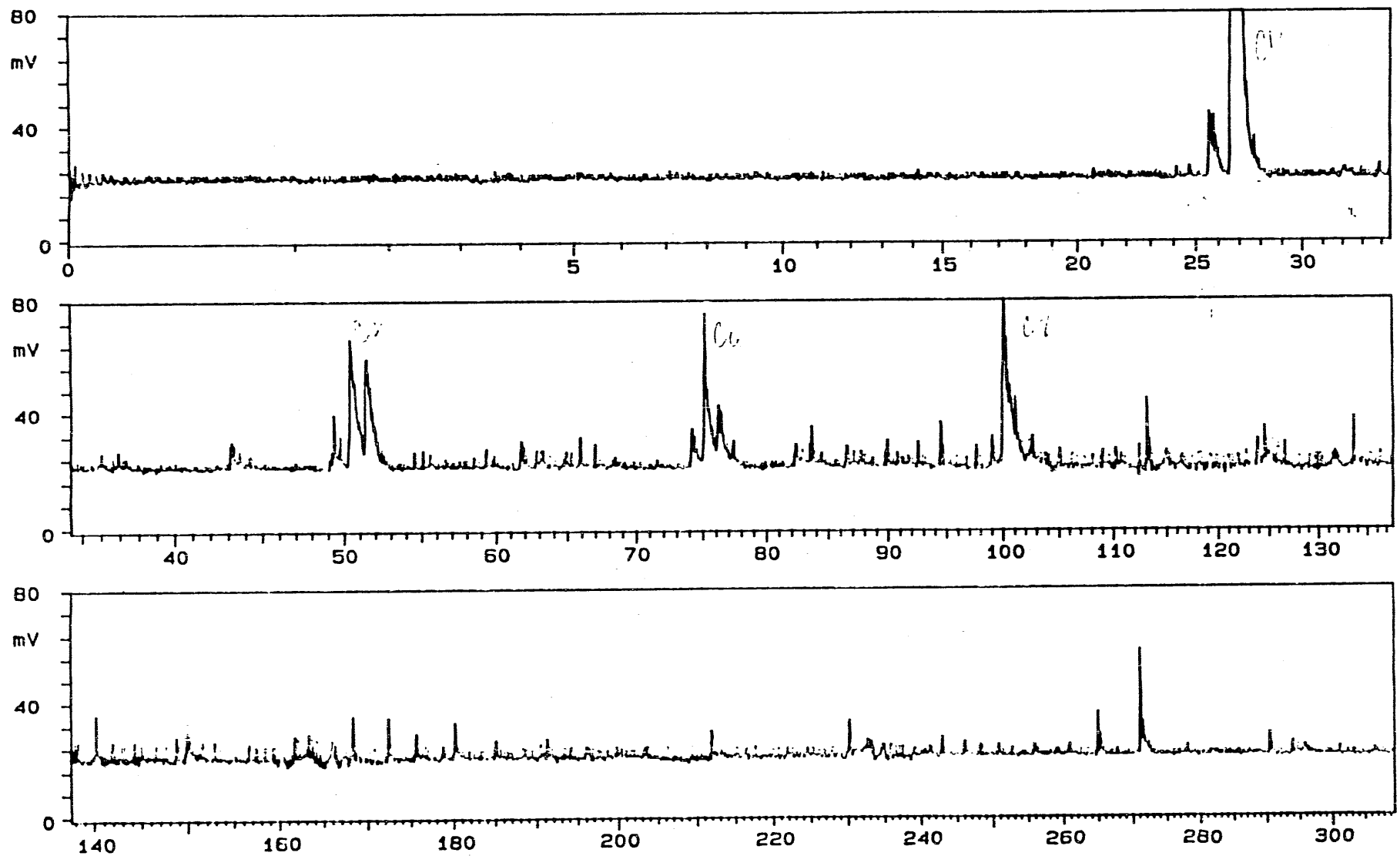

SSL# 3915-1188 Spectrum 2B'

X=743.9, COAL SAMP B, FOC=-1.0 ATT=0.25%, 0.6UJ

COLUMBIA U

SPEKTRUM 7030

POLARITY -

RANGE .16 V

21/12/1988

LASER .610uJ

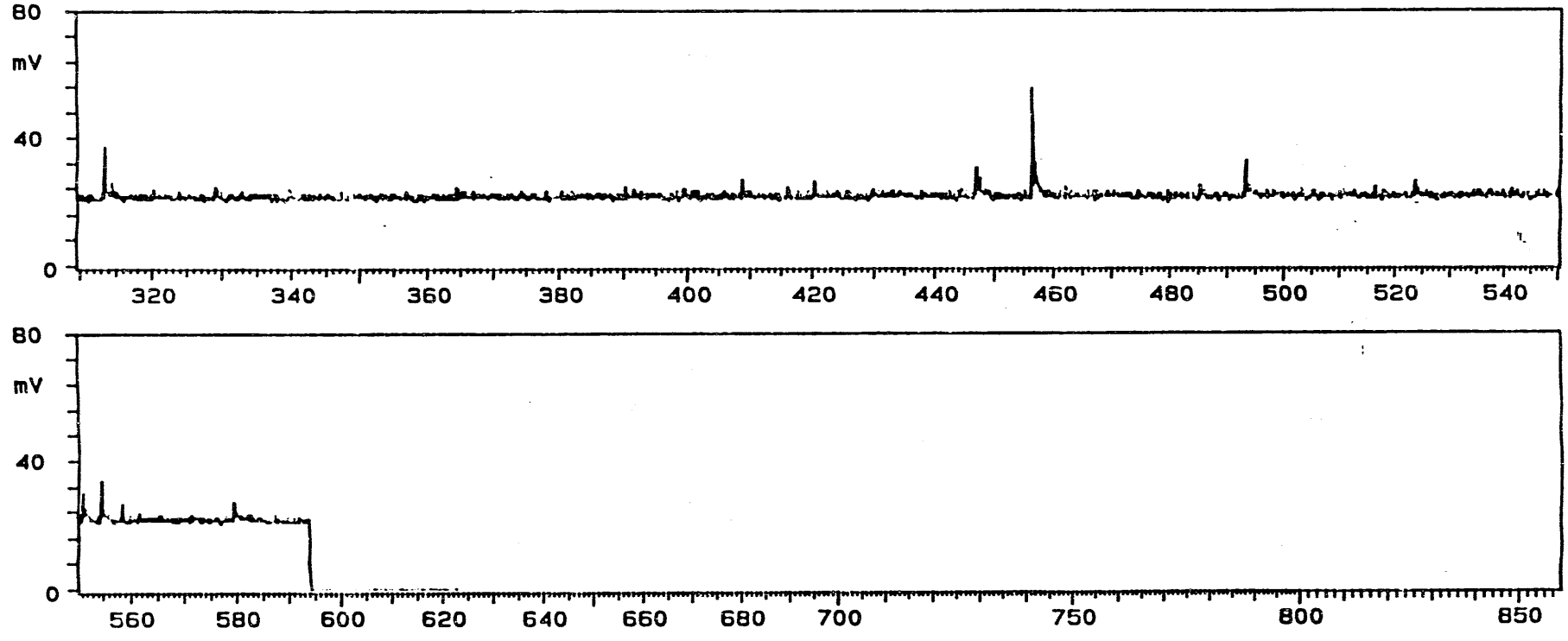

SSL# 3915-1188 Spectrum 3B

X=744.3, COAL SAMP B, FOC=-1.0 ATT=0.25%, 0.6UJ

COLUMBIA U

SPEKTRUM 7090

POLARITY -

RANGE .16 V

21/12/1988

LASER .530uJ

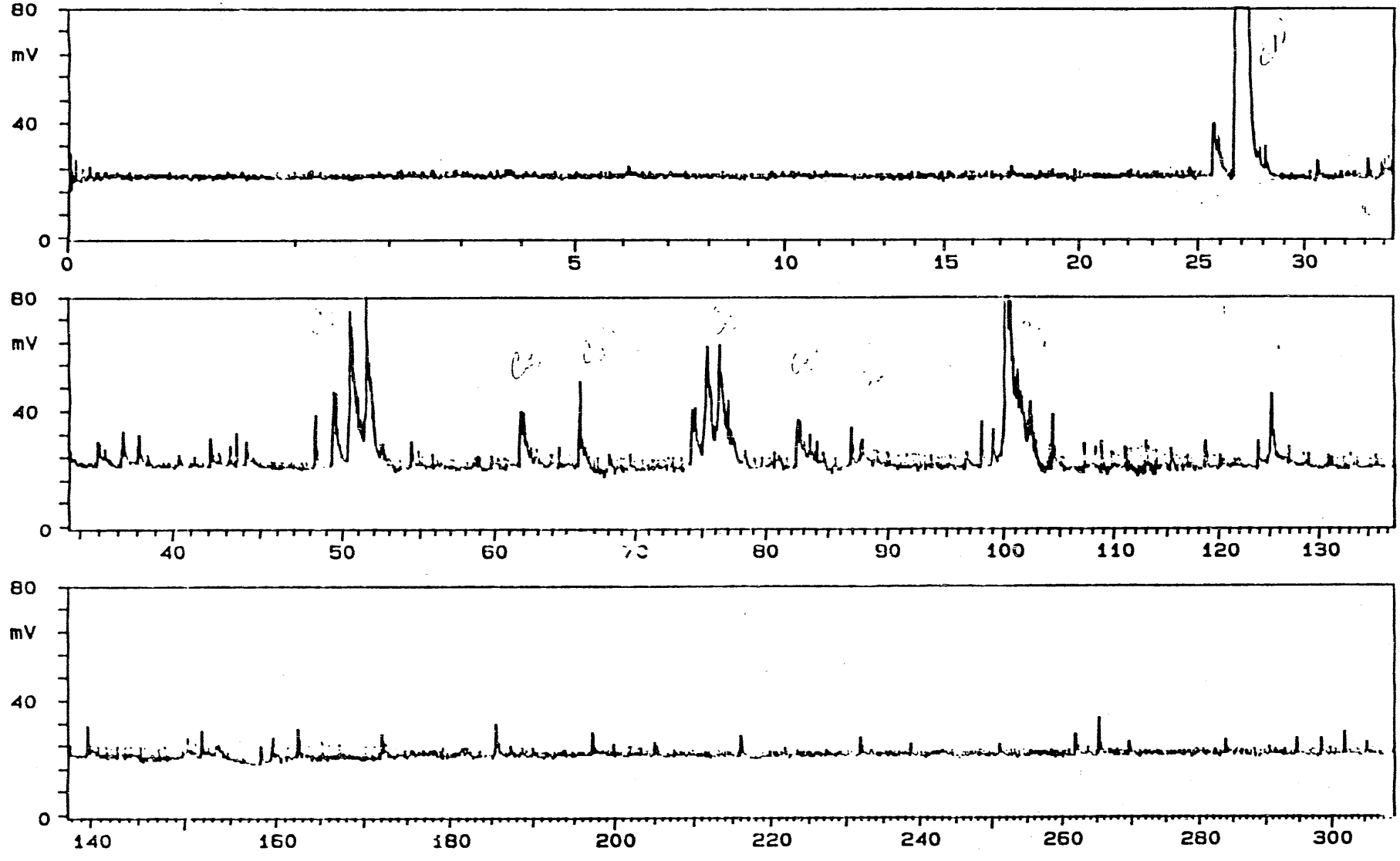

SSL# 3915-1188 Spectrum 38'

X=744.3, COAL SAMP B. FOC=-1.0 ATT=0.25%, 0.6UJ

COLUMBIA U

SPEKTRUM 7090

POLARITY -

RANGE .16 V

21/12/1988

LASER .530UJ

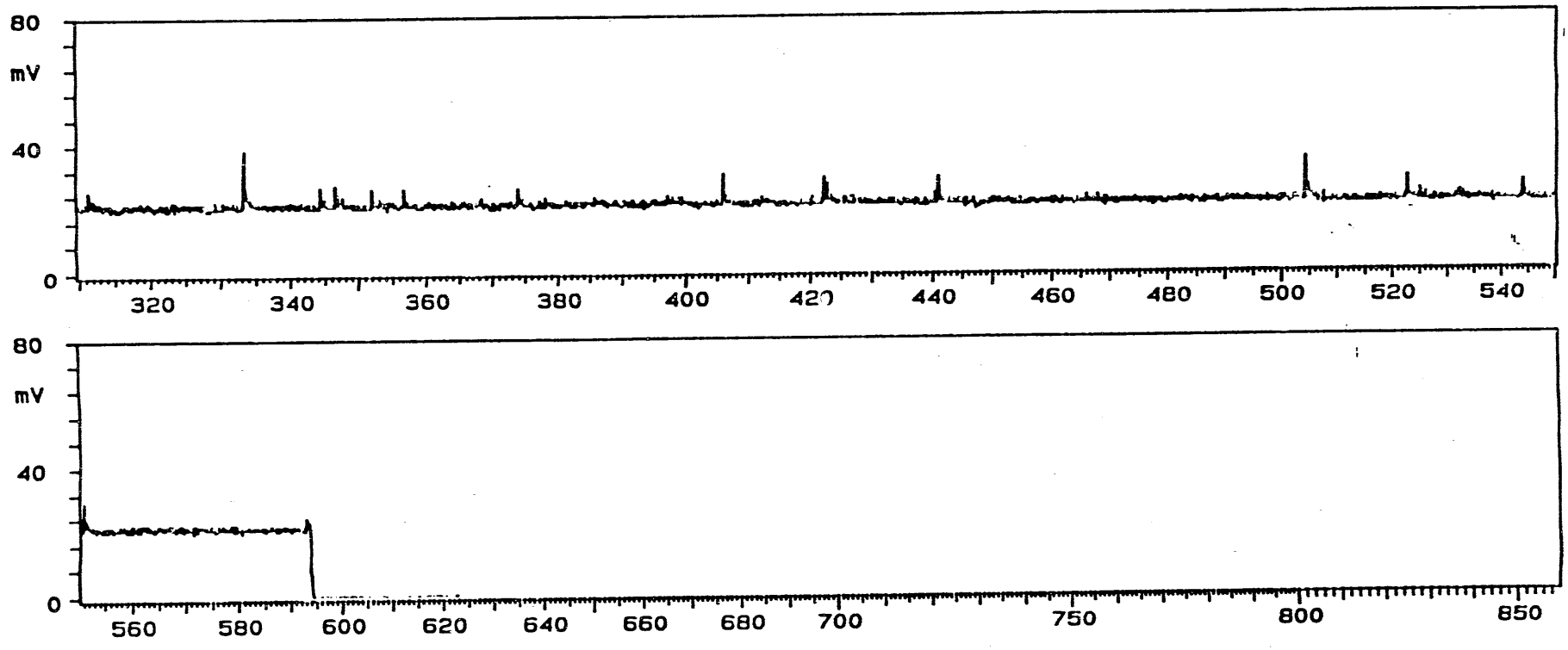

SSL# 3915-1188 Spectrum 4B
X=744.7, COAL SAMP B, FOC=-1.0 ATT=0.25%, 0.6UJ
COLUMBIA U

SPEKTRUM 7150
POLARITY -
RANGE .16 V

21/12/1988
LASER .620uJ

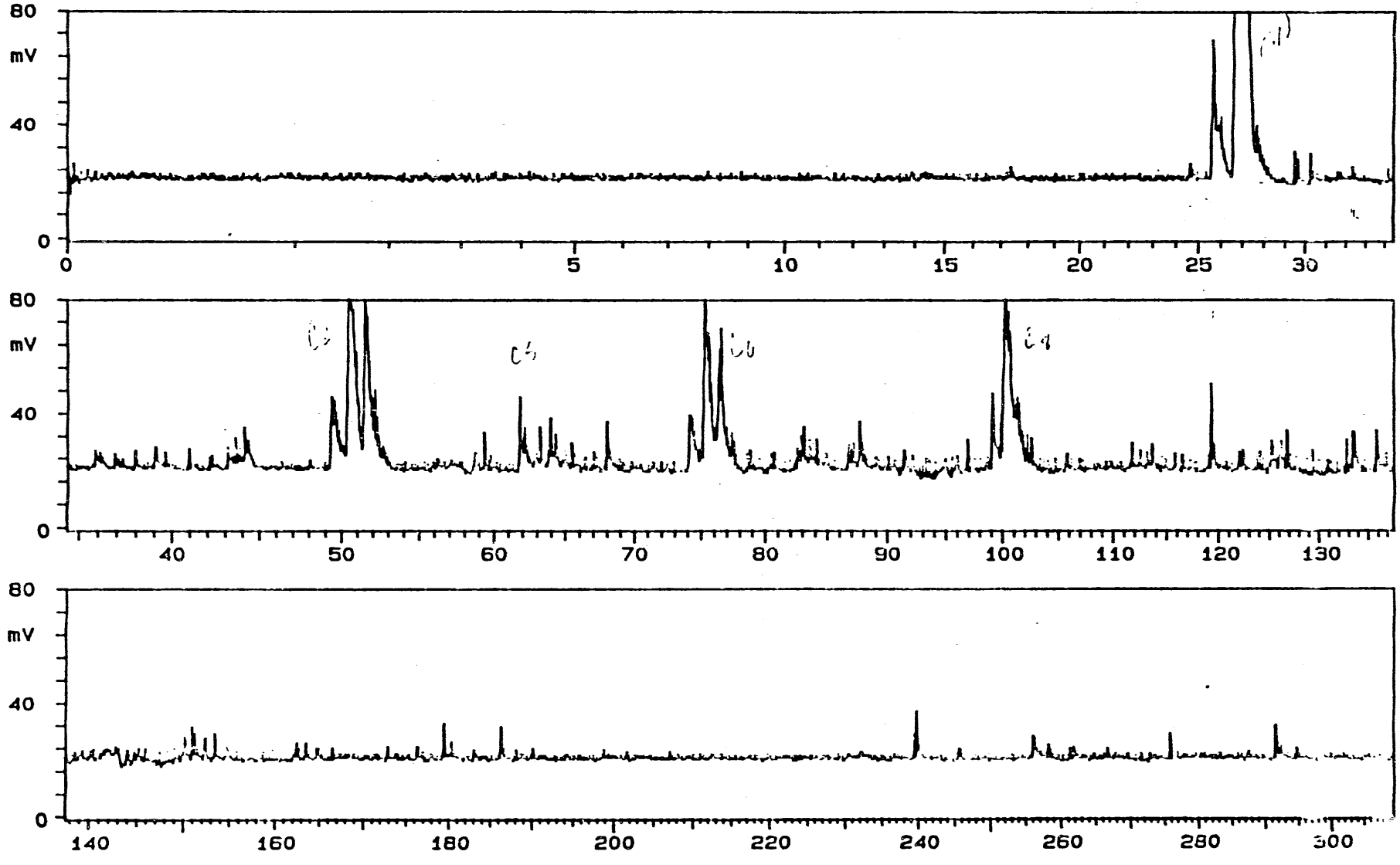

SSL# 3915-1188 Spectrum 4B'
X=744.7, COAL SAMP B, FOC=-1.0 ATT=0.25%, 0.6UJ
COLUMBIA U

SPEKTRUM 7150
POLARITY -
RANGE .16 V

21/12/1988
LASER .620uJ

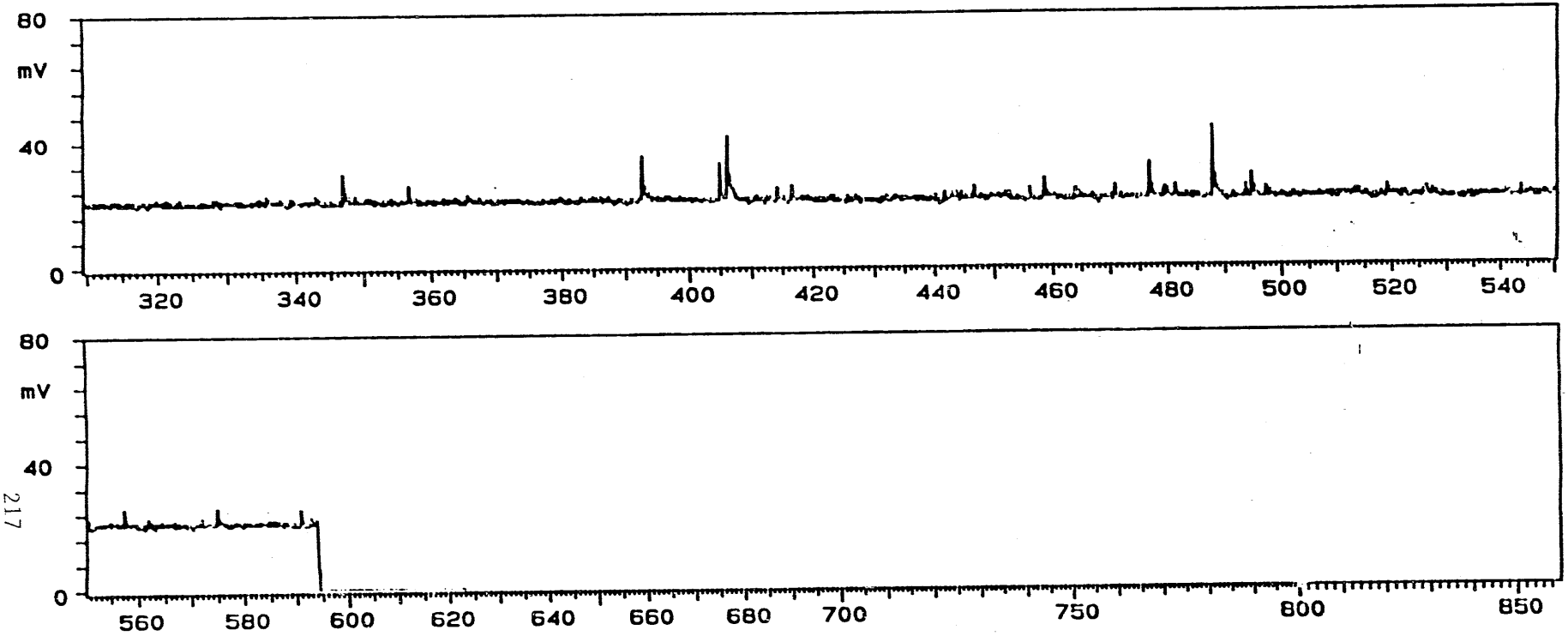

SSL# 3915-1188 Spectrum 5B

X-745.1, COAL SAMP B, FOC=-1.0 ATT=0.25%, 0.6UJ

COLUMBIA U

SPEKTRUM 7210

POLARITY =

RANGE .16 V

21/12/1988

LASER .590uJ

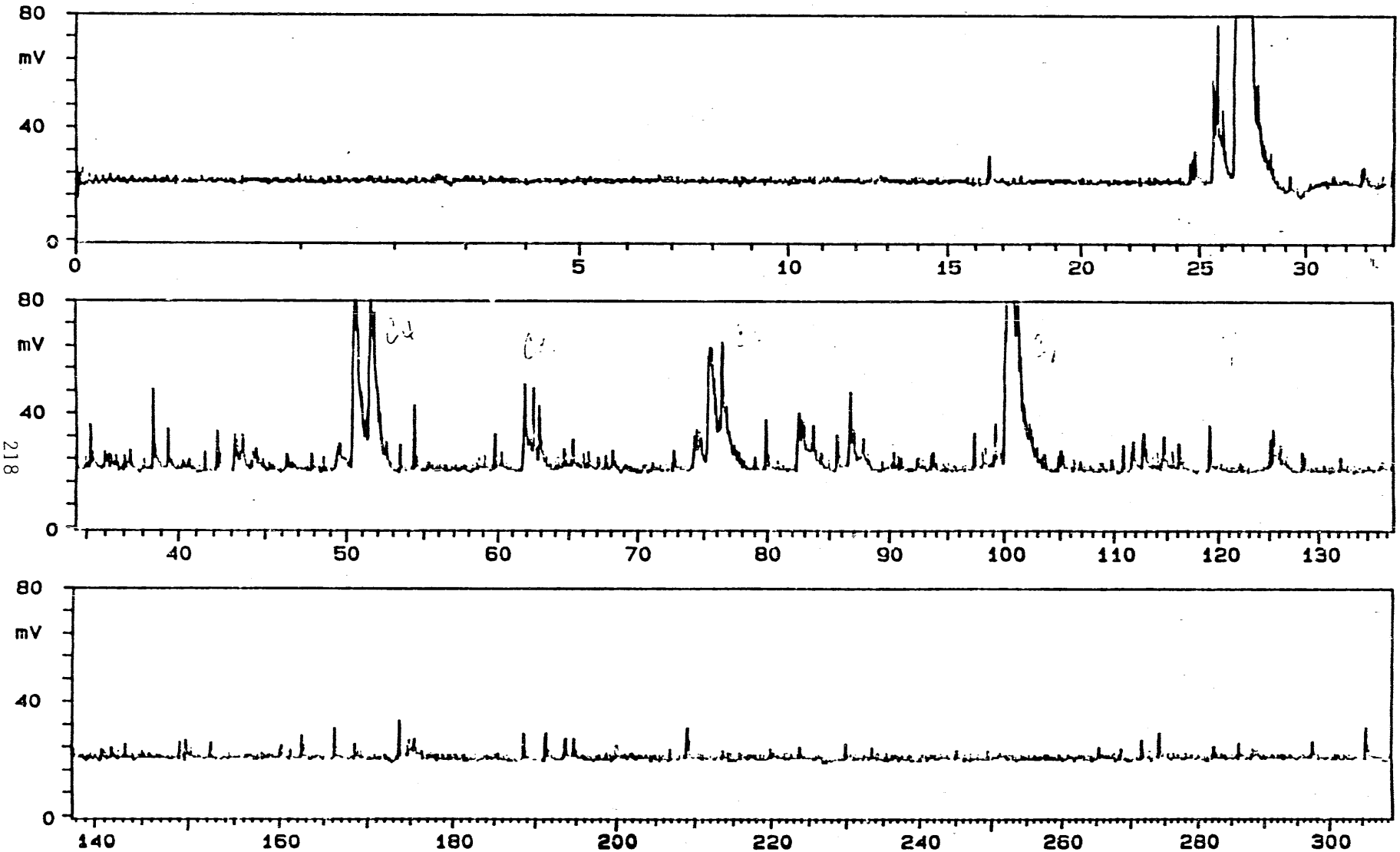

SSL# 3915-1188 Spectrum 5B'
X-745.1. COAL SAMP B. FOC=-1.0 ATT=0.25%. 0.6UJ
COLUMBIA U

SPEKTRUM 7210
POLARITY -
RANGE .16 V

21/12/1988
LASER .590uJ

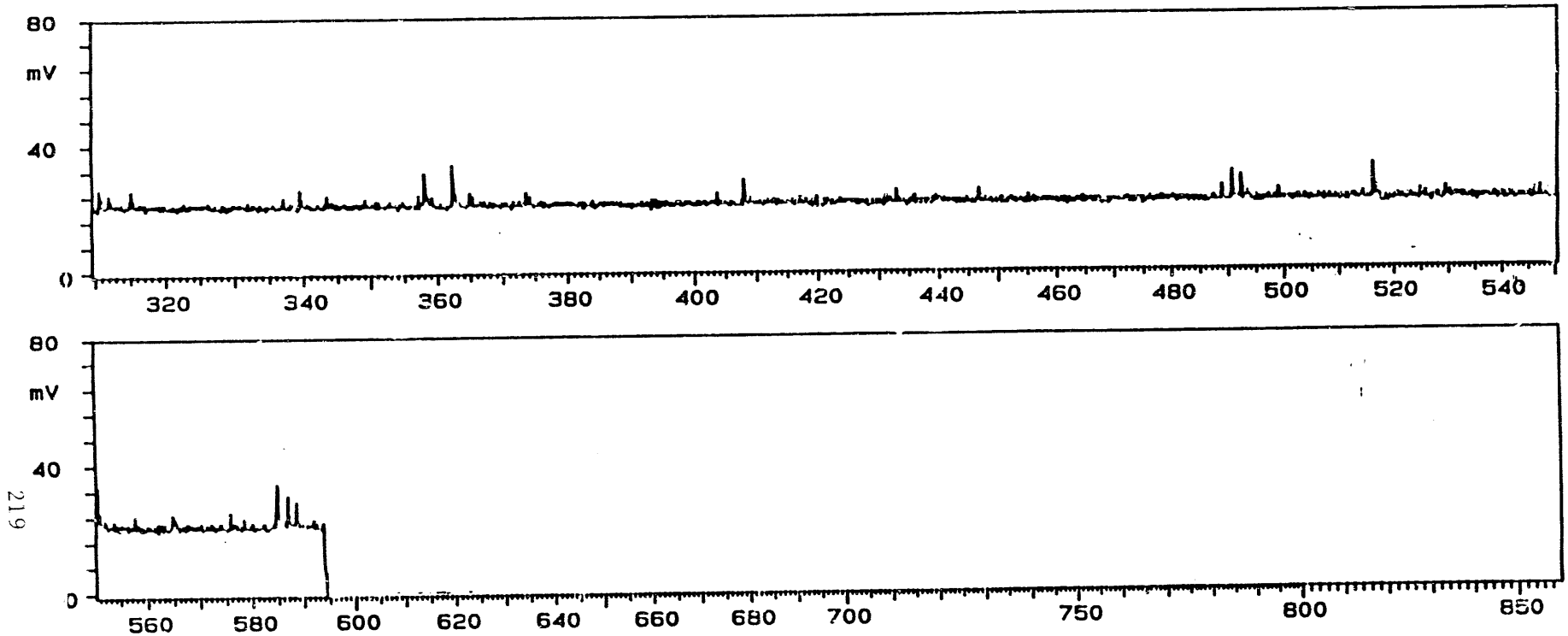

219

SSL# 3915-1188 Spectrum 6B

X=745.5, COAL SAMP B, FOC=-1.0 ATT=0.25%, 0.6UJ

COLUMBIA U

SPEKTRUM 7270

POLARITY -

RANGE .16 V

21/12/1988

LASER .590uJ

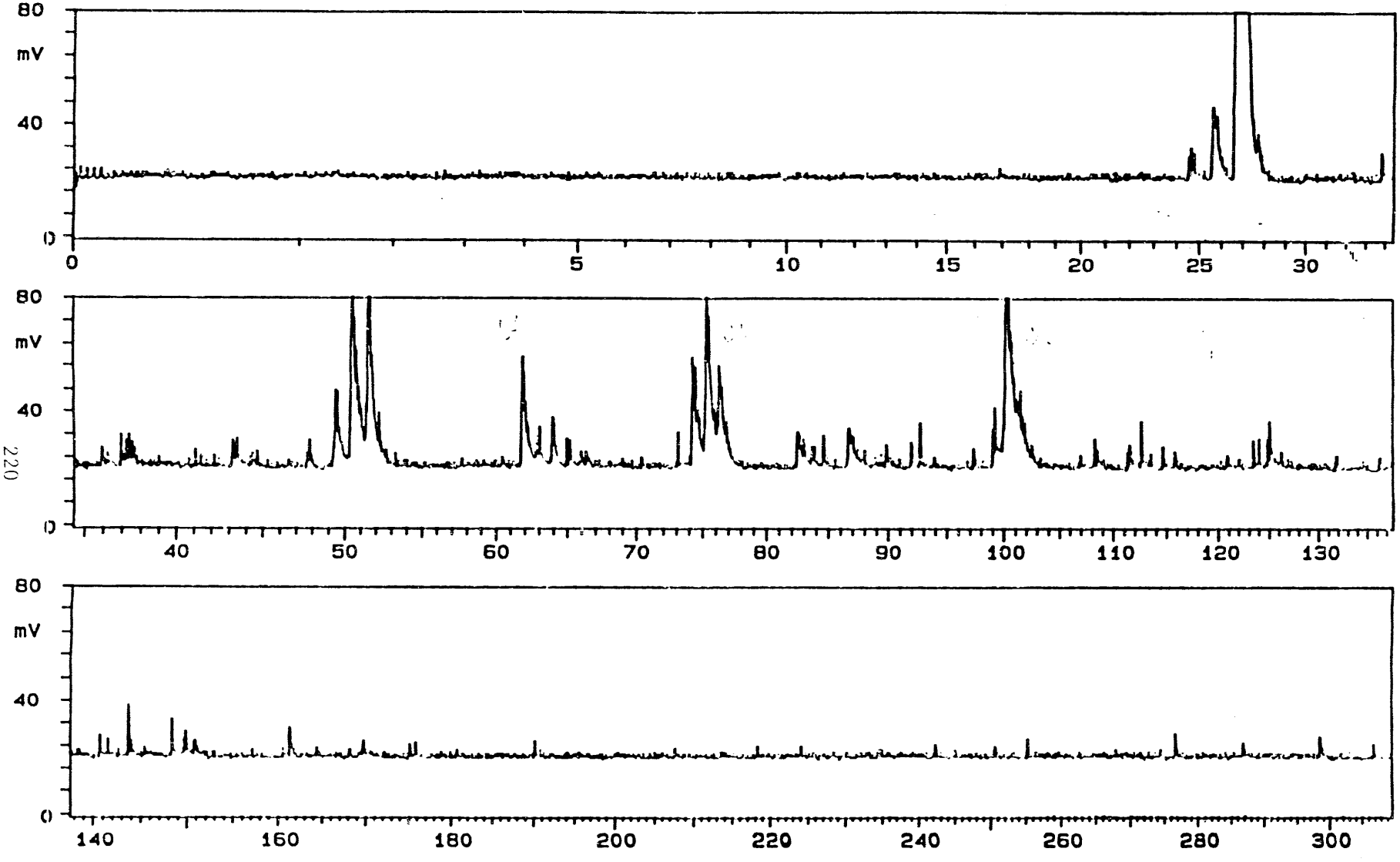

SSL# 3915-1188 Spectrum 66'
X=745.5, COAL SAMP B, FOC=-1.0 ATT=0.25%, 0.6UJ
COLUMBIA U

SPEKTRUM 7270
POLARITY -
RANGE .16 V

21/12/1988
LASER .590uJ

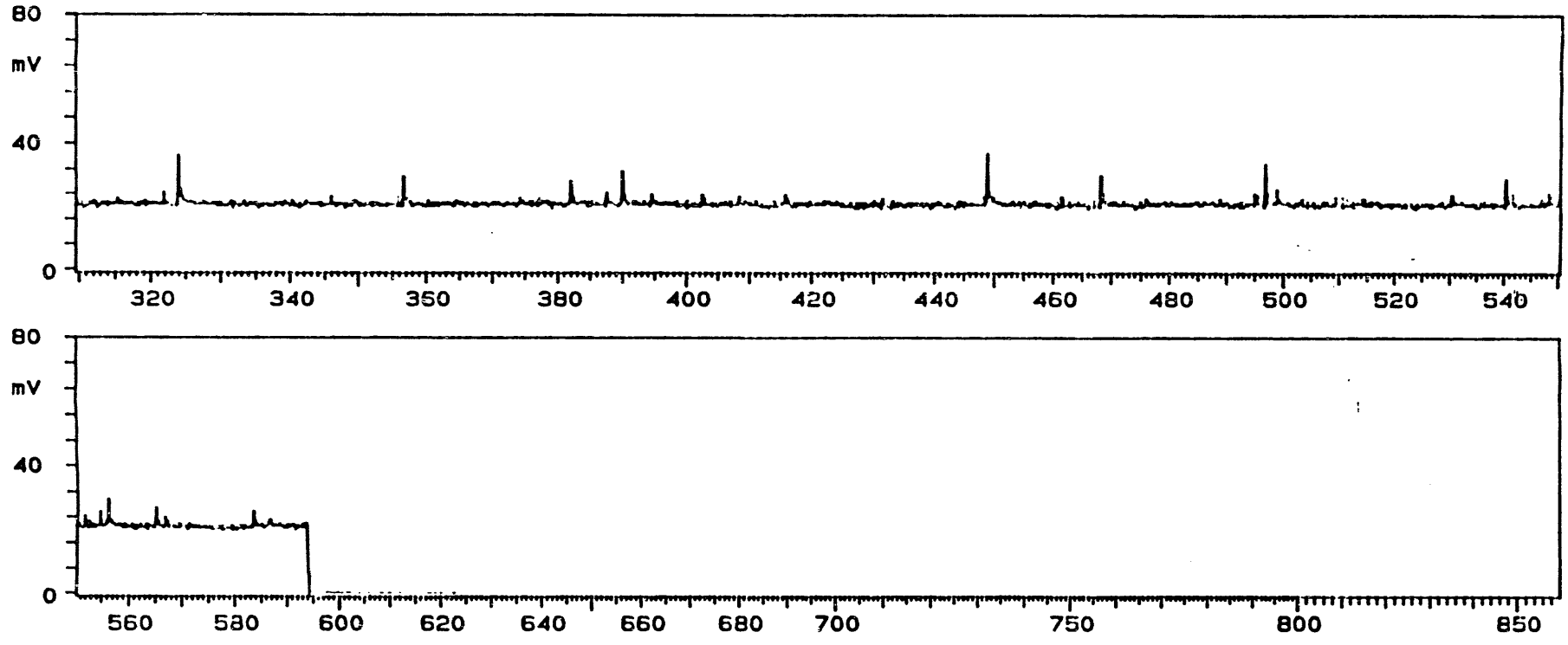

SSL# 3915-1188 Spectrum 7B

SPEKTRUM 7330

21/12/1988

X=745.9, COAL SAMP B, FOC=-1.0 ATT=0.25%, 0.6UJ

POLARITY -

LASER .600uJ

COLUMBIA U

RANGE .16 V

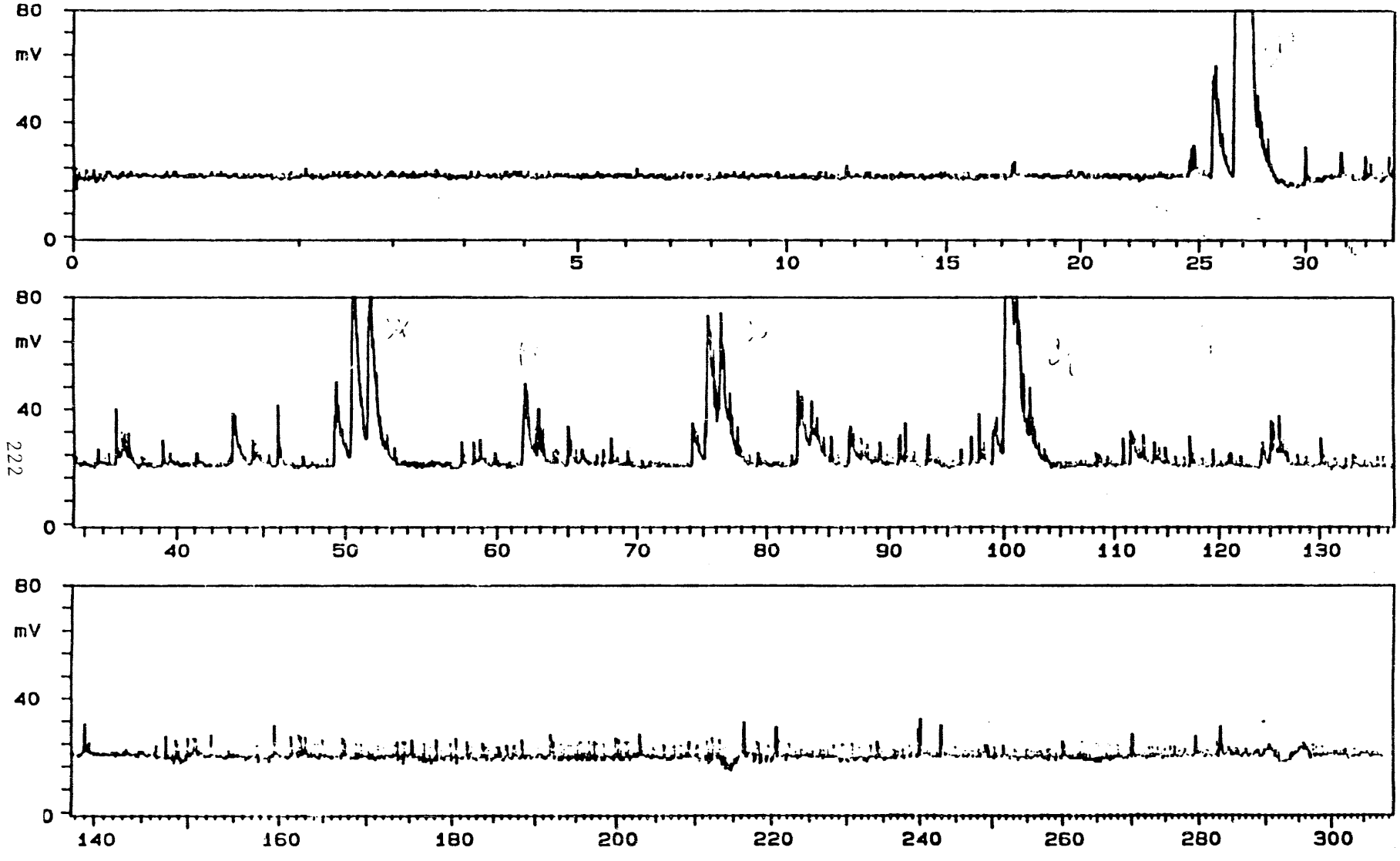

SSL# 3915-1188 Spectrum 78'

SPEKTRUM 7330

21/12/1988

X-745.9, COAL SAMP B, FOC=-1.0 ATT=0.25%, 0.6UJ

POLARITY -

LASER .600uJ

COLUMBIA U

RANGE .16 V

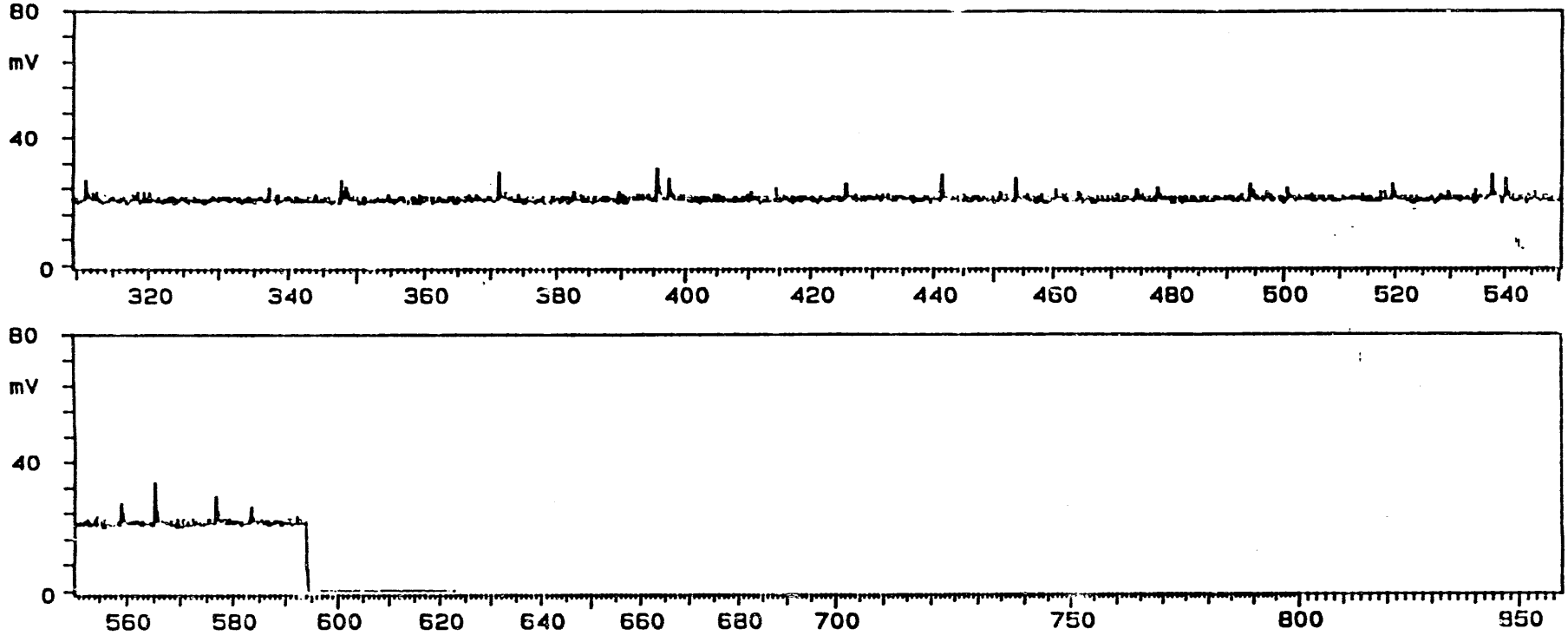

SSL# 3915-1188 Spectrum 8B
X=746.3, COAL SAMP B, FOC=-1.0 ATT=0.25%, 0.6UJ
COLUMBIA U

SPEKTRUM 7390
POLARITY -
RANGE .16 V

21/12/1988
LASER .590uJ

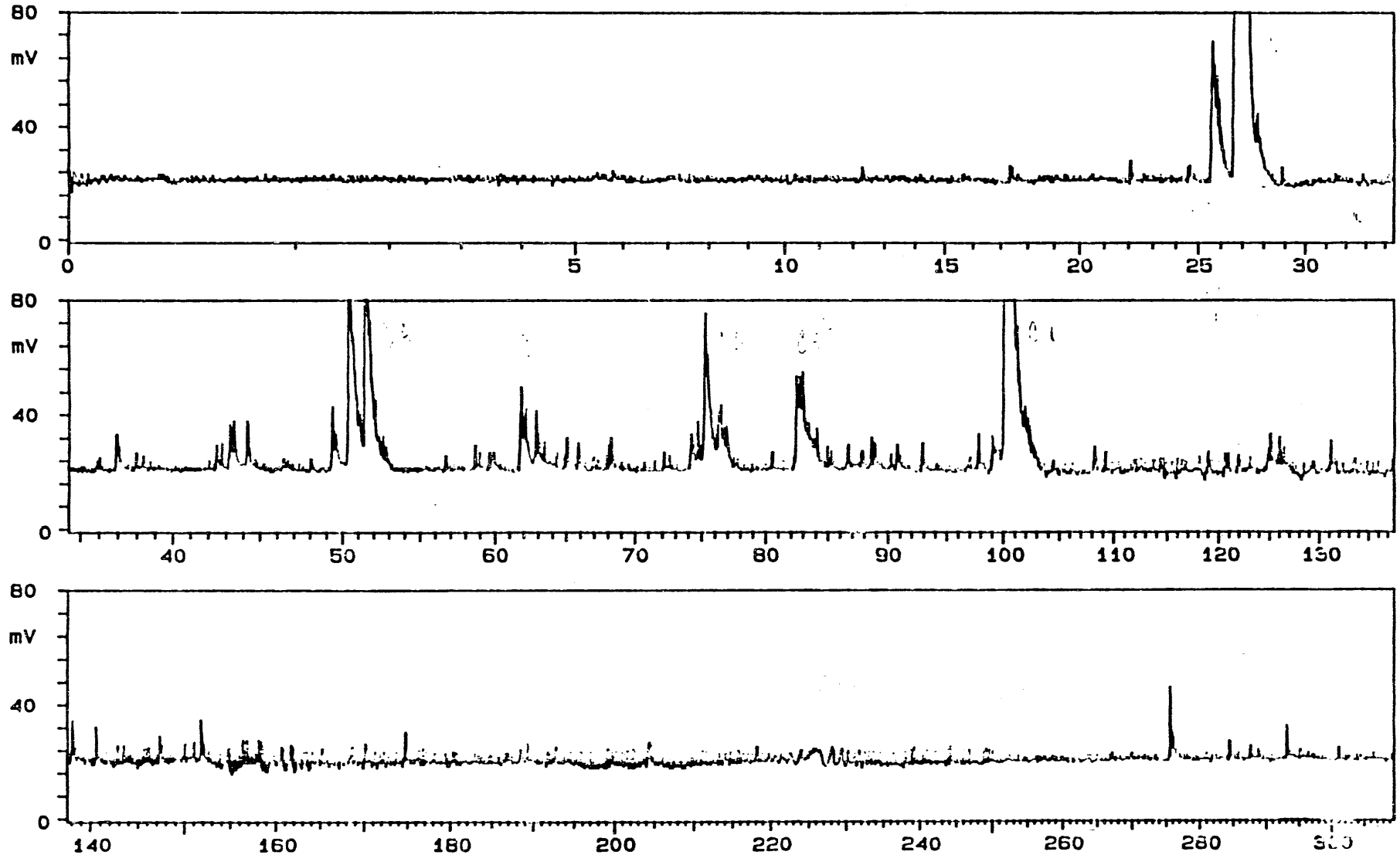

SSL# 3915-1188 Spectrum 8B' SPEKTRUM 7390 21/12/1988

X=746.3. COAL SAMP B. FOC=-1.0 ATT=0.25%. 0.6UJ POLARITY - LASER .590uJ

COLUMBIA U RANGE .16 V

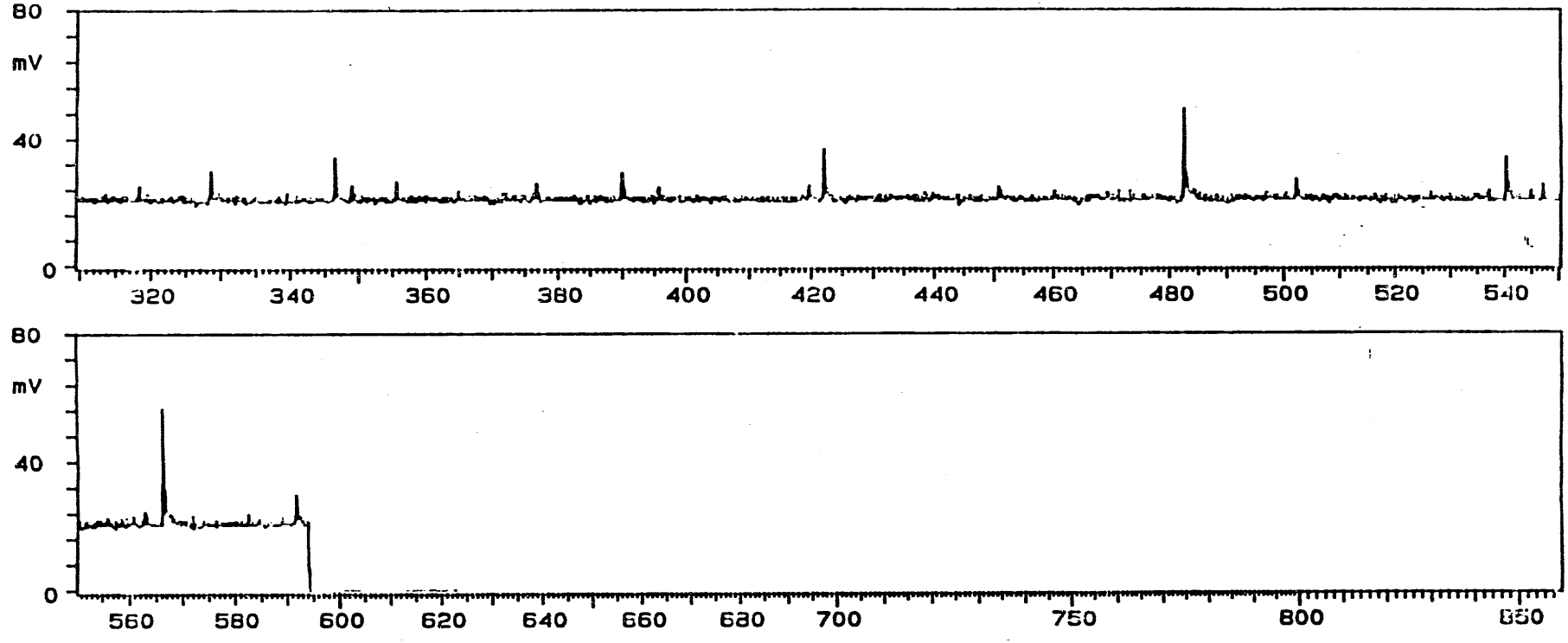

SSL# 3915-1188 Spectrum 9B

X-746.7, COAL SAMP B, FOC=-1.0 ATT=0.25%, 0.6UJ

COLUMBIA U

SPEKTRUM 7450

POLARITY -

RANGE .16 V

21/12/1988

LASER .620uJ

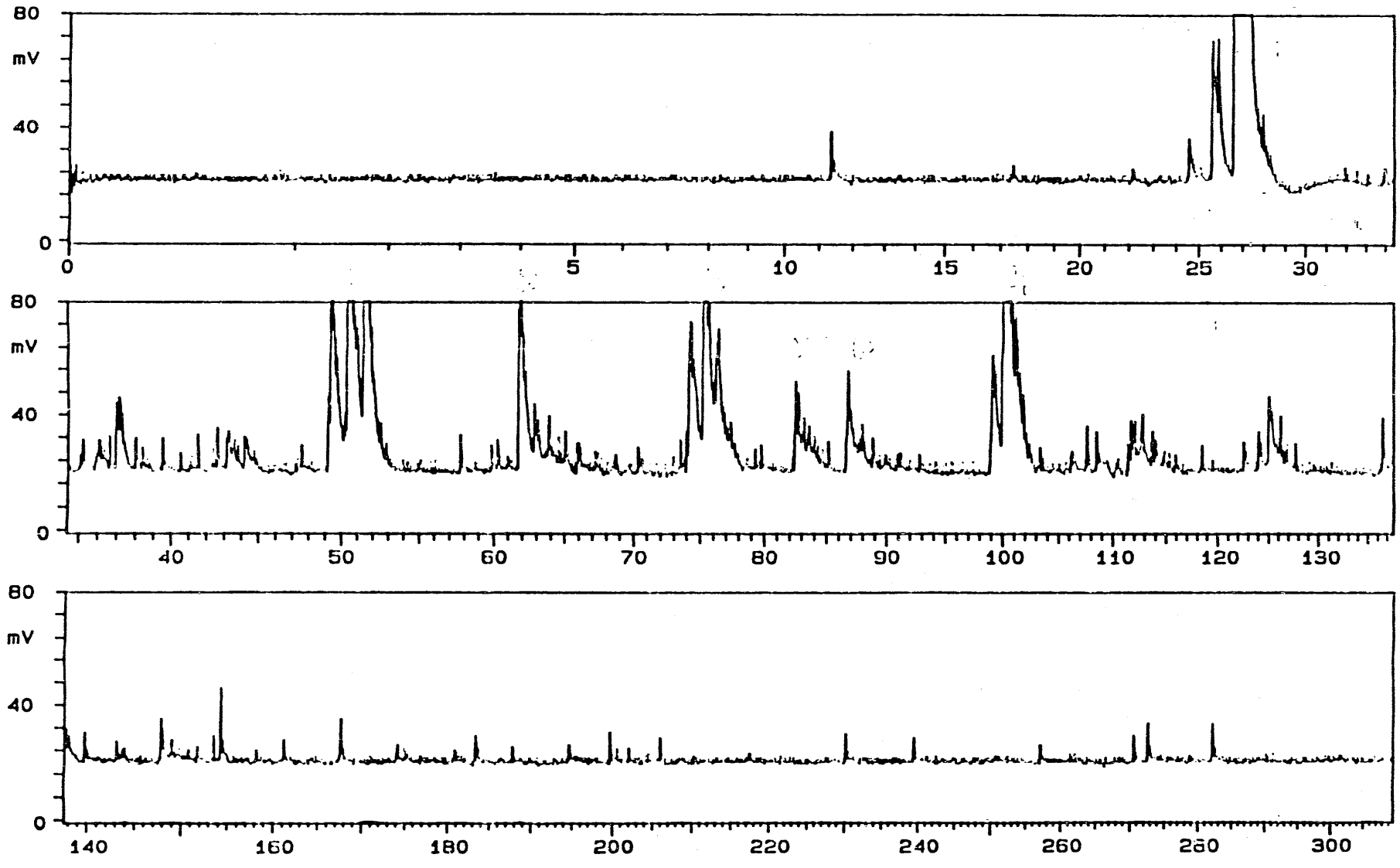

SSL# 3915-1188 Spectrum 9B'

X=746.7, COAL SAMP B. FOC=-1.0 ATT=0.25%. 0.6UJ

COLUMBIA U

SPEKTRUM 7450

POLARITY -

RANGE .16 V

21/12/1988

LASER .620uJ

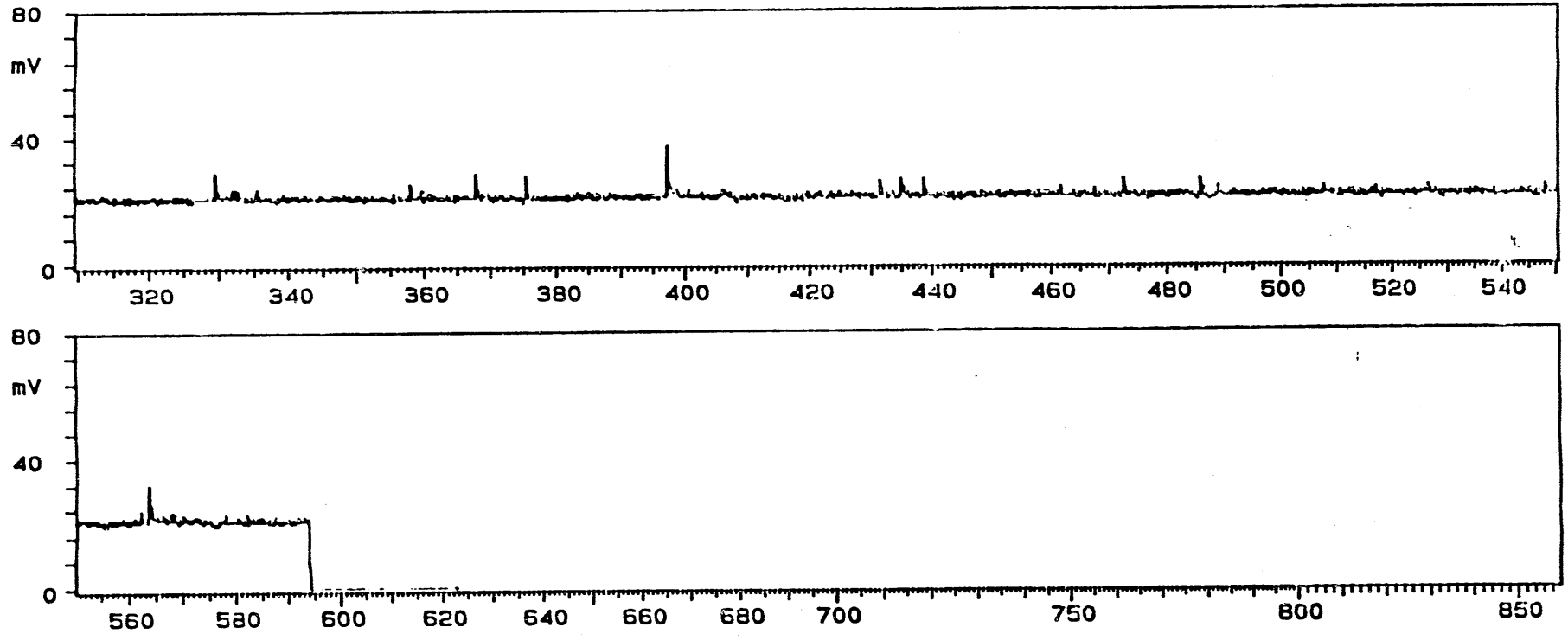

SSL# 3915-1188 Spectrum 10B
X=747.1. COAL SAMP B. FOC=-1.0 ATT=0.25%. 0.6UJ
COLUMBIA U

SPEKTRUM 7510
POLARITY -
RANGE .16 V

21/12/1988
LASER .590uJ

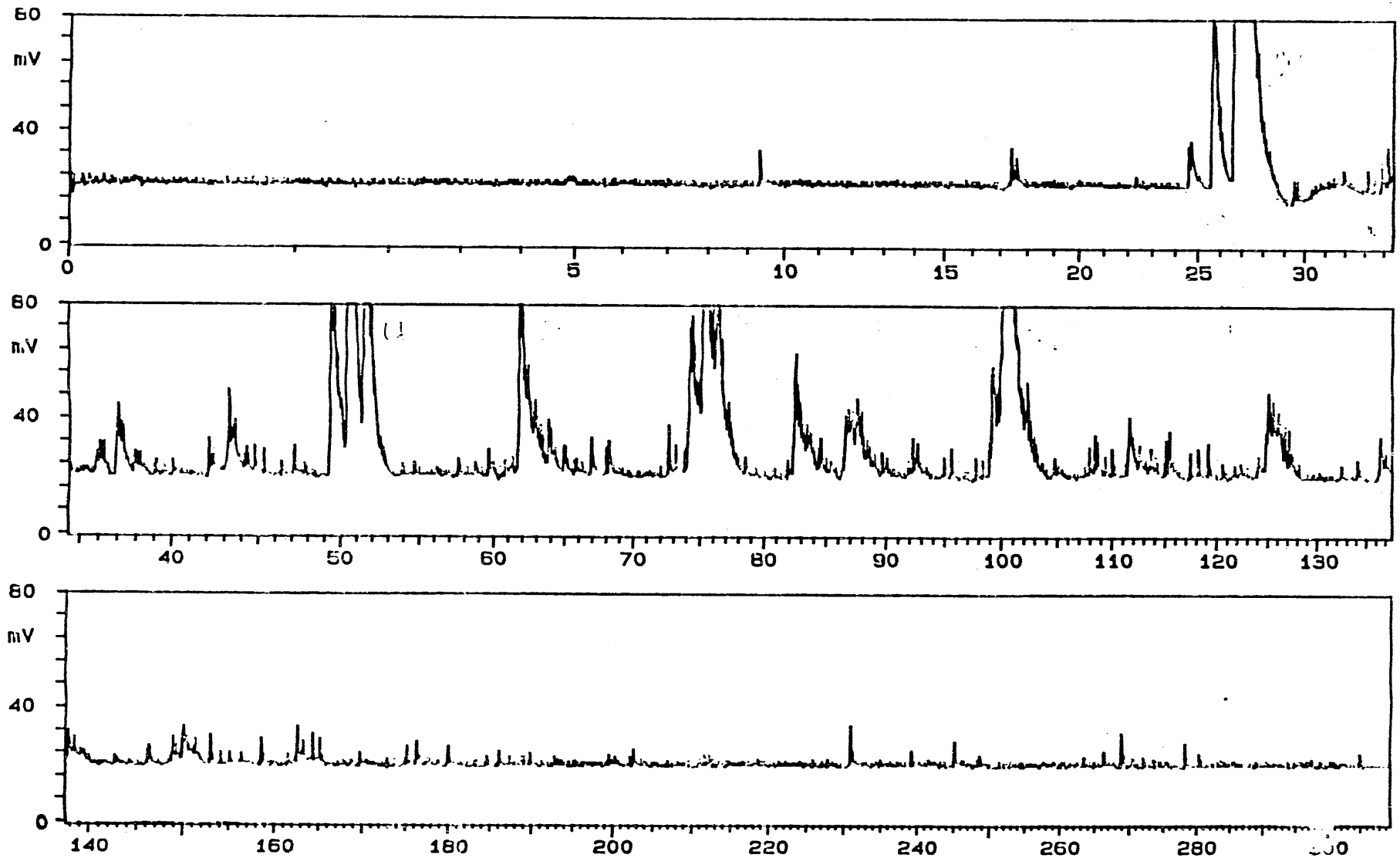

SSL# 3915-1188 Spectrum 10B'
X=747.1, COAL SAMP B, FOC=-1.0 ATT=0.25%, 0.6UJ
COLUMBIA U

SPEKTRUM 7510
POLARITY -
RANGE .16 V

21/12/1988
LASER .590uJ

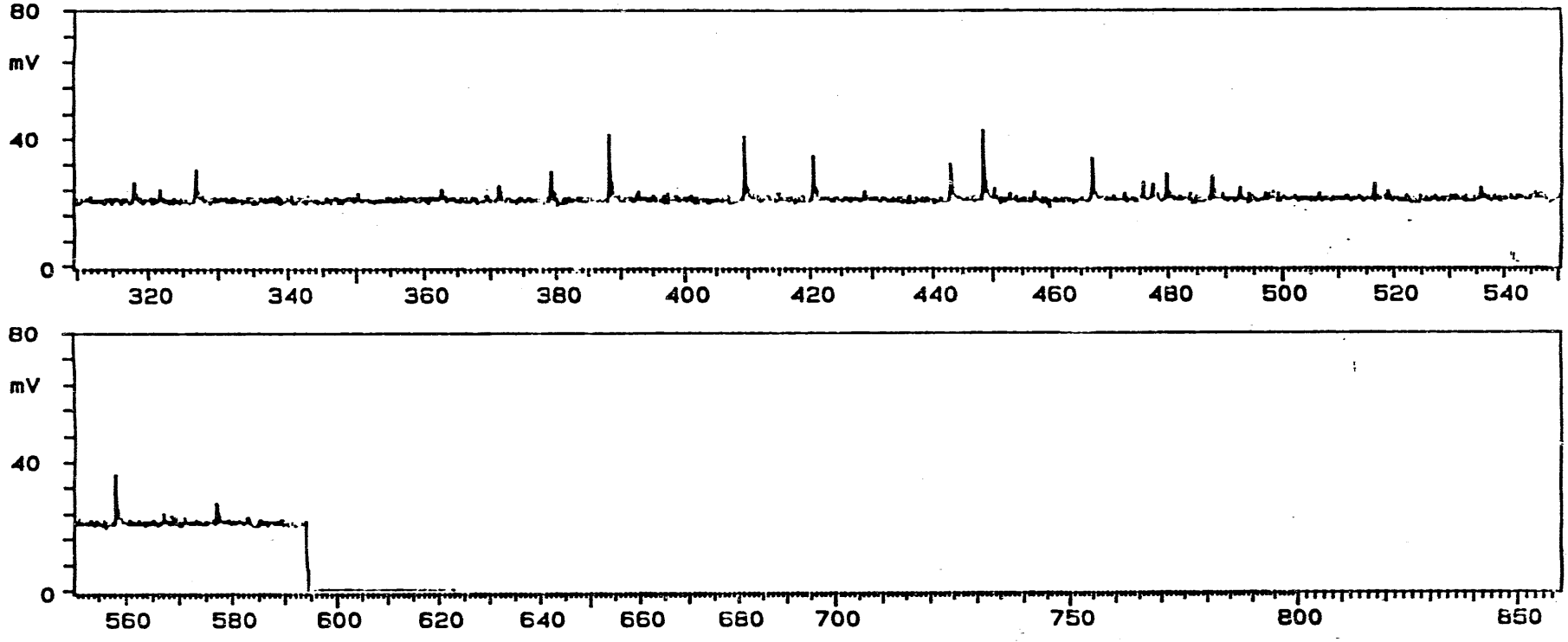

SSL# 3915-1188 Spectrum 11B
X=747.1, COAL SAMP B, FOC=-1.0 ATT=0.25%, 0.6UJ
COLUMBIA U : REPEAT SAME LOCATION, DEPTH 2

SPEKTRUM 7570
POLARITY -
RANGE .16 V

21/12/1988
LASER .610uJ

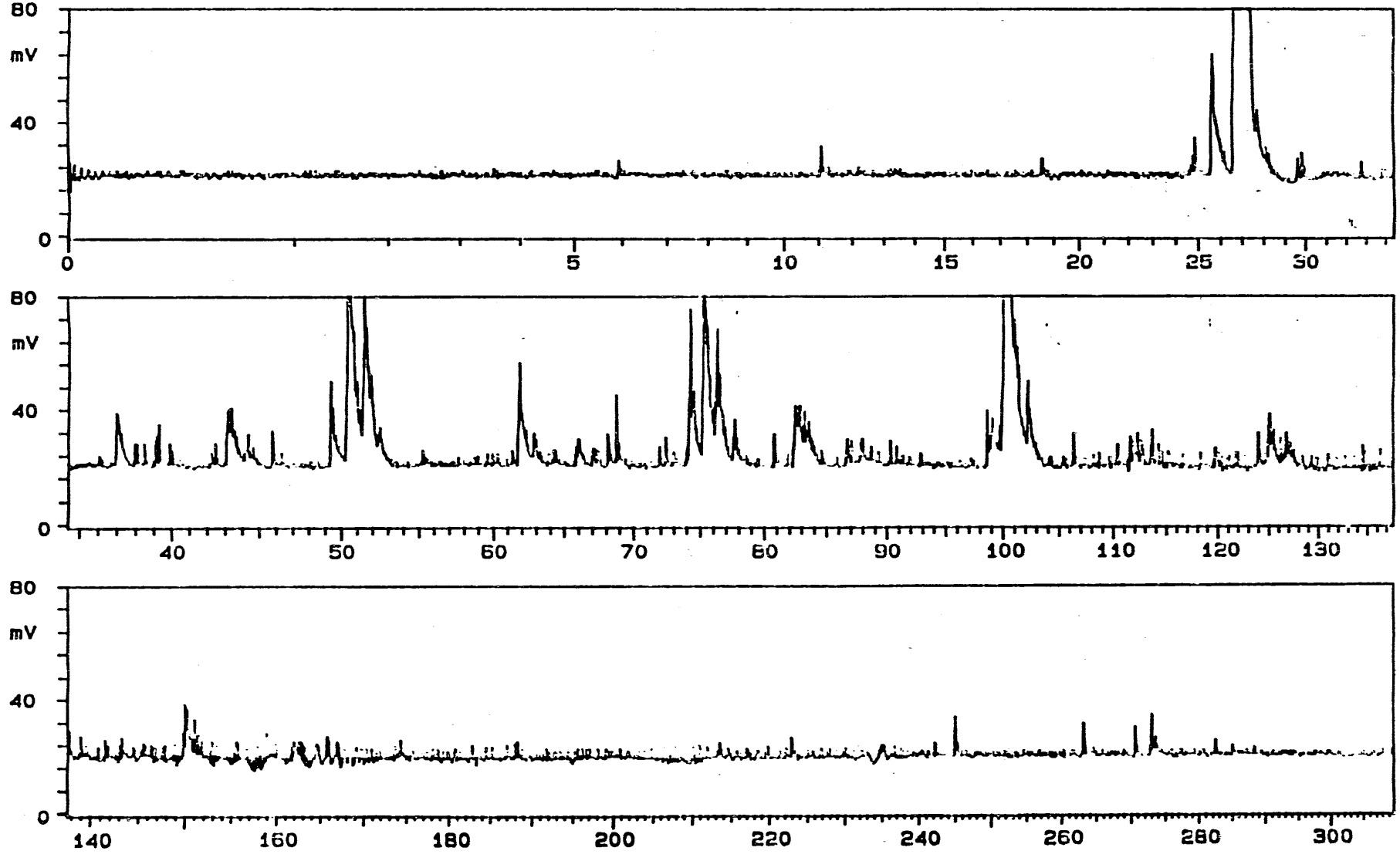

SSL# 3915-1188 Spectrum 11B'
X=747.1, COAL SAMP B, FOC=-1.0 ATT=0.25%, 0.6UJ
COLUMBIA U : REPEAT SAME LOCATION, DEPTH 2

SPEKTRUM 7570
POLARITY -
RANGE .16 V

21/12/1988
LASER .610uJ

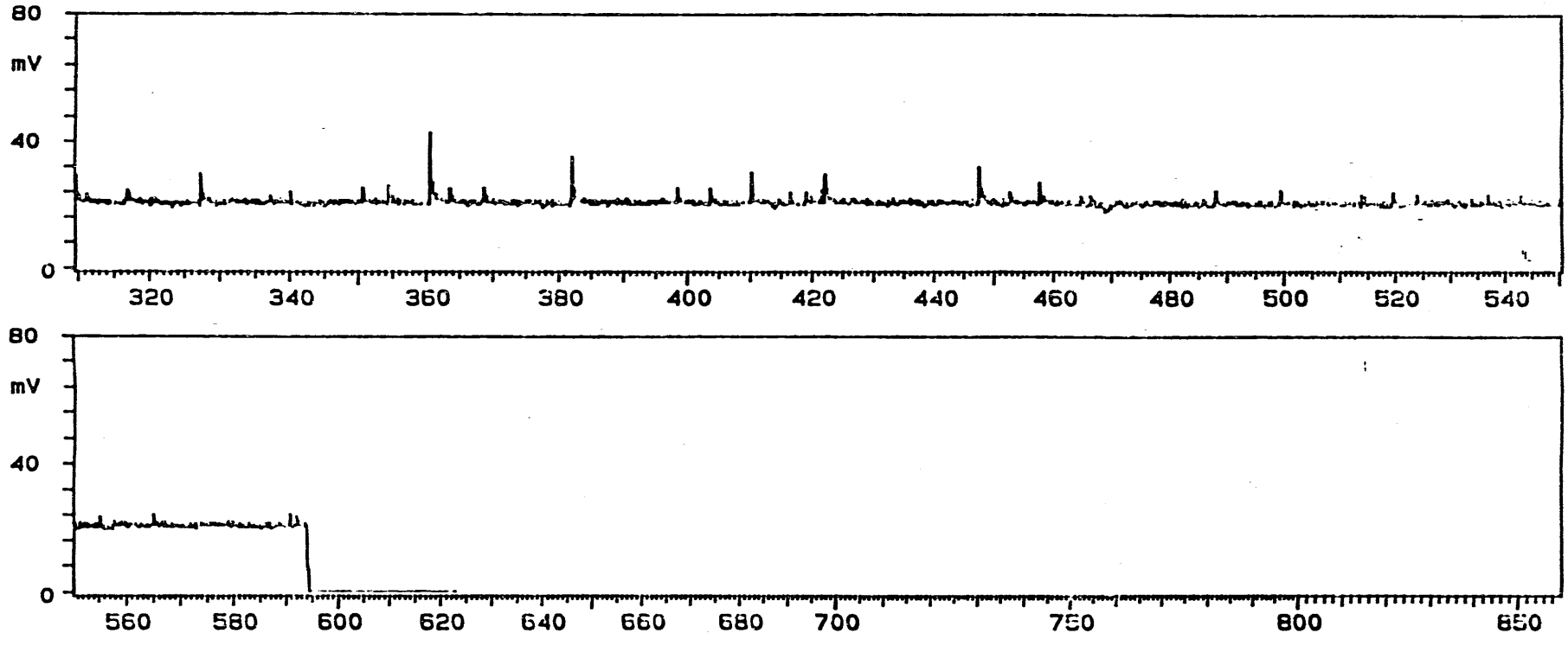

*US GOVERNMENT PRINTING OFFICE:1990-548-138/20006

END

DATE FILMED

01/07/91